THE SYNTHESIS OF NOVEL BIODEGRADABLE POLYESTERS AND COPOLYESTERS FROM ANHYDROSULFITES

KARINE LINE ROSE N'GOALA

Doctor of Philosophy

THE UNIVERSITY OF ASTON IN BIRMINGHAM

April 1996

SUMMARY

The University of Aston in Birmingham

THE SYNTHESIS OF NOVEL BIODEGRADABLE POLYESTERS AND COPOLYESTERS FROM ANHYDROSULFITES

Karine Line Rose N'Goala

A thesis submitted for the degree of Doctor of Philosophy

1996

This thesis was concerned primarily with the synthesis and the ring-opening polymerization of anhydrosulfites (1,3,2-dioxa-thiolan-4-one-2-oxides), and secondly with the copolymerization of anhydrosulfites with ε-caprolactone. The polyesters and copolyesters synthesised are of considerable interest in medical applications and also for use as environmental friendly packaging.

A range of anhydrosulfites were prepared according to an established method. Aliphatic anhydrosulfites were obtained with a level of purity satisfactory for polymerization whereas aromatic anhydrosulfites decomposed during distillation and purification by chromatographic techniques. Aliphatic anhydrosulfites with a substituent, such as methyl, isopropyl, n-butyl and isobutyl were studied by NMR spectroscopy. Analysis of these spectra revealed that the five-membered anhydrosulfite ring was puckered and that when the substituent was bulky, rotations about the alkyl chains were restricted.

A wide range of anionic initiators may be used to initiate anhydrosulfites. Lithium alkyls turned out to be more successful than alkali metal alkoxides and amides. The molecular weights were found to depend on the basicity of the initiator, the monomer-to-initiator ratio, the nature of the solvent and the polymerization temperature. The molecular weight $\overline{M}_n$ of poly(L-lactic acid) ranged from (0.5 to 6)x10^4. Highly crystalline and purely isotactic poly(lactic acid) was synthesised from L-lactic acid anhydrosulfite (L-LAAS) whereas DL-LAAS led to an amorphous polymer with randomly distributed D- and L-lactic units. This indicated that this polymerization was not stereoselective. However, the bulkiness of the substituent in the anhydrosulfites molecule was found to influence the stereoselectivity of the polymerization, thus polyesters with isobutyl or n-butyl pendant group were preferentially isotactic.

Block-copolymers of ε-caprolactone and several anhydrosulfites were successfully produced. Block-copolymers of LAAS with ε-caprolactone were also synthesised, but the incorporation of caprolactone units was rather small. In contrast, random copolymerization of LAAS and ε-caprolactone led to polymers with blocky structures similar to those obtained in the block-copolymerization of LAAS with ε-caprolactone.

Keywords

ANHYDROSULFITE, POLY(LACTIC ACID), BIODEGRADABLE, ALIPHATIC COPOLYESTERS, POLY(CAPROLACTONE).

To my mother

ACKNOWLEDGEMENTS

My sincere thanks go to my supervisor Dr Allan J. Amass for his advice and encouragement throughout the period of this work and to my co-supervisor Prof Brian J. Tighe for his helpful comments. I also wish to gratefully acknowledge the European Community for their financial support under Brite Euram program.

I would like to thank Dr Luke Adams for his help and 'precious' advice, and Dr Gilles Piquet for his collaboration and partnership in the synthesis of the copolymers.

I also wish to acknowledge the help of the support staff in the chemistry department, in particular, Dr Mike Perry for NMR spectroscopy, Denise Ingram and Mike Houghton for FT-IR spectroscopy and HPLC.

Thanks are also due to my friends and fellow research students, Babs, Monali, Wendy, Val, Fred, Rob, Colin, Phil, Mike, Mark, Andy, Monique, Udkhar and Steve, whose humour, advice and kindness contributed so much to this work.

Finally, I wish to express my sincere thanks to my mother and my father for their encouragement, and also to Guillaume for his invaluable support and patience over the last three years.

LIST OF CONTENTS

CHAPTER 1

INTRODUCTION

CHAPTER 2

EXPERIMENTAL TECHNIQUES

CHAPTER 3

MONOMER SYNTHESIS

CHAPTER 4

POLY(LACTIC ACID) SYNTHESIS

CHAPTER 5

SYNTHESIS OF NOVEL POLYESTERS

CHAPTER 6

COPOLYMERIZATION OF LACTIC ACID ANHYDROSULFITE WITH ε-CAPROLACTONE

CHAPTER 7

SYNTHESIS OF NOVEL COPOLYESTERS

CHAPTER 8

CONCLUSION

LIST OF FIGURES

LIST OF TABLES

LIST OF ABBREVIATIONS

BAAS	Benzilic acid anhydrosulfite
CL	Caprolactone
COP	Copolymer
DSC	Differential scanning calorimetry
FT-IR	Fourier transform infrared
GPC	Gel permeation chromatography
HCAAS	Hydroxy caproic acid anhydrosulfite
HICAAS	Hydroxy isocaproic acid anhydrosulfite
HIVAAS	Hydroxy isovaleric acid anhydrosulfite
HPLC	High performance liquid chromatography
LAAS	Lactic acid anhydrosulfite
MAAS	Mandelic acid anhydrosulfite
$\overline{M_n}$	Number average molecular weight
$\overline{M_w}$	Weight-average molecular weight
$\overline{M_w}/\overline{M_n}$	Polydispersity
MW	Molecular weight
NMR	Nuclear magnetic resonance
PCL	Poly(caprolactone)
PHCAAS	Poly(hydroxy caproic acid anhydrosulfite)
PHICAAS	Poly(hydroxy isocaproic acid anhydrosulfite)
PHIVAAS	Poly(hydroxy isovaleric acid anhydrosulfite)
PLAAS	Poly(lactic acid anhydrosulfite)
THF	Tetrahydrofuran
TLC	Thin layer chromatography

CHAPTER 1

INTRODUCTION

1.1. Applications of polyesters

Polymers as biomaterials have received considerable attention. Biodegradable polymers from glycolic acid (hydroxy acetic acid) or from lactic acid (2-hydroxypropionic acid) are the simplest linear aliphatic polyesters, which are currently the most widely used synthetic, degradable polymers in human medicine. They display an excellent biocompatibility and do not exhibit any toxicity. When devices from these materials are implanted in living organisms including the human body, they are hydrolyzed to their constituent α-hydroxy acid which is eliminated by general metabolic pathways.

In particular, poly-α-esters play an important role in controlled-release technology [1]. Their primary function is to regulate the release of a drug in a predictable manner by progressive chemical erosion of the polymer backbone. There is also considerable interest in using these polymers because devices made with these materials shrink with time and eventually disappear. This property is particularly suitable for implants and injectables because the device does not have to be removed from its site of application in the body once the delivery role is complete.

Thus, biodegradable polyesters have many important applications in medicine and in agriculture : in medicine as surgical implants, absorbable sutures [2,3], implants for controlled release of drugs [4], carriers of drugs [5] and in agriculture, mainly as controlled release of fertilizers and pesticides.

Their properties such as transparency, mechanical strength, safety and degradability in compost are also of considerable interest and open up their use as consumer goods packaging, an application with potentially huge markets. Additionally, they can be utilized in a wide variety of consumer products such as paper coatings, films, moulded articles, foamed articles and fibers [6]. But, the availability of lactic acid, in particular, and

its low production cost make this hydroxy acid even more interesting for industrial production.

Copolymerization of ε-caprolactone with hydroxy acids provides a variety of polyesters with a wide range of degradability. Indeed, PCL is degraded very slowly when compared with polylactic acid. However, the biodegradability can be enhanced greatly by copolymerization. For example, the amorphous copolymer poly(ε-caprolactone-co-DL-lactic acid) undergoes degradation at a greater rate than either of the homopolymers, as shown in table 1.1.

Table 1.1. Biodegradation of polyesters.

Polymer	Approximate time for biodegradation (months)
Poly(L-lactide)	18 -24
Poly(DL-lactide)	12-16
Poly(glycolide)	2 - 4
50:50 Poly(DL-lactide-co-glycolide)	2
85:15 Poly(DL-lactide-co-glycolide)	5
90:10 Poly(DL-lactide-co-caprolactone)	2

(source : reference Chasin and Langer [1])

Because of the wide range of biodegradation profiles available with lactic and glycolic acids, and caprolactone polymers, the duration of action of drug delivery products range from a few days to about 2 years, as shown in table 1.1.

1.2. Synthetic routes to poly-α-esters

Poly-α-esters can be synthesised by different methods, either by direct polycondensation of α-hydroxy acids or by ring-opening polymerization of cyclic monomers such as cyclic dimers (glycolide and lactide), anhydrosulfites or anhydrocarboxylates. Each method

provides specific degrees of control of the molecular weight, the molecular weight distribution and the stereochemical structure of the resulting polymer. Each of these characteristics, in turn, is important in defining the degradability of the polyester.

1.2.1. Structural aspect of poly(lactic acid)

Due to its asymmetrical β-carbon, the starting material lactic acid, exists as two different stereoisomers D and L, D referring to the sign of rotation of the polarized light (-) and analogously (L) to (+). For expressing its absolute configuration in a more appropriate manner, the (R)-(S) system would be used, with the assignments (R)-lactic acid = D-lactic acid and (S)-lactic acid = L-lactic acid.

In the chains of the resulting polymer, polylactic acid, a true asymmetric centre is also found, which is the reason why this polymer can exhibit optical activity. This asymmetric centre can be either in D- or L- configurations, which have, in this case, nothing to do with optical activity and merely refer to the methyl group being positioned either below or above the chain in a planar position.

In addition, polylactic acid is called either D-, L- or DL- when obtained from D-, L- or DL-monomers, respectively. In each case, there is a distinctive distribution of the D- and L-forms among the units in the poly(lactic acid) chains and this decide the chain tacticity. To define the stereochemical structure of polymer chains, it is convenient to consider that the polymer chain is comprised of a number of dyad units or sequences of two monomer units. There are two possible types of dyads, the isotactic or meso dyad (m) and the syndiotactic or racemic dyad (r).

Both D- and L-polylactic acid produced from a pure enantiomeric monomer are expected to be isotactic. Using an extended zig-zag structure, these polymers can be defined as meso dyads (m), where the methyl group alternates across the plane containing the main chain bonds, as shown in figure 1.1. But, in some cases, the polymerization, which yields polylactic acid, involves racemization of the asymmetric centre, as part of the mechanism, so that the polymer obtained has a partially irregular structure. For more information see section 1.2.3.2.

In general, DL-polylactic acid obtained from an enantiomeric mixture of D- and L-monomers can be either syndiotactic, also defined as racemic dyads (r), where all the methyl groups are located on one side, as shown in figure 1.1., or atactic with a random distribution of D- and L-forms. But again, in some cases, the polymerization producing polylactic acid is stereoselective, so that the polymer formed has a predominantly isotactic structure, as discussed in section 1.2.4.4.

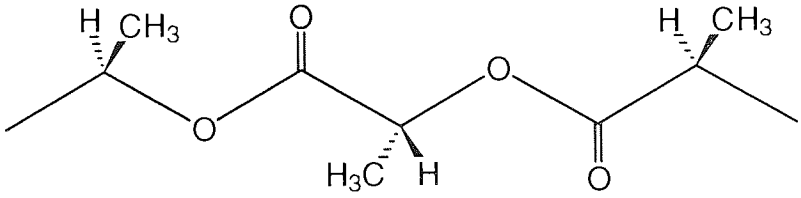

(a)

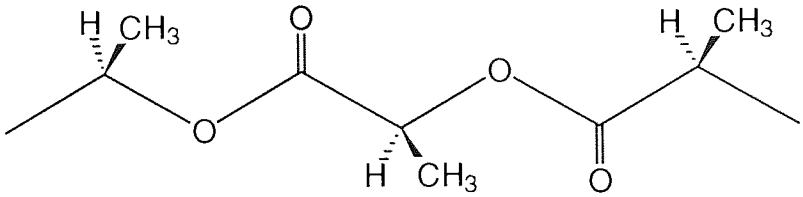

(b)

Figure 1.1. (a) Isotactic and (b) syndiotactic structures of poly(lactic acid).

In the case of an atactic poly(lactic acid), the possible stereosequences are numerous and sometimes can be observed in ^{1}H and ^{13}C NMR spectra. Interpretation of these spectra depends on consideration of the sequences of several monomer units or n-ads. Table 1.2. shows the several sequences involved in dyad, triad, and tetrad sensitivity together with their frequency of occurrence as a function of P_m, according to Bernouillian statistics [7]. P_m designates the probability that the polymer chain will add a monomer unit to give the same configuration as that of the last unit at its growing end.

Table 1.2. Dyad, Triad, and Tetrad sequences.

n-ad	Designation	Bernouillian probability
Dyad	meso, m	P_m
	racemic, r	$(1 - P_m)$
Triad	isotactic, mm	P_m^2
	heterotactic, mr	$2P_m(1 - P_m)$
	syndiotactic, rr	$(1 - P_m)^2$
Tetrad	mmm	P_m^3
	mmr / rmm	$2P_m^2(1 - P_m)$
	rmr	$P_m(1 - P_m)^2$
	mrm	$P_m^2(1 - P_m)$
	rrm / mrr	$2P_m(1 - P_m)^2$
	rrr	$(1 - P_m)^3$

(Source : reference Bovey [7])

Measurement of the relative intensities of the different sequences from the NMR spectra gives a valid statistical representation of the microstructure of the polymer and these data give, in turn, a considerable insight into the mechanism of chain propagation.

Jedlinski *et al* [8,9] synthesised poly(lactic acid) from DL-lactide with various initiators and investigated the microstructure of the polymers by NMR spectroscopy. Indeed, in ^{13}C NMR spectroscopy, the signals of methine and carbonyl carbons of poly(lactic acid) were found to be sensitive to the chain sequences. By comparing line intensities in these regions and theoretical stereosequence distributions given by models based on Bernouillian statistics for single and pair addition of lactic repeating units in growing chains, they found that methine and carbonyl carbons were sensitive to tetrads and hexads, respectively. Thereby, the several tetrads could be attributed to the spectral lines of the methine carbon signal in particular. Kricheldorf [10-13] and Vert [14] published results in agreement with these assignments, which results are discussed in detail in section 1.2.3.2.

These differences in structure of poly(lactic acid) are directly reflected in their properties. D- and L-poly(lactic acid) or syndiotactic DL-poly(lactic acid) are crystalline, tough, inelastic materials of low permeability that degrade slowly by hydrolysis over several months. In contrast, atactic DL-poly(lactic acid) is amorphous, more permeable and degrades more rapidly than the two stereoregular polymers.

1.2.2. Polycondensation of α-hydroxycarboxylic acids

1.2.2.1. General characteristics

α-Hydroxy acids contain two functional groups in their chemical structure and so can, under certain conditions, react between them. In this way, they can yield linear polymers by stepwise intermolecular condensation of the reactive groups, as shown in figure 1.2. If significant polymer formation is to be achieved, the water must be removed continuously from the reaction to displace the equilibrium.

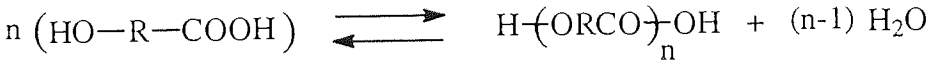

Figure 1.2. Polycondensation reaction of α-hydroxy acids.

In this step-growth polymerization, all functional groups are equally reactive. This means that a monomer will react with both monomer and polymer species with equal ease but monomers, being the most predominant species, will tend to react most often. Consequently, all the monomer will be incorporated into a chain molecule in the early stages of the reaction and the chains will be rather short. Thus, if chains of significant size are to be obtained, very high conversions and long reaction times will be necessary. In any case, this process yields polymers with chains of widely varying lengths, the polydispersities obtained are close to 2.

Lactic and glycolic acids can be polymerized by simple condensation effected at temperatures above 120°C. Under these conditions, polymerization rates are higher than at ambient temperature but at such high temperatures, side-reactions are more likely to occur. Fukuzaki and Aiba [15-18] synthesised poly(lactic acid) ($\overline{M_n}$ = 4900) and copolymers of lactic acid with various aromatic hydroxy acids ($\overline{M_n}$ < 3000) by polycondensation. These polymerizations were carried out at 200°C, in the absence of a catalyst which produced polymers of low molecular weight ($\overline{M_n}$ < 10,000). The formation of cyclic dimers along with the equilibrium between free acids, water and polyesters prevented the formation of higher molecular weight polymers.

Alternatively, below this temperature direct polymerization can be effected by the use of highly energetic reactants, such as heavy-metal containing catalysts. Yamaguchi *et al* [19] synthesised poly(lactic acid) by direct polycondensation of L-lactic acid using a solvent such as diphenyl ether and catalysts such as Sn, SnO or $SnCl_2$. Materials with $\overline{M_w}$ > 200,000 were obtained, but these polymers also contained low molecular weight components. Nevertheless, removing water from the reaction media during the initiated polymerization of lactic acid under mild conditions appeared to be the key to the production of polymers with useful properties.

This process is limited to lactic and glycolic acids, attempted polymerization of higher acids yielded unwanted by-products and the polymers produced usually exhibit a low molecular weight and a rather broad molecular weight distribution.

1.2.2.2. Stereochemical aspects of poly(lactic acid) produced by polycondensation

On one hand, the polycondensation of D- or L-lactic acid leads to isotactic polymer. On the other hand, because the formation of long chain polymers by direct condensation is a random process, the polymers produced from racemic lactic acid have an atactic structure with a random distribution of L- and D- units obeying Bernouillian statistics.

1.2.3. Ring-opening polymerization of lactide and glycolide

1.2.3.1. General characteristics

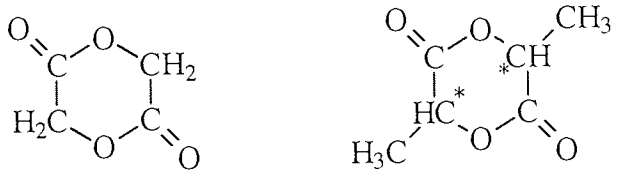

(a) (b)

Figure 1.3. Structure of glycolide (a) and lactide (b).

The preferred method for producing higher molecular weight polyesters ($\overline{M_n} \approx 10^6$), required for pharmaceutical applications, is the ring-opening polymerization of cyclic dimers, lactide or glycolide shown in figure 1.3. These polymerizations can be carried out either in solution or in bulk and are usually performed in a sealed, clean, dry container under reduced pressure and at high temperature. A broad variety of initiators such as tin-, zinc-, or aluminium-containing catalysts can be used in this process, e.g. tetraphenyl tin or stannous octanoate (tin ethyl-2 hexanoate) [19-21], aluminium isopropoxide or zinc powder [22]. These compounds are believed to initiate the cyclic diesters by a non-ionic insertion mechanism [12].

On the other hand, the polymerization of lactide can be effected anionically at room temperature. Jedlinski and Walach [23] used potassium methoxide to initiate L- and DL-lactide polymerizations in THF, which proceeded with good yields. The molecular weight obtained were relatively high with an upper limit of 40,000 for $\overline{M_n}$.

The anionic polymerization of L-lactide was also performed by Kricheldorf and Kreiser-Saunders [10] by using initiators such as potassium *tert*-butoxide and butyllithium. They reported that the mechanism consisted in a deprotonation of L-lactide followed by a

nucleophilic initiation of the lactide anion, then the propagation proceeded via alkoxide chain ends, as shown in figure 1.4.

It is known however, that these methods are limited to glycolide and lactide, increased substitution reduces the polymerizabitility of the cyclic diester.

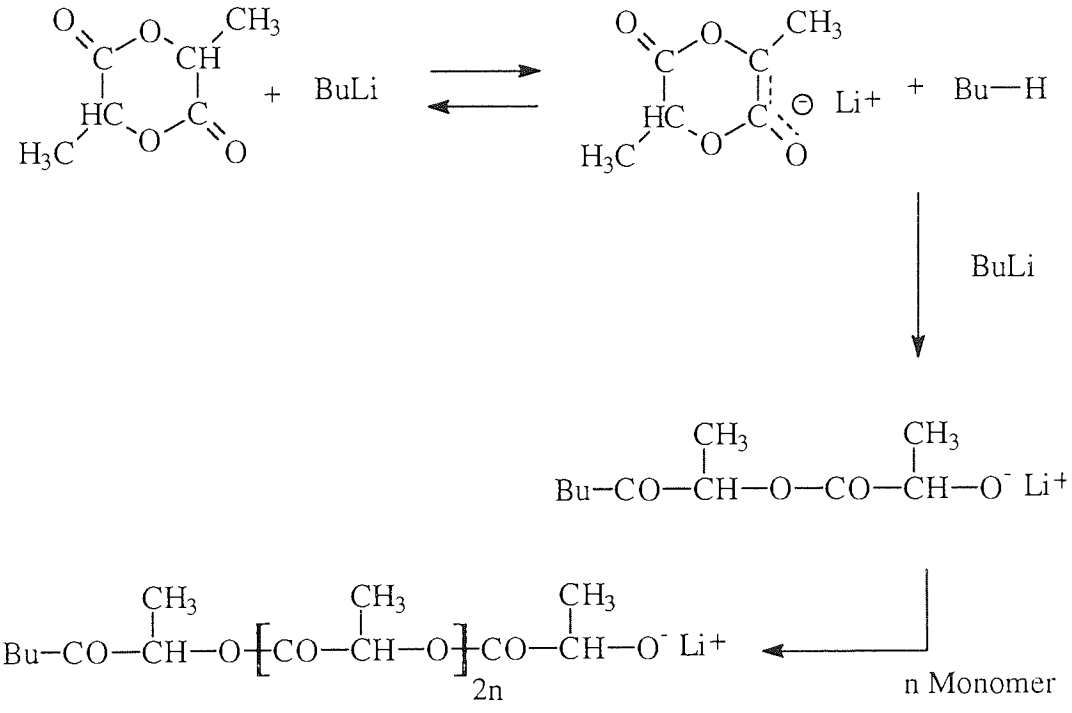

Figure 1.4. Anionic ring-opening polymerization of lactide.

1.2.3.2. Stereochemical aspects of polylactic acid produced by ring-opening polymerization of lactide

The polymerization of cyclic lactide proceeds through pair-addition of lactic acid repeating units which yields polydimers, with the initial configuration of the lactide retained in the process. This implies that polymers with various configurational structures can be obtained.

The ring-opening polymerization of a pure enantiomer (optically active D or L monomer) D,D- or L,L-lactide results in an isotactic polylactic acid, if no racemization occurs. In some cases, the polymer obtained is not totally stereoregular. For example, the anionic polymerization of L-lactide at room temperature with strong bases like potassium *tert*-butoxide and butyllithium involved partial racemization of lactic units in the resulting polymer because of the deprotonation of L-lactide [10], as described previously.

On the other hand, racemic lactide (racemic combinations of D,D- and L,L-lactides) gives a 'predominantly isotactic' polymer (Vert's terminology [22]) as meso diads are favoured by L,L- and D,D- repeating units. In contrast, the D,L- diastereoisomer or meso lactide gives a polymer predominantly syndiotactic as racemic diads are favoured by the meso diastereoisomeric structure. The corresponding tetrads and their probabilities of occurrence are listed in table 1.3.

Table 1.3. Tetrad probabilities for the different types of poly(D,L-lactide)s.

Random stereosequence		Bernouillian poly(*rac*-D,L-lactide)		Bernouillian poly(*meso*-D,L-lactide)	
Tetrad	Probability	Tetrad	Probability	Tetrad	Probability
mmm	0.125	mmm	0.375	-	-
mmr	0.125	mmr	0.125	-	-
rmm	0.125	rmm	0.125	-	-
mrm	0.125	mrm	0.250	mrm	0.125
rmr	0.125	rmr	0.125	rmr	0.250
rrm	0.125	-	-	rrm	0.125
mrr	0.125	-	-	mrr	0.125
rrr	0.125	-	-	rrr	0.375

(Source : reference Kricheldorf [12])

The ring-opening polymerization of lactides does not necessarily follow Bernouillian statistics for a pair-addition mechanism because side-reactions, such as transesterification and racemization can also occur during the process and lead to random stereosequences. The level of transesterification depends on the initiator used and high reaction temperatures usually increase this contribution. Kricheldorf and Boettcher [12] reported that the transesterification reactions occurred at temperatures above 120°C for the polymerization of *meso*-D,L-lactide with aluminium-containing initiators. Jedlinski and co-workers [8] found also that poly(lactic acid) synthesised from racemic lactide at 150°C with zinc chloride was essentially atactic. Vert *et al* [14] compared the configurational structure of poly(racemic-lactide) obtained from a polymerization initiated with stannous octoate or zinc and found that the nature of the initiator and the temperature were not the only variables influencing the occurrence of intermolecular transesterification, but the monomer-to-initiator ratio and the polymerization time also had an effect. However, the transesterification contribution was, in general, greater in the zinc-initiated polymerization than stannous octoate-initiated polymerization.

1.2.3.3. Copolymerization of lactide and ε-caprolactone

Block-copolymers of ε-caprolactone with lactide were prepared in THF and benzene with lithium *tert*-butoxide by Bero and co-workers [23]. The molecular weight and the molecular weight distribution of the copolymers were found to be affected by the nature of the solvent.

In contrast, many attempts to synthesise random copolymers of lactide (or glycolide) and ε-caprolactone failed. The copolymers obtained had a blocky structure, because of the larger reactivity of lactide compared to ε-caprolactone. Grijpma and Pennings [24] carried out a ring-opening polymerization of a 50/50 mixture of L-lactide and ε-CL in bulk with stannous octoate. The polymerization temperature and the reaction time were found to influence the copolymer composition and structure because of a diminution of the difference in reactivity between lactide and ε-CL at high temperature, but in a greater part, because of the occurrence of transesterification reactions.

Perego and Vercellio [25] conducted similar copolymerizations of L- and DL-lactide with ε-CL and observed a difference between feed ratio and copolymer composition, along with a certain quantity of unreacted ε-CL.

1.2.4. Ring-opening polymerization of anhydrosulfites and anhydrocarboxylates

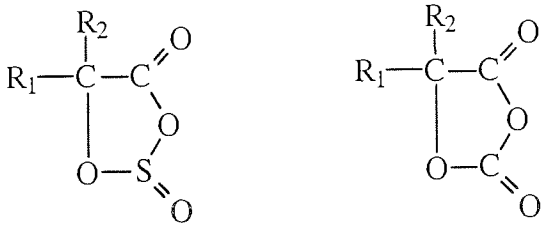

(a) (b)

Figure 1.5. Structure of anhydrosulfites (a) and anhydrocarboxylates (b).

Anhydrosulfites and anhydrocarboxylates, shown in figure 1.5., provide an interesting and convenient route to poly-α-esters with a variety of R_1 and R_2 substituents. The synthesis of anhydrosulfites and anhydrocarboxylates involves the direct reaction of α-hydroxycarboxylic acids with thionyl chloride and carbonyl chloride, respectively, under suitable conditions, principally a dry atmosphere and a relatively low temperature. For more information about the synthesis of anhydrosulfites see section 3.1.

There are several known ways of polymerizing these heterocyclics. Thermal decomposition [26-41], nucleophile (aprotic and protonic)- and base-initiated polymerization [42-50] have all been reported. In contrast, the use of cationic initiators appeared to be unsuccessful. Crowe [48] attempted to polymerize α-ethyl-α-hydroxy butyric acid anhydrosulfite (DEAS) with boron trifluoride etherate and no polymer was produced.
For each type of ring-opening polymerization of these compounds, a small molecule (sulphur dioxide or carbon dioxide) is eliminated from the ring, so these processes, so-

called 'extrusion polymerizations', are irreversible. The over-all polymerization schemes are summarized in figure 1.6.

However, anhydrosulfites and anhydrocarboxylates differ in reactivity. Anhydrosulfites undergo spontaneous polymerization at high temperature and in the presence of nucleophiles whereas anhydrocarboxylates are thermally stable and not very susceptible to hydroxyl-initiated polymerization. This arises from their differences in structure. The sulphonyl group in the anhydrosulfite molecules, being larger than a carbonyl, is forced out of the plane of the ring, as discussed in section 3.4., imposing a ring-strain on the molecule and distorting it whereas anhydrocarboxylate rings are planar.

1.2.4.1. Thermal decomposition

The mechanism involved in the thermal decomposition starts with a contraction of the ring leading to the formation of an α-lactone with elimination of sulphur dioxide or carbon dioxide. Then, this unstable intermediate takes part in a rapid chain-propagation reaction initiated by a trace of moisture or other nucleophile and via the hydroxyl group produced by the decomposition of the α-lactone, as shown in figure 1.6.
The rate of polymerization of anhydrosulfites was found to increase with increasing ring substitution. Blackbourn and Tighe [32] reported that the rate of thermal polymerization of anhydrosulfites, derived from symmetrically substituted α-hydroxy acids, increased as C(5) substituents methyl, ethyl, n-propyl and n-butyl were successively introduced. This was so because bulky substituents increased the ring-strain of the monomer.

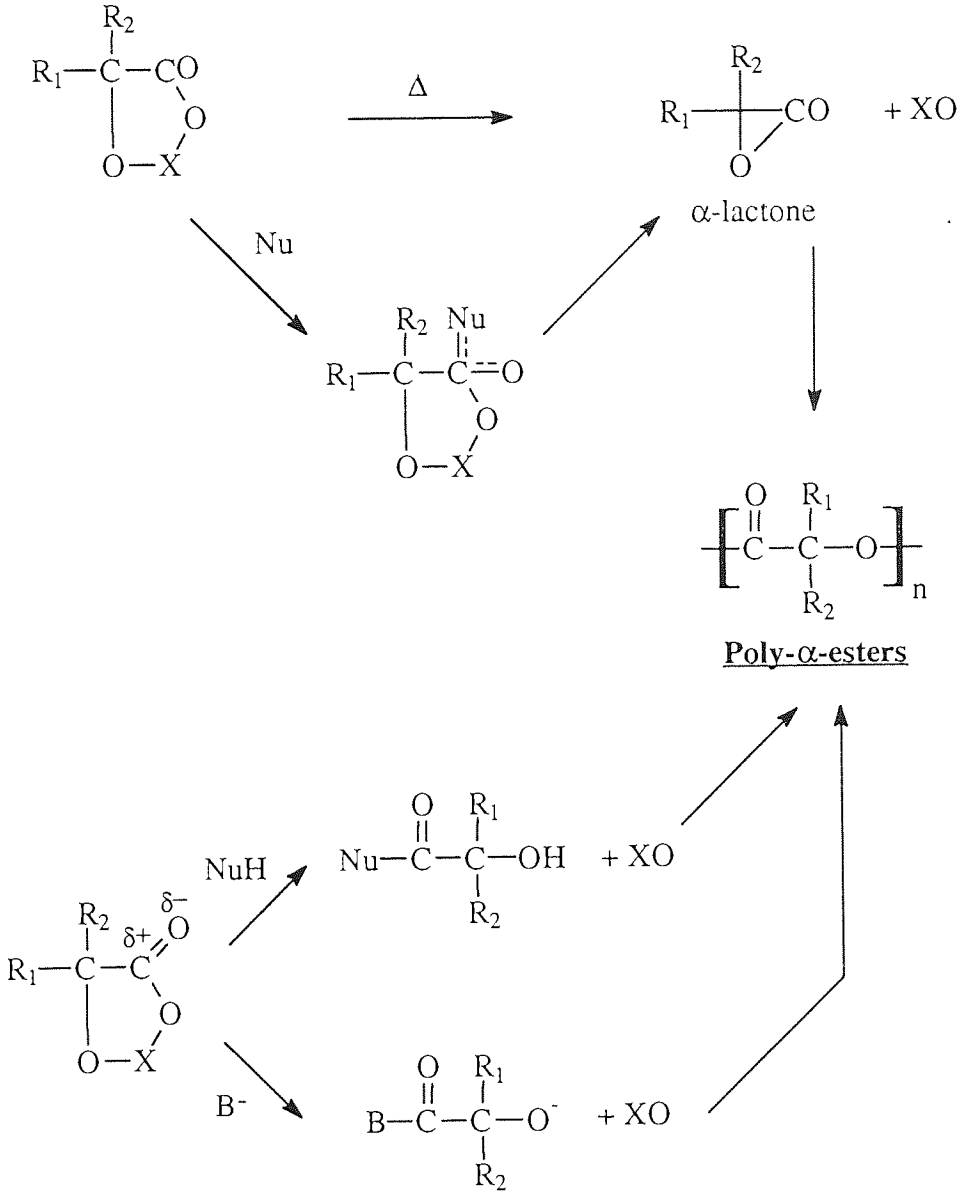

X : S = O or C = O.

Nu : aprotic nucleophile (e.g. pyridine)

NuH : protonic nucleophile (e.g. benzylalcohol)

B^- : Strong base (e.g. alkoxide).

Figure 1.6. Different routes to poly-α-esters from anhydrosulfites and anhydrocarboxylates

1.2.4.2. Protonic nucleophile-initiated polymerization

Anhydrosulfites and anhydrocarboxylates undergo similar reactions to N-carboxy-α-amino acid anhydrides (NCAs) in the presence of protonic nucleophiles e.g. primary and secondary amines and alcohols, but the polymers formed from NCAs are poly-α-amino acids [51], as shown in figure 1.7.

The mechanism consists of a direct nucleophilic attack on the carbonyl group of the ring and formation of a terminal hydroxyl group. Propagation then proceeds by further attack on the ring by the hydroxyl-end group, as shown in figure 1.6. Experimental results obtained by Tighe *et al* [29,39] indicate that protonic nucleophiles are not useful as initiators in the polymerization of these heterocyclics. Only low molecular weight polymers are produced.

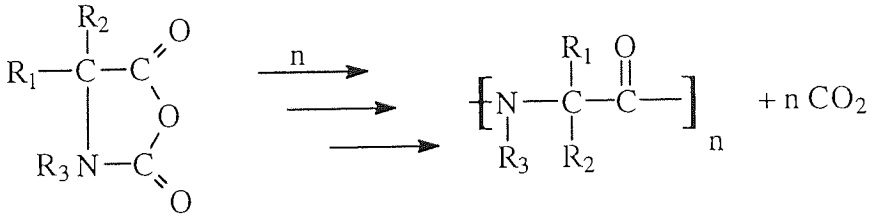

Figure 1.7. Polymerization of N-carboxy-α-amino acid anhydrides (NCAs).

The nature of the C(5) substituent in the anhydrosulfite ring was found to have a profound effect on the decomposition of anhydrosulfites with alcohol. This was attributed to the combined steric and electronic effects of the C(5) substituents which influenced the susceptibility of the C(4) carbonyl group to nucleophilic attack. In particular, the phenyl substituent had an activating influence because of its electron-withdrawing power [29].

1.2.4.3. Aprotic nucleophile-initiated polymerization

The aprotic nucleophiles e.g. triethylamine, pyridine initiate the polymerization of anhydrosulfites and anhydrocarboxylates. The mechanism involved in this polymerization is a nucleophilic attack on the carbonyl carbon of the ring producing a complex intermediate which decomposes to an α-lactone. This unstable ring is then initiated by nucleophiles present in the reaction media and repetitive attack on the heterocyclic ring yields a polymer, as shown in figure 1.6.

Adams [50] reported that lithium and potassium alkoxides, as well as butyllithium and *sec*-butyllithium were much more effective as initiators for the polymerization of L-lactic acid anhydrosulfite (L-LAAS), even though products of relatively low molecular weight were produced ($\overline{M_n}$ < 20,000). In this case, the attack of the *tert*-butoxide ion or the butyl group, on the carbonyl carbon is strong enough to cause an acyl-oxygen bond scission and, in this way, leads to the formation of an active alcoholate anion, the propagating species, as shown in figure 1.6.

The polymerization mechanism is comprised of chain initiation and chain propagation with no termination reactions. Thus, the active centres still remain after complete polymerization so that some monomer subsequently introduced in the polymerization mixture will add to the existing chains. Hence, the term 'living' polymerization is often used to describe these systems which are of great potential for the synthesis of block-copolymers.

However, experiments carried out by Adams[50] indicated that although the polymerization of lactic acid anhydrosulfite with lithium *tert*-butoxide in nitrobenzene had some degree of 'living' character, only a fraction of the propagating chain ends remained active . This probably meant that accidental termination by impurity was occurring.

1.2.4.4. Stereospecificity of ring-opening polymerization of anhydrosulfites and anhydrocarboxylates

Very little is known about the stereospecificity of the ring-opening polymerization of anhydrosulfites and anhydrocarboxylates. Inoue *et al* [45] have reported that the polymerization of racemic anhydrosulfites was asymmetrically selective when brucine, an optically-active tertiary amine, was employed as catalyst. Additionally, Kricheldorf and Jonte [52] have observed that the polymerization of D,L-lactic acid anhydrocarboxylate, using a variety of anionic initiators, behaved like most polymerizations of D,L-α-amino acid carboanhydride (NCAs) and, in particular, was stereoselective like NCAs. Thus, when a racemic mixture of L- and D-monomers was polymerized, the enantiomorphic monomers (D) were incorporated preferentially into polymer growing chains already containing D units, just as L-monomers into chains containing L units. Therefore the polymer produced was preferentially isotactic, its structure being either a mixture of isotactic L and isotactic D chains or chains formed with isotactic sequences L and isotactic sequences D.

1.2.4.5. Copolymerization of anhydrosulfites

Inoue *et al* [53] examined the possibility of the copolymerization of α-hydroxy isobutyric acid anhydrosulfite (HBAS) with vinyl compounds and found that at 80°C and in the presence of azo-bis-isobutyronitrile, the copolymerization of HBAS with styrene, vinyl chloride or methyl methacrylate led to the formation of homopolymers of the vinyl compounds only.

On the other hand, Adams [50] reported that block-copolymerizations of styrene and 1,3-butadiene with L-LAAS appeared to be possible whereas random copolymerization of L-LAAS with butadiene was unsuccessful.

1.3. Anhydrosulfites

1.3.1. Historical development of anhydrosulfite chemistry

In 1922, Blaise and Montagne [54] were the first to describe methods for the preparation of anhydrosulfites from lactic and α-hydroxy isobutyric acids by their reaction with thionyl chloride. They found that thermal decomposition of these compounds gave sulphur dioxide and the corresponding polyester.

Later, in 1953, the preparation of α-hydroxy isobutyric acid anhydrosulfite and its thermal polymerization were examined in greater details by Alderson [55] who developed improved experimental techniques for the synthesis of polyesters of high molecular weight.

Then, in 1965, Rose and Warren [56] extended the range of anhydrosulfites to other di-substituted α-hydroxy acids and also used pyridine in the thermal polymerization of these compounds.

From 1967, Ballard and Tighe [26-27] developed an alternative route to anhydrosulfites involving the anhydrous copper (II) salt of the acid, which enabled the synthesis of anhydrosulfites in good yield, and in so doing, extended the number of anhydrosulfites which might be prepared. Table 1.4. presents the range of anhydrosulfites with a variety of R_1 and R_2 which have been synthesised to date.

Table 1.4. List of anhydrosulfites.

R_1	R_2	α-hydroxy acid anhydrosulfite	References
H	H	glycolic	27, 28
H	CH_3	lactic	27, 50
CH_3	CH_3	α-hydroxyisobutyric	26
H	C_6H_5	mandelic	29, 30
C_6H_5	C_6H_5	benzilic	29, 30
CH_2Cl	CH_2Cl	α,α-(bischloromethyl)-α-hydroxyacetic	29
C_2H_5	C_2H_5	α-hydroxy-α-ethyl butanoic	31, 32, 36
n-C_3H_7	n-C_3H_7	α-hydroxy-α-n-propyl pentanoic	31, 32
n-C_4H_9	n-C_4H_9	α-hydroxy-α-n-butyl hexanoic	31, 32
- $(CH_2)_x$ - where x = 3, 4, 5, 6		α-hydroxy-cyclobutane, -pentane, -hexane, -heptane	31, 33
CH_3	C_2H_5	α-hydroxy-α-methyl butanoic	37
CH_3	n-C_3H_7	α-hydroxy-α-methyl valeric	37
CH_3	iso-C_3H_7	α-hydroxy-α-methyl isovaleric	37
CH_3	n-C_4H_9	α-hydroxy-α-methyl caproic	37
CH_3	n-C_6H_{13}	α-hydroxy-α-methyl octanoic	37
CH_3	n-C_8H_{17}	α-hydroxy-α-methyl decanoic	37
H	COOH	tartronic	43, 49
CH_3	C_6F_5	α-pentafluorophenyl-α- hydroxy propanoic	39

1.3.2. Anhydrosulfite monomers

Anhydrosulfites (1,3,2-dioxathiolan-4-one-2-oxides) are five-membered heterocyclics based upon α-hydroxy acids and containing two oxygens, one sulphonyl and one carbonyl group. They are prepared by the reaction of thionyl chloride with either the

parent acid, as shown in figure 1.8. or its corresponding copper (II) salt, for more information see section 3.1.

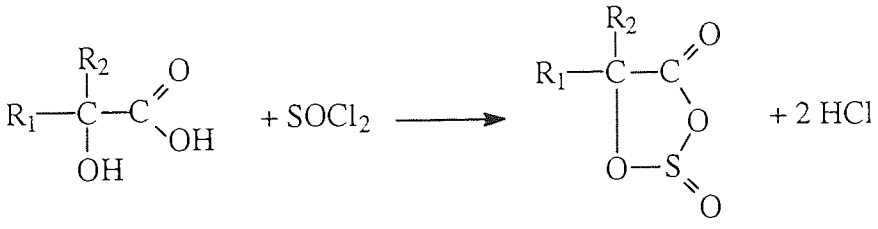

Figure 1.8. Reaction of α-hydroxy acids with thionyl chloride.

Because of the importance of monomer purity in obtaining high molecular weight polyesters, Tighe *et al* [31] developed a purification method with silver oxide for aliphatic anhydrosulfites, in order to remove the chlorine-containing impurities synthesised simultaneously with the anhydrosulfites.

On the introduction of C(5)-phenyl substituent, the anhydrosulfites become viscous oils and these compounds were found to be purified only with difficulty [30].

On the other hand, anhydrosulfites are very sensitive to water and react rapidly with it to yield the parent acid, as shown in figure 1.9.

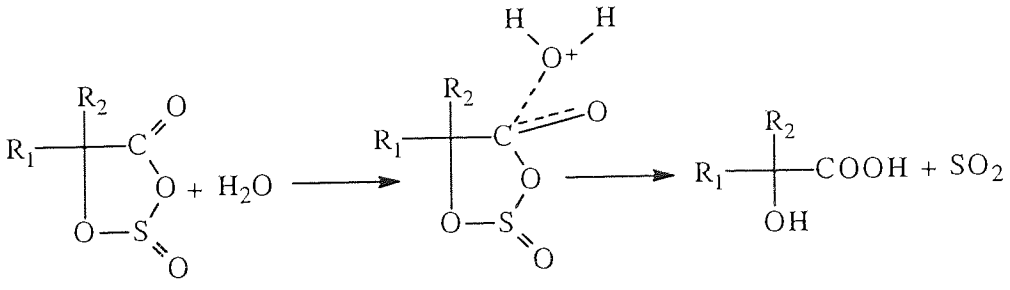

Figure 1.9. Decomposition of α-hydroxy acid anhydrosulfites to the corresponding acid when in contact with water.

1.4. Biodegradation

1.4.1. Definition

There is an absence of consensus on definitions and on reliable testing procedures, protocols and standards for biodegradation. Nevertheless, it is reasonable to say that biodegradation refers to the chemical reactions that destroy the polymer structure and this degradation of macromolecules can be triggered either by a chemical process, such as hydrolysis or oxidation, or by biological agents, such as microorganisms or released enzymes, or both. The enzymatic process is restricted to the polymer surface and occurs concurrently with bulk aqueous hydrolysis.

1.4.2. Biodegradation of poly-α-esters

At the moment, degradation of poly(α-hydroxy acids) is increasingly regarded as depending on chemical hydrolysis only, although an enzymatic contribution to in-vivo degradation is still questioned.

Indeed, polymers having hydrolyzable groups, such as esters, are more susceptible to biodegradation via hydrolysis. Their degradation proceeds in two stages. The first stage is a random hydrolytic scission of ester linkages, the ester bond being cleaved by reaction with one molecule of water to form acid and alcohol end groups, as shown in figure 1.10. The resulting decrease in the molecular weight produces some changes in mechanical properties and morphology, but no weight loss [57]. The second stage involves measurable weight loss in addition to chain cleavage.

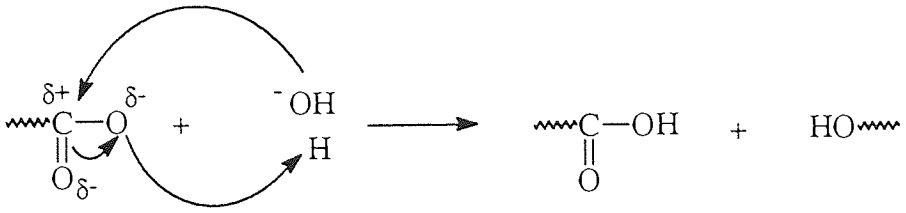

Figure 1.10. Hydrolytic degradation of polyesters.

1.4.3. Factors affecting polymer degradation

The biodegradability of a synthetic polymer may be affected by different factors, (i) its chemical structure involving steric and electronic effects in the chain, and also its hydrophilic-hydrophobic character, (ii) its morphology (crystallinity and tacticity), and also (iii) its physical properties (glass transition temperature Tg) as well as (iv) its molecular weight.

1.4.3.1. Chemical structure

Changing the chemical structure of polyesters may be used to control the rate of hydrolysis. The increased hydrophobicity of polylactic acid relative to polyglycolic acid together with the steric effect of the methyl side chain is enough to reduce the rate of degradation dramatically, see table 1.1.

Since polyesters are degraded by hydrolysis, the hydrophobic-hydrophilic character influences the degradation greatly. In a hydrophobic polymer, the degradation is limited to the surface of the materials whereas in a hydrophilic polymer, water is present in the bulk of the material by virtue of its swelling and degradation may occur throughout the bulk of the material.

1.4.3.2. Morphology

The crystalline phase of polymers is a regular close-packing of chains which is inaccessible to water. As a result, its hydrolytic degradation is not favoured and a reduction in crystallinity would yield an increase in the rate of hydrolysis. In a semi-crystalline polymer, the amorphous regions are degraded prior to the crystalline regions and because hydrolytic chain cleavage occurs randomly in the amorphous phase of the polymer, the degree of crystallinity of the polymer is an important factor in the determination of its biodegradability.

Chain symmetry and flexibility both affect the crystallinity of a polymer. If a chain possesses large pendant groups, these will increase the rigidity but also increase the difficulty of close-packing to form a crystalline array. In addition, chains containing irregular units, which detract from the linear geometry, reduce the ability of a polymer to crystallize. Thus, the presence of a chiral center in the main chain is also essential in regard to the morphology of a material. Vert *et al* [58,59] have exemplified the effects of configurational structure on physical, mechanical and biological properties and consequently on the degradation rate in the case of a series of lactic acid stereocopolymers.

1.4.3.3. Physical properties

Because water and perhaps enzymes are involved in biodegradation, polymer flexibility can play a significant role. The more flexible the polymer chain, the greater the potential for interacting with water and the active sites of the enzyme. Consequently, the glass transition temperature Tg of a material is important in regard to its degradability, a reduction of Tg resulting in an increase of chain mobility and a reduction of the energy required to achieve the transition state. In particular, by copolymerization, the glass transition temperatures Tg can be varied. The Tg of copolymers of lactide and ε-caprolactone was found to increase in proportion to the lactide content and this affected directly the biodegradability of the material [1].

1.4.3.4. Molecular weight

Molecular weight of polymers has a significant effect on their biodegradability. The higher the starting molecular weight, the faster the degradation. Bendix *et al* [60] reported that in 10 weeks, when implanted in a rat, poly(L-lactide) with a high molecular weight could lose 70 % of its initial molecular weight compared to 40 % for a lower molecular weight sample. Nevertheless, differences in biodegradation of polymer samples of different molecular weight can also be attributed to crystallinity.

1.5. Biocompatibility

Biocompatibility is concerned with the interactions between foreign materials and living tissue. The original definition of a biocompatible material as one that is inert toward the physiological environment has been modified to include materials having minimal interaction with the environment [61].

When a polymer is implanted into soft tissue, an interface is created between the polymer surface and the tissue fluid that contains various surface active macromolecules such as proteins. The interface depends very much on the adsorption of these proteins which occurs very soon after contact. In this way, the polymer surface is modified and the interfacial free energy is lowered. But, the desorption of the adsorbed species can take place depending on the nature of the polymer. The major adsorbed species are likely to be plasma proteins, and their adsorption onto hydrophobic surfaces is largely irreversible[62].

Thus, if a polymer is to be used in the human body, it is preferable if this material is hydrophobic because it would induce minimal responses in soft tissue.

1.6. Scope and object of the present work

Poly(α-hydroxy acids), in particular polylactic acid- and their copolymers, represent an important class of synthetic biodegradable polymers. However, there are not many ways to synthesise them.

On one hand, direct polycondensation of α-hydroxy acid does not yield polymers with useful properties and ring-opening polymerization of lactide is most frequently initiated with toxic heavy-metal compounds which have to be removed if polymers are to be used for medical applications. In addition, the polymers obtained from D,L-lactide cannot be totally atactic, with randomly distributed D- and L-units, which usually undergo higher rate of degradation.

On the other hand, these methods do not offer much control over the molecular weight and the molecular weight distribution of the polymers. Therefore, a route to polylactic acid which provides control over characteristics such as molecular weight, molecular weight distribution and configuration will be of considerable interest.

Polyesters have been successful in delivery of conventional pharmaceuticals. But some limitations on their use appeared for protein delivery because of their incompatibility with some of these macromolecules [1]. Therefore, introducing a hydrophobic alkyl group in the polyester might be an alternative to this problem.

In any case, polyesters with aromatic rings or hydrophobic alkyl as side groups can be expected to give interesting results in their degradation process and the need for expanding the spectrum of available degradable polyesters is evident. Thereby, it was our interest to develop a novel series of biodegradable and biocompatible poly-α-esters via anhydrosulfites with a variety of substituents such as phenyl, isopropyl, n-butyl or isobutyl.

In this present work, we report the synthesis of a range of anhydrosulfites with their structure determination by NMR spectroscopy and their general properties, followed by their anionic homopolymerization and copolymerization with ε-caprolactone. The polyesters and copolyesters synthesised were characterized with respect to structure (^{1}H and ^{13}C NMR spectroscopy) and molecular weight (gel permeation chromatography).

CHAPTER 2

EXPERIMENTAL TECHNIQUES

2.1. Purification of materials

2.1.1. α-Hydroxy acids

2.1.1.1. Lactic acid

L- and DL- lactic acid (2-hydroxypropionic acid) were both supplied by Aldrich Co. as 85 % w/v solutions in water which contained varying amounts of intermolecular esterification products. Indeed, pure lactic acid cannot be obtained because any removal of water leads to a formation of lactides [63].

2.1.1.2. DL-2-hydroxy isovaleric acid

DL-2-hydroxy isovaleric acid (2-hydroxy-3-methyl butyric acid) of 99% purity was also purchased from Aldrich Co. as a solid.

2.1.1.3. DL-2-hydroxy caproic acid

DL-2-hydroxy caproic acid (2-hydroxy hexanoic acid) was obtained from Sigma Co. as a white powder with a purity of 95-98 %.

2.1.1.4. L-2-hydroxy isocaproic acid

L-2-hydroxy isocaproic acid (L-2-hydroxy-4-methyl pentanoic acid) of 99 % purity was supplied by Sigma Co. as a solid.

2.1.1.5. Mandelic and benzilic acids

Mandelic and benzilic acids of 99 % purity were purchased from Aldrich Co. and were used as supplied.

2.1.2. Solvents

2.1.1.1. Tetrahydrofuran

Tetrahydrofuran was used as solvent in many operations, either as eluent in gel permeation chromatography and high performance liquid chromatography or as solvent in the purification and polymerization of anhydrosulfites.

Hplc grade THF was utilized as eluent in the chromatographic techniques and was supplied by Fisons Chemicals Co., without further purification. Solutions of polymers samples or impure anhydrosulfites were prepared in this solvent and used for analysis.

On the other hand, a dried distilled grade tetrahydrofuran was purchased from Fisons Chemicals Co. and used as solvent in the purification of anhydrosulfites (for purification of both aliphatic and aromatic anhydrosulfites). Its water content was below 0.01 %.

When used as solvent in the polymerization of anhydrosulfites, dried distilled grade THF was further dried by standing over sodium wire and then by refluxing over sodium and benzophenone until the mixture developed the deep purple colour of sodium benzophenone ketyl. THF was finally distilled on the vac-line prior to use from this drying agent as required.

2.1.2.2. Toluene

Toluene was dried successively over calcium hydride, phosphorus pentoxide and then fractionally distilled under argon. The distillation apparatus is shown in figure 2.1.

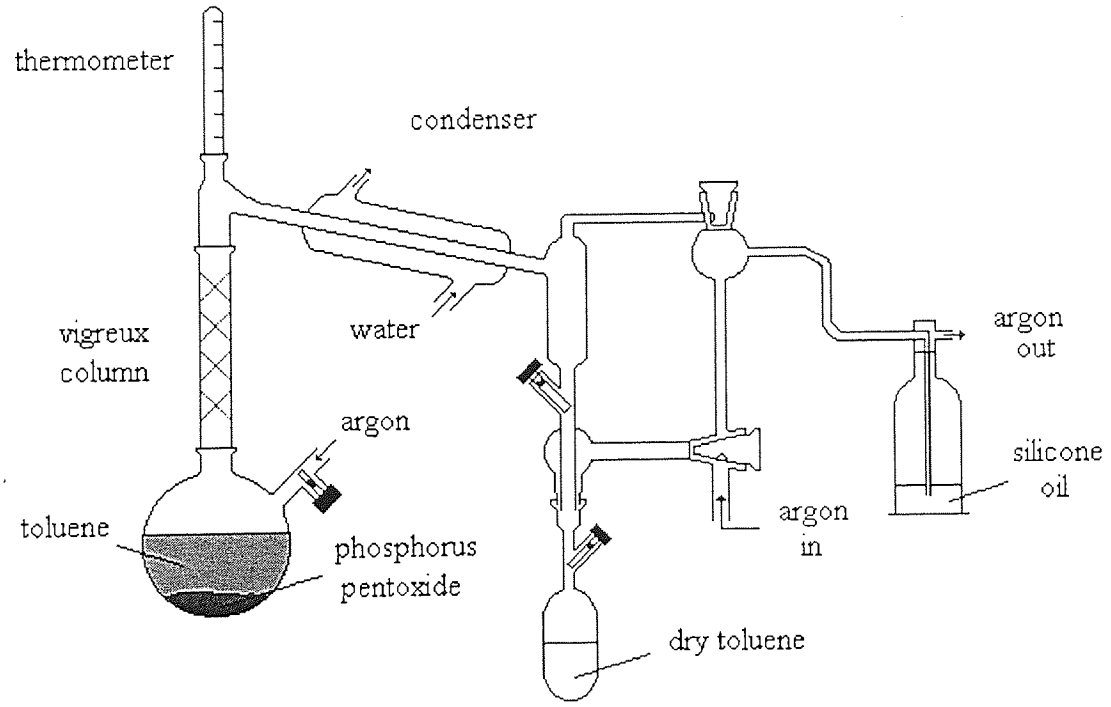

Figure 2.1. Apparatus for distillation under argon atmosphere.

2.1.2.3. Diethyl ether

Primar grade diethyl ether, obtained from Fisons Chemicals Co. and containing less than 0.01 % water (Karl Fischer), was stored over sodium wire and used as solvent in the synthesis of anhydrosulfites without distillation.

2.1.2.4. Dichloromethane

Dichloromethane (high purity grade) was obtained from Fisons Chemicals Co. and placed over calcium hydride for 72 hours. It was then fractionally distilled under an inert atmosphere of argon. The distillation apparatus used was similar to that shown in figure 2.1. Before starting the distillation the system was purged with argon and refluxed for 2 hours.

2.1.2.5. Other solvents

Acetone and methanol were used as supplied by Fisons Chemicals Co.

2.1.3. Drying agents

2.1.3.1. Sodium metal

Sodium metal was supplied in paraffin oil by BDH. The oil was removed by washing with hexane and tarnished surfaces cut away before use.

2.1.3.2. Benzophenone

Benzophenone was supplied by Janssen Chemica, and used without further purification.

2.1.3.3. Phosphorus pentoxide

Phosphorus pentoxide was used as supplied by Fisons Chemicals Co.

2.1.3.4. Calcium hydride

Calcium hydride was supplied by Aldrich Co. A 40 mesh powder was found to be the most efficient for drying dichloromethane.

2.1.4. Initiators

2.1.4.1. Butyllithium and *sec*-butyllithium

Butyllithium and *sec*-Butyllithium were obtained from Aldrich Co. as 1.6 M and 1.3 M cyclohexane solutions, in bottles fitted with a 'sure seal' top. This enabled the connection of the bottle to an argon line, whilst a sample of the solution was taken by syringe and so contamination of the catalyst was prevented. The solutions were stored in the refrigerator under a slight argon pressure to reduce decomposition.

2.1.4.2. *tert*-Butyllithium

tert-Butyllithium was supplied by Aldrich Co. as a 1.7 M pentane solution. This was treated as described for butyllithium and *sec*- butyllithium to prevent contamination and decomposition.

2.1.4.3. Potassium *tert*-butoxide

Potassium *tert*-butoxide was obtained from Aldrich Co. as a solid. This was directly transferred to the dry box where solutions in THF were prepared.

2.1.4.4. Lithium diisopropylamide

Lithium diisopropylamide was supplied by Aldrich Co. as a powder. This was transferred directly to the dry box where the initiator solutions were prepared.

2.1.4.5. Trifluoromethanesulfonic acid

Triflic acid (trifluoromethane sulphonic acid) was obtained from Aldrich Co. in a 10g ampoule. Very hygroscopic, it gives toxic fumes with moisture. A solution in dry dichloromethane was kept in a storage flask in the dry box.

2.2. Techniques for synthesising and handling air-sensitive compounds

In general, work with air-sensitive compounds requires a good over-all plan, because the experiment is frequently less flexible than laboratory operations which are performed in the presence of air.

One approach to the handling of air-sensitive compounds involves manipulations in a previously evacuated system, vacuum-line techniques. This technique was utilized only for the distillation and storage of solvents like THF.
A second method involves manipulation in an inert gas to exclude air, sometimes in a dry box or a glove bag. The storage of dry solvents and reactive initiators, as well as, the preparation of catalyst systems were carried out in a dry box whereas all the other operations, involved in the synthesis and purification of anhydrosulfites, were performed in an atmosbag.

2.2.1. Vacuum line

The high vacuum line (figure 2.2.) consisted of a manifold and four greaseless taps where distillation could be carried out. The manifold was evacuated using an Edwards rotary pump and a mercury diffusion pump, thereby achieving a pressure as low as 10^{-5} mm/Hg in the best cases. This pressure could be checked approximatively by the MacLeod Gauge. To condense any vapour coming from the manifold or diffusion pump two liquid nitrogen traps were used.

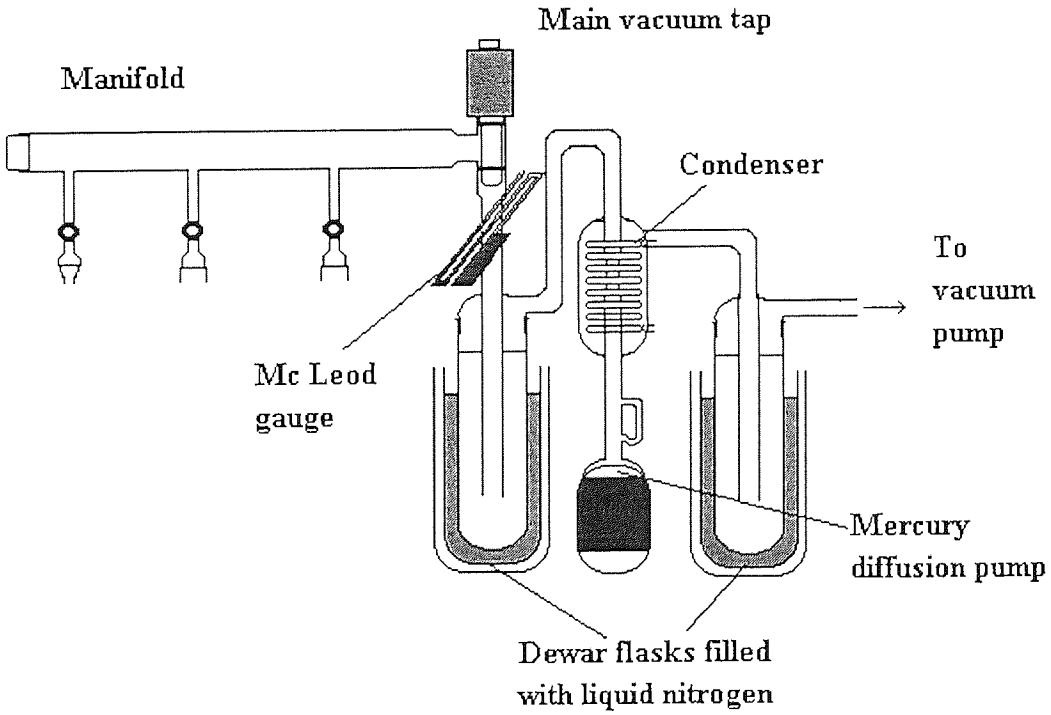

Figure 2.2. Diagram of the high vacuum-line.

2.2.1.1. Freeze-thaw degassing of solvents

The degassing of the liquids prior to their distillation was carried out by attaching the solvent flask to the vacuum line with the main tap closed. A Dewar vessel filled with liquid nitrogen was placed around the flask. When frozen, the appropriate taps were

opened and the system evacuated. After a while, the main tap was closed and the solvent allowed to thaw. This procedure was repeated until no gas bubbles escaped from the liquid on warming to room temperature.

2.2.1.2. Trap to trap distillation

The degassed solvent or monomer could be transferred to another flask using the high vacuum line. An empty receiver flask, which had been dried in an oven at 240°C was attached to the vacuum line, evacuated, and allowed to cool. This was then immersed in liquid nitrogen. By closing the main tap and opening the appropriate taps the liquid could be distilled from the solvent or monomer flask into the second flask.

2.2.2. Inert-atmosphere glove box

The inert-atmosphere glove box provides a straightforward means of handling air- and moisture-sensitive products. In its simple form, it consists of a gas-tight box fitted with a window, a pair of gloves, and a gastight door or transfert port. The entire box is flushed with an inert gas, after which compounds may be manipulated in the inert atmosphere. The glove bag is a simple, portable and convenient variant of the dry box.

2.2.2.1. Glove bag

The Atmosbag ®, as described in figure 2.3., was used in the synthesis and purification of anhydrosulfites because of their high sensitivities to water. The 'Atmosbag' consists of a large polyethylene bag fitted with different inlets, two of them were used, one for the argon flush and one for connection with a vacuum pump, and also an open end which may be closed by rolling and clamping. The bag is purged by several cycles of filling with inert gas and collapsing.

In this technique, great care was necessary to maintain a water- and oxygen-free atmosphere.

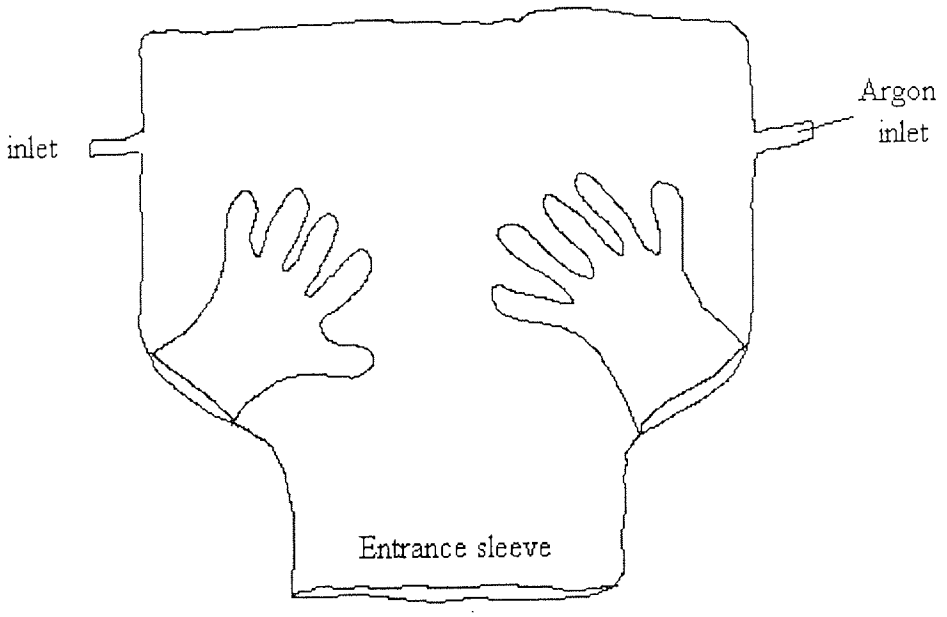

Figure 2.3. Polyethylene glove bag.

2.2.2.2. Dry box

The dry box was obtained from Halco engineering and was used to store and manipulate the different initiators and solvents.

The working atmosphere within the glovebox, argon, was continuously recirculated through columns of chemical adsorbent to remove unwanted components particularly water and oxygen from the gas phase. Typically BASF R311 catalyst and 3 Å molecular sieve were employed to remove oxygen and water to below 2 ppm and 10 ppm negative systems and 1 ppm and 5 ppm positive systems respectively.

For component entry, a fully evacuable double door posting port was used. To prevent impairment of the working atmosphere once items were placed in the port and the outer door sealed, the atmosphere was purged to create a complimentary parts per million level of oxygen and water and then filled with argon before opening the inner door.

2.3. Analytical techniques

2.3.1. Chloride titration

Assessment of the quantities of chlorine-containing impurities present in the monomers was made by the modification of Ingram's technique [64]. This method determines the level of chloride impurities, the predominant impurity in the monomer synthesis being known to be an α-chloro acid chloride.

An accurately weighed sample of anhydrosulfite (ca. 0.1 g) was added to an excess of water-acetone mixture (3:1) and a few drops of 1N-nitric acid. The solution was heated, cooled and titrated potentiometrically against 0.01 N silver nitrate. The instrument used was a Corning pH meter model 220 equipped with a coaxial electrode filled with gel and a solution of KCl (Russel).

2.3.2. High Performance Liquid Chromatography (HPLC)

This chromatographic technique uses solvent under pressure to elute components of a sample. HPLC grade THF was used without further preparation.

The equipment

The chromatograph is shown in block diagram form in figure 2.4. Samples for analysis were introduced through a multiport valve which permitted precise, repeatable sample loading with minimal disturbance of solvent flow. A solvent delivery system (the star 9010 from Varian) was connected to a column placed in a column heater (Jones Chromatography) to control of the temperature. The column was a stainless steel tube packed with a silica-based reverse phase consisting of extremely fine, regularly sized, spherical particles (5 μm in diameter). In reverse phase chromatography a highly polar solvent system is used for elution (THF). Under such conditions polar compounds prefer

to stay in the mobile phase and are eluted before nonpolar materials which have a greater affinity for the stationary phase.

A UV diode array (Polychrom 9065-Varian) detector was used for the detection of the eluted components in the samples. The detector was a computer controlled instrument comprising software for complete spectral and chromatographic peak processing. The polyview spectral processing application provided post-run analysis of data from the diode array detector. It enabled a spectrum to be taken at any time during the running of the chromatogram, or to generate an absorbance chromatogram at any wavelength within the wavelength range (190-367 nm).

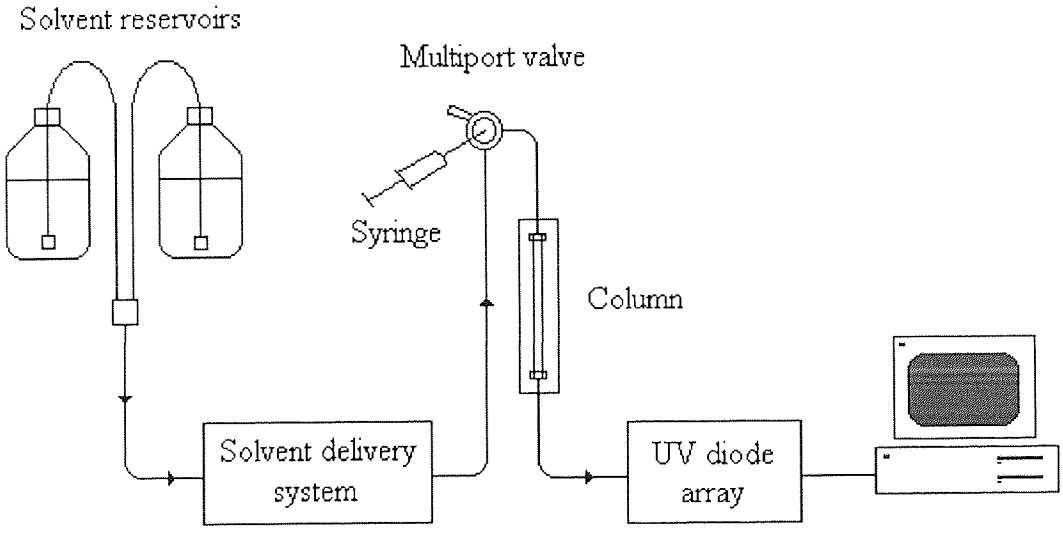

Figure 2.4. The High Performance Liquid Chromatography (HPLC)

2.3.3. Infrared Spectroscopy

Infrared spectra were determined with a Perkin Elmer Model Paragon 1000 Infrared Fourier Transform Spectrometer over the range 4000-400 cm^{-1}. This computer controlled instrument, including Grams Analyst 1000 software enabled a complete analysis of infrared spectra.

Solid samples were studied as KBr disc whereas liquid samples were handled in a cell with KBr windows.

2.3.4. Nuclear Magnetic Resonance Spectroscopy

All NMR spectra were obtained from a Bruker 300 MHz FT-NMR Spectrometer using the P.E.N.D.A.N.T. [65,66] technique (Polarization Enhancement Nurtured During Analysis Nucleide Technique). This technique is applicable to any insensitive nucleus (coupled to sensitive nuclei). In particular, ^{13}C were coupled to ^{1}H. Thereby, PENDANT enables to obtain ^{13}C NMR spectra that show alternating phases of isolated (quarternary), CH, CH_2 and CH_3 carbon resonances but it also permits the simultaneous detection of all of these resonances. ^{13}C NMR spectra were obtained in a J-Modulated form with CH_3 and CH carbons appearing as positive peaks and CH_2 and C appearing as negative peaks.

^{1}H and ^{13}C chemical shifts were reported in ppm with tetramethylsilane as the internal reference. Solid samples were dissolved in deuterated chloroform ($CDCl_3$), thereby in the ^{13}C spectra, the three characteristical peaks centred at 77.00 ppm could be seen whereas in the ^{1}H spectra, water in the solvent might appear as a single signal at 2.15 ppm and residual protons as a single signal at 7.24 ppm.

Both ^{1}H and ^{13}C NMR spectra were integrated and edited on a PC computer using WinNMR software from Bruker.

2.3.5. Gel Permeation Chromatography

Gel Permeation Chromatography (G.P.C.) is one of the most important techniques for the determination of the molecular weights of polymers and their distribution. Its aim is to separate a sample of a polymer into its component fractions according to their sizes. The column is filled with a cross linked polymer which forms a gel in the presence of the solvent (THF). The gel contains pores of different-sized diameters, then small molecules may penetrate a greater fraction of the pores, consequently larger polymer molecules will

elute from the column first, followed progressively by molecules of lower molecular weights.

A differential refractometer continously monitors the refractive index (R.I.) of the eluting solution and compares it with that of the pure solvent. Differences in refractive index between solution and solvent cause a deflection on the chart recorder.

Once calibrated by samples of known molecular weights, the interpretation of chromatograms can be carried out.

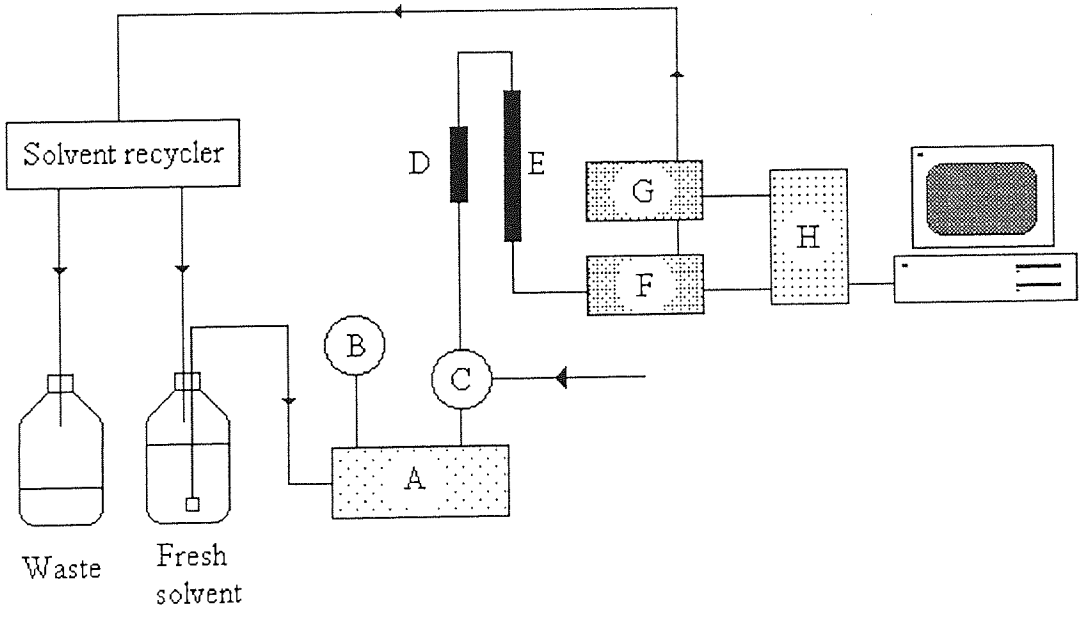

A- HPLC pump
B- Pressure gauge
C- Loop injector
D- Guard column
E- Gel column
F- RI detector
G- UV detector
H- DCU

Figure 2.5. The Gel Permeation chromatography.

The equipment

The eluent THF was delivered at 1 ml per minute by a Knauer high performance liquid chromatography pump. Samples of polymer, made up in THF (1-2 % w/v), were introduced into the column using a 100 ml valve and loop injector system. The solution

passed first through a short guard column designed to filter the solution and then prevent blockages in the rest of the system, before entering then the main column set, supplied by Polymer Laboratories. A differential refractometer monitors continously the refractive index of the eluted solution and compares it with the refractive index of the eluent. Any difference owing to the presence of any polymer in the eluent generates a deflection which is proportional to the concentration of the eluting polymer at that time.

The output of this detector was recorded by a data collecting unit (DCU), which is monitored by a PC computer running the software PL Caliber (from Polymer Laboratories).

Calibration of the column

The GPC column is calibrated with a series of narrow standards, each of which has a known Mp the peak maximum of the raw data chromatogram. A series of narrow dispersity polymers from the same homologous series (polystyrene) are dissolved in the eluent (THF) and injected on the column set. The elution volumes are recorded for each of the peaks and then a plot of Log (Molecular Weight) versus elution volume is constructed as shown below (figure 2.6.). Assuming that the known molecular weight of the polymer standards are precise, it is now feasible to derive a function of the form Log(M) = f (V) such that the molecular weight corresponding to any elution volume can be deduced.

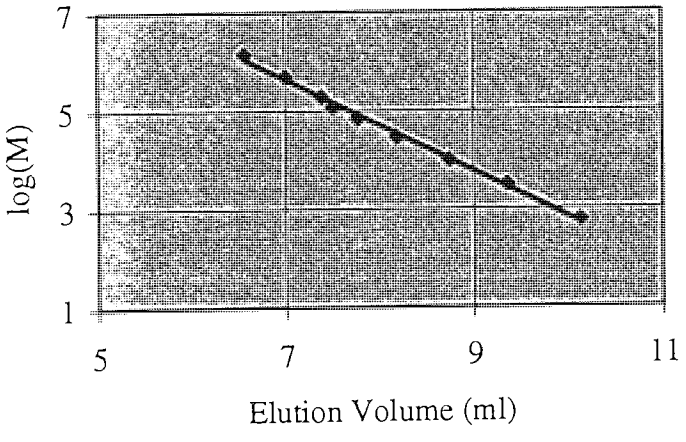

Figure 2.6. GPC calibration curve (Polystyrene).

GPC calculation

The average molecular weights calculated may be defined as follows :

$$\overline{M_n} = \frac{\sum N_i M_i}{\sum N_i} \qquad (1)$$

$$\overline{M_w} = \frac{\sum N_i M_i^2}{\sum N_i M_i} \qquad (2)$$

$\overline{M_n}$: number average molecular weight

$\overline{M_w}$: weight average molecular weight

N_i : number of molecules of molecular weight M_i

M_i : molecular weight of a given molecule

If W_i is the weight of molecular weight M_i in a given fraction then

$$N_i = \frac{W_i}{M_i}$$

Therefore,

$$\overline{M_n} = \frac{\sum W_i}{\sum W_i / M_i} \quad \text{and} \quad \overline{M_w} = \frac{\sum W_i M_i}{\sum M_i}$$

Since the refractive index response is a measure of the concentration of the polymer of molecular weight M_i at a given height h_i, hence,

$$\overline{M_n} = \frac{\sum h_i}{\sum h_i / M_i} \qquad (3)$$

$$\overline{M_w} = \frac{\sum h_i M_i}{\sum h_i} \qquad (4)$$

Some samples insoluble in THF were also processed by RAPRA Technology using a Gel Permeation Chromatograph. A solution of each sample was prepared by adding 10 ml of chloroform stabilised with ethanol to 20 mg of sample. A small amount of 1,2 dichlorobenzene was also added as an internal marker for flow-rate correction purposes. Each solution was run in duplicate.

The GPC system used was calibrated with polystyrene and all of the results, referring to the soluble material within each sample, are expressed as the 'polystyrene equivalent' molecular masses. In view of the difference in chemical type between the samples and the calibrants, it follows that there could be a considerable difference between these polystyrene equivalents and the actual molecular masses of the samples.

2.3.6. Differential Scanning Calorimetry (D.S.C.)

Polymer samples were characterized by Differential Scanning Calorimetry (D.S.C.) using a Polymer Laboratories Thermal Sciences PL-DSC instrument. A temperature programme was followed whereby samples were heated from -100 to 200°C under an nitrogen atmosphere.

Differential Scanning Calorimetry is a useful technique for identifying the thermal transitions of a polymer e.g. melting points and glass transition temperature. In this technique, a sample is sealed in a small aluminium pan and placed in a heating block. A reference sample (either alumina or an empty pan) is placed in a separate block. Both the sample and reference are heated and their temperatures measured by thermocouples so that the heat input to the sample may be adjusted so that the temperatures of each block are always identical. In this way, both endothermic and exothermic transitions may be identified and the area under the peaks will be proportional to the change in enthalpy occurring.

CHAPTER 3

MONOMER SYNTHESIS

3.1. Synthetic route to anhydrosulfites

Two methods for the preparation of α-hydroxy acid anhydrosulfites have been established : both involved the action of thionyl chloride, in the one case on the free α-hydroxy acid and in the other on the anhydrous copper (II) salt of the acid. The latter route was chosen as the method of synthesis in these studies because it was reported that more satisfactory results, in terms of purity and yield were obtained . As prepared by this method, the anhydrosulfites were impure and therefore were distilled and treated with a metal oxide in order to achieve a level of purity sufficient for successful polymerization. Thus, a general procedure, described below in figure 3.1. was used to prepare a range of anhydrosulfites ready for polymerization.

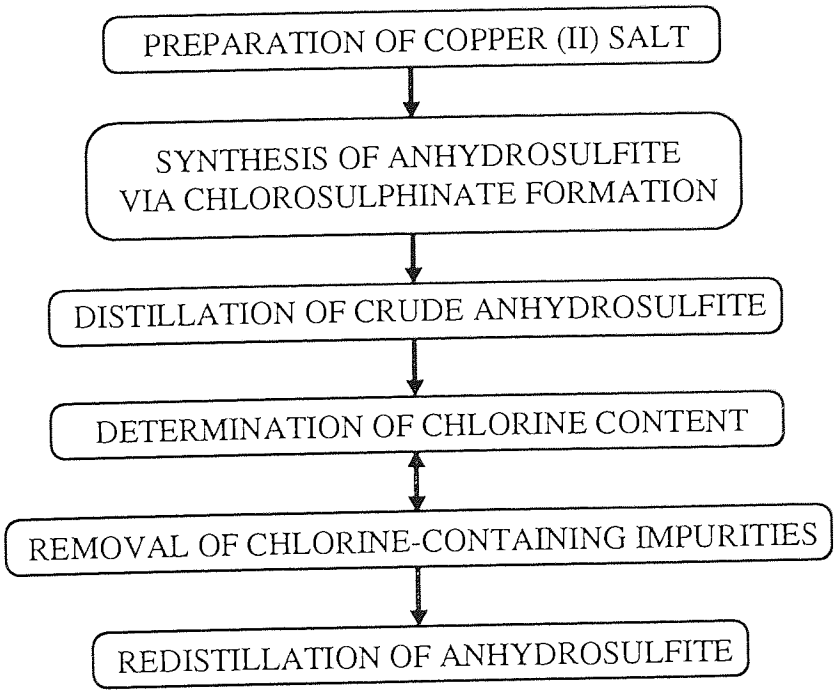

Figure 3.1. Schematic diagram of anhydrosulfites synthesis

3.1.1. Preparation of copper (II) salt

3.1.1.1. Experimental

The preparative scheme of the formation of copper (II) salt is presented in figure 3.2. α-Hydroxy acid (2 moles) dissolved in water was neutralised with ammonia solution and then heated to boiling. Cupric chloride (1 mole) was dissolved in a minimum quantity of methanol [50] and slowly added to the solution of the ammonium salt. The mixture was then cooled in an ice bath to obtain a precipitate of fine crystals which were isolated by filtration. The product was a green or blue solid containing large quantities of water which was then completely removed under vacuum at 80°C for 48 hours.

Prior to use, the copper salt prepared was further dried at 80°C for 20 hours in a vacuum oven, then released to atmospheric pressure by admitting dry argon.

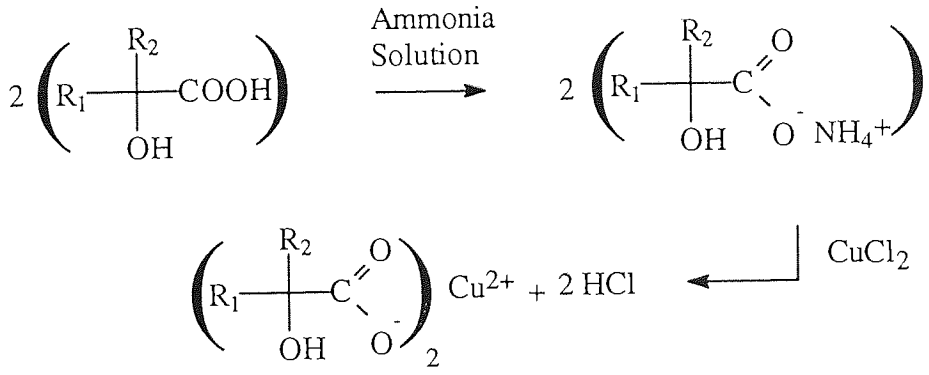

Figure 3.2. Formation of copper (II) salt from the corresponding hydroxy acid.

3.1.1.2. Discussion

For successful synthesis of anhydrosulfites, the reaction of thionyl chloride must first take place at the carboxylate group. The formation of an ammonium salt is a means of favouring the reaction of the hydroxy acid with the copper (II) chloride and by producing

the copper (II) salt the attack of thionyl chloride will take place preferentially on the negatively charged oxygen atom of the carboxylate anion rather than on the α-hydroxyl group which is co-ordinated to the central copper ion, thereby reducing electron density at the oxygen atom, as shown in figure 3.3. The complexation can be confirmed by the infrared data, the free hydroxyl stretching absorption in the region of 3400 cm^{-1} observed with the acid is displaced and changed in shape in the spectrum of the copper (II) salt, as shown in figures 3.4. and 3.5.

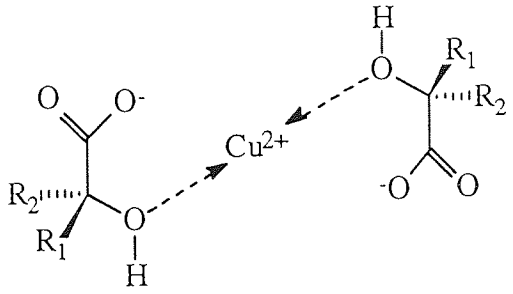

Figure 3.3. Structure of the copper(II) salts of α-hydroxy acids.

The formation of the copper salt may be followed by infrared analysis. The FT-IR spectra of hydroxy acids show carboxylic carbonyl peaks at 1705-1720 cm^{-1} whereas the FT-IR spectra of the copper salts show carboxylate carbonyl peaks at 1570-1650 cm^{-1}. Figures 3.4. and 3.5. show the spectra for lactic acid and its copper (II) salt.

Use of other metal salts, like lithium and sodium has been attempted and has not shown any great advantage over the use of copper salt [67].

The yields of the different copper (II) salts prepared were between 80-90%, except for copper (II) lactate, for which the yield was only 50% because of the presence of varying amounts of intermolecular esterification products in lactic acid, an 85% solution in water. Pure free lactic acid is difficult to obtain and removal of water causes the formation of lactides which can not be separated from lactic acid [63]. However, the route via the copper salt permits the removal of the undesirable lactides at the initial stage.

Figure 3.4. FT-IR spectrum of lactic acid.

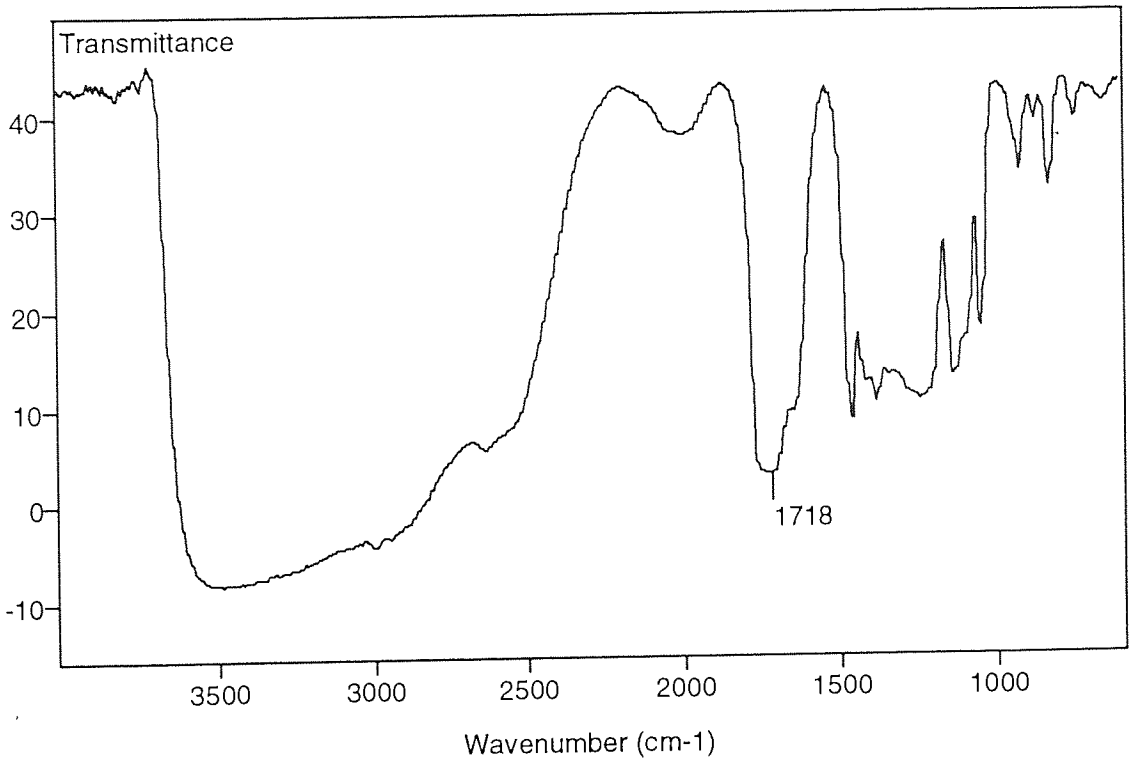

Figure 3.5. FT-IR spectrum of the copper (II) salt of lactic acid.

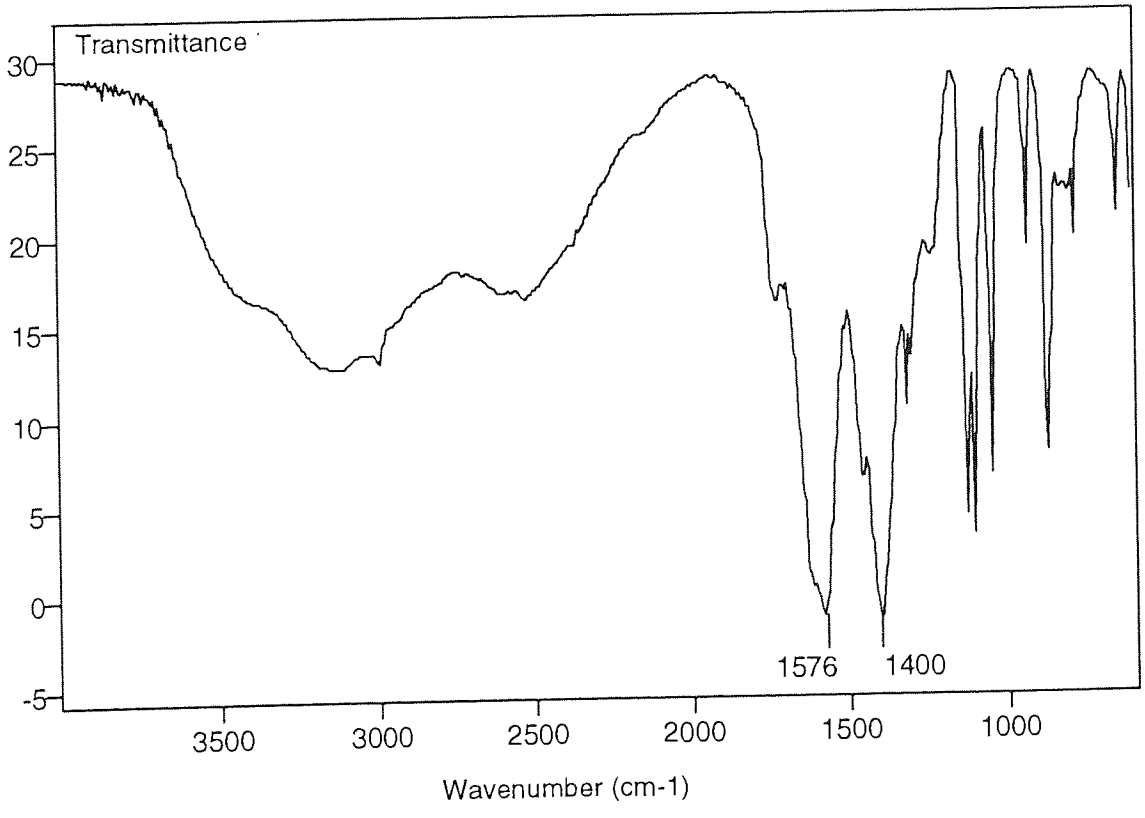

3.1.2. Synthesis of anhydrosulfites

3.1.2.1. Experimental

The preparation of the anhydrosulfite was carried out in an 'atmosbag' filled with argon using glassware that dried at 240°C. These precautions were taken because anhydrosulfites are very sensitive to water, which decomposes them very quickly to the corresponding acid.

The dry anhydrous copper salt (0.5 mole) prepared as described in section 3.1.1.1. was slurried in dry ether (300 ml) and thionyl chloride (supplied by Aldrich Co.) was added dropwise in excess (2 moles) at low temperature. The preferred reaction temperature ranged from -20°C to 0°C depending on the α-hydroxy acid anhydrosulfite prepared. The reaction vessel was maintained at this temperature for the duration of the reaction especially when the exothermic conversion of copper (II) salt to hydroxy acid chlorosulphinate occurred. The mixture was stirred for 20-30 minutes. A change in the colour of the precipitate was observed from blue-green to a dark reddish-brown. The precipitate of copper chloride obtained was filtered off but a small amount of fine copper salt passed through a grade 4 porosity sintered glass Buchner funnel. The filtrate was left for 1 hour under reduced pressure at room temperature. Ether and final traces of thionyl chloride were evaporated off.

3.1.2.2. Discussion

Thionyl chloride can react with the α-hydroxyl group or on the negatively charged oxygen atom of the carboxylate anion to form respectively an alkyl chlorosulphinate (A) or an acyl chlorosulphinate (B), as shown in figure 3.6. The acyl chlorosulphinate is thought to be more stable than the alkyl form and therefore less likely to eliminate sulphur dioxide.

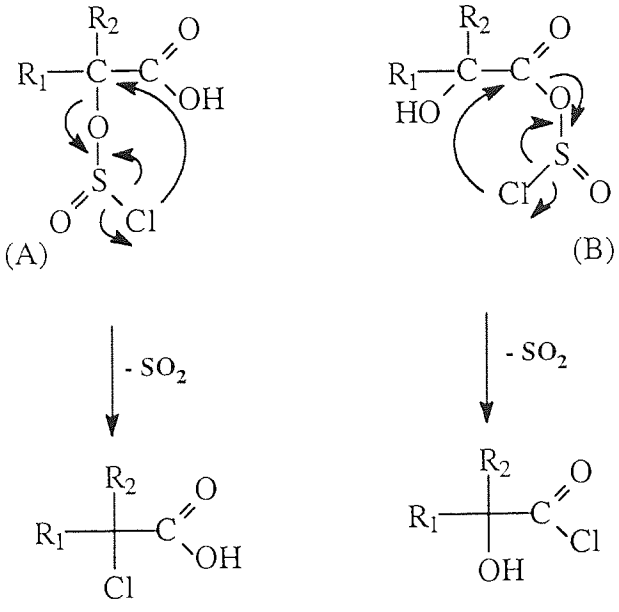

Figure 3.6. Elimination of sulphur dioxide from chlorosulphinate.

Once formed the chlorosulphinates can react further by three different routes:

(i) ring closure via intramolecular elimination of hydrogen chloride to form an α-hydroxy carboxylic acid anhydrosulfite.

(ii) S_Ni type reaction with elimination of sulphur dioxide to form an α-chloro acid or an α-hydroxy acid chloride.

or (iii) further attack of thionyl chloride on the α-chloro acid or on the α-hydroxy acid chloride to produce an α-chloro acid chloride.

These different routes are presented in figure 3.7. and the proportions of the different species present in the final product of the reaction vary depending on the substituents on the C(2) carbon atom of the hydroxy acid. Nevertheless, the α-chloro acid chloride was found as the main impurity, the α-chloro acid and the α-hydroxy acid chloride being less stable, especially in the presence of an excess of thionyl chloride.

Small amounts of thionyl chloride were found to produce unconverted acid, whereas large amounts or elevated temperatures resulted in higher yields of chloride by-products.

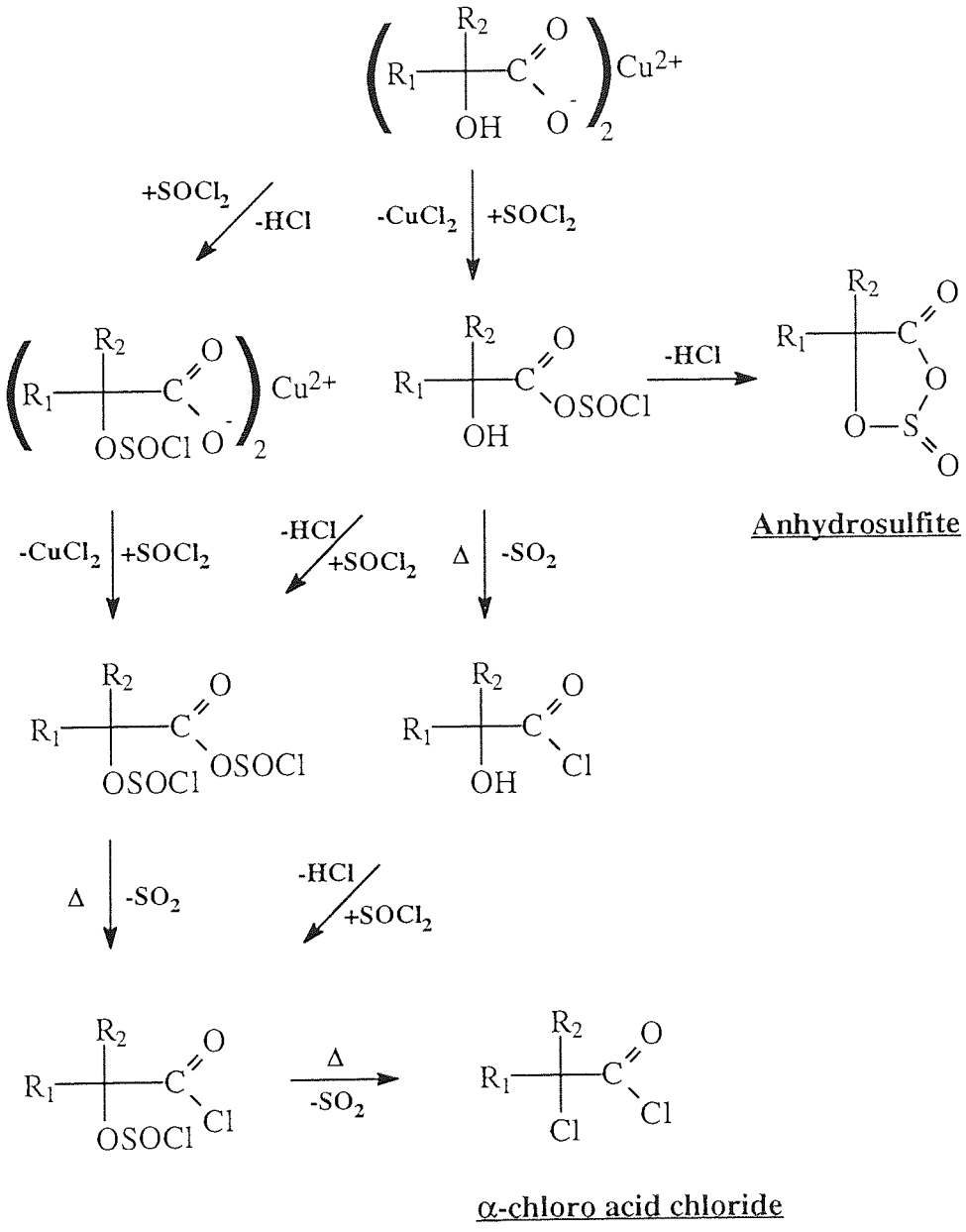

Figure 3.7. Reactions of the copper (II) salt with thionyl chloride.

3.1.3. Distillation of crude anhydrosulfite

3.1.3.1. Experimental

The crude anhydrosulfite was distilled at reduced pressure through a small Vigreux column, so as to separate the anhydrosulfite from the unchanged acid and the little amount of copper salt which was too fine to be stopped in the filtration. The distillation was carried out at 0.1-0.2 mm/Hg and the boiling point at this reduced pressure ranged from 20 to 50°C depending on the anhydrosulfites prepared, see section 3.2. for more information.

3.1.3.2. Discussion

Once distilled, the product was analysed by infrared to confirm the synthesis of anhydrosulfite. Figure 3.8. presents the different changes of the carbonyl absorptions during the synthesis of lactic acid anhydrosulfite, from the acid to the final product via the intermediate copper salt. Thereby, infrared spectroscopy turned out to be a useful technique in this synthesis.

The major impurities in anhydrosulfite preparation have been shown to be i) chlorine-containing compounds having either acyl or akyl chlorine or both, ii) the parent α-hydroxy acid resulting from unreacted starting materials or from presence of moisture in the medium and also iii) some fine copper salt. A simple fractional distillation eliminates efficiently the acid and the copper salt but does not remove the chlorine-containing impurities with similar boiling points to their corresponding anhydrosulfites.

Figure 3.8. FT-IR carbonyl peak absorptions during the synthesis of LAAS.

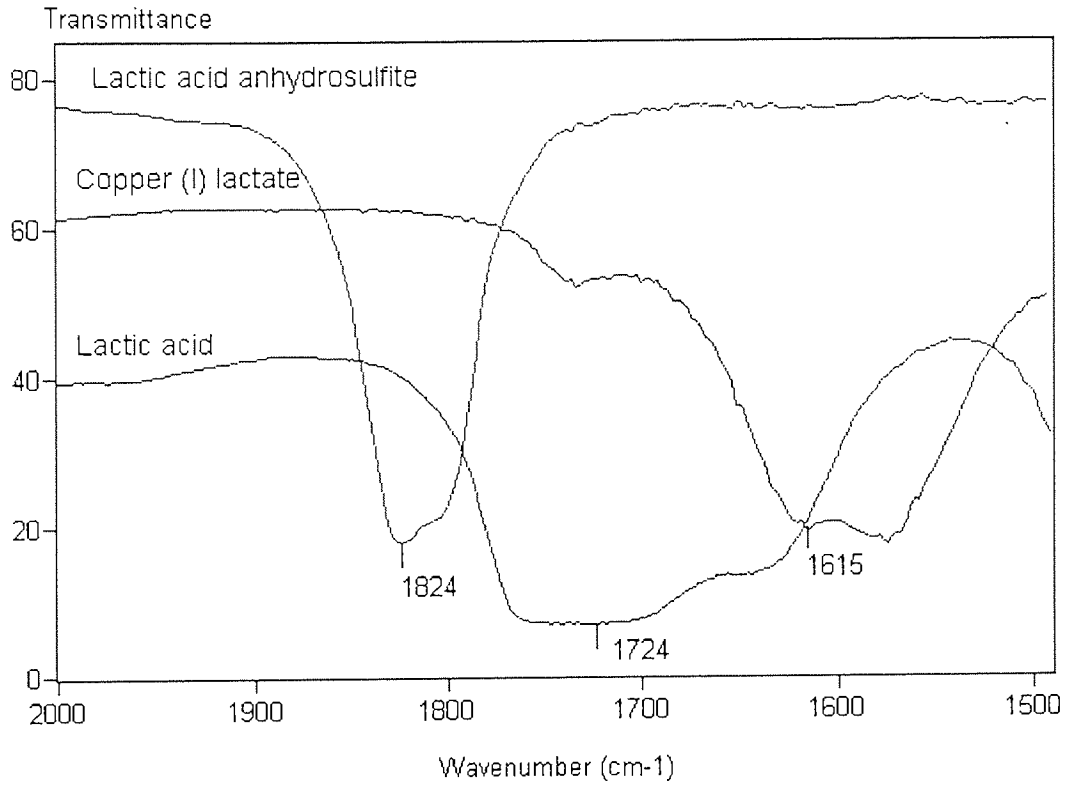

FT-IR and NMR spectra provide a useful indication of anhydrosulfite purity. Chlorine-containing impurities can be shown to be present in the product after distillation. The infrared carbonyl peak of the anhydrosulfite prepared appears relatively broad, as shown in figure 3.9. because of the similarity of the carbonyl absorptions of the anhydrosulfite, the chloro acid chloride, the chloro acid and the acid chloride, as presented in table 3.1. for lactic acid anhydrosulfite.

Table 3.1. FT-IR carbonyl absorptions for the impurities of lactic acid anhydrosulfite.

Impurities	Structure	FT-IR data (cm^{-1}) C = O
2-Chloropropionyl chloride	CH_3-CH(Cl)-CO(Cl)	1795.8
Propionyl chloride	CH_3-CH_2-CO(Cl)	1813.4
2-Chloropropionic acid	CH_3-CH(Cl)-COOH	1727.7

(source : reference Aldrich catalogue [68])

Figure 3.9. FT-IR spectra of LAAS before and after purification.

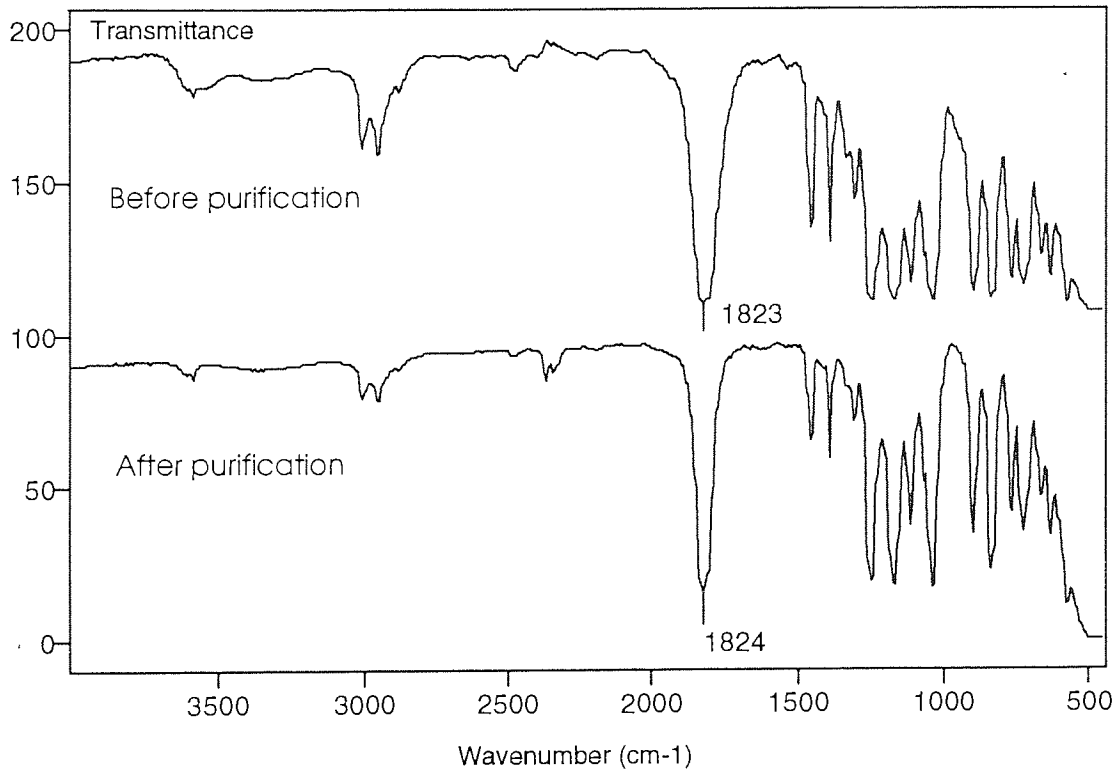

Analysis of the ^{1}H NMR spectrum of the unpurified product reveals the presence of impurities, several quartets at around 5.5 ppm and doublets at 1.3-1.8 ppm are observed, as shown in figure 3.10.

Figure 3.10. ^{1}H NMR spectrum of impure LAAS

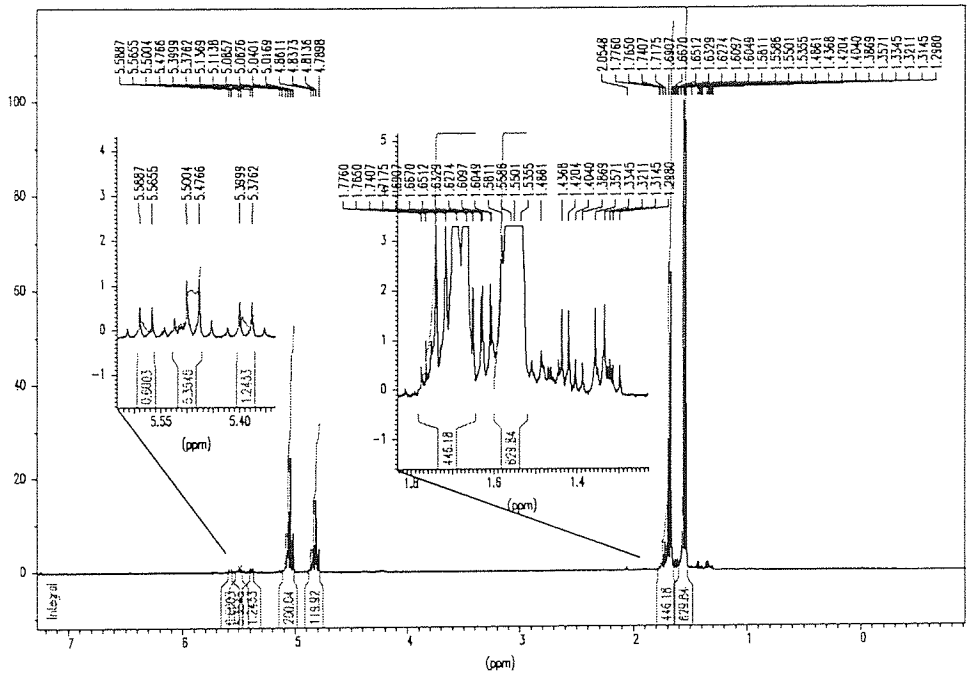

3.1.4. Determination of chlorine content

Potentiometric chloride titration was the method used (see section 2.) for the determination of chlorine-containing impurities level in the distilled anhydrosulfite. Typical values for the crude product were between 1 and 16%, this was calculated as follow :

$$\% \text{ of chlorine-containing impurities} = n_{Cl}/n_{product}$$

with n_{Cl} : number of moles of chloride determined by titration

$n_{product}$: number of moles of product calculated as a pure product.

3.1.5. Removal of chlorine containing impurities

3.1.5.1. Experimental

The impure anhydrosulfite (0.5 mole) was dissolved in dried THF (50 ml) and placed in a flask with copper (I) oxide (1 mole) (supplied by Aldrich Co.) dried in the oven at 80°C beforehand. This mixture was agitated with a magnetic stirrer and maintained at 0-5°C with an ice bath for 4-5 hours. The mixture was filtered off and THF removed under vacuum. After re-distillation, the chloride content was determined by potentiometric titration, and if necessary, the treatment repeated.

Chloride contents below 4% were found to be necessary if the monomer was to be polymerized. Above this value polymerization would start but be quickly stopped by impurities and resulted in formation of oligomers only.

3.1.5.2. Discussion

In order to produce high molecular weight polymers a specific purification procedure was established. Treating the impure monomer with copper (I) oxide was found to be the most effective [50]. This method gave satisfactory results, as presented in table 3.2.

Table 3.2. Effectiveness of copper (I) oxide as purifying agents for LAAS.

Monomer		Chloride content / %	Yields / %
LAAS	-Before purification	13	35
	-After purification	0.5 - 4	20

3.1.6. Redistillation of anhydrosulfite

The purified anhydrosulfite was redistilled under reduced pressure and stored under argon in a stoppered flask which was then protected from light with aluminium foil and kept in a dessicator containing a drying agent such as phosphorus pentoxide, at a temperature below 0°C.

Just before polymerization, the anhydrosulfite was still re-distilled using a micro-distillation apparatus so as to remove any acid possibly formed in spite the precautions taken. The monomer was used immediately after such distillation.

3.2. Synthesis of aliphatic anhydrosulfites

α-Hydroxy acids with one aliphatic substituent on the α-carbon were successfully converted to the corresponding anhydrosulfites (1,3,2-dioxa-thiolan-4-one-2-oxides) by reaction of the hydroxy acid with thionyl chloride according to the procedure described in section 3.1. Their general structure is presented in figure 3.11. and the aliphatic anhydrosulfites prepared by this method are listed in table 3.3.

Figure 3.11. Anhydrosulfites structure.

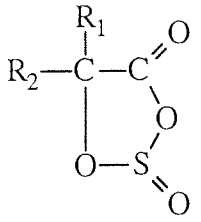

Table 3.3. Aliphatic anhydrosulfites prepared.

Anhydrosulfites abbreviation	Parent α-hydroxy acid	R_1	R_2
LAAS	Lactic acid	H	$-CH_3$
HIVAAS	2-Hydroxy isovaleric acid	H	$-CH(CH_3)_2$
HCAAS	2-Hydroxy caproic acid	H	$-(CH_2)_3-CH_3$
HICAAS	2-Hydroxy isocaproic acid	H	$-CH_2-CH(CH_3)_2$

3.2.1. Properties of aliphatic anhydrosulfites

Aliphatic anhydrosulfites, when pure, are colourless liquids and possess a characteristically strong odour. They are soluble in most organic solvents and decompose quickly to the corresponding acid when in contact with water. They exhibit a strong

carbonyl peak at around 1820 cm^{-1} and a less intense peak at 1240 cm^{-1} attributable to the sulphonyl group, as shown in table 3.4. This is illustrated by the infrared spectrum of LAAS in figure 3.12. Normally their boiling points are greater than 200°C at atmospheric pressure. However, they can be easily distilled at a reasonable temperature under reduced pressure without leading to decomposition of the product, as shown in table 3.4.

Table 3.4. Boiling points and FT-IR absorptions for the different aliphatic anhydrosulfites synthesised.

Anhydrosulfites	Boiling point / °C for 0.1-0.2 mm.Hg	FT-IR / cm^{-1}	
		C = O	S→O
LAAS	22	1824	1240
HIVAAS	26	1823	1247
HCAAS	42	1824	1245
HICAAS	49	1823	1244

Figure 3.12. FT-IR spectrum of LAAS

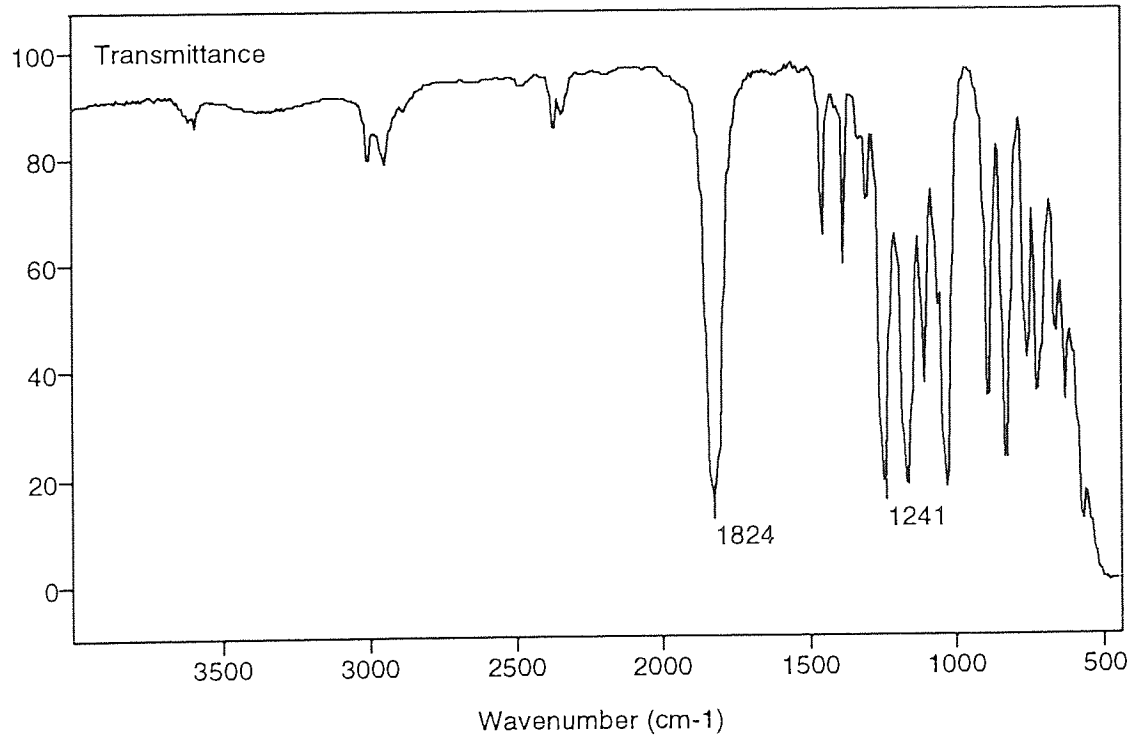

3.2.2. NMR studies

As the five-membered anhydrosulfite ring is puckered with the sulfur atom out of the plane [70], anhydrosulfites exist in two different conformations. These are shown in figure 3.13. Thus, the ^{1}H NMR spectra of L- and DL-LAAS show two sets of doublets for the methyl protons and two sets of quartets for the methine protons, as shown in figures 3.14 and 3.18. The integral values of the signals confirm these assignments. There is not an equal distribution of the two forms, (1) contributing more to the structure than (2), because the conformation (1) is the less sterically hindered. There is an equilibrium between the two forms and the position of equilibrium can be affected by a change in temperature.

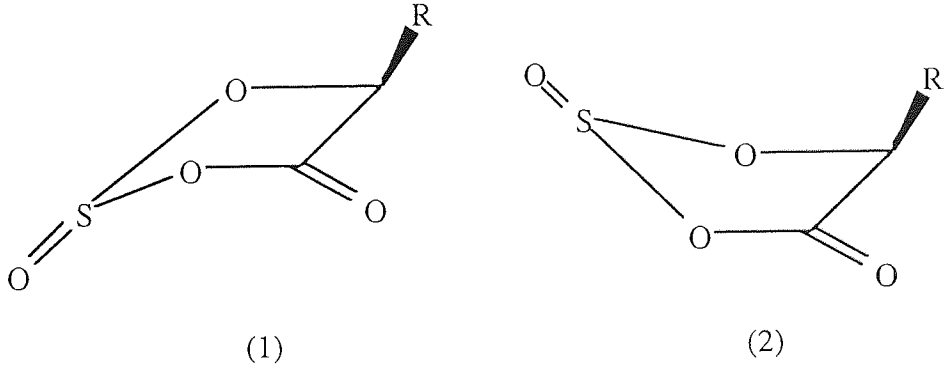

Figure 3.13. The two possible conformations of anhydrosulfites.

Figure 3.14. ^{1}H NMR spectrum of DL-LAAS

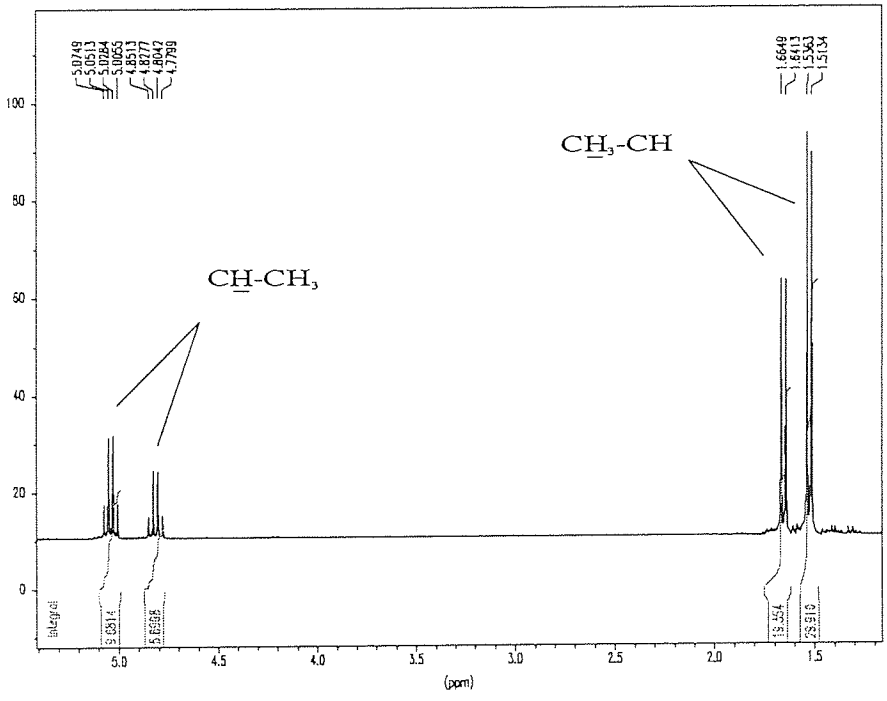

3.2.2.1. Homodecoupling on the methyl protons

So as to give an insight into the structure of the anhydrosulfites, spin decoupling was effected on the anhydrosulfite molecule. The sample used for this experiment was analysed beforehand by HPLC, only one component being detected by UV and therefore, the sample of LAAS was assumed to be pure.

A double resonance was applied on one of the two methyl protons signals at 1.51 -1.54 ppm, as shown in figure 3.15. Thus, this particular doublet collapsed to a singlet and caused one of the two quartets attributed to the methine protons to collapse to a singlet also. By repeating the experiment, the collapse of the other quartet could be observed as a result of the spin decoupling on the second doublet. Thus, the doublet at 1.51 - 1.54 ppm was found to be associated with the quartet at 5.00 - 5.07 ppm whilst the doublet at 1.64 - 1.66 ppm to the quartet at 4.78 - 4.85 ppm. This inter-connection of pairs of the

different methyl and methine protons signals revealed the position of these two types of protons on a common carbon and confirmed the two different positions of the protons relative to the sulfonyl group.

Figure 3.15. Homodecoupling applied on the methyl proton in the ^{1}H NMR spectrum of DL-LAAS

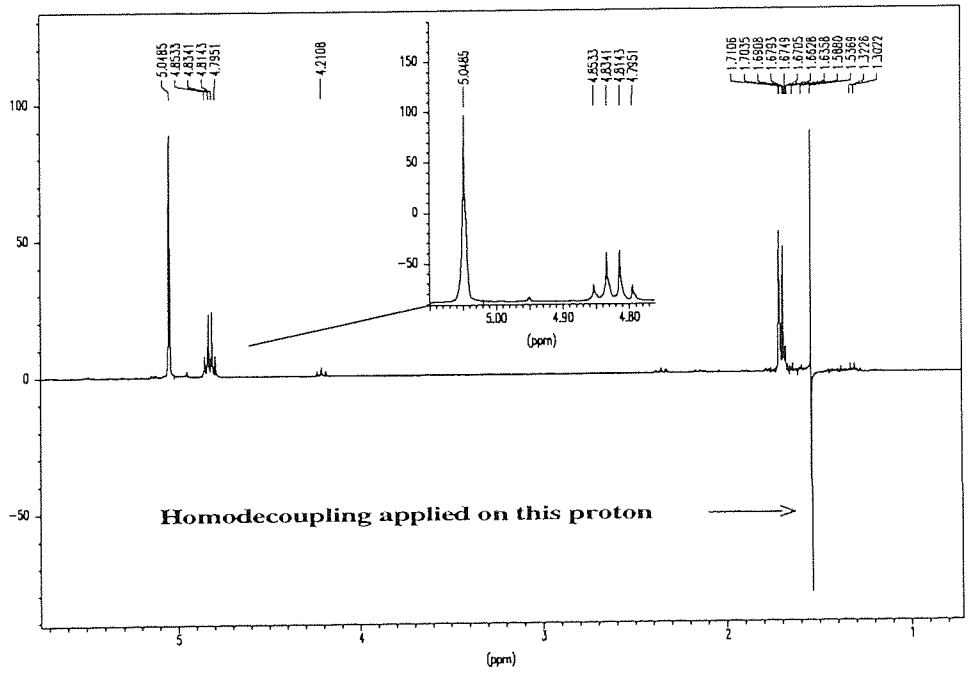

3.2.2.2. Effect of the temperature on the structure of anhydrosulfites

^{1}H NMR analysis of DL-LAAS at different temperatures was also employed to confirm the inter-connection between the signals. The spectral analyses were carried out at room temperature, 0°C, -20°C and -40°C and the associated spectra are presented in the appendix. The chemical shifts of the two types of protons and their relative peak areas are listed in table 3.5. A shift in the chemical resonances of the methine or methyl protons, as well as a change in the ratio of the two structural forms, was observed when the temperature was changed.

Table 3.5. Methine signals in the ^1H NMR spectrum of DL-LAAS at different temperatures.

Temperature / °C	δ.ppm	Relative peak area
20	4.81 - 4.88	0.59
	5.05 - 5.12	1.00
0	4.83 - 4.91	0.55
	5.07 - 5.14	1.00
-20	4.86 - 4.93	0.53
	5.08 - 5.15	1.00
-40	4.88 - 4.95	0.51
	5.10 - 5.17	1.00

In the following equilibrium, for a pure anhydrosulfite (LAAS),

$$LAAS_{(1)} \rightleftharpoons LAAS_{(2)}$$

the ratio of the concentrations of both configurations (1) and (2) is independent of the volume of the system and depends only on the temperature.

In reversible isothermal changes at constant pressure, the difference in available energy for this system may be defined by :

$$\Delta G = \Delta H - T\Delta S \quad (a)$$

with ΔS the difference in entropy of the system,

and if all the pressures are unity (e.g. 1 atm),

$$\Delta G = -RT \times \ln K \quad (b)$$

giving another expression for the standard available energy change.

Therefore, if the difference in heat content of this system equal to the increase of energy absorbed by the system in this change of state, ΔH is assumed constant over a small range of temperature, it may be deduced as follows :

$$\text{From (a) and (b) :} \quad \ln K = -\frac{\Delta H}{RT} + \text{constant} \quad \text{(c)}$$

K, the equilibrium constant at the temperature T may be defined by :

$$K = \frac{C_1}{C_2}$$

with C_1 : concentration of LAAS in the configuration (1)

C_2 : concentration of LAAS in the configuration (2)

Hence ΔH may be deduced as follows:

$$\Delta H = -R \times m$$

with R : the general gas constant ($R = 8.3178\ J^{\circ}.C^{-1}.mol^{-1}$).

m : slope of the straight line defined by (c).

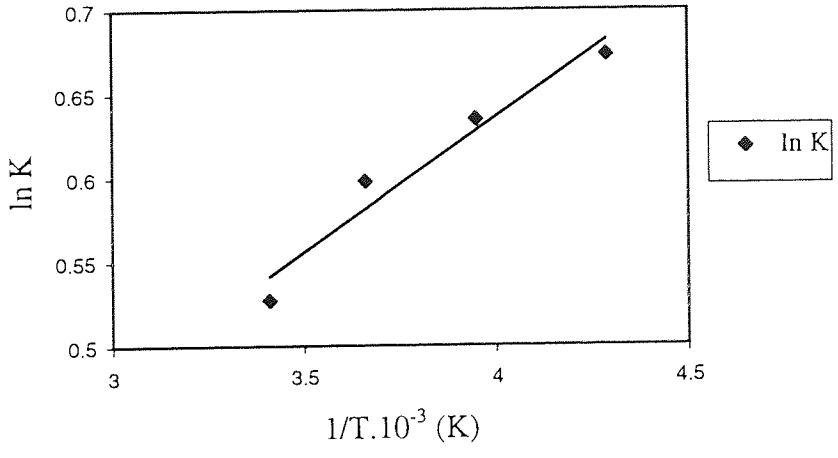

Figure 3.16. Graph of ln K plotted against 1/T for the equilibrium between the two conformations of DL-LAAS.

The variables of the equation defining the straight line ln K = f(1/T) were calculated from the values presented in table 3.5. and plotted, as shown in figure 3.16. Hence, the equation (c) could be determined, as follow :

$$\ln K = 160/T - 0.0042 \text{ (temperature in K)}$$

The change of enthalpy for this equilibrium was determined as 1.3 $kJ.mol^{-1}$.

3.2.3. Examples of aliphatic anhydrosulfites

A thorough knowledge of the starting monomer is always of considerable interest in an understanding of producing polymers derived from them. Thus, FT-IR and NMR spectra were used to analyse the detailed chemical structures of the range of monomers synthesised.

3.2.3.1. Lactic acid anhydrosulfite (LAAS)

Because the C(5) carbon of LAAS is asymmetric, D and L stereoisomers exist, as shown in figure 3.17. Thus, L- and DL-LAAS were prepared and studied in parallel.

Figure 3.17. Structure of LAAS.

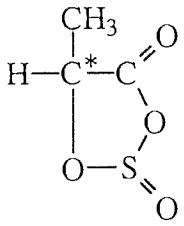

DL- and L-LAAS both exhibit a sharp carbonyl peak at 1824 cm^{-1}, a less intense peak at 1240 cm^{-1} due to the sulphonyl group and weak C-H stretching absorptions at 2946 cm^{-1} and 2999 cm^{-1}, as shown in figure 3.12.

Despite the presence of the two stereoisomers in the racemic DL-LAAS, the ^{1}H NMR spectra of DL- and L-LAAS are similar and show two sets of doublets for the methyl protons and two sets of quartets for the methine protons, as shown in figures 3.14. and 3.18.,and also in table 3.6. The peak areas of the two types of protons correspond approximately to the 3:1 ratio, the number of methyl protons compared to the numbers of methine protons, for both L- and DL-LAAS. Additionally, the molecule is

preferentially in the configuration (1), approximatively 1.7 more than in the configuration (2) for DL- and L-LAAS.

Figure 3.18. ^{1}H NMR spectrum of L-LAAS

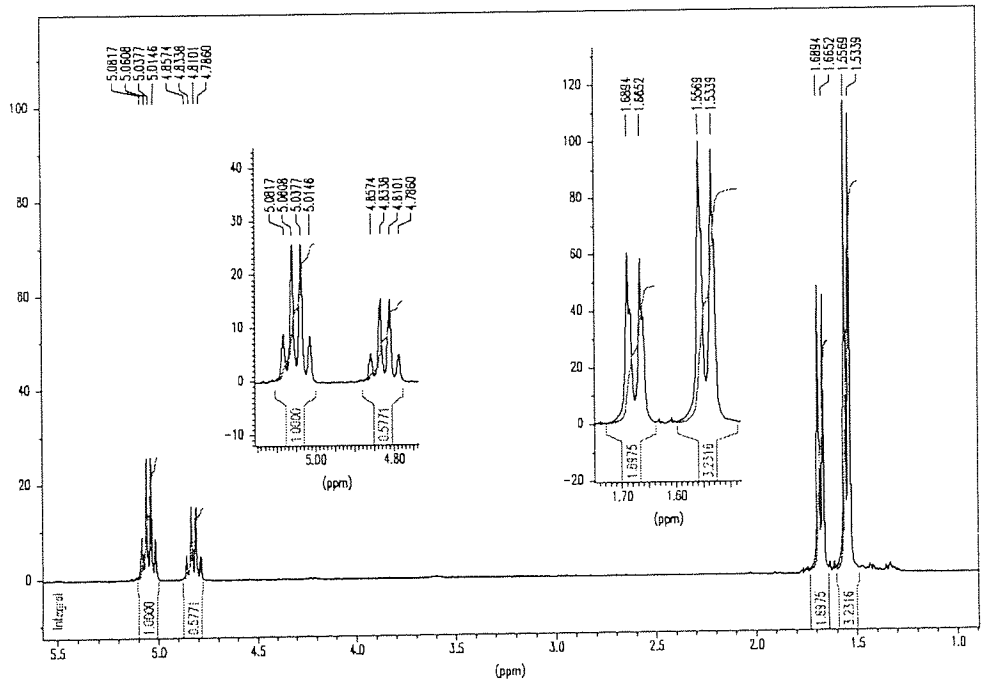

Table 3.6. ^{1}H NMR data of L-LAAS and DL-LAAS.

Anhydrosulfite	δ.ppm	Peak shape	Relative peak area	Assignment
L-LAAS	1.53 - 1.56	doublet	2.99	CH-CH_3
	1.67 - 1.69	doublet	1.81	CH-CH_3
	4.79 - 4.86	quartet	0.54	CH_3-CH
	5.01 - 5.08	quartet	0.93	CH_3-CH
DL-LAAS	1.51 - 1.54	doublet	2.99	CH-CH_3
	1.64 - 1.66	doublet	1.94	CH-CH_3
	4.78 - 4.85	quartet	0.58	CH_3-CH
	5.01 - 5.07	quartet	0.97	CH_3-CH

As expected, the ^{13}C NMR spectra of both DL- and L-LAAS exhibit two signals for the methyl and methine carbons because of the two possible conformations. The chemical shifts for those carbons are presented in table 3.7. and this is illustrated by the ^{13}C NMR spectrum of DL- LAAS in figure 3.20.

Whereas the ^{1}H NMR spectra of DL- and L-LAAS are identical, a difference between DL- and L-LAAS is noticeable in the ^{13}C NMR spectra. This is so for the carbonyl peak, as it could be observed in figure 3.19. and table 3.7. The ^{13}C NMR spectrum of DL-LAAS, the racemic combination of D- and L-LAAS, exhibits two carbonyl signals originating from the two configurations D and L. Nevertheless four carbonyl absorptions for the DL- and two for the L-LAAS might be expected because of the two possible conformations, probably the low intensity absorption usually obtained for this functional group does not permit a better definition.

Figure 3.19. Carbonyl signals in the ^{13}C NMR spectrum of DL-LAAS

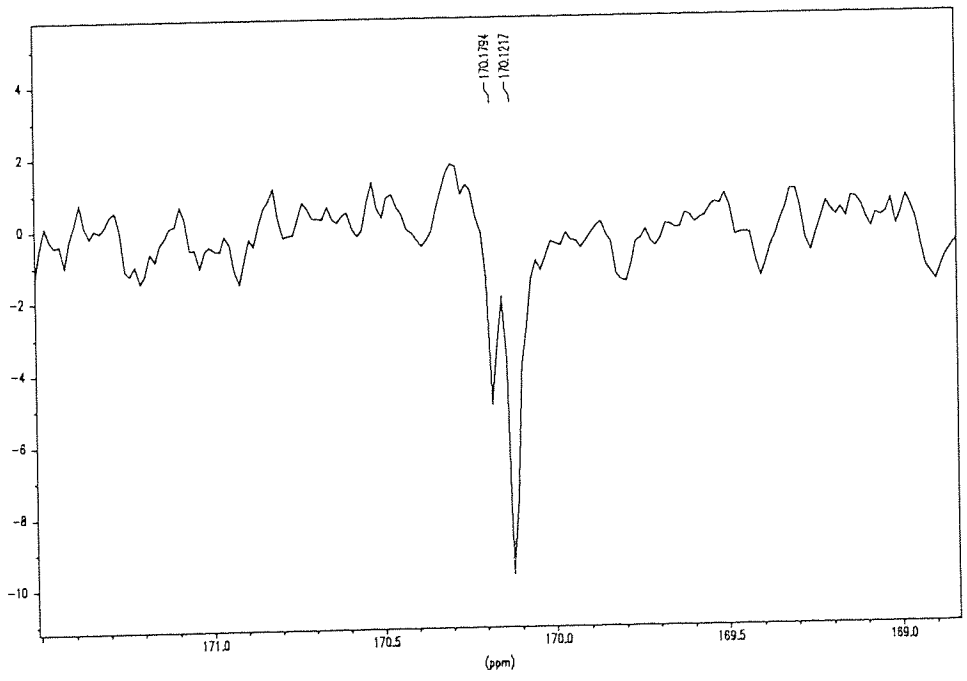

Figure 3.20. ^{13}C NMR spectrum of DL-LAAS

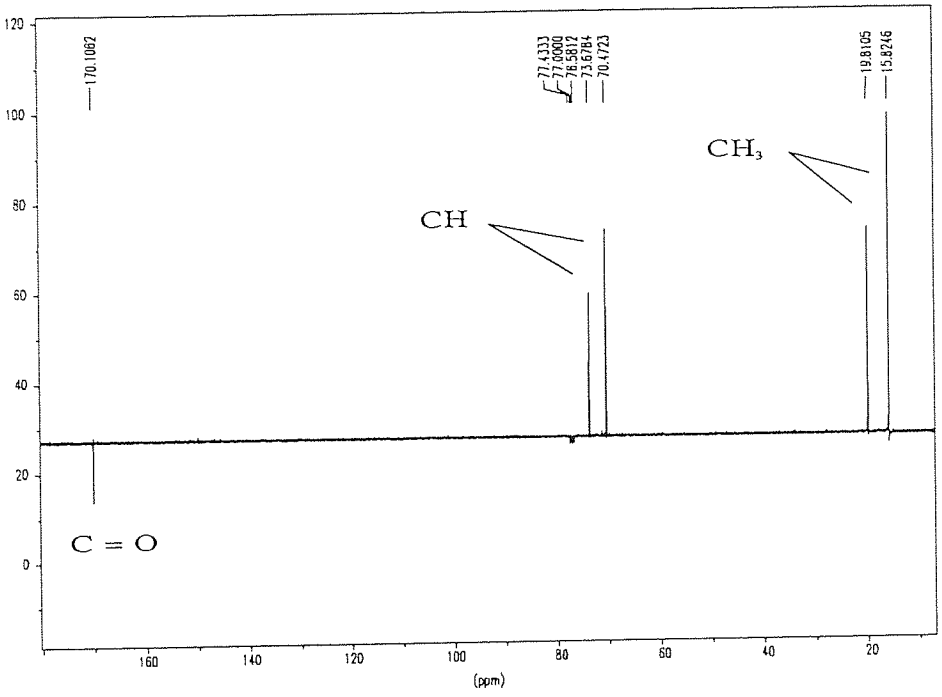

Table 3.7. ^{13}C NMR data of L-LAAS and DL-LAAS.

Anhydrosulfite	δ. ppm	Assignment
L-LAAS	15.91	CH_3
	19.90	CH_3
	70.46	CH
	73.68	CH
	170.09	C = O
DL-LAAS	16.24	CH_3
	20.27	CH_3
	70.43	CH
	73.71	CH
	170.12	C = O
	170.18	C = O

3.2.3.2. DL-2-Hydroxy isovaleric acid anhydrosulfite (DL-HIVAAS)

DL-HIVAAS shows two characteristic peaks of the carbonyl and sulphonyl groups in the infrared, at 1823 cm^{-1} and 1247 cm^{-1} respectively and also strong absorptions at 2973 cm^{-1} attributable to the C-H stretch, as shown in figure 3.21.

Figure 3.21. FT-IR spectrum of DL-HIVAAS

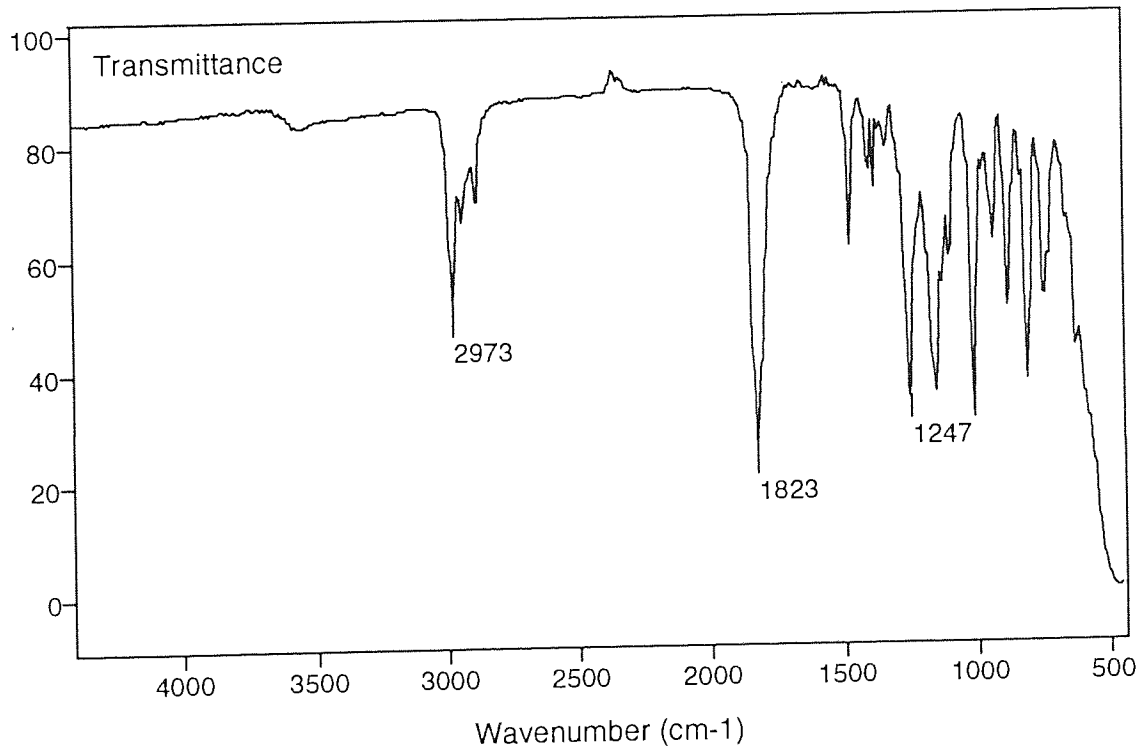

The relative peak areas in the ^1H NMR spectrum of DL-HIVAAS do not correspond exactly to the 6:1:1 ratio expected for the methyl, methine and ring protons, but 7:1:1, as shown in table 3.8. The three signals could still be attributed to the different types of protons which are represented as H_a, H_b and H_c in figure 3.22.

Inspection of the ^1H NMR spectrum of DL-HIVAAS in figure 3.23. shows that like LAAS, there is a ring effect visible on the ring proton H_c, two doublets are attributed to the ring proton instead of one doublet as expected.

From the relative peak areas of the proton H_c in the two configurations, the relative proportions of configuration (1) to configuration (2) is 1.8 for HIVAAS. Compared with LAAS, the bulkiness of the substituent on the α-carbon seems to influence slightly the equilibrium between the two conformations.

Figure 3.22. Key to NMR spectra of DL-HIVAAS.

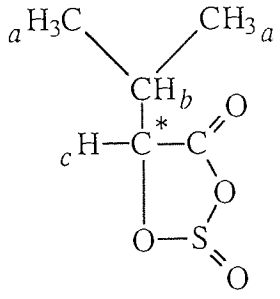

Figure 3.23. ^{1}H NMR spectrum of DL-HIVAAS

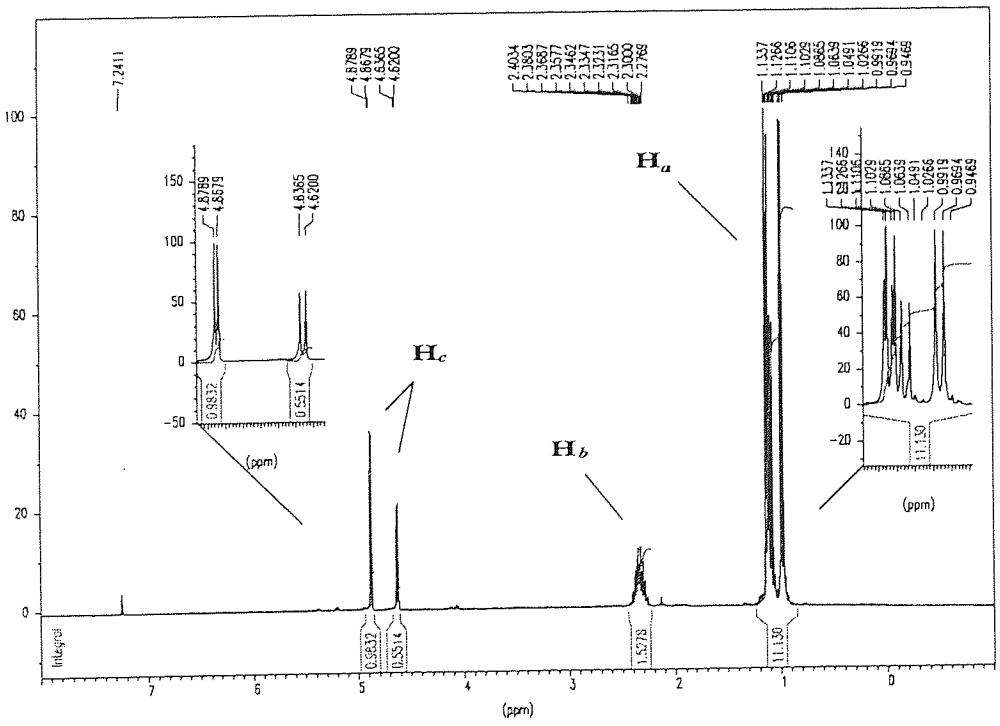

Table 3.8. ^{1}H NMR data of DL-HIVAAS.

Anhydrosulfite	δ.ppm	Peak shape	Relative peak area	Expected	Assignment
DL-HIVAAS	0.95 - 1.13	4 doublets	11.13	9.6	$(CH_3)_2$-CH
	2.28 - 2.40	multiplet	1.53	1.6	CH-$(CH_3)_2$
	4.62 - 4.64	doublet	0.55	0.6	CH-CH-$(CH_3)_2$
	4.87 - 4.88	doublet	0.98	1.0	CH-CH-$(CH_3)_2$

The methyl resonance is also of interest because one doublet was expected whereas the spectrum shows four doublets, as shown in figure 3.24. This could be explained by restricted rotation around the CH_c-CH_b bond. The expected doublet for the methyl protons is transformed into two doublets if the two methyl groups are non-equivalent. Additionally, the methyl groups are affected by the sulphonyl group, giving rise to four doublets and this effect is greater for one of the methyl groups, presumably when this group is the closest to the sulphonyl group.

Figure 3.24. Methyl protons signals in the ^{1}H NMR spectrum of DL-HIVAAS

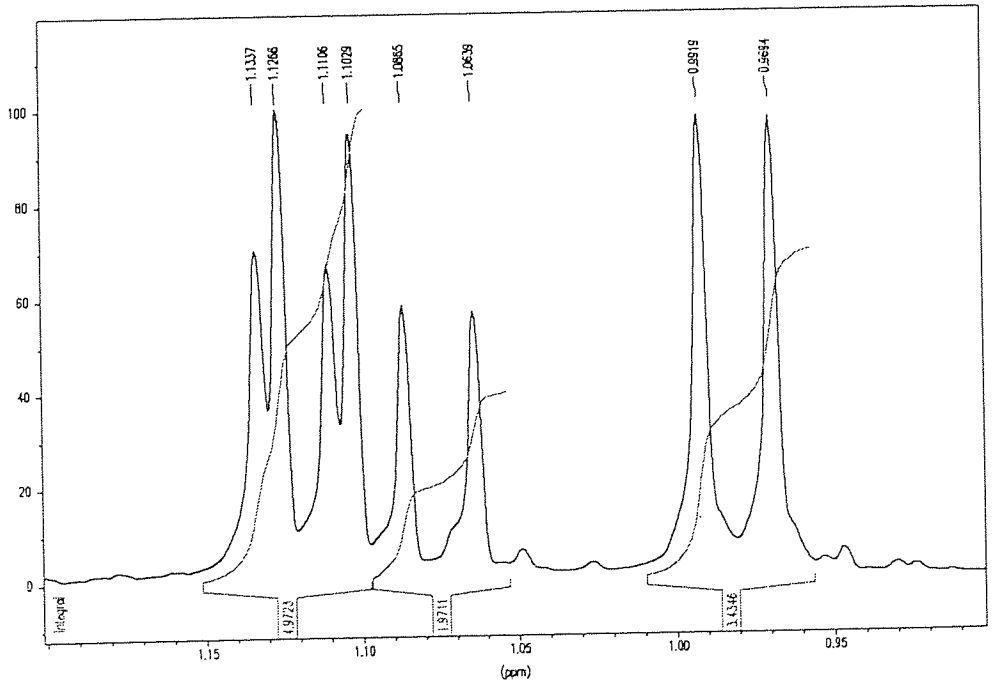

The ^{13}C NMR spectrum and the corresponding peak table for DL-HIVAAS are shown in figure 3.25. and table 3.9., respectively.

Figure 3.25. ^{13}C NMR spectrum of DL-HIVAAS

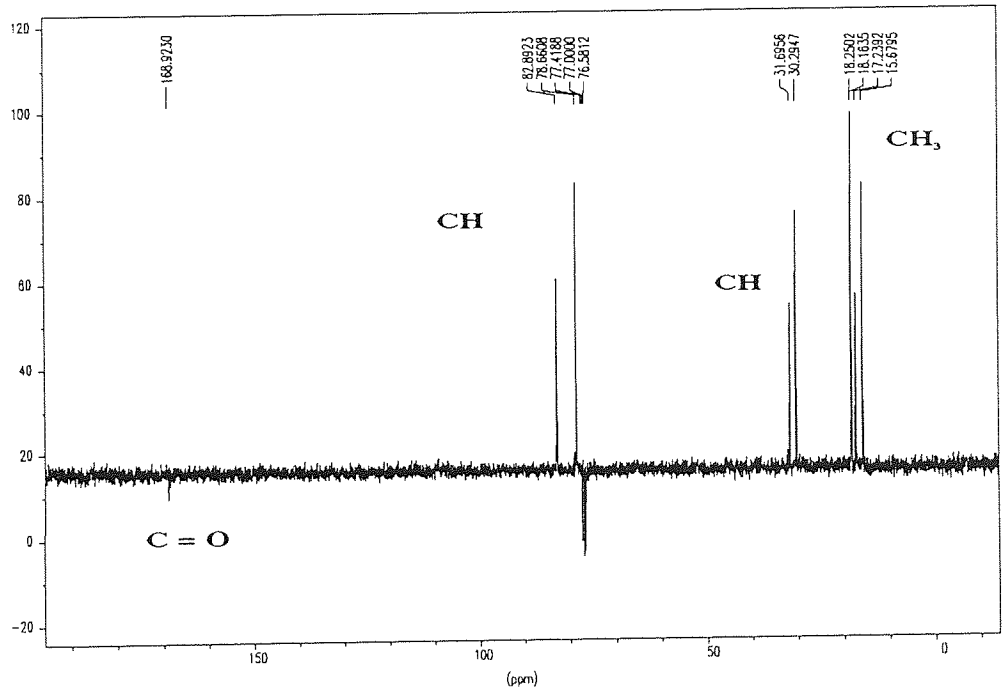

Table 3.9. ^{13}C NMR data of DL-HIVAAS.

Anhydrosulfite	δ. ppm	Assignment
DL-HIVAAS	15.68 - 17.24	CH_{3a}
	18.16 - 18.25	CH_{3a}
	30.29	CH_b
	31.70	CH_b
	78.66	CH_c
	82.89	CH_c
	168.92	C = O

In the ^{13}C NMR spectrum of DL-HIVAAS, several signals were observed, four signals for CH_3, two for CH_b, two signals for CH_c and only one for C = O, as shown in figure 3.24. and table 3.9. This confirmed the different effect observed for the ^{1}H NMR spectrum, in particular for the methyl carbons, for which four resonances arose. This fine structure was associated with steric hindrance along with the two possible positions of the sulphonyl group, as it has been previously explained. An expansion of this region is shown in figure 3.26.

There was also insufficient sample to permit a thorough detection of the two close signals of the carbonyl group.

Figure 3.26. Methyl signals in the ^{13}C NMR spectrum of DL-HIVAAS

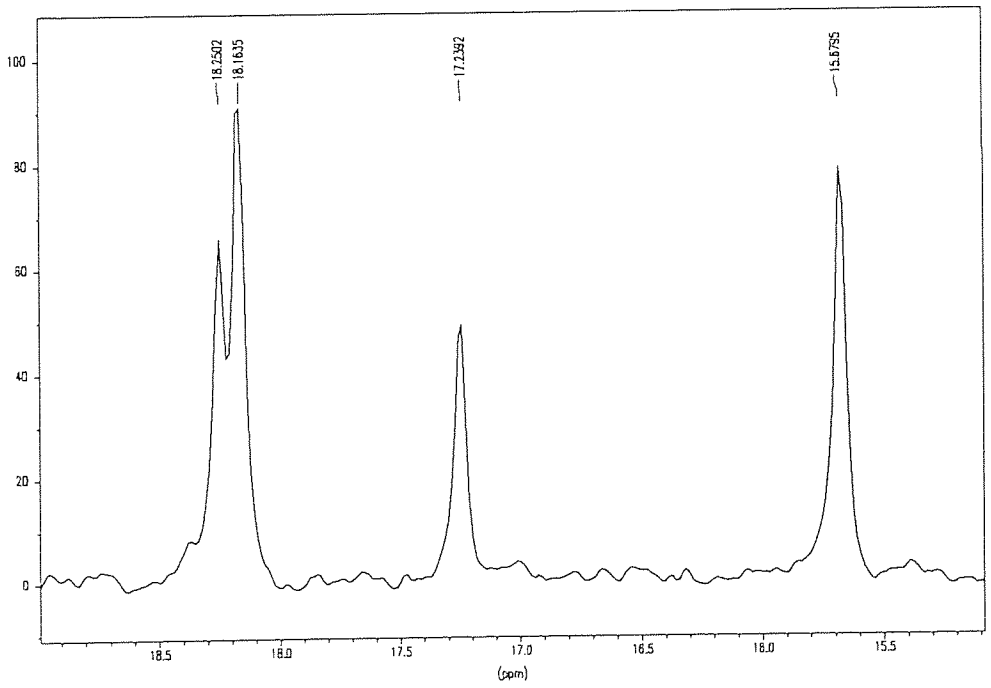

3.2.3.3. DL-2-Hydroxy caproic acid anhydrosulfite (DL-HCAAS)

In the FT-IR spectrum of DL-HCAAS, the characteristic strong anhydrosulfite carbonyl peak at 1824 cm^{-1} can be seen along with the less intense peak at 1245 cm^{-1} associated with the sulphonyl group and the C-H stretching absorptions around 2961 cm^{-1}, see in appendix.

Figure 3.27. Key to NMR spectra of DL-HCAAS.

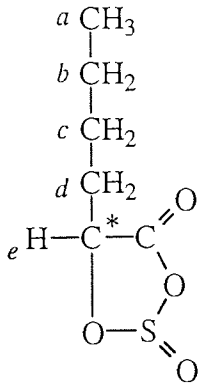

In the ^1H NMR spectrum of DL-HCAAS, the peak areas of the five different protons present in the molecule, as represented in figure 3.27., do not correspond exactly to the ratio 3:4:2:1 for H_a:(H_b, H_c):H_d:H_e, as demonstrated in table 3.10.

Analysis of the spectrum revealed a pair of quartets instead of the expected triplet for the resonance of the ring proton (H_e). Steric hindrance restricts rotation about the CH_e-CH_{2d} bond and so the two hydrogens are not equivalent. Thus, the proton in question, H_e, is coupled independently to the two individual protons H_d of the first carbon atom. This gave rise to the shape of a quartet equivalent to two doublets. In addition, the ring proton H_e has two positions relative to the sulphonyl group, which lead to a pair of quartets for this proton, as shown in figure 3.28.

The bulkiness of the substitutent on the α-carbon was also found not to influence the equilibrium between the two configurations.

It is interesting to note that in the case of the methyl group the two effects have virtually disappeared, the resonance is a simple triplet of a proton adjacent to a methylene group and the chemical shift between the two triplets is so small that a pseudo-triplet can be seen in the spectrum, as shown in figure 3.28.

Figure 3.28. ^{1}H NMR spectrum of DL-HCAAS

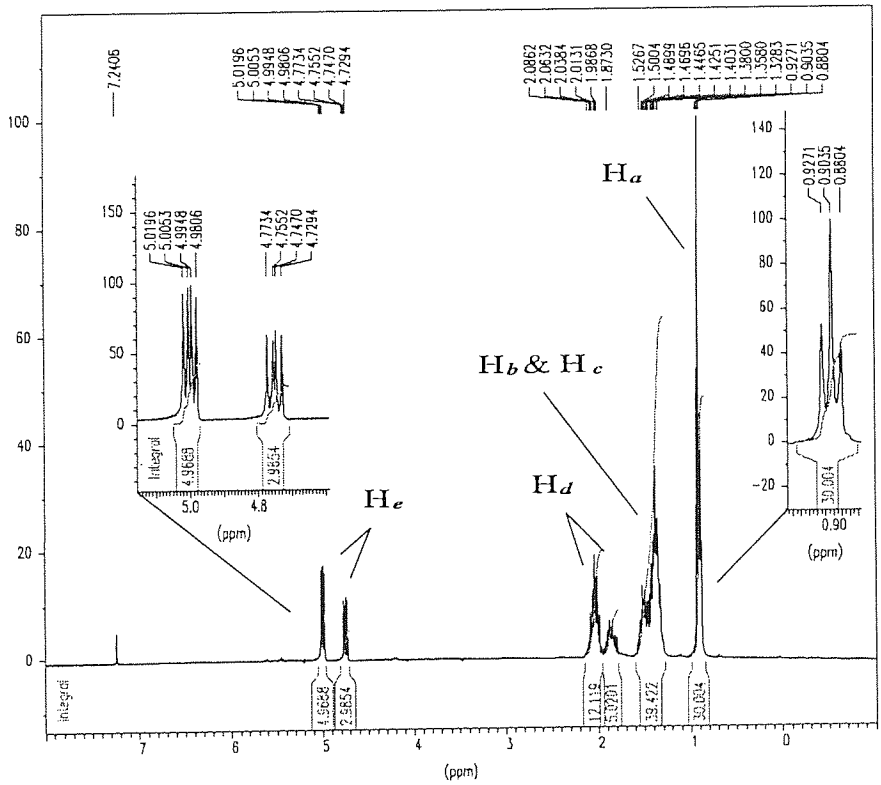

Table 3.10. ^{1}H NMR data of DL-HCAAS.

Anhydrosulfite	δ.ppm	Peak shape	Relative peak area	Expected	Assignment
DL-HCAAS	0.88 - 0.93	triplet	30.00	30	H*a*
	1.33 - 1.53	multiplet	39.42	40	H*b* & H*c*
	1.87 - 1.99	multiplet	5.02		H*d*
	2.01 - 2.09	multiplet	12.12	20	H*d*
	4.73 - 4.77	quartet	2.99		H*e*
	4.98 - 5.02	quartet	4.97	10	H*e*

The ^{13}C NMR spectrum of DL-HCAAS in figure 3.29. confirmed the different effect revealed in the ^{1}H NMR spectrum.

Figure 3.29. ^{13}C NMR spectrum of DL-HCAAS

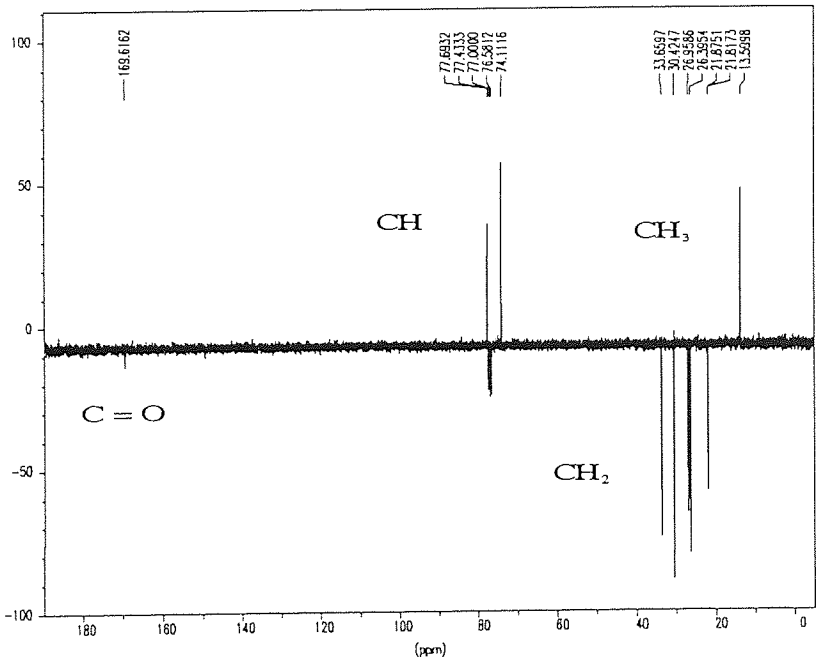

Table 3.11. ^{13}C NMR data of DL-HCAAS.

Anhydrosulfite	δ. ppm	Assignment
DL-HCAAS	13.60	$CH_{3\text{-}a}$
	21.82	$CH_{2\text{-}b}$
	21.88	$CH_{2\text{-}b}$
	26.40	$CH_{2\text{-}c}$
	26.96	$CH_{2\text{-}c}$
	30.42	$CH_{2\text{-}d}$
	33.66	$CH_{2\text{-}d}$
	74.11	$CH_{\text{-}e}$
	77.69	$CH_{\text{-}e}$
	169.62	C = O

In particular, the ^{13}C NMR spectrum demonstrates clearly the reduction of the ring effect along the n-butyl chain. The ring effect is most marked for methylene closest to the ring and diminishes as the carbon moves further away from the ring so that the ring effect in the case of the methyl carbon has practically disappeared. The methylene carbons all appear as doublets and the spacing decreases as the carbon moves away from the ring, as shown in figure 3.30. and table 3.11.

Additionally, just as for DL-HIVAAS, the two carbonyl signals due to the D and L conformations of the carbon asymmetric present in DL-HCAAS could not be detected.

Figure 3.30. Methylene signals in the ^{13}C NMR spectrum of DL-HCAAS

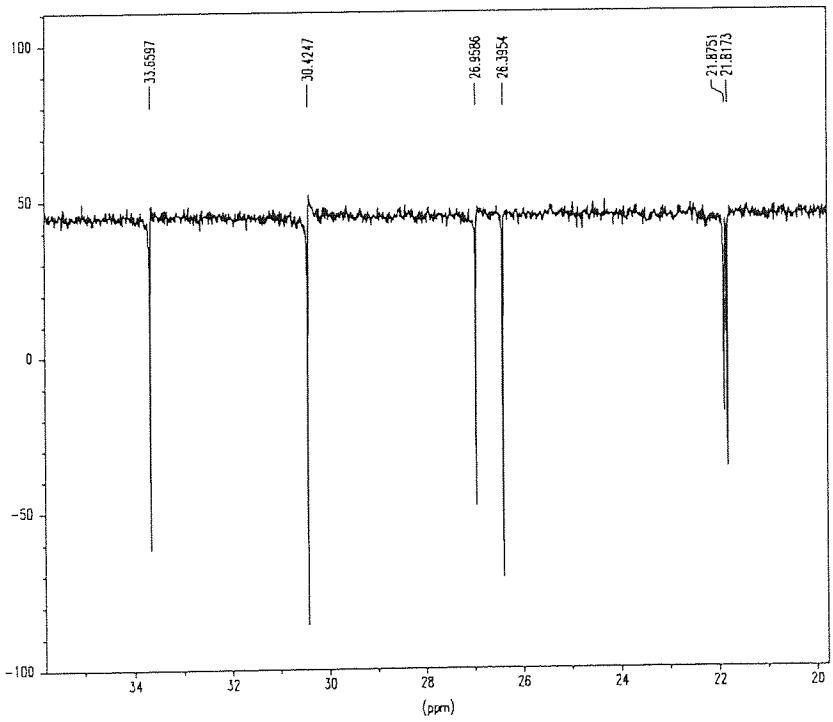

3.2.3.4. L-2-Hydroxy isocaproic acid anhydrosulfite (L-HICAAS)

L-HICAAS was synthesised in very small quantity, allowing a restrictive analysis of the molecule. Thus, the FT-IR and NMR spectroscopy were performed on a sample containing still 24 % of chlorine-containing impurities, which was determined by chlorine potentiometric titration.

The FT-IR spectrum of L-HICAAS in the appendix shows the two characteristic peaks of the carbonyl and the sulphonyl groups, at 1823 cm^{-1} and 1244 cm^{-1} respectively and also strong absorptions around 2963 cm^{-1} attributed to the C-H stretch.

The structure of L-HICAAS along with the several protons and carbons on the α-carbon are presented in figure 3.31.

Figure 3.31. Key to NMR spectra of L-HICAAS.

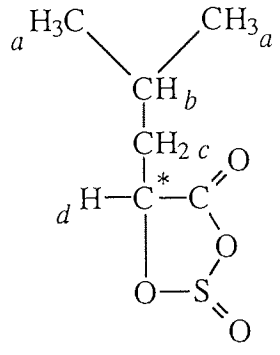

The ^1H NMR spectrum and the corresponding peak table for L-HICAAS are shown in figure 3.32. and table 3.12.

Figure 3.32. ^{1}H NMR spectrum of L-HICAAS

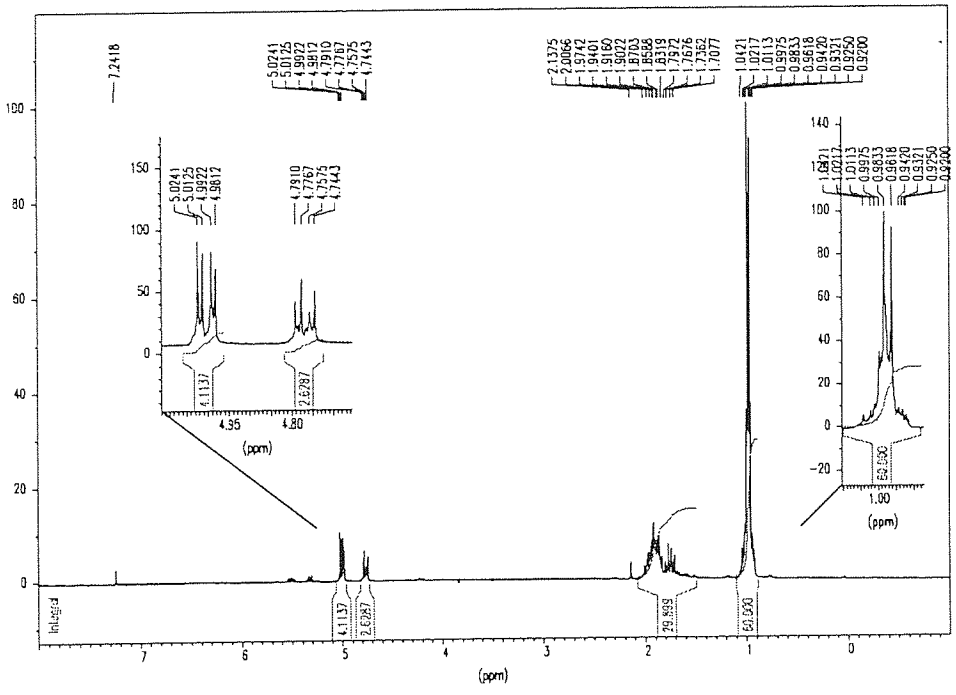

Table 3.12. ^{1}H NMR data of L-HICAAS.

Anhydrosulfite	δ.ppm	Peak shape	Relative peak area	Expected	Assignment
DL-HICAAS	0.92 - 1.04	multiplet	60.0	60	$(CH_3)_2$-CH
	1.71 - 2.14	multiplet	29.9	30	CH_2-CH-$(CH_3)_2$
	4.74 - 4.79	quartet	2.6	10	CH-CH_2-CH
	4.98 - 5.02	quartet	4.1		CH-CH_2-CH

In the ^{1}H NMR spectrum of L-HICAAS, the peak areas of the methyl, methylene and methine protons did not correspond to the ratio 6:3:1 for H_a:(H_b, H_c):H_d, but 9:4:1 This could be explained by the presence of impurities in the sample used for the NMR analysis. Potentiometric titration showed the sample to contain 24% of impurities and this was confirmed by the ^{1}H NMR analysis which revealed that the two quartets centred

at 5.32 and 5.50 ppm represented 15 % of the two other quartets, the resonances of the ring proton H_d in L-HICAAS, as shown in figure 3.33. and table 3.12.

Figure 3.33. Methine protons signals in the ^{1}H NMR spectrum of L-HICAAS

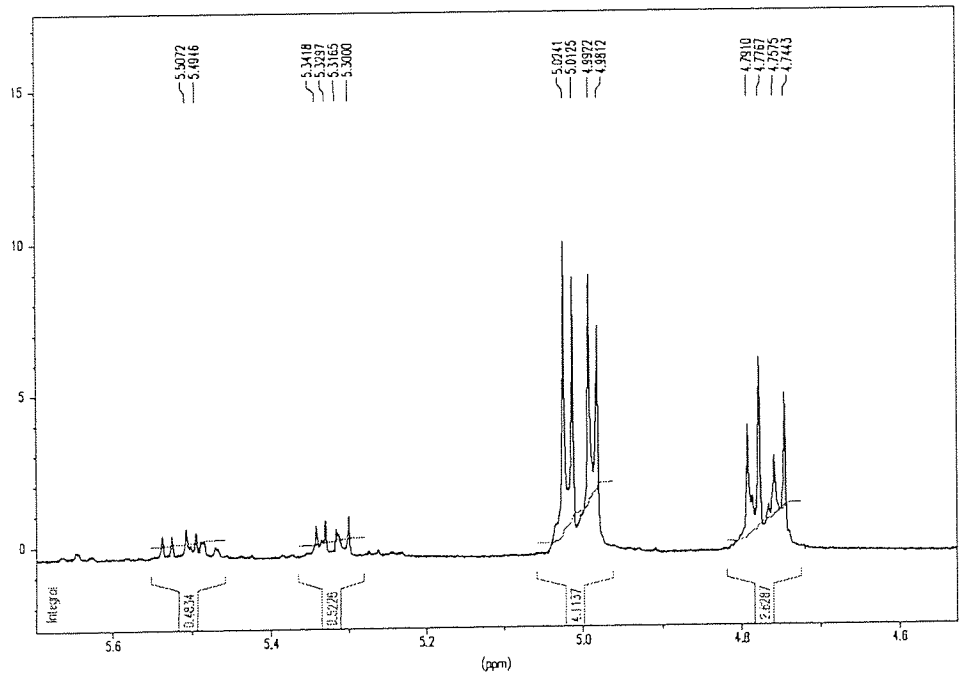

In the molecule, there is again a ring effect as well as a restriction around the CH_d-CH_{2c} bond because of steric hindrance and this results in the shape of a pair of quartets in the ^{1}H NMR spectrum instead of a triplet, as explained previously for DL-HCAAS in greater details.

Similarly, the methyl protons resonances might be expected in the shape of two doublets with each of them affected by the sulphonyl group. In fact, it appears as a pseudo-doublet resulting probably from four doublets slightly shifted from one another. This could mean that for these methyl protons, H_a, the rotation around the CH_d-CH_{2c} bond is less restricted and the sulphonyl group effect is reduced compared with the methyl protons in the molecule of DL-HIVAAS, because they are further away from the ring. Indeed, these effects still play an important role in the structure of this anhydrosulfite and are more visible in the ^{13}C NMR spectrum presented in figure 3.34., with the corresponding peak table in table 3.13.

Figure 3.34. ^{13}C NMR spectrum of L-HICAAS

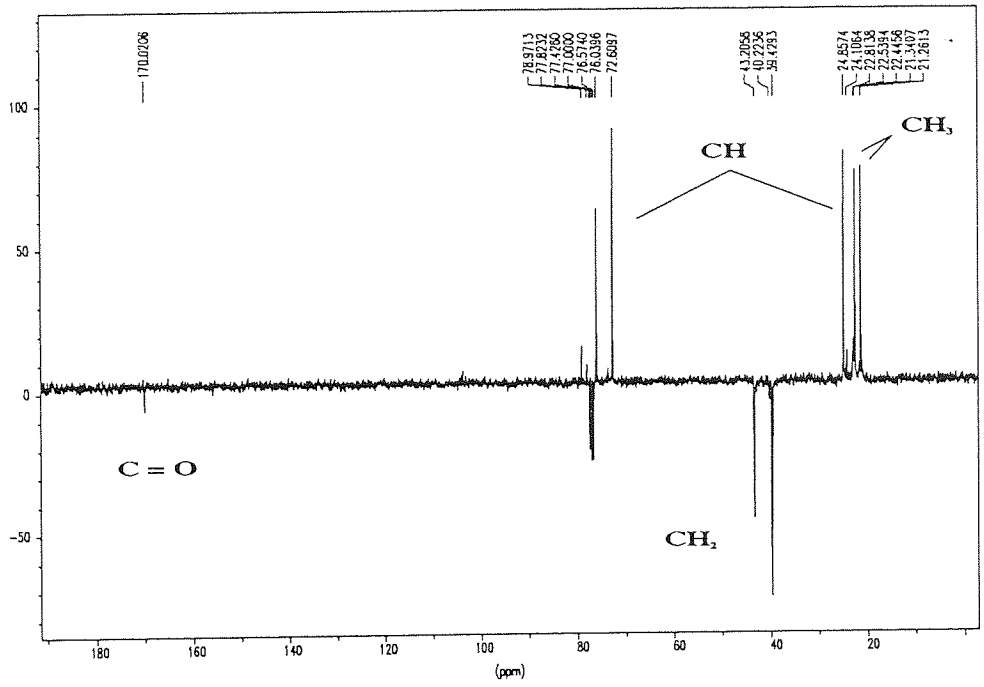

Table 3.13. ^{13}C NMR data of L-HICAAS.

Anhydrosulfite	δ. ppm	Assignment
DL-HICAAS	21.26 - 21.34	CH_{3a}
	22.44 - 22.54	CH_{3a}
	22.81 - 24.10	CH_3 (impurity)
	24.86	CH_b
	39.43	CH_{2c}
	40.22	CH_2 (impurity)
	43.21	CH_{2c}
	72.61	CH_d
	76.04	CH_d
	77.82 - 78.97	CH (impurity)
	170.01	C = O

Analysis of the ^{13}C NMR spectrum of L-HICAAS revealed two resonances for the methyl carbons owing to the non-equivalence of the methyl carbons and these signals were split in two, as shown in figure 3.35. Impurities could be involved in these peaks, but because of the high intensity of these signals, it was more likely that the methyl carbons were affected by the sulphonyl group, as observed for DL-HIVAAS in section 3.2.3.2. However, this ring effect in L-HICAAS was reduced compared to the one observed in DL-HIVAAS, probably because the methyl carbons in L-HICAAS were further away from the ring and the sulphonyl group. Moreover, this effect had practically disappeared, for the methine carbon CH_b, the CH being smaller than a methyl group.

Figure 3.35. Methine and methyl signals in the ^{13}C NMR spectrum of DL-HICAAS

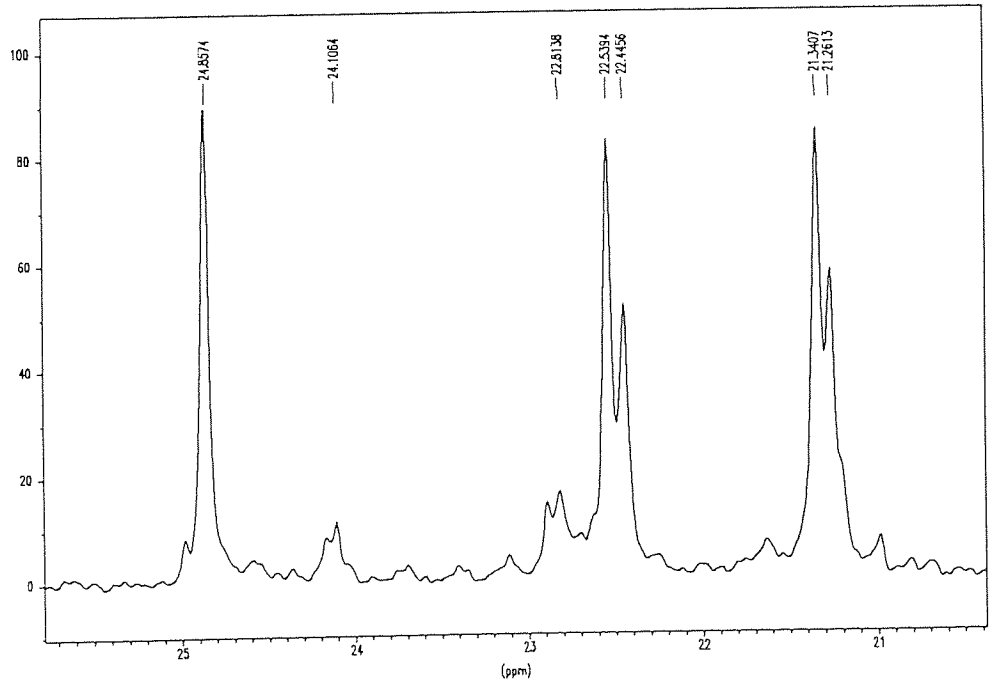

3.3. Synthesis of aromatic anhydrosulfites

α-Hydroxy acids with an aromatic substituent on the α carbon were converted to the corresponding anhydrosulfite by reaction with thionyl chloride. But distillation was not satisfactory as a means of purification of the product, in the procedure described in section 3.1. Complete decomposition of the monomer took place under such conditions (100°C, 0.1 mm/Hg).

Because product had to be highly pure if it was to be polymerized, alternative techniques of purification were investigated for these compounds, in particular chromatographic techniques. Thin layer chromatography (TLC), high performance liquid chromatography (HPLC), FT-IR and UV spectroscopy were used to assist the separation of aromatic anhydrosulfites from the unwanted by-products (chlorinated impurities, the parent acid and its copper salt) by different techniques of purification. The aromatic anhydrosulfites synthesised and then purified are listed in table 3.14., and their structures described in figure 3.36.

Figure 3.36. Aromatic anhydrosulfites structure.

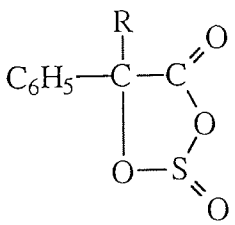

Table 3.14. Aromatic anhydrosulfites prepared.

Anhydrosulfites abbreviation	Parent α-hydroxy acid	R
MAAS	Mandelic acid	H
BAAS	Benzilic acid	C_6H_5

3.3.1. Benzilic acid anhydrosulfite (BAAS)

3.3.1.1. Experimental

The preparation of BAAS was carried out under conditions similar to those described in section 3.1., with the temperature maintained below -20°C. Copper (II) salt of benzilic acid was converted by reaction with thionyl chloride to a red oil. The FT-IR spectrum of the resulting product exhibited three carbonyl peaks at 1660, 1733 and 1819 cm^{-1}, as shown in figure 3.37. These peaks corresponded to the copper (II) salt, the acid and the anhydrosulfite absorptions respectively. Thus, the anhydrosulfite BAAS was synthesised but was also mixed with other unwanted compounds, the unreacted acid and its copper salt.

Figure 3.37. FT-IR carbonyl absorptions of crude BAAS, benzilic acid and its copper (II) salt.

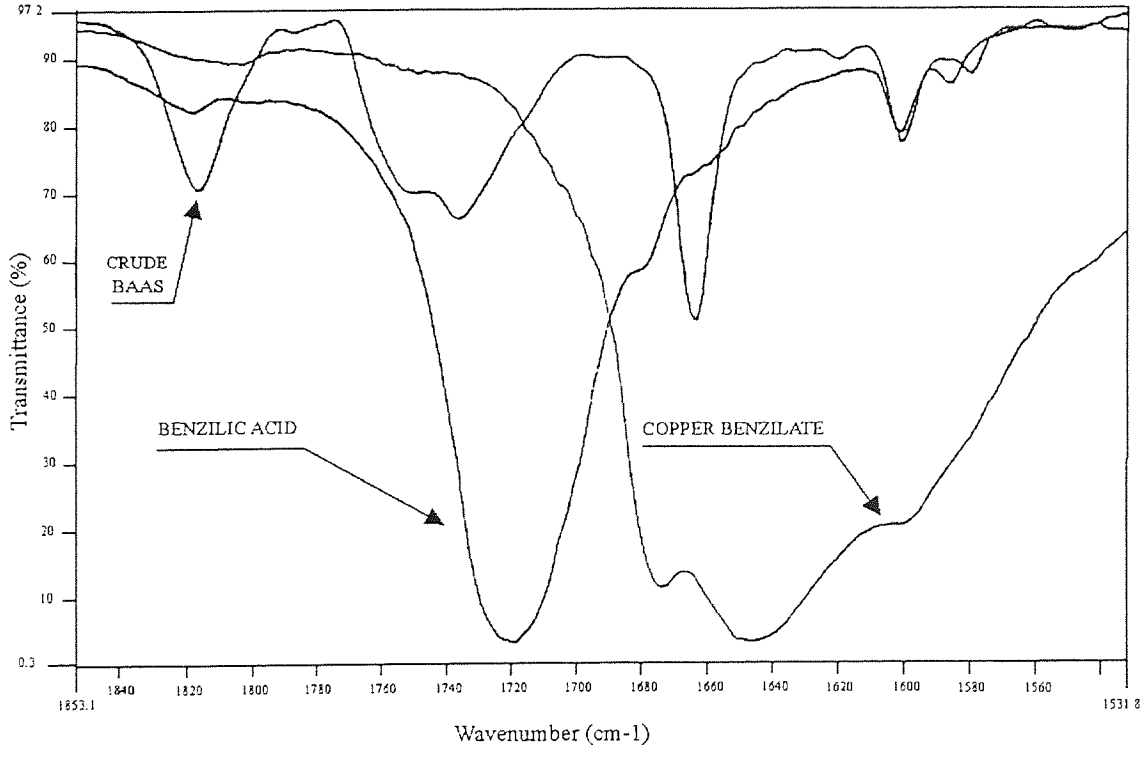

A vacuum distillation was first performed on crude BAAS. No distillate was obtained even at 100°C (0.1 mm/Hg). The commensurate disappearance of the FT-IR characteristic anhydrosulfite carbonyl peak of the sample indicated that decomposition of the anhydrosulfite had taken place. Therefore, crude BAAS was analysed by HPLC and TLC before 'Dry Flash' chromatography, with particular precautions, could be attempted in order to obtain BAAS sufficiently pure for polymerization.

3.3.1.2. HPLC analysis

The crude BAAS was analysed by HPLC, analysis of the eluent was by a UV diode array as detector (for more information see section 2). using a silica based reverse phase column with dry THF as solvent. Under such conditions, polar compounds are eluted before non-polar materials.

Three components eluted on the column appeared with very close retention times, as shown in table 3.15. Figure 3.37. shows the UV spectra of these components revealed by HPLC. They all display a spectrum that is consistent with an aromatic ring in the structure. The FT-IR data together with the UV spectrum of pure LAAS (in appendix) permitted the characterization of the different components, as presented in table 3.15.

Table 3.15. The components of crude BAAS revealed by HPLC.

Components	Retention time (min)	UV data λ_{max} (nm)	Assignment
No 1	3.803	206	benzilic acid
No 2	4.049	212	copper (II) benzilate
No 3	4.252	204 - 250	BAAS

Figure 3.38. UV spectra of the components present in crude BAAS.

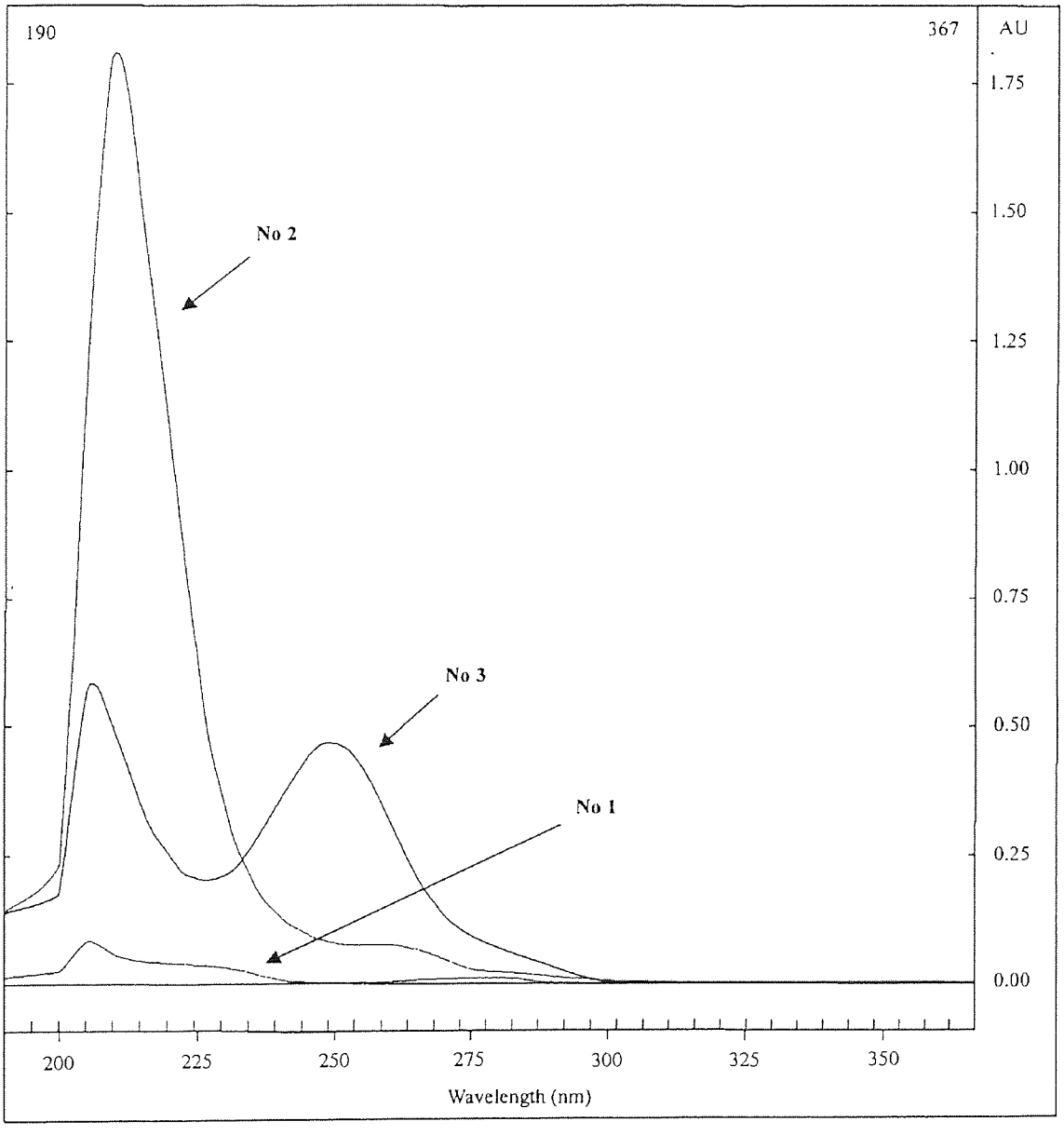

3.3.1.3. TLC analysis

TLC analyses of crude BAAS were carried out with different solvents so as to determine the best solvent system for separation by 'Dry Flash' Chromatography. Volume of the

different fractions to be collected was also estimated. The TLC silica plates were supplied by Merck. Dried solvents like tetrahydrofuran (THF), diethyl ether, chloroform and hexane in different combinations were used.

Because the different spots were naturally coloured, there was no need of staining agent. The analysis of the different TLC showed that THF:Hexane was most efficient for separating the best the different components and probably four compounds were present in the red oil. From the FT-IR data, three of them could be attributed to BAAS, benzilic acid and the copper salt, the fourth compound was supposed to be a chlorine-containing impurity.

Small fractions (20 ml) were found necessary to separate the different compounds because of the closeness of the different spots, as shown in figure 3.39.

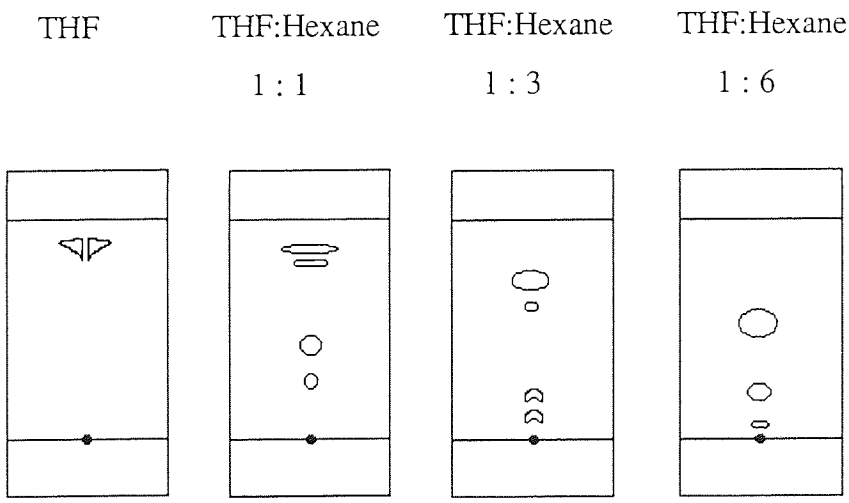

Figure 3.39. TLC plates with unpurified BAAS.

3.3.1.4. 'Dry Flash' Column Chromatography with silica as adsorbant

As anhydrosulfites are very sensitive to water and decompose quickly to the corresponding acid in its presence, rigorous precautions were taken to exclude moisture in the process. All glassware was left in the oven at 240°C for 24 hours prior to use and

the solvents were dried as described in section 2. The procedure was carried out in an 'Atmosbag' containing argon.

The packing material for the column was silica gel which was dried at 240°C for several hours so as to remove the 10-20 % water that it usually contains and also to increase its activity as adsorbant.

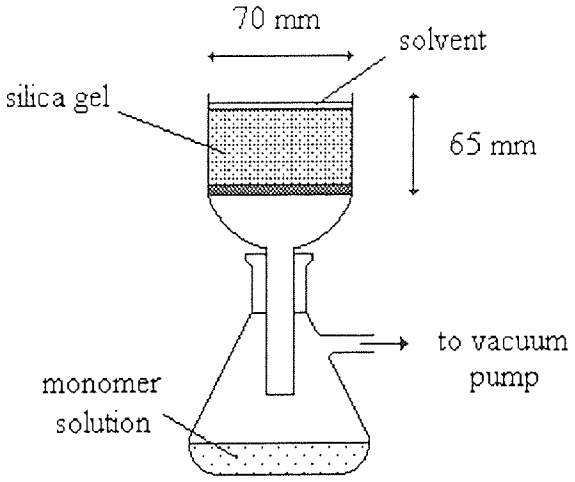

Figure 3.40. 'Dry Flash' Chromatography apparatus.

A grade 3 porosity sintered glass funnel, with a 'quickfit' joint was fitted to a Buchner flask, as shown in figure 3.40., and filled with a slurry of around 30 g of TLC standard grade silica gel without binder (supplied by Aldrich Co.) in THF:Hexane (1:6). Suction was applied using a vacuum pump until the packing was dry. It was then pressed down with a large stopper to ensure good packing and provide a smooth, flat surface. The column was loaded with the crude product and sucked dry. Previous TLC data was used to select the solvent system. The column was then washed with 20 ml fractions of THF:Hexane of increasing polarity 1:6 to 1:1 and finally pure THF. The different samples collected were checked by TLC before evaporation. The first two components to pass through were analysed by FT-IR and found to be the copper (II) salt and the acid followed by the anhydrosulfite decomposed into the acid. There was no indication of a fourth component.

In conclusion, it turned out to be impossible to purify BAAS under these conditions. The retention times of the different components present in the crude product were too close and the sensitivity of the anhydrosulfites to water and acidic compounds, together with being the third component to be eluted were making the purification more difficult.

3.3.2. Mandelic acid anhydrosulfite (MAAS)

3.3.2.1. Experimental

Under the same reaction conditions as copper benzilate, the copper (II) salt of mandelic acid was converted by reaction with thionyl chloride to a dark brown liquid which contained insoluble particules, copper by-products which could be separated from a yellow liquid by centrifugation. The FT-IR spectrum of the liquid phase shown in figure 3.41. exhibited two strong carbonyl peaks at 1823 and 1735 cm^{-1} which corresponded respectively to the anhydrosulfite and probably one of its derivative ester. Distillation under reduced pressure (100°C, 0.1 mm/Hg) to obtain product was then attempted without success.

Figure 3.41. FT-IR spectrum of crude MAAS

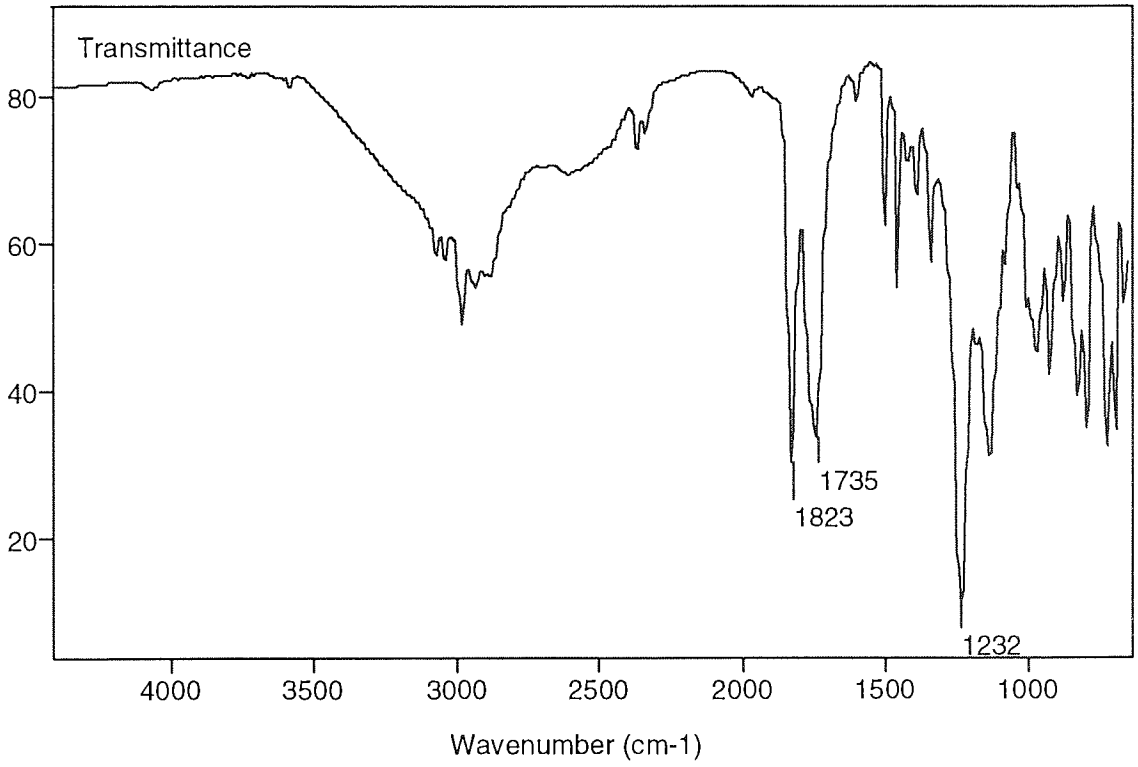

Despite care being taken to store it in dry conditions and at low temperature, when left overnight this product decomposed to white crystals, probably due to the presence in excess of thionyl chloride.

These crystals were separated and purified by successive washing with THF before analysing them by FT-IR and NMR spectroscopy. The FT-IR spectrum is presented in appendix whereas the ^{1}H and ^{13}C NMR spectra are shown in figures 3.42. and 3.43. with their corresponding peak tables 3.16 and 3.17.

Analysis of the NMR spectra allowed determination of this decomposition product, as mandelic acid chloride with its methine carbon resonance at 58.64 ppm characteristic for a CH-Cl, which resonance differs from a peak between 70 - 80 ppm for CH-OH.

Consequently, the purification was effected just after the synthesis, before any decomposition could take place.

Figure 3.42. ^{1}H NMR spectrum of the decomposition product of MAAS.

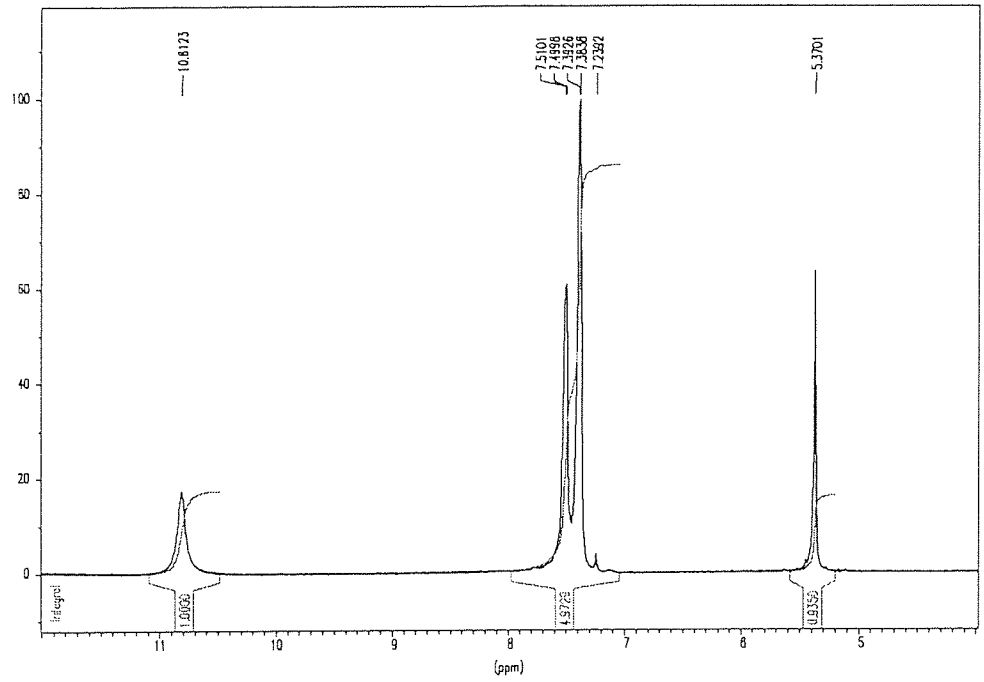

Table 3.16. ^{1}H NMR data of the decomposition product of MAAS.

δ.ppm	Peak shape	Relative peak area	Assignment
5.37	singlet	0.94	CH
7.23 - 7.51	multiplet	4.97	C_6H_5
10.81	singlet	1.00	OH

Figure 3.43. ^{13}C NMR spectrum of the decomposition product of MAAS.

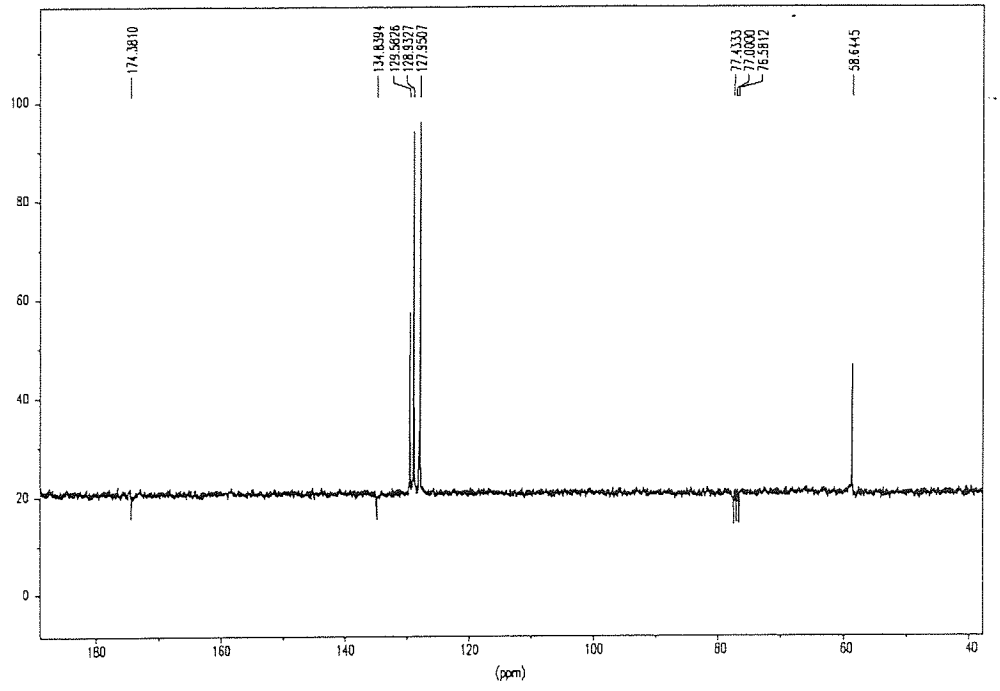

Table 3.17. ^{13}C NMR data of the decomposition product of MAAS.

δ.ppm	Assignment
58.64	CH
127.95 - 134.83	C_6H_5
174.38	C = O

3.3.2.2. HPLC analysis

Immediately after its synthesis, the crude MAAS was analysed by HPLC using the same reverse phase column as for BAAS and dry THF as solvent. Two components were revealed on the chromatogram with very close retention times on the column, as shown in table 3.18. Figure 3.44. shows the UV spectra of the two components.

Table 3.18. The components of crude MAAS revealed by HPLC.

Components	Retention time (min)	UV data λ_{max} (nm)	Assignment
No 1	4.319	208 - 270	MAAS
No 2	4.135	208	ester by-product

Figure 3.44. UV spectra of components present in crude MAAS and revealed by HPLC.

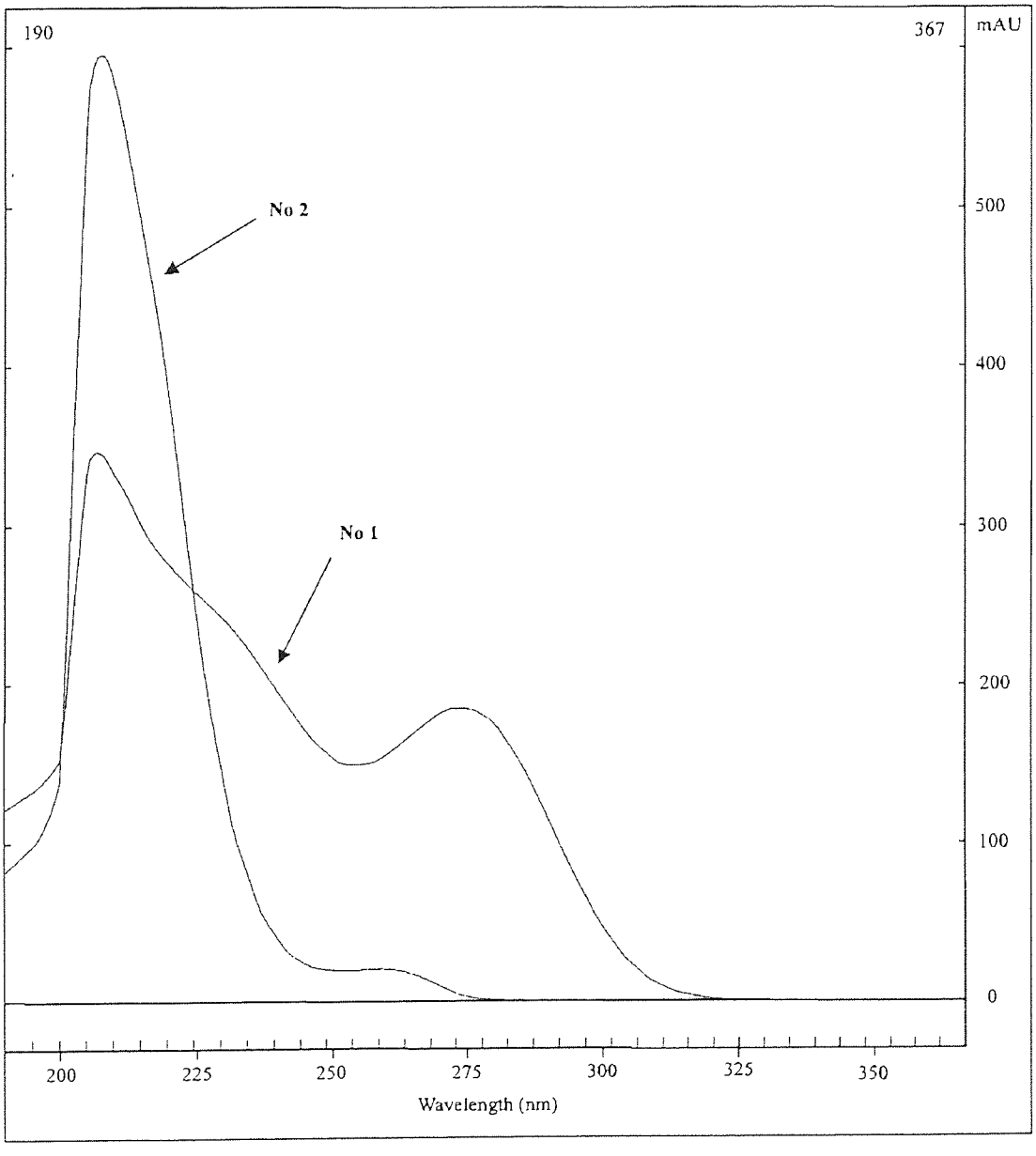

3.3.2.3. TLC analysis

TLC was used to analyse crude MAAS and silica was replaced by neutral alumina in order to prevent decomposition on the column packing. Silica usually contains about 10-20 % water and is acidic in nature whereas alumina possess very little water (The TLC alumina sheets were purchased from Merck Co).

A range of solvents was investigated in this analysis and amongst solvents like THF, diethyl ether, chloroform, dichloromethane, hexane, ethyl acetate and acetonitrile, the system, THF:hexane (1:2), turned out to be the most satisfactory, but the two spots were still very close.

Unlike BAAS, impure MAAS was not colored and a staining agent was necessary. A solution of 10 % phosphomolybdic acid in ethanol (supplied by Aldrich Co.) was applied to the plate in the form of a spray and then heated. The reagent was usually used for the detection of lipids, lactone, ketoacids, hydroxy acids and unsaturated fatty acids.

3.3.2.4. 'Dry Flash' chromatography with alumina as adsorbant

The precautions and the procedure were similar to those employed for BAAS (see in section 3.3.1.4.). Grade 1 aluminium oxide was purchased from BDH Co. The eluting system of solvent THF:hexane (1:2) was kept at this ratio throughout the process. The samples collected were checked by TLC before evaporation. MAAS could be slightly purified, the ester partially removed, as shown in figure 3.45. and only a small percentage of anhydrosulfite was obtained because of its partial decomposition.

Figure 3.45. FT-IR spectrum of MAAS after flash chromatography

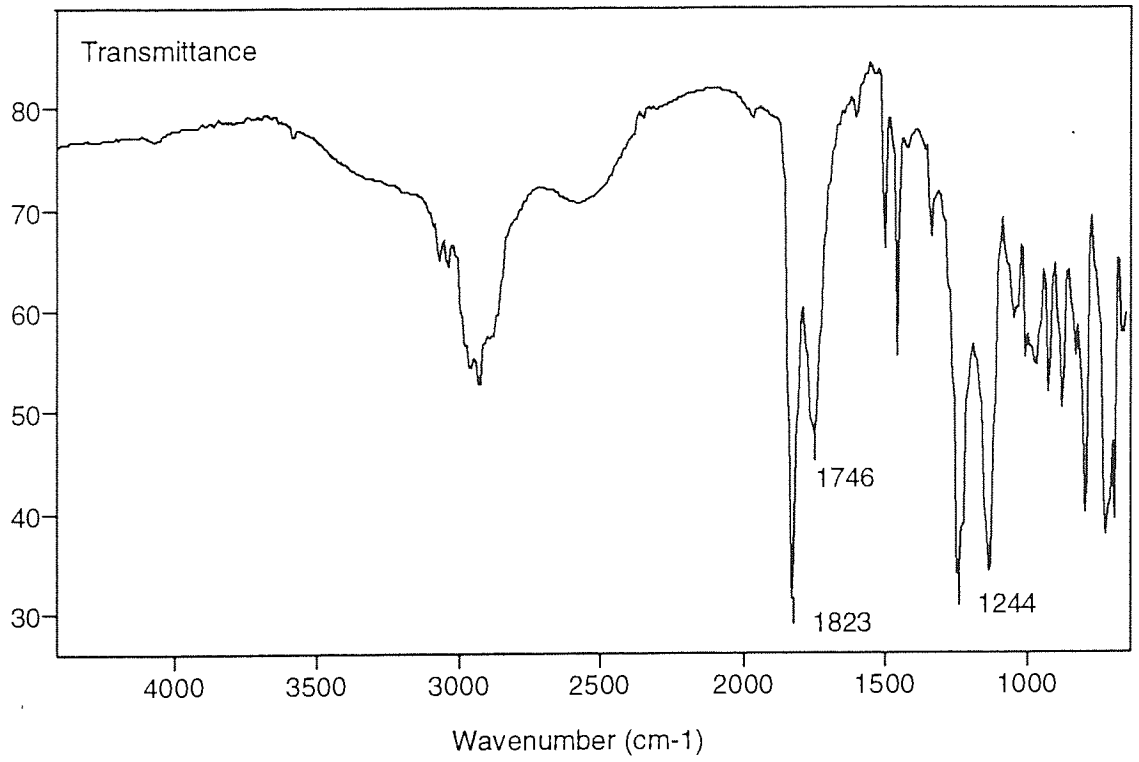

When the fractions resulting from the flash chromatography were analysed by TLC, a new spot was discovered at the solvent front as early as the second fraction and was present in all the following fractions. This new product turned out to have an FT-IR carbonyl absorption in infrared at 1807 cm^{-1} and was always mixed with the ester derivative (carbonyl absorption at 1749 cm^{-1}), as shown in figure 3.46. This new carbonyl peak at the wavelength 1807 cm^{-1} corresponds presumably to the α-chloro mandelic acid.

Figure 3.46. FT-IR spectrum of MAAS when decomposed in flash chromatography

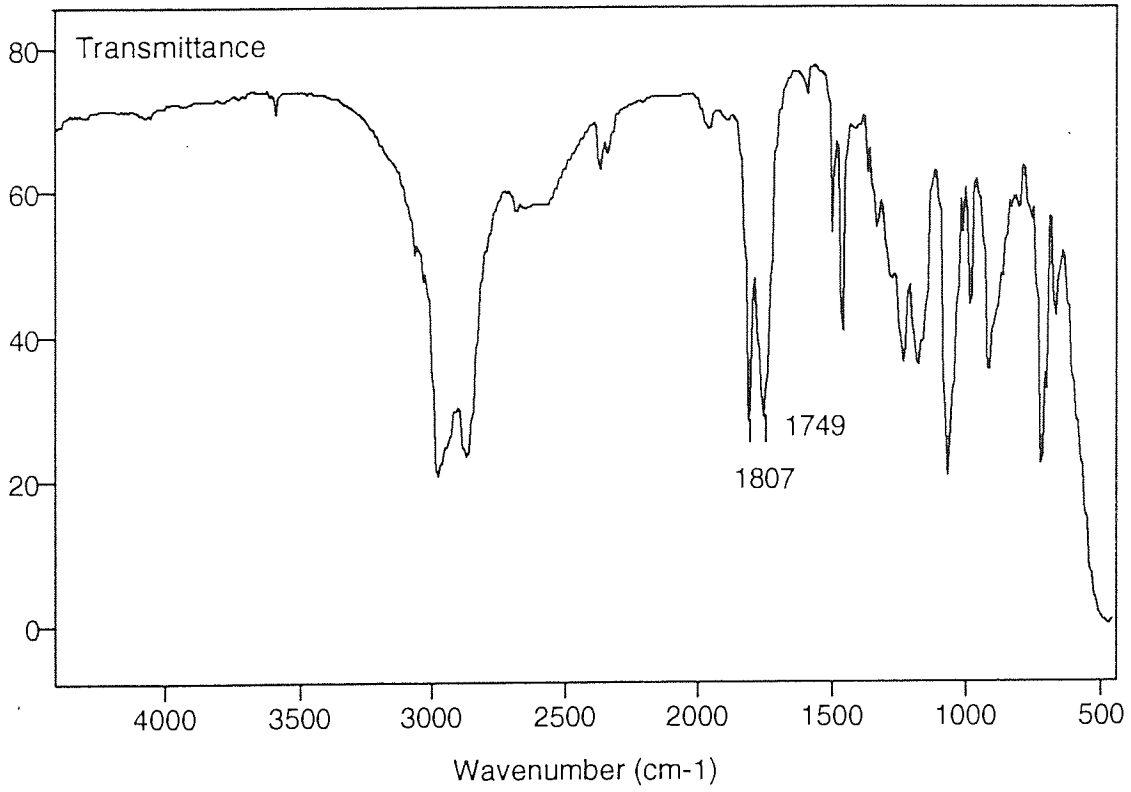

In conclusion, it was found to be impossible to separate MAAS from its ester derivative under these conditions. The requirements for successful purification could not be reached. A relatively fast process involving a short stay in the packing material was recommended to prevent any decomposition of MAAS whereas several repeated chromatography were necessary to enable a complete separation of the two similar compounds.

Accordingly, a relatively slower elution chromatography on an alumina gel column was investigated.

3.3.2.5. Elution Chromatography on an alumina gel column

The column was constructed from a length of wide bore glass tubing tapered at one end and attached at the head by a regulating device for controlling the pressure by hand, as shown in figure 3.47. For security, the column was wrapped in adhesive tape.

The eluting system of solvent was again THF:hexane (1:2) and neutral alumina the adsorbant.

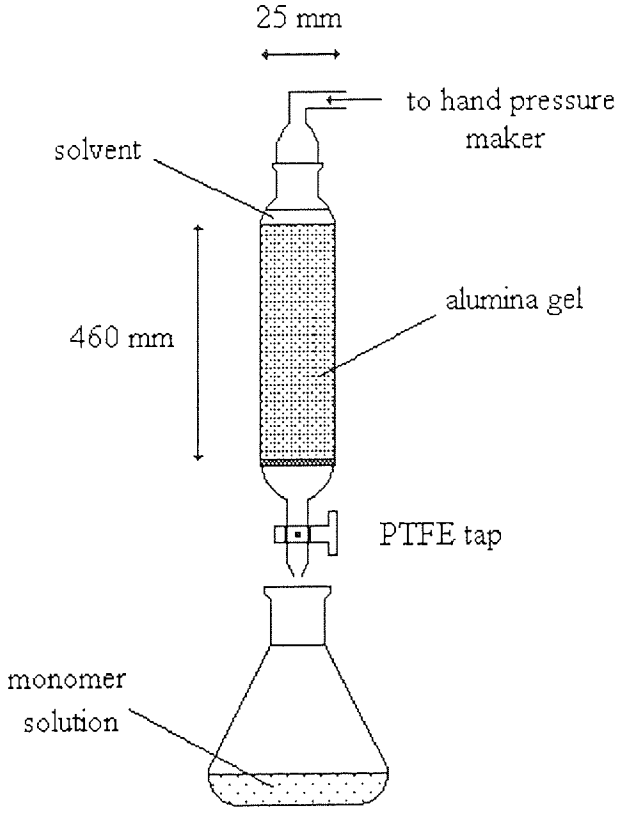

Figure 3.47. Elution Chromatography apparatus.

The purification was unsuccessful, the material obtained at the end of the column was the anhydrosulfite decomposed to the α-chloro acid, as shown by its characteristics FT-IR carbonyl absorption at around 1807 cm^{-1}.

Pure MAAS could not be obtained by 'Dry Flash' chromatography. An ester derivative was always present and attempts to separate them with elution column chromatography ended in decomposition of the anhydrosulfite to the α-chloro acid.

CHAPTER 4

POLY(LACTIC ACID) SYNTHESIS

4.1. Experimental

4.1.1. Procedure

Since the anhydrosulfite monomers were very sensitive to water and the propagating growing carbanions (or carbanion pairs) were extremely reactive towards traces of oxygen, water or carbon dioxide, great care was taken in purification and drying of the solvent, in cleaning and drying of the glassware and also in handling the initiator solutions under dry atmosphere, as described in section 2. Thereby, all polymerization experiments were also conducted under argon and the temperature was kept constant.
The diagram of the polymerization vessel used in this study is shown in figure 4.1. This vessel, equipped with a magnetic stirring bar, was attached to the vacuum line at (B) and evacuated before filling it with argon through tap (C). Water at constant temperature was continually passed through the double jacket. Then the polymerization could be carried out according to one of the following procedures.

Procedure 1 : The desired amount of freshly distilled monomer in solution in THF was injected by syringe into the vessel through (A) and the required quantity of initiator, which was kept at the same temperature as the monomer, was subsequently injected through a suba seal stopper.

Procedure 2 : This procedure differs from procedure 1 in the order of injections of the different compounds involved in the polymerization. The solvent was first injected in the polymerization vessel, followed by the desired quantity of initiator. Shortly after, the

required amount of pure monomer was added into the vessel. All different injections were effected through suba seal stoppers (A).

In both procedures, the mixture was then further agitated for 6 minutes, this reaction time was chosen for reasons explained in the next section. Subsequently, the solvent (THF or toluene) was removed from the reaction products by simple evaporation. When the monomer was the mixture of the two enantiomers, a precipitation in hexane of the polymers produced was found to be necessary followed by filtration and drying in a dessicator for 5 hours.

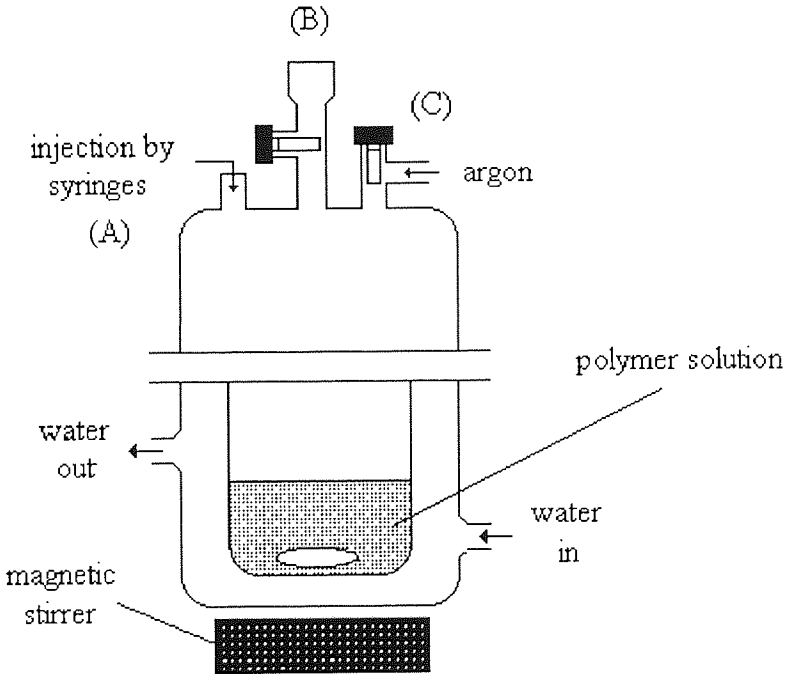

Figure 4.1. Diagram of the polymerization vessel.

Under similar conditions (initiator, monomer-to-initiator ratio, temperature), the molecular weight of polymers produced according to procedure 1 differed to those obtained with procedure 2, as presented in table 4.1. In procedure 1 the initiator was more efficient in comparison with procedure 2 where the initiator was further dissolved and likely to react with other species than the monomer present in the reaction medium, consequently higher molecular weight polymers were usually obtained for procedure 2.

Table 4.1. Differences between the two procedures in the polymerization of L-LAAS with butyllithium as initiator at 25°C.

Procedure	$\overline{M_{theor}}$ $10^{-3}.mol.g^{-1}$	$\overline{M_n}$ $10^{-3}.mol.g^{-1}$	$\overline{M_w}$ $10^{-3}.mol.g^{-1}$	$\overline{M_w}/\overline{M_n}$
No 1	6.84	6.0	6.9	1.15
No 2	6.62	7.3	8.0	1.09

0.04 mol of DL-LAAS, 10 ml of THF, 4 10^{-4} mol of n-BuLi,
$[n\text{-BuLi}]_0$ = 1.6 M in hexanes, procedure 2.

4.1.2. Time of reaction

The ring-opening polymerization of anhydrosulfites is an exothermic process. Therefore a system which records the temperature change allows the extent of polymerization to be followed. In this way, the kinetics of polymerization can be defined and the end of the reaction established.

However, the experiment described below was performed with the aim of determining a suitable reaction time only, even though in most anionic polymerizations of anhydrosulfites carried out in this work, the appearance of bubbles in the reaction medium, originating from the release of sulphur dioxide during polymerization (see mechanism in section 4.4.) was a visual indication of the polymerization taking place and thereby the end of the reaction could be assumed when evolution had stopped.

The increase in temperature associated with the ring-opening polymerization was measured using a GL23 2kΩ thermocouple (supplied by RS Components Ltd.). The change in resistance as a function of temperature was measured by a Knauer auto potentiometer bridge itself linked to a Servoscribe IS Chart recorder. After calibration the apparatus was found to have a linear sensitivity to increases in temperature.

In a typical experiment, the vessel in figure 4.1. was filled with argon after evacuation as described previously. A thermistor placed in the reaction medium was connected to the

potentiometer bridge. Water from a thermostated bath at 25°C was continually passed through the double jacket. The balancing bridge was connected to chart recorder and the whole system was left to equilibrate for 20 minutes at 25°C.

When the bridge was adjusted to zero and a stable line was obtained on the chart recorder, the required amount of initiator was injected by a syringe through the suba seal.

Figure 4.2. Typical of the calorimetric trace of LAAS polymerization

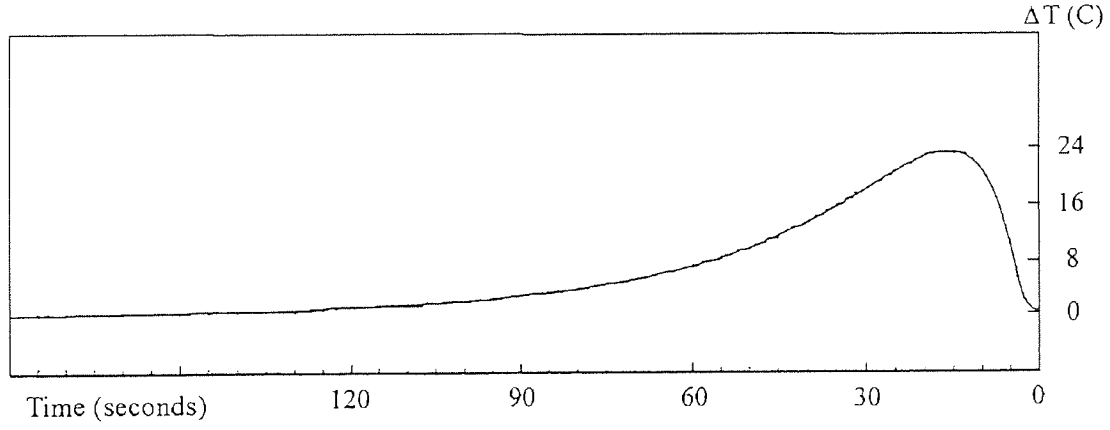

The trace of deflection against time obtained for a typical polymerization of LAAS is shown in figure 4.2. At the time zero the initiator is injected and soon after, polymerization takes place generating heat and causing a rise in temperature on the chart recorder. Then when the temperature maximum is reached, after a few seconds, the end of the polymerization is assumed and the cooling down of the system occurs.

Consequently, after the addition was realized, the mixture was further agitated for 6 minutes knowing that the polymerization of lactic acid anhydrosulfite was completed within a minute, as shown in figure 4.2.

4.2. Comparison of different initiator systems

The polymerization of anhydrosulfites can be carried out thermally [26-41] or by using pyridine as initiator [44,46] but control over those catalyst systems was difficult and only low molecular weight polymers were produced. In addition, polymerization involving multicomponent catalyst systems, described as proceeding by a coordinated anionic process were found unsuccessful for lactic acid anhydrosulfite [50].Therefore, conventional anionic initiators and cationic systems were investigated for the polymerization of anhydrosulfites.

4.2.1. Anionic initiators

Different anionic initiators such as alkali metal alkoxides, amides and alkyls were used to initiate the polymerization of L-LAAS.

All the following polymerizations were carried out in THF according to procedure 1 and the temperature was kept constant at 25°C in order to compare the different initiator systems.

4.2.1.1. Alkali metal alkoxides

Alkali metal alkoxides are important as catalysts for polymerization of organic carbonyl or unsaturated monomers. Because of the strong electronegative character of oxygen, they exhibit a strong polar character and thus the metal-oxygen bonds are highly ionic [70]. But, the metal-oxygen-carbon bonds are also affected by the nature of the alkyl group with its electron releasing tendency (the + I inductive effect) which makes the bond less polar.

On the other hand, metal alkoxides very easily undergo hydrolysis reactions which lead to the formation of hydroxides or hydrated oxides and when only a small amount of

water is available, a partial hydrolysis occurs yielding oxide alkoxides $MO_n(OR)_x$ [71]. Consequently great care was taken in the preparation of the initiator solution in THF.

Two solutions with dried THF as solvent were prepared one containing the freshly distilled monomer and the other the alkali metal alkoxide precautiously preserved from air and moisture. They were then used in different amounts in the polymerization of L-LAAS with potassium *tert*-butoxide as initiator.

The results obtained for this series of polymerization are shown in table 4.2. The yields of polymer were high and the molecular weights generally low. As illustrated in figure 4.3., the molecular weight distributions were bi-modal when the monomer-to-initiator ratio was above 200. In the case of bi-modal molecular weight distributions, the figures in the table 4.2. refer to the estimates of the molecular weights of the two fragments.

Table 4.2. Polymerization of L-LAAS with potassium *tert*-butoxide as initiator at 25°C.

Sample No	[M] $mol^{-1}.dm^3$	[I] $mol^{-1}.dm^3$	[M] / [I]	$\overline{M_n}$ $10^{-3}.mol.g^{-1}$	$\overline{M_w}$ $10^{-3}.mol.g^{-1}$	$\overline{M_w}/\overline{M_n}$	Yield %
1	1.05	1.9	60	4.8	11.3	2.35	-
2	1.30	6.3	200	7.5	10.8	1.45	90
3	1.33	5.2	250	10.7 5.8	12.3 7.3	1.14 1.26	94
4	1.35	4.4	300	20.9 9.1	22.3 10.4	1.07 1.14	90
5	1.37	3.8	350	20.6 10.0	21.3 10.7	1.03 1.07	-

$[L\text{-}LAAS]_0 = 1.5$ M, $[(CH_3)_3COK]_0 = 0.05$ M, THF as solvent.

Figure 4.3. GPC trace of L-PLAAS initiated with potassium *tert*-butoxide in THF at 25°C, [M] / [I] = 250.

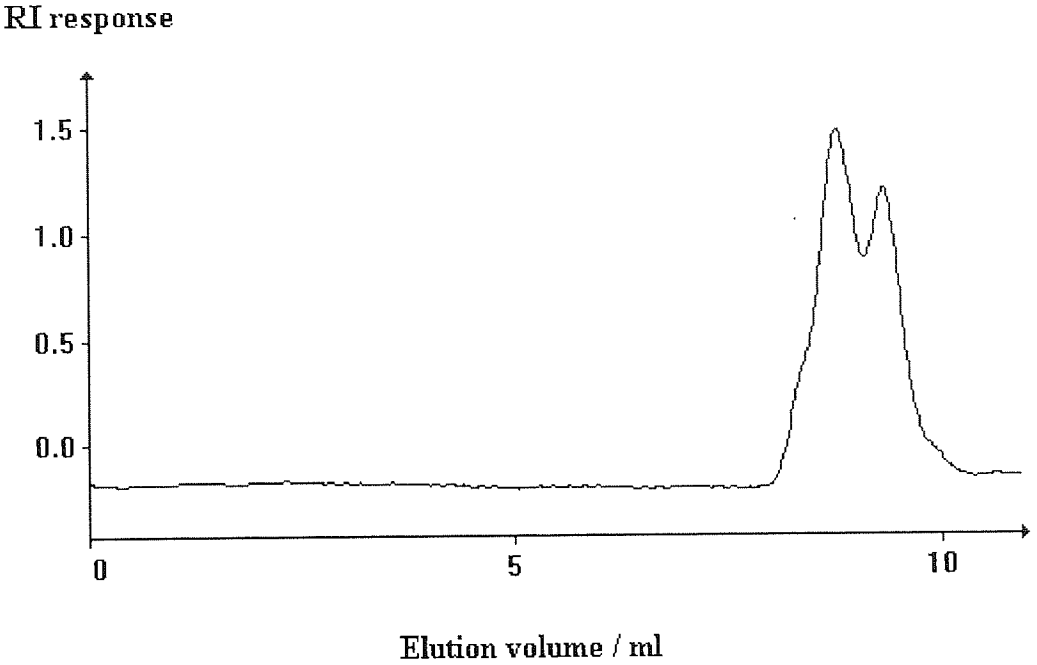

4.2.1.2. Alkali metal amides

It was reported that tertiary amines (e.g. triethylamine, pyridine) and tertiary amides (e.g. N.N-dimethylformamide) initiate the polymerization of anhydrosulfites at room temperature [46]. L-LAAS was polymerized using lithium diisopropylamide as initiator, the results are listed in table 4.3. Again the yields of polymer were high but all the molecular weight distributions were bi-modal, probably because of the presence of two different propagating species in the polymerization mixture, as explained in section 4.4. in greater detail. It is interesting to note that the molecular weight distributions of the individual component polymers are quite narrow. This suggests that each propagating species taken individually will yield polymers of narrow molecular weight distribution.

Additionally, by adding more monomer in the reaction mixture after 6 minutes when the polymerization was complete, an increase of the molecular weight was observed, as shown in table 4.3. Thus, this system seemed to be living.

Table 4.3. Polymerization of L-LAAS with lithium diisopropylamide as initiator at 25°C.

Sample No	[M] $mol^{-1}.dm^3$	[I] $10^3.mol^{-1}.dm^3$	[M] / [I]	$\overline{M_n}$ $10^{-3}.mol.g^{-1}$	$\overline{M_w}$ $10^{-3}.mol.g^{-1}$	$\overline{M_w}/\overline{M_n}$	Yield %
6	1.28	8.7	150	9.8 5.0	10.4 6.0	1.06 1.19	91
7	1.40	4.7	300	12.2 6.5	12.9 7.5	1.06 1.17	89
8	1.44	3.7	410	14.4 7.5	15.6 9.9	1.08 1.33	99
7 + inj(LAAS)	1.46	2.7	480	19.9 9.4	20.9 11.2	1.05 1.19	99

$[L\text{-}LAAS]_0 = 1.5$ M, $[((CH_3)_2\text{-}CH)_2N\text{-}Li]_0 = 0.05$ M, THF as solvent,

7 + inj(LAAS) : addition of monomer L-LAAS in the polymer 7 after completion (6 minutes).

4.2.1.3. Alkali metal alkyls

The properties of lithium alkyls have been studied and indicate a rather complex behaviour [72,73]. Association of organolithium compounds in non polar solvents is known to take place. Hexameric association was found when the alkyl group was primary whereas *tert*-butyl lithium was tetrameric. The lithium atoms are in the aggregate centre surrounded by the alkyl groups, each of which appears to be bonded to more than one lithium. Although the bonding type in the lithium alkyls is not simple, the carbon-lithium bond is partly covalent and an ionic dissociative process is possible.

In contrast, associations in basic solvents like ether and THF are very difficult to investigate because of the extreme reactivity of the organolithium reagent towards the solvent. It was previously [74] reported that butyllithium reacts smoothly with THF to give butane, ethylene and the lithium enolate of acetaldehyde, as shown in figure 4.4.

Figure 4.4. Reaction of butyllithium with THF

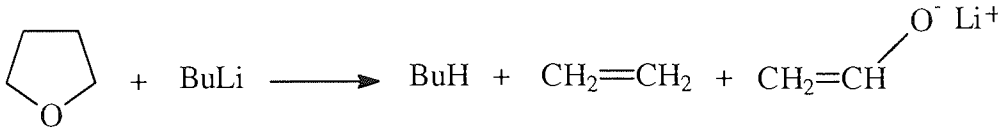

In the polymerization of lactic acid anhydrosulfite with *sec*-butyllithium, higher molecular weights of polymer were obtained and with the exception of sample 1 the molecular weight polydispersities were approximatively 1.5, as shown in table 4.4. The efficiencies of the initiator were lower. The lithium alkyls are stronger nucleophiles than the alkoxides and amides and so will react with any impurities present in the polymerization. But this is a minor effect compared to their reaction with basic solvents like THF. Consequently, a smaller amount of initiator is available for the polymerization and higher molecular weight polymers are produced.

Table 4.4. Polymerization of L-LAAS with *sec*-butyllithium as initiator at 25°C.

Sample No	[M] $mol^{-1}.dm^3$	[I] $10^2.mol^{-1}.dm^3$	[M] / [I]	$\overline{M_n}$ $10^{-3}.mol.g^{-1}$	$\overline{M_w}$ $10^{-3}.mol.g^{-1}$	$\overline{M_w}/\overline{M_n}$	Yield %
10	2.26	6.0	40	3.5	10.9	3.14	92
11	2.33	2.0	110	21.6	32.1	1.49	99
11 + inj(LAAS)	2.34	1.4	170	25.1	38.5	1.54	99

$[L\text{-}LAAS]_0$ = 2.5 M in THF, $[C_2H_5\text{-}CH(CH_3)\text{-}Li]_0$ = 1.45 M in cyclohexane,

11 + inj(LAAS) : addition of monomer L-LAAS in the polymer 11 after completion (6 minutes).

When *tert*-butyllithium was used as initiator in this polymerization, higher molecular weights were obtained and the molecular weight polydispersities were approximately 1.5, as shown in table 4.5. The efficiencies of the initiator were even lower than those of *sec*-

butyllithium, being an evidence that the initiator, as a stronger nucleophile, reacted even more strongly with THF and any impurities present in the polymerization.

Table 4.5. Polymerization of L-LAAS with *tert*-butyllithium as initiator at 25°C.

Sample No	[M] $mol^{-1}.dm^3$	[I] $10^2.mol^{-1}.dm^3$	[M] / [I]	$\overline{M_n}$ $10^{-3}.mol.g^{-1}$	$\overline{M_w}$ $10^{-3}.mol.g^{-1}$	$\overline{M_w}/\overline{M_n}$	Yield %
13	3.22	4.1	80	16.1	26.3	1.64	77
14	3.25	2.8	120	30.8	45.6	1.48	91
15	3.27	1.3	250	37.7	70.9	1.88	97

$[L\text{-}LAAS]_0$ = 3.3 M in THF, $[(CH_3)_3C\text{-}Li]_0$ = 1.7 M in pentane.

As illustrated in figure 4.5., the molecular weights did not parallel the theoretical molecular weights or the monomer-to-initiator ratio ([M] / [I]). Thus, this polymerization did not seem to obey the typical linear dependence of a 'living' polymerization. Nevertheless, when some more monomer was added to the polymerization mixture (polymer 11 in table 4.4.), the molecular weight of polymer increased, meaning that this system was living.

Figure 4.5. Polymerization of L-LAAS with *tert*-butyllithium at 25°C.

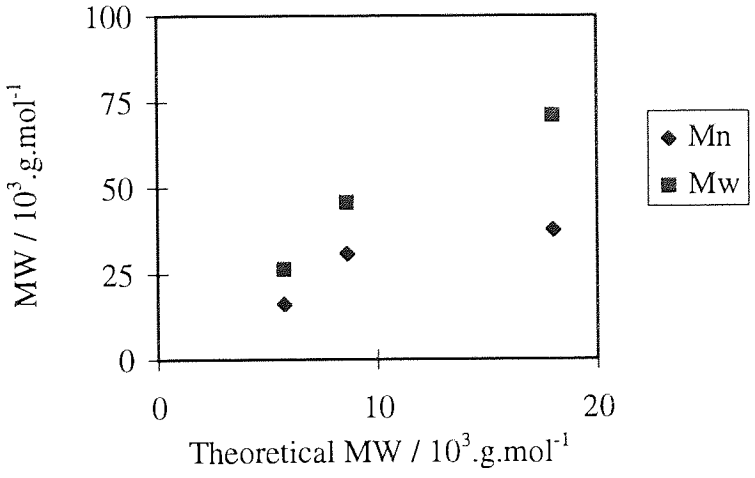

The polymerization of anhydrosulfites with alkali metal alkyl initiators proceeded with good yields and showed great promise as an initiator system for the synthesis of poly(α-esters) by ring-opening polymerization.

4.2.2. Cationic initiator

4.2.2.1. Experimental

The experimental conditions were similar to those used in the anionic-catalysed polymerizations. Two solutions were prepared, one containing trifluoromethanesulfonic acid (triflic acid) in dichloromethane and the other L-LAAS in THF. Two polymerizations of L-LAAS were then carried out according to procedure 1.

In these experiments, there was no appearance of bubbles (sulphur dioxide released during polymerization) in the reaction medium when the initiator was injected in the polymerization vessel, as usually observed in the anionic polymerization of LAAS. This was a sign that no polymerization of LAAS had occurred. Consequently, the reaction mixture was stirred for 30 minutes instead of 6 minutes. Then, the samples were left to evaporate overnight.

4.2.2.2. Results & Discussion

The results for the cationic polymerization of L-LAAS with triflic acid are presented in table 4.6. Polymers of $\overline{M_n} \approx 7000$ were detected by GPC and analysis of the ^{1}H and ^{13}C NMR spectra of these materials, presented in the appendix, showed that the polymers produced were poly(THF) only. Triflic acid is known to initiate the ring-opening polymerization of cyclic ethers.

Table 4.6. Polymerization of L-LAAS with triflic acid as initiator.

Sample No	[M] $10^{-2}.mol^{-1}.dm^3$	[H] $10^{-2}.mol^{-1}.dm^3$	[M] / [I]	Temperature °C	Observation
16	1.52	2.7	40	25	No L-PLAAS
17	1.52	10.8	10	50	No L-PLAAS

$[L\text{-}LAAS]_0 = 1.5$ M in THF, $[CF_3SO_3H]_0 = 0.7$ M in dichloromethane.

Thus, the cationic polymerization with the strong acid, triflic acid, has been attempted without success for the polymerization of L-LAAS, although the proton could have reacted with the different oxygen atoms present in the molecule and sulphur dioxide as a good leaving group would have permitted the propagation to proceed.

4.2.3. Discussion

A wide range of anionic initiators may be used to initiate the polymerization of L-lactic acid anhydrosulfite whereas triflic acid as a cationic initiator was found inefficient to polymerize L-LAAS.

Although the yields of L-polylactic acid were all relatively high, the molecular weights and the molecular weight distribution of L-PLAAS depended on the nature of the initiator. Bi-modal polymers were obtained with lithium diisopropylamide and potassium *tert*-butoxide (for a monomer-to-iniator ratio above 200). This was probably caused by the presence of two propagating species in the polymerization medium. In contrast, uni-modal polymers were produced with *sec*- and *tert*-butyllithium.

The molecular weights of L-PLAAS appeared to increase when the initiator was a strong base and also to depend on the monomer-to-initiator ratio, so that a control of the molecular weight might be possible. In addition, the molecular weights of L-PLAAS

were higher than predicted, probably because of the occurrence of side-reaction between alkyl lithium and THF.

Thus, alkyl lithium turned out to be more successful than alkali metal alkoxides and amides. In particular, L-polylactic acid of relatively high molecular weight, $\overline{M_n}$ of 37700 was synthesised with *tert*-butyllithium at 25°C.

4.3. Effect of multiple additions of monomer on molecular weight distribution of polymer

In anionic polymerization, the mechanism for a number of monomers is comprised of chain initiation and chain propagation with no termination reactions, e.g. styrene [75]. In those polymerizations, the end groups remained active and these systems are so-called 'living'. Thereby, it was interesting to investigate the "living" character of the present system PLAAS by adding more monomer to the polylactic chains.

4.3.1. Experimental

Two solutions in THF were prepared, one containing the freshly distilled monomer L-LAAS ([M] = 1.5 M) and the other the initiator, potassium *tert*-butoxide ([I] = 0.05 M). At the start, 10 ml of the L-LAAS solution was introduced in the polymerization vessel before adding 2 ml of the initiator solution. The mixture was then further agitated for 6 minutes. Subsequently, 2 ml of this reaction mixture was extracted by a syringe and 2 ml of monomer solution was added. The polymer solution was left under stirring for 6 more minutes. This procedure was repeated for a number of subsequent additions.

4.3.2. Results

Figure 4.6. and table 4.7. show the molecular weight changes that took place in this type of experiment. The molecular weight increased when some more monomer was added at the completion of the polymerization. However, the molecular weight distribution became multi-modal after a few additions.

Figure 4.6. Multiple addition of monomer in the polymerization of lactic acid anhydrosulfite with potassium *tert*-butoxide as initiator at 25°C.

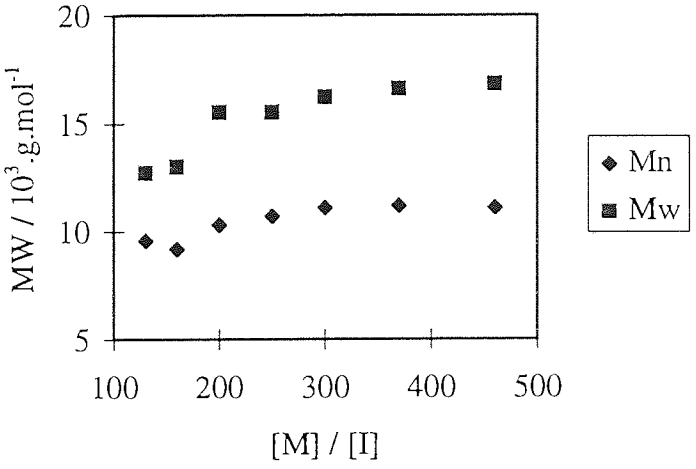

Table 4.7. Multiple addition of monomer in the polymerization of L-LAAS with potassium *tert*-butoxide at 25°C.

Sample No	[M] / [I]	$\overline{M_n}$ 10^{-3}.mol.g^{-1}	$\overline{M_w}$ 10^{-3}.mol.g^{-1}	$\overline{M_w}/\overline{M_n}$	Observation
20	130	9.6	12.7	1.33	uni-modal
20 + inj (LAAS)	160	9.2	13.0	1.42	bi-modal
21 + inj (LAAS)	200	10.3	15.5	1.51	multi-modal
22 + inj (LAAS)	250	10.7	15.5	1.46	multi-modal
23 + inj (LAAS)	300	11.1	16.2	1.46	multi-modal
24 + inj (LAAS)	370	11.2	16.6	1.48	multi-modal
25 + inj (LAAS)	460	11.1	16.8	1.51	multi-modal

4.3.2. Discussion

The results suggested that some propagating centres were still active and so addition of monomer on these chains was taking place whereas some other centres were undergoing termination reactions due to the inevitable presence of impurities and moisture.

But it appeared that the solvent THF might also be responsible for the termination of the chains. A similar decrease in reactivity of the carbanions of the 'living' polystyrene systems in THF was previously [76] reported, in particular, for the living α-methylstyryl potassium oligomers. This decay of the living carbanions was attributed to the occurrence of aging processes which involved reaction with the solvent THF, as presented in figure 4.7.

Figure 4.7. Decay of the living oligomers of α-methylstyrene

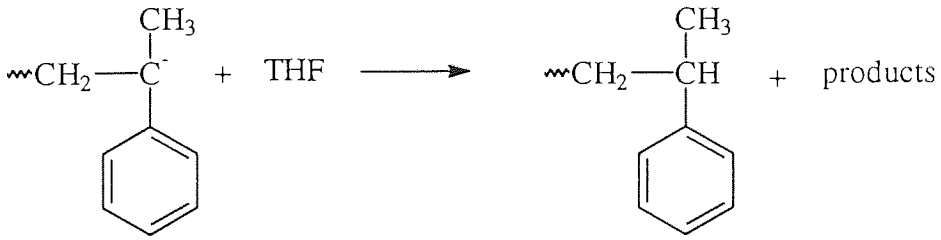

4.4. Mechanism for the anionic polymerization of lactic acid anhydrosulfite

The sheme in figure 4.8. may be proposed as a mechanism for the anionic polymerization of lactic acid anhydrosulfite initiated with alkyl lithiums. The polymerization mechanism is comprised of a rapid chain initiation and chain propagation with no real termination reaction, even though, in the previous section, the polymerization of L-LAAS did not appear to be totally 'living'.

The alkyl anion attacks the carbonyl atom in the monomer molecule with acyl-oxygen bond scission and formation of the alkyl end group. The active propagating species is thought to be an alcoholate. The further propagation proceeds via acyl-oxygen bond scission and the resulting alcoholate anions are regenerated after addition of each subsequent monomer molecule. The mechanism would be similar for alkali metal alkoxides and amides.

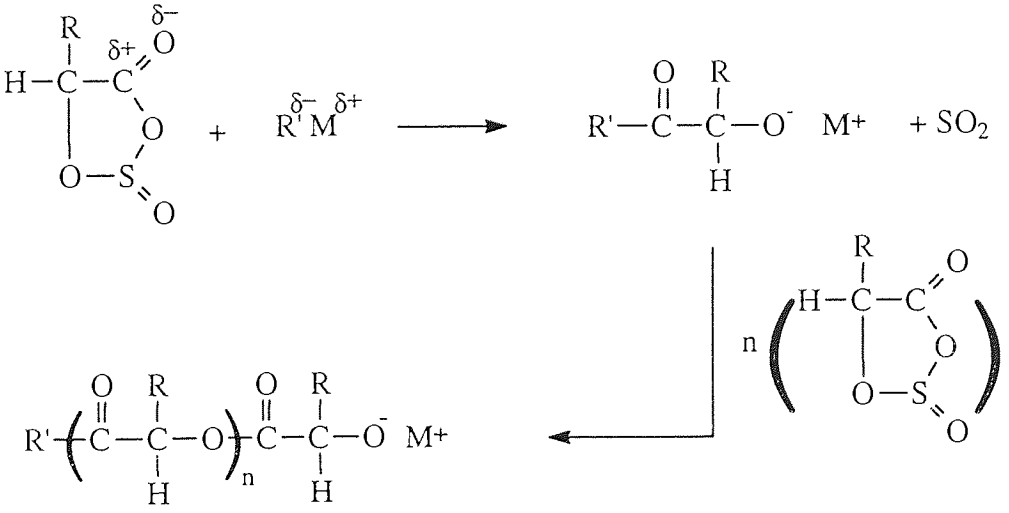

+ n SO_2

R' = alkyl, amide or alkoxide.

M = Li or K.

Figure 4.8. Mechanism for the anionic polymerization of aliphatic anhydrosulfites.

The propagating active centers in anionic polymerization are basically ion pairs. They can be present in several forms, as shown in figure 4.9., depending on the solvent, the temperature, and the counterion. These range from aggregated ion pairs to free solvated ions. Any of these forms can be active in the addition of monomer. Polar solvents (e.g. tetrahydrofuran, dielectric constant = 7.6) favour the three species on the right whereas non-polar solvents (e.g. hexane, dielectric constant = 1.9) the two on the left.

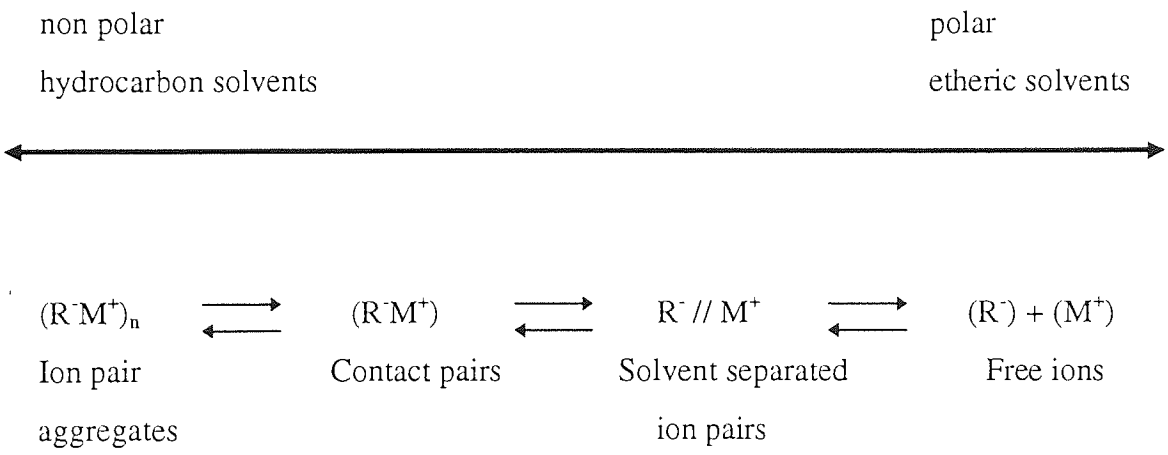

Figure 4.9. Effect of solvent polarity on nature of propagating species.

Since free ions react with the monomer much faster than ion pairs and covalent molecules, rates of propagation can be quite different. In addition, if the exchange between the species, ion pairs and free ions is slow, two polymers of different molecular weight may be produced. Therefore, bi-modality of the molecular weight distribution of polymers synthesised with initiators such as potassium-*tert*-butoxide and lithium diisopropylamide might be caused by the presence of two different active species in the polymerization medium.

4.5. Effect of solvent

A series of polymerizations of L- and DL-LAAS using butyllithium as initiator at 25°C were conducted in two different solvent, THF and toluene in order to investigate the effect of the solvent in this system.

4.5.1 Results

Solvents utilized in the polymerization were dried and distilled, prior to use, as described in section 2. The polymerizations were equally easily carried out in both solvent, THF and toluene. The polarity of the solvent did not appear to affect the structure of the polymers, but differences in molecular weight and molecular weight distribution were observed, in particular for L-PLAAS, as shown in table 4.8.

Table 4.8. Polymerization of L and DL-LAAS with n-BuLi in different solvents at 25°C.

Poly-α-esters	Solvent	[M] / [I]	$\overline{M_n}$ 10^{-3}.mol.g^{-1}	$\overline{M_w}$ 10^{-3}.mol.g^{-1}	$\overline{M_w}/\overline{M_n}$
L-PLAAS	THF	100	15.0	26.8	1.8
	Toluene		9.1	12.0	1.3
DL-PLAAS	THF	95	7.3	8.0	1.1
	Toluene		7.1	7.9	1.1

0.04 mol of L- and DL-LAAS, 10 ml of THF and toluene

$[n\text{-BuLi}]_0$ = 1.6 M in hexanes, procedure 2.

Also, the enantiomeric nature of the monomer had a profound effect on the molecular weight of polylactic acid. L-LAAS was found to yield higher molecular weight polymers than DL-LAAS under similar reaction conditions, as shown in table 4.8. This suggested that the mixture of enantiomers caused a hindrance in the polymerization and so polymerized less easily than the pure enantiomer. The relatively narrow molecular weight

distribution of PLAAS was also confirmed by GPC. As illustrated in figure 4.10., the polydispersities of polymers produced from DL-LAAS were close to 1.

Figure 4.10. GPC trace of DL-PLAAS initiated by n-BuLi in THF at 25°C.

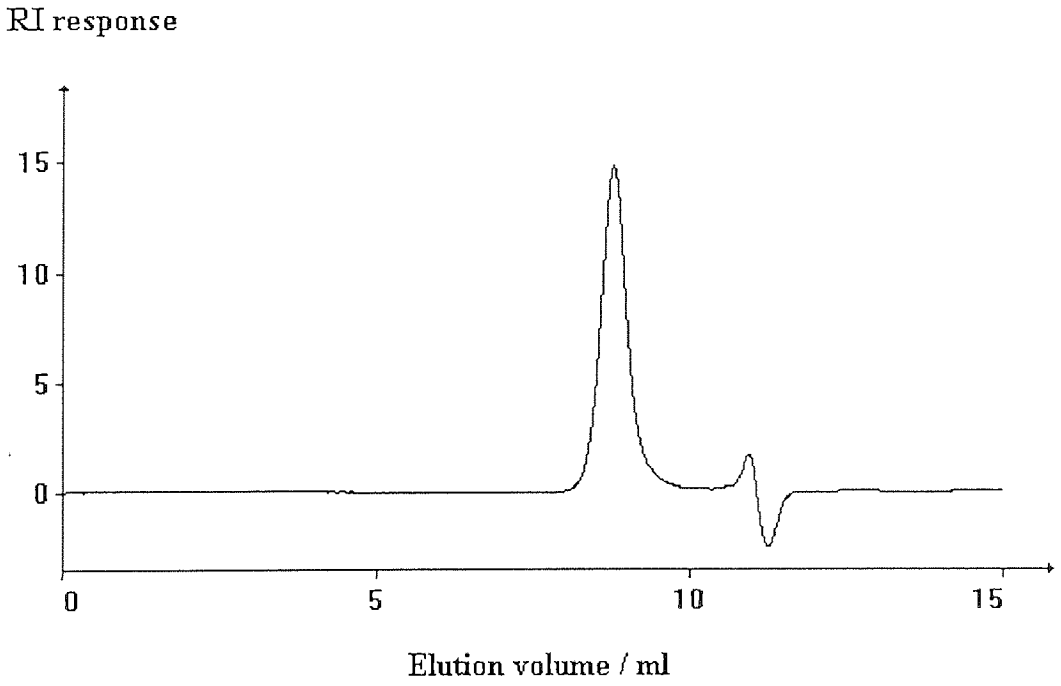

4.5.2. Discussion

Because the organolithium reagent is reactive towards solvents like ethers, as discussed in section 4.2.1.3., the amount of catalyst available for the initiation of monomers is reduced and so higher molecular weight polymers are synthesised in THF.

Moreover, as THF favours the presence of free ions, the carbanion or the active chain end is expected to be more reactive in THF than in toluene, as previously explained. This would mean a faster initiation reaction and so narrower polydispersities would be obtained. This is contrary to the results presented in table 4.8., in the case of L-PLAAS where the polydispersity was narrower when toluene was used. This can be explained if termination reactions occurred in THF, but not in toluene. This confirms that a reaction between THF and the active chain ends occurred, as discussed in section 4.3.2.

Different visual characteristics were also observed in these polymerizations depending on the solvent used. In THF, when the polymerization had occurred the mixture, initially transparent, was turned into a yellow solution, the sulphur dioxide was presumably trapped in THF. This was not the case in toluene. Additionally, when the monomer was the pure enantiomer, the polymer produced was highly crystalline and not very soluble in THF. So during polymerization, the mixture was turned into a solution containing insoluble particles whereas in toluene it was only more viscous.

Thereby, the solubility of the polymer may also be a factor that has to be taken into account, in particular this may be an explanation for the difference in polydispersities of L-PLAAS synthesised in THF or toluene, as shown in table 4.8.

4.6. Effect of the temperature

The molecular weight of polymers depended on the temperature, at which the polymerization was carried out and its evolution against temperature differed when the initiator used was potassium *tert*-butoxide or butyllithium.

4.6.1. Potassium tert-butoxide as initiator

4.6.1.1. Results

The polymerization of L-LAAS initiated with potassium *tert*-butoxide was performed at different temperatures according to procedure 1 and the molecular weights increased with temperature, as shown in tables 4.9. and 4.10. The values of initiator efficiency presented in these tables were calculated, as follow :

$$\text{Initiator efficiency} = \frac{[M]_0}{[I]_0} \times \frac{\text{conversion}}{\overline{x_n}}$$

with $\overline{x_n}$: number-average degree of polymerization

Table 4.9. Polymerization of L-LAAS with potassium *tert*-butoxide and [M] / [I] = 110 at different temperatures.

Temperature °C	$\overline{M_n}$ 10^{-3}.mol.g^{-1}	$\overline{M_w}$ 10^{-3}.mol.g^{-1}	$\overline{M_w}/\overline{M_n}$	Yield %	Efficiency of the initiator / %
30	6.7	8.8	1.32	78	92
40	10.5	18.2	1.73	99	75
50	10.4	14.1	1.36	94	72
60	10.7	14.5	1.35	92	68

$[L\text{-}LAAS]_o = 1.24$ M, $[(CH_3)_3COK]_o = 0.011$ M, THF as solvent, procedure 1.

Table 4.10. Polymerization of L-LAAS with potassium *tert*-butoxide and [M] / [I] = 200 at different temperatures.

Temperature °C	$\overline{M_n}$ 10^{-3}.mol.g^{-1}	$\overline{M_w}$ 10^{-3}.mol.g^{-1}	$\overline{M_w}/\overline{M_n}$	Yield %	Efficiency of the initiator / %
30	7.7	14.7	1.91	79	150
40	14.7	29.4	1.99	98	96
50	13.8	23.7	1.71	97	100
60	17.4	28.8	1.65	84	70

$[L\text{-}LAAS]_o = 1.4$ M, $[(CH_3)_3COK]_o = 0.007$ M, THF as solvent, procedure 1.

4.6.1.2. Discussion

A decrease of the efficiency of the initiator was observed when the temperature was increased. Probably the reaction between the initiator and the impurities was favoured at higher temperature leading to less available catalyst for the initiation of monomers, and as a result, the molecular weights of polymers produced were higher.

As more time is needed for polymerization to complete at higher monomer-to-initiator ratio, the chance for termination reactions to occur is expected to be greater. This is probably the reason why the polydispersities of polymers for a monomer-to-initiator ratio of 110 were narrower than those obtained for a ratio of 200, as shown in tables 4.9. and 4.10. Additionally, the polydispersity of polymers tended to decrease with increasing polymerization temperature, probably because of faster initiation reaction at higher temperature than at room temperature.

4.6.2. Butyllithium as initiator

4.6.2.1. Results

When the polymerization of L-LAAS was carried out with butyllithium in THF according to procedure 2, the change of molecular weights against temperature showed another pattern, an increase and then a decrease of the molecular weight, as shown in table 4.11.

Table 4.11. Polymerization of L-LAAS with n-BuLi as initiator and [M] / [I]= 100 at different temperatures in THF.

Temperature °C	$\overline{M_n}$ 10^{-3}.mol.g^{-1}	$\overline{M_w}$ 10^{-3}.mol.g^{-1}	$\overline{M_w}/\overline{M_n}$
30	45.1	60.6	1.3
40	60.6	84.3	1.4
50	25.2	34.9	1.4

$[L\text{-}LAAS]_0 = 2.6$ M, $[n\text{-}BuLi]_0 = 1.6\ 10^{-4}$ M, procedure 2.

4.6.2.2. Discussion

When *n*-BuLi was injected in the polymerization vessel and then mixed with the solvent before adding the monomer, it appeared that it not only initiated the polymerization of the anhydrosulfite but also reacted with the solvent. These two reactions were in competition with each other and behaved differently with respect to temperature. The results presented in table 4.11. suggested that the reaction between the initiator and the solvent was favoured up to 40°C whereas at 50°C, the initiation of anhydrosulfite was then predominant. Hence, the molecular weight of the polymers produced increased with a rise of the temperature up to 40°C and then decreased.

Thus, by increasing the polymerization temperature, it became possible to synthesise high molecular weight polymers from anhydrosulfites. Polylactic acid with $\overline{M_n}$ of 60600 was obtained by performing the polymerization with butyllithium at 40°C, for a monomer-to-initiator of only 100.

4.7. Characterisation of L- and DL-PLAAS

FT-IR and NMR spectroscopy, differential scanning calorimetry (D.S.C.) were used to characterize the polylactic acid produced, L-PLAAS and DL-PLAAS.

4.7.1. FT-IR analysis

The infrared spectra of L- and DL-PLAAS are presented in figures 4.11. and 4.12., respectively.

Figure 4.11. FT-IR spectrum of L-PLAAS

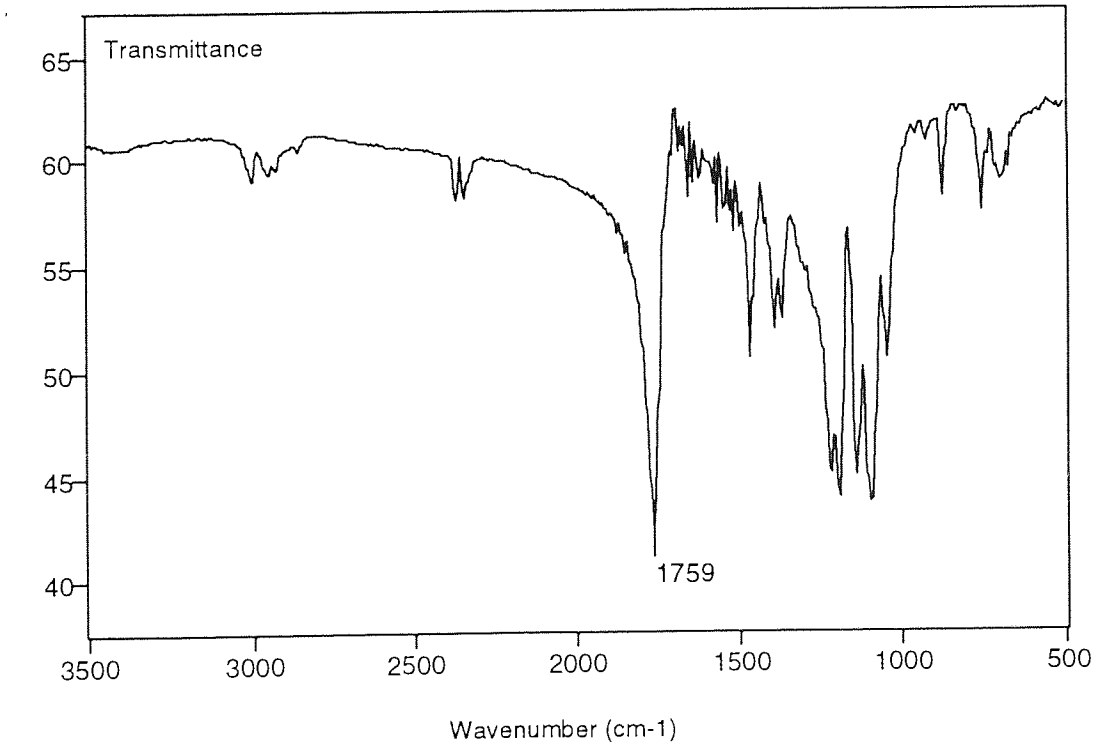

The infrared spectra of L- and DL-PLAAS exhibited both the weak stretching absorption around 2990 cm^{-1} but were still distinguishable by their strong carboxylic peak which appeared at different wavelengths, 1759 cm^{-1} for L-PLAAS and 1752 cm^{-1} for DL-

PLAAS. They also differed in shape, small shoulders were visible only on the carboxylic peak in the FT-IR spectrum of DL-PLAAS, as well as new absorptions between 1000 and 1500 cm^{-1}. But, these differences were more likely to be attributed to crystallinity rather than tacticity as such.

Figure 4.12. FT-IR spectrum of DL-PLAAS

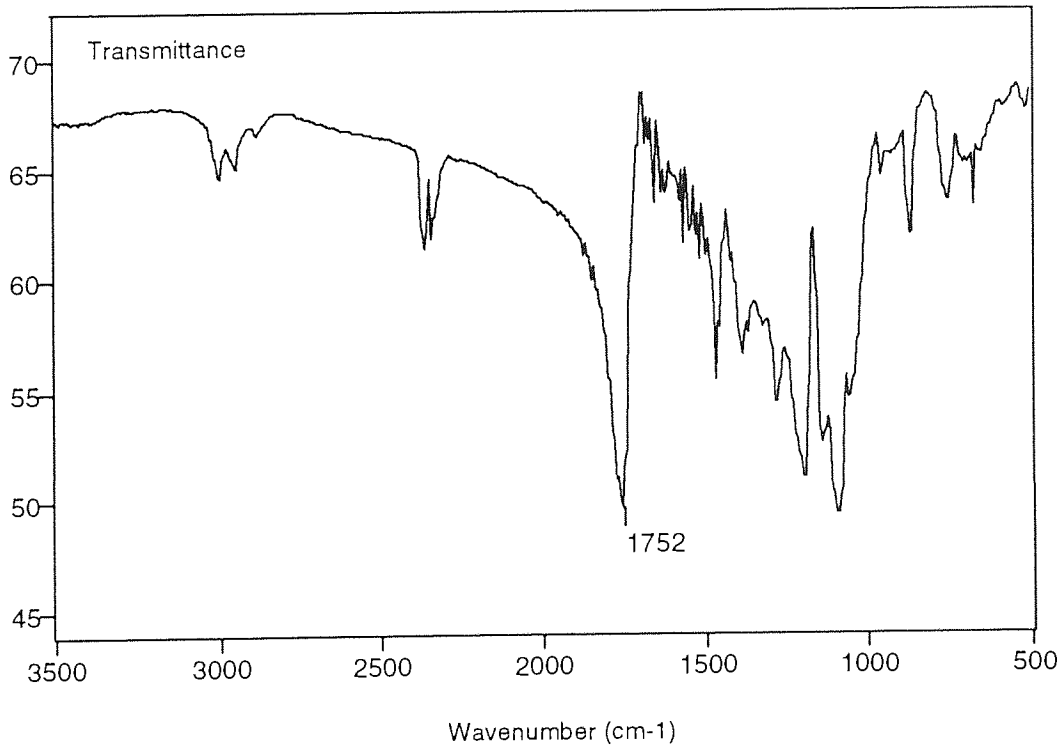

4.7.2. NMR analysis

The polymers produced L-PLAAS and DL-PLAAS were characterized structurally by analysing information obtained from ^{1}H and ^{13}C NMR spectra of their solutions in $CDCl_3$. NMR spectroscopy is a particularly effective way of examining the microstructure of the polymers and determining their tacticity, as shown in section 1.2.1.

4.7.2.1. L-PLAAS

Figure 4.13. shows a ^{1}H NMR spectrum of a sample of L-PLAAS. Analysis of the ^{1}H NMR spectrum of L-PLAAS revealed a doublet at 1.55 ppm assigned to the CH-C**H**$_3$ signal and a 1:3:3:1 quartet centred at 5.13 ppm assigned to the C**H**-CH_3. The integral values of the signals confirm these assignments. As CH-C**H**$_3$ and C**H**-CH_3 appear as a quartet and a doublet, those protons are expected to be in a stereospecific environment.

Figure 4.13. ^{1}H NMR spectrum of L-PLAAS

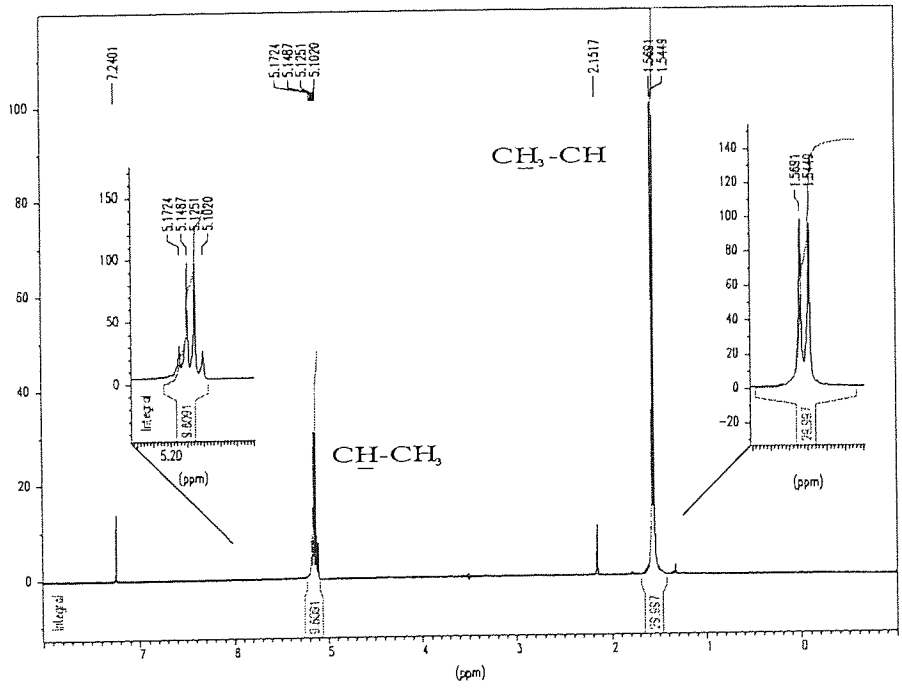

A spin decoupling experiment was performed on the L-PLAAS sample by applying a double resonance on the methyl protons at 1.54-1.56 ppm. As expected, this resulted in a collapse of the 1:3:3:1 quartet to a singlet at 5.14 ppm, as shown in figure 4.14. This meant that there was only one stereospecific environment for the methine proton in the polymer chains, therefore L-PLAAS was expected to be stereoregular.

Figure 4.14. ^{1}H homodecoupling on the methyl of L-PLAAS

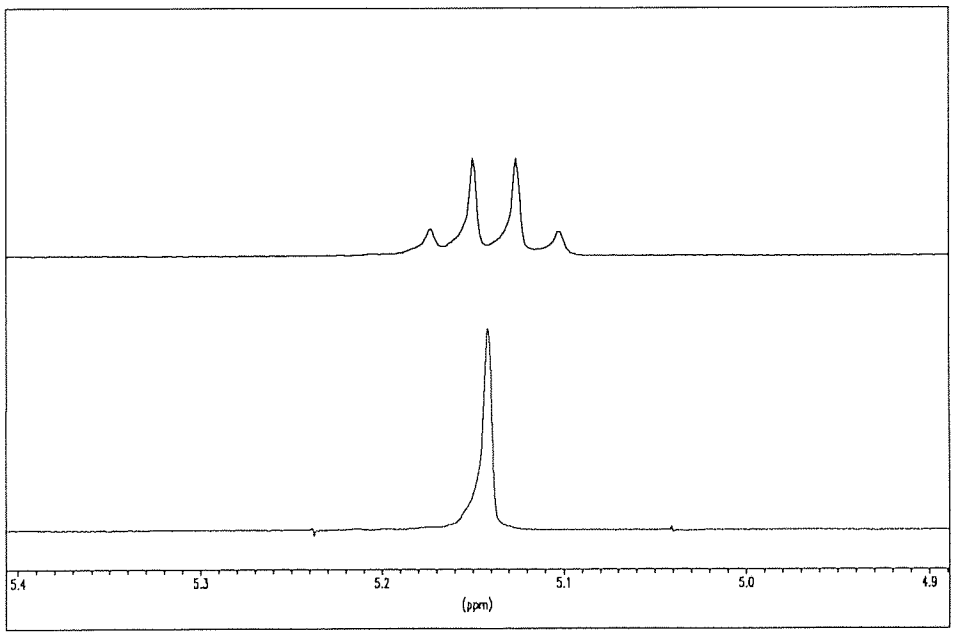

The ^{13}C NMR spectrum showed signals at 169.6 ppm assigned to the C=O carbon, at 68.9 ppm assigned to the CH carbon and at 16.6 ppm assigned to the CH_3 carbon, as presented in figure 4.15.

In ^{13}C NMR, the methine and carbonyl carbons are known to be very sensitive to the chain sequences. An expansion of the different regions shows clearly a single peak for each carbon, in particular the carbonyl signal presented in figure 4.16. This confirms the stereoregularity of L-PLAAS.

Figure 4.15. ^{13}C NMR spectrum of L-PLAAS

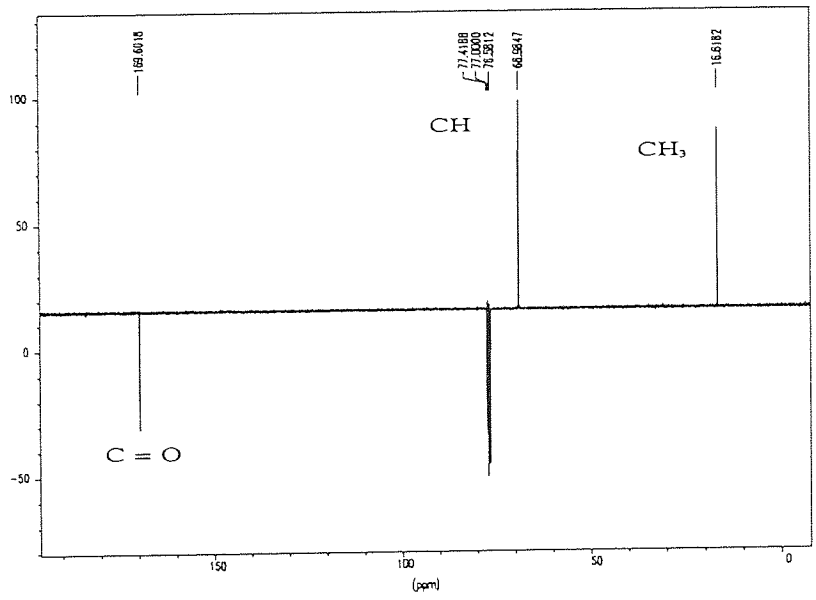

Figure 4.16. Carbonyl signal in the ^{13}C NMR spectrum of L-PLAAS.

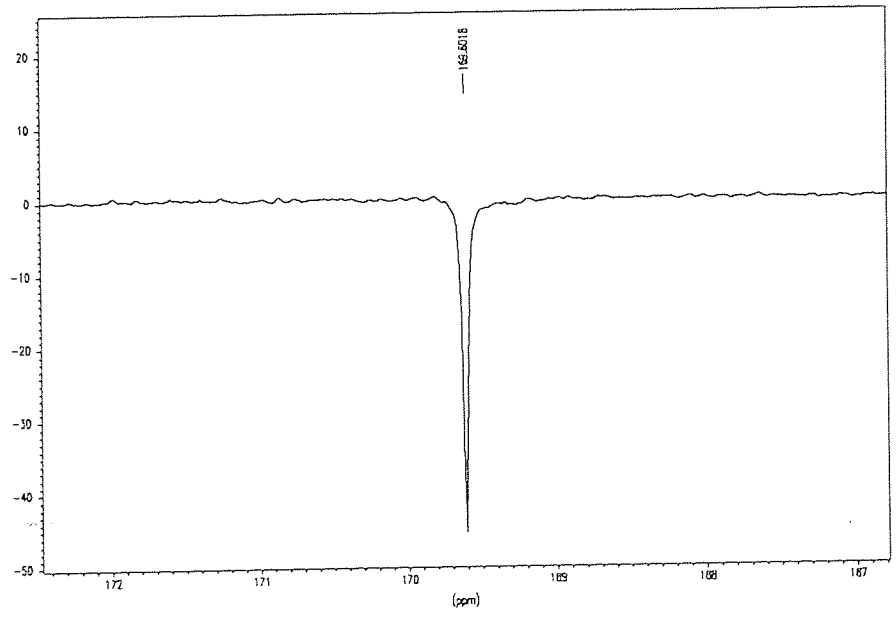

Thus, the anionic ring-opening polymerization of the pure enantiomer L-LAAS yielded a stereoregular polymer. This indicated that first, the anhydrosulfite had the enantiomeric nature of lactic acid, the starting material and secondly the polymerization did not involve racemization of the asymmetric centre, as expected from the mechanisms presented in sections 3.1. and 4.4. It should be mentioned that partial racemization by deprotonation could be observed for a number of initiated-polymerization of L-lactide, as discussed in section 1.2.3.2.

As the steric structure of the substituted carbon atom is not affected, the polymerization of the pure enantiomer (optically active L monomer) results in an isotactic polymer where the methyl group alternates across the plane containing the main chain bonds, as described in section 1.2.1.

4.7.2.2. DL-PLAAS

The ^{1}H NMR spectrum of DL-PLAAS in figure 4.17. shows a distorted doublet at 1.53 ppm attributed to the methyl protons and a multiplet at 5.15 ppm attributed to the methine protons. The integral values of the signals confirm these assignments.

The signal at 7.24 ppm corresponds to residual proton present in $CDCl_3$ whereas the signals at 0.9 ppm were attributed to n-hexane, in which the polymer was precipitated. Unlike L-PLAAS, DL-PLAAS was found very difficult to dry.

Figure 4.17. ^{1}H NMR spectrum of DL-PLAAS

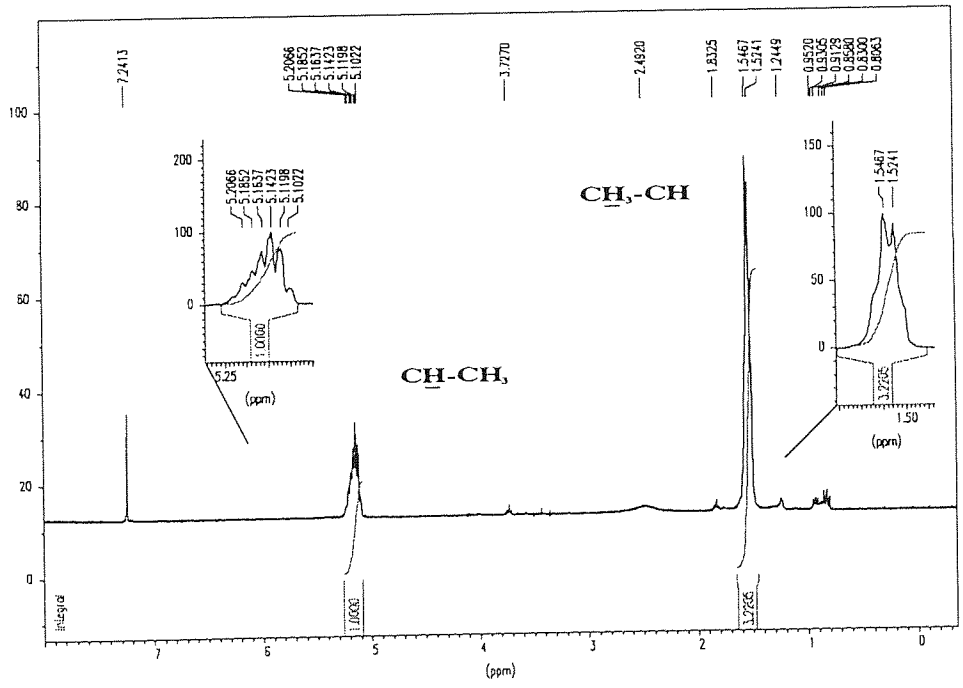

The methine region was simplified to singlets by ^{1}H-decoupling of the methyl frequencies, as shown in figure 4.18. This homodecoupling revealed several resonances with a major peak at 5.13 ppm which practically coincided with the only resonance obtained from a similar homodecoupling experiment on the methyl protons of L-PLAAS shown in figure 4.14.

Thereby, the methine region probably consisted of several overlapping quartets, each having line intensities 1:3:3:1, the typical multiplet pattern for a proton coupled to three equal protons of a methyl group. Thus, the methine proton was expected to be in different stereospecific environments in the polymer chains.

Figure 4.18. ^{1}H homodecoupling on the methyl of DL-PLAAS.

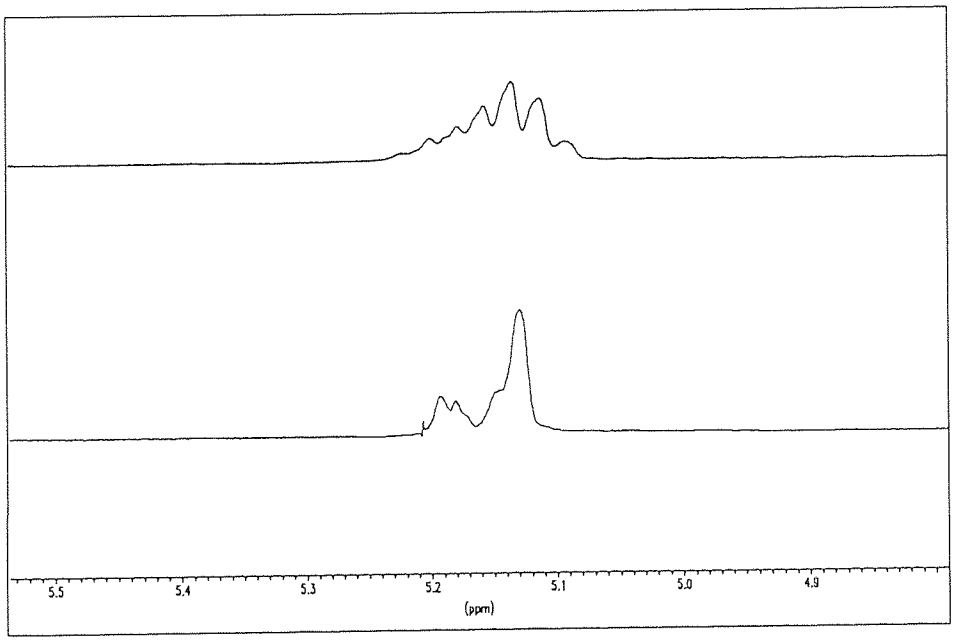

The ^{13}C NMR spectrum showed signals at 169.2 ppm assigned to the C=O carbon, at 69.2 ppm assigned to the CH carbon and at 16.6 ppm assigned to the CH_3 carbon, as shown in figure 4.19.

Figure 4.19. ^{13}C NMR spectrum of DL-PLAAS

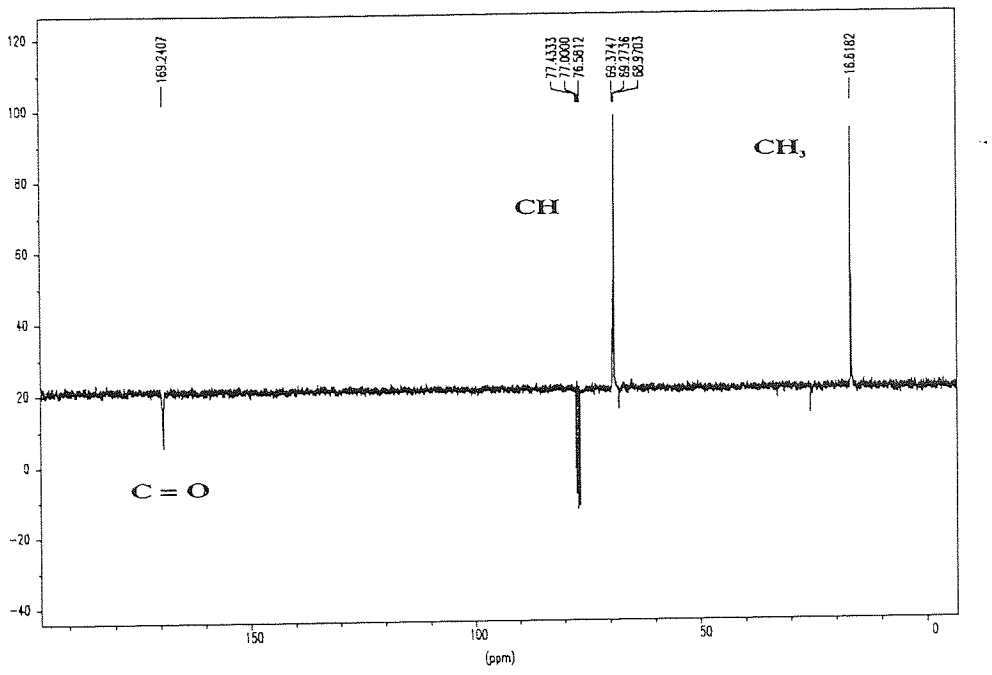

Closer examination of the methine and carbonyl regions show fine structure. It can be seen that there are 5 lines in each region, without taking into account the several shoulders observable on the carbonyl signals, as shown in figures 4.20. and 4.22. These fine structures correspond to residual resonances of the stereoirregular portions of the chains which arise from sensitivity to longer stereochemical sequences than triad (referring to α-carbons).

If D and L lactic units are distributed statistically along the chain according to Bernouillian single-addition statistics, stereosensitivity to triads, tetrads and pentads should give 4, 8 and 16 components, respectively [7]. This is outlined in greater detail in section 1.2.1.

Figure 4.20. Methine carbon signals in the ^{13}C NMR spectrum of DL-PLAAS

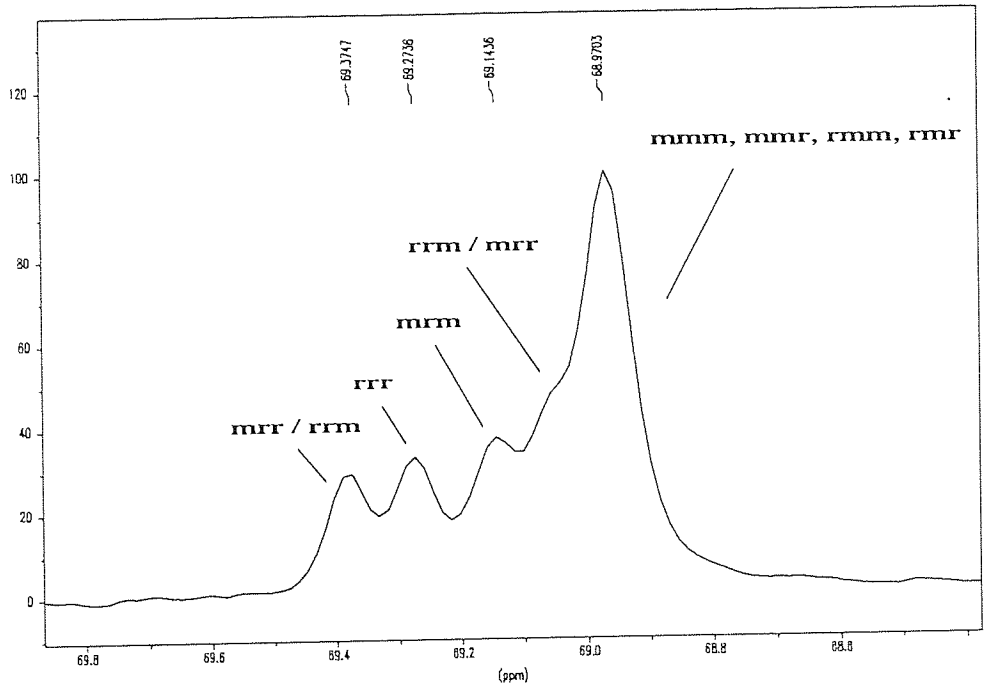

On the basis of work by Jedlinski [8,9] and Kricheldorf [10-13] on poly(DL-lactide) initiated with several catalysts, it was possible to make the different assignments for the methine carbon signals. They demonstrated that the methine carbon of poly(DL-lactide) was sensitive to tetrads and the signal obtained for DL-PLAAS exhibited a pattern similar to some signals they have reported. They differed slightly in the intensities of the various peaks. Therefore the stereosequences of DL-PLAAS were analyzed by NMR on the basis of tetrad effects and the structures of polymers obtained were described by the single-addition Bernouillian statistics. In this case, the following eight tetrads would be formed in the polymer chains, mmm, mmr, rmm, mrm, rmr, rrm, mrr, rrr with equal probability if no stereoselection occurred. The different assignments are presented in figure 4.20. Beside the lines of the tetrad characteristic for an isotactic tetrad mmm, the mmr, rmm and rmr tetrads were also present and this was in agreement with the fact that the methine carbon signal of L-PLAAS coincided with the main methine signal of DL-PLAAS.

Figure 4.21. Relative peak intensities of the methine carbon signals in the ^{13}C NMR spectrum of DL-PLAAS

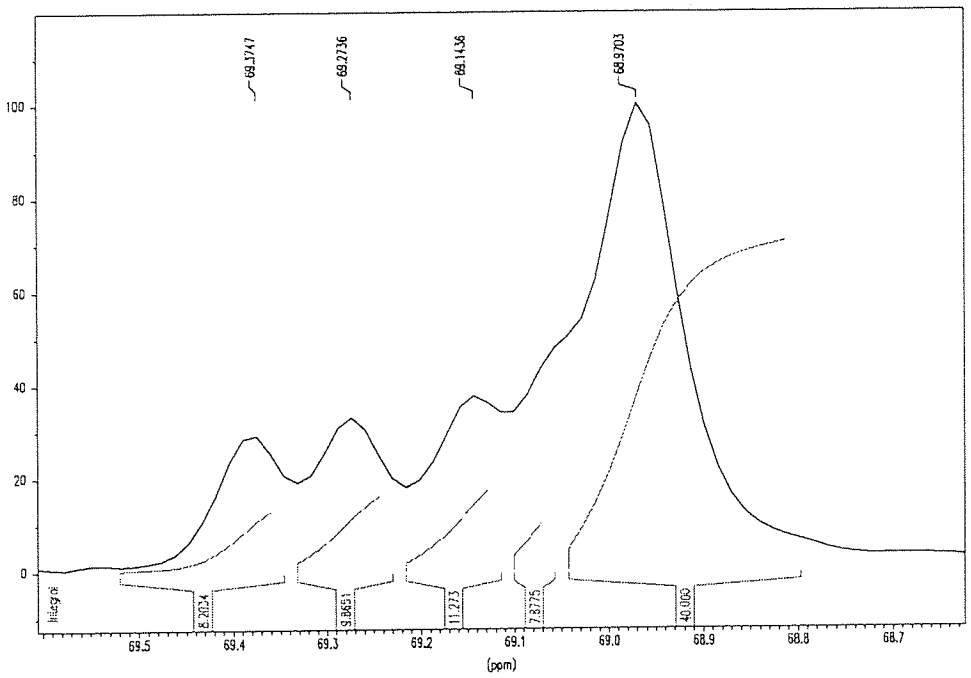

Table 4.12. ^{13}C NMR data of the methine carbon of DL-PLAAS

δ.ppm	Relative peak intensity	Assignment
68.97	40	mmm, mmr, rmm, rmr
-	8	rrm / mrr
69.14	11	mrm
69.27	10	rrr
69.38	8	mrr / rrm

The Nuclear Overhauser Effect (NOE) is important in ^{13}C NMR spectroscopy and causes an increase in the signal intensity, but this effect is similar for each peak corresponding to a same carbon, so a determination of relative peak intensity for the several tetrads peaks of the methine carbon is possible and gives satisfactory data.

The intensity of one of the tetrads peak was not accurate because of its poor resolution, as shown in figure 4.18. Nevertheless, by observation of tetrads intensities, DL-PLAAS would appear to be random or atactic, since P_m, the probability of generating a meso sequence when a new monomer unit is added at the growing chain was equal to 0.5 or since the main methine peak intensity was equal to the intensity of the four other peaks.

According to Bernouillian statistics for tetrads, outlined in section 1.2.1., the main methine peak (mmm, mmr, rmm, rmr) is equal to :

$$P_m^3 + 2P_m^2(1-P_m) + P_m(1-P_m)^2$$

which, by simplification, gives P_m.

In addition, from the NMR data in table 4.12., the normalised intensity of the main methine peak (mmm, mmr, rmm, rmr) is equal to 40/77 or 0.52.

Therefore, considering the error on one of the tetrads intensity, P_m could be assumed to be equal to 0.5 and this confirmed the atacticity of the polymer DL-PLAAS, with D- and L-lactic units randomly distributed in the polymer chains.

The expansion of the carbonyl region is presented in figure 4.22. From work by jedlinski and Kricheldorf, tetrad stereosensitivity of the carbonyl carbon could be deduced. As the carbonyl carbon signal of L-PLAAS coincided with the downfield peak of DL-PLAAS, this peak could be partly attributed to isotactic tetrads mmm.

Figure 4.22. Carbonyl signals in the ^{13}C NMR spectrum of DL-PLAAS

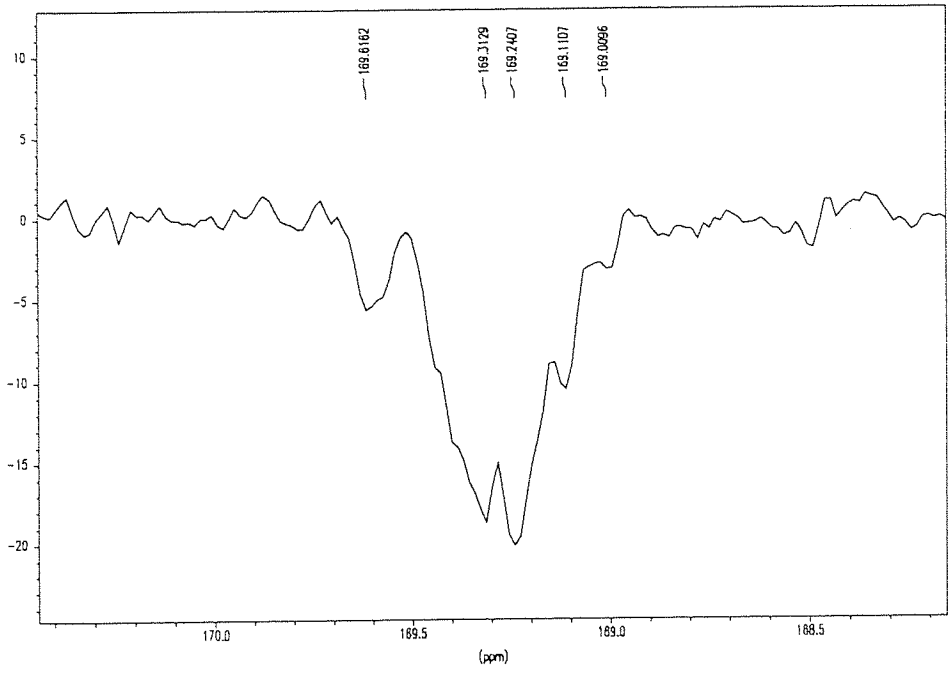

4.7.3. DSC analysis

Because of its regular symmetrical structure and therefore its tendency to form ordered structure, L-PLAAS was found highly crystalline and hardly soluble in THF. This behaviour was reflected in the DSC trace presented in figure 4.23. A highly endothermic melting transition was visible for L-PLAAS at 140-150°C, this melting temperature depended on its molecular weight, but no glass transition was detected.

In contrast, DL-PLAAS with unsymmetrical chains in its structure was soluble in THF and amorphous, as shown in its DSC trace presented in figure 4.24. Only a glass transition at 35°C was observed.

Figure 4.23. DSC trace of L-PLAAS.

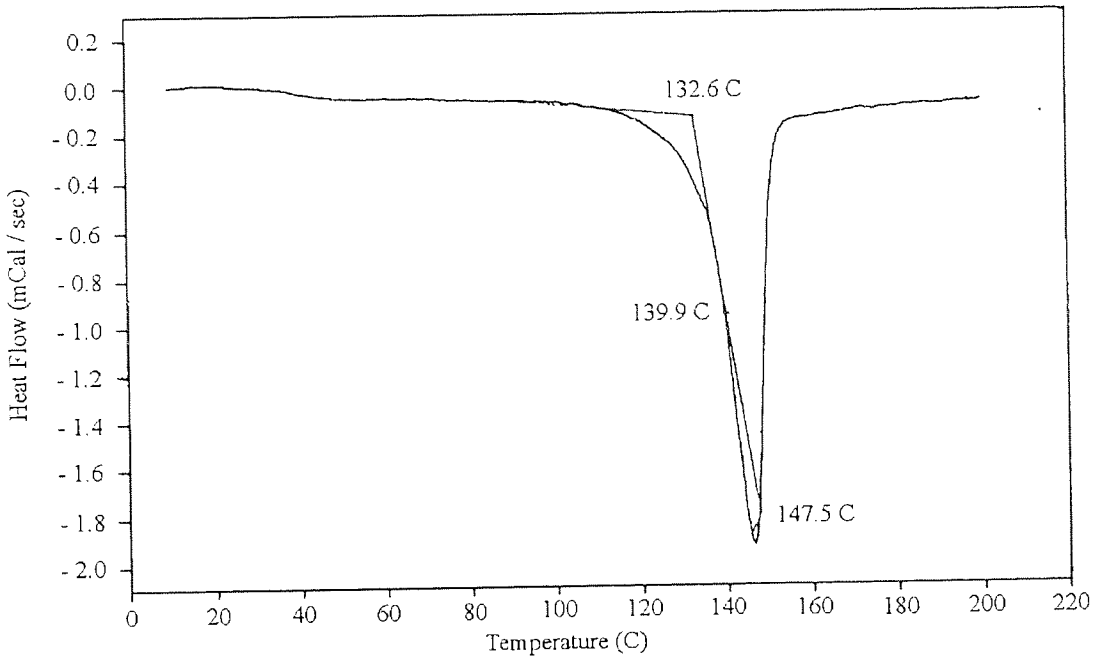

Figure 4.24. DSC trace of DL-PLAAS.

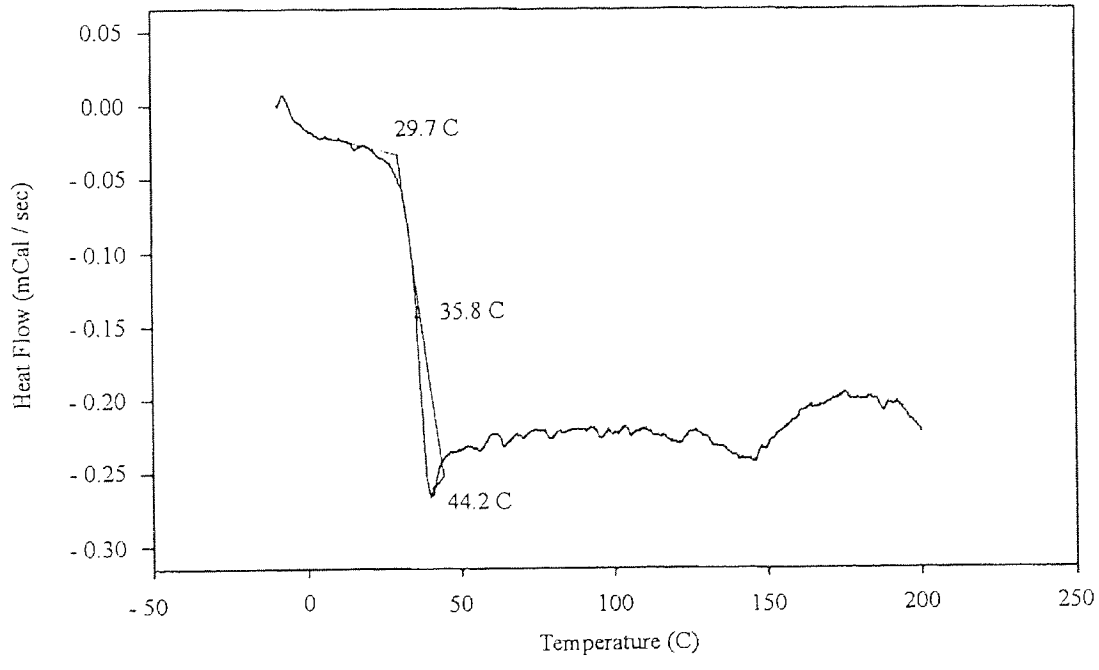

4.7.4. Discussion

Analysis of the ^{1}H and ^{13}C NMR spectra of L-PLAAS and DL-PLAAS revealed that L-LAAS led to a purely isotactic poly(lactic acid) while DL-LAAS produced a polymer with randomly distributed L- and D-lactic units.

These results were in agreement with the DSC traces of the two polymers. The stereoregular polymer L-PLAAS exhibited an endothermic melting transition at 140-150°C and so was highly crystalline whereas the atactic polylactic acid DL-PLAAS showed only a glass transition at 35°C. As a consequence, the highly crystalline L-PLAAS was hardly soluble in THF, unlike the amorphous DL-PLAAS.

These results indicated that the formation of L (or DL)-LAAS from L (or DL)-lactic acid did not involve inversion of configuration and this configuration was retained in the ring-opening polymerization, as expected from the mechanisms shown in sections 3.1. and 4.4. Also, as a truly atactic polylactic acid was formed from racemic LAAS, the anionic polymerization of LAAS was not stereoselective.

CHAPTER 5

SYNTHESIS OF NOVEL POLY-α-ESTERS

A series of experiments designed to produce poly-α-esters from other anhydrosulfites was conducted. The structure of the different aliphatic polymers to be synthesised by this method are shown in figure 5.1.

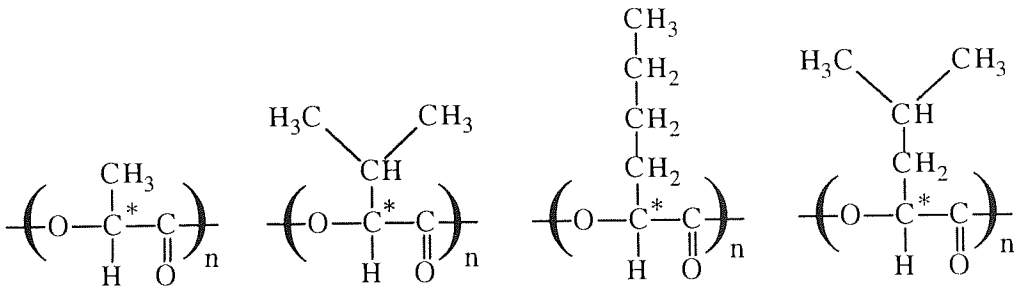

DL-PLAAS DL-PHIVAAS DL-PHCAAS L-PHICAAS

PLAAS	Poly(lactic acid anhydrosulfite)
PHIVAAS	Poly(hydroxy isovaleric acid anhydrosulfite)
PHCAAS	Poly(hydroxy caproic acid anhydrosulfite)
PHICAAS	Poly(hydroxy isocaproic acid anhydrosulfite)

Figure 5.1. Poly-α-esters synthesised.

5.1. Experimental

Since LAAS was successfully polymerized by alkyls lithium in tetrahydrofuran (THF) at room temperature (see section 4.), the other aliphatic anhydrosulfites polymerizations were carried out under similar conditions. Polymerizations were performed under a dry

argon atmosphere, in the vessel described in figure 4.1. Thus, the polymerizations proceed through a similar mechanism as LAAS, as shown in details in section 4.4.

The solvent THF (10 ml) was first dried and introduced in the polymerization vessel, then the initiator butyllithium (0.10 ml) was injected through a suba seal stopper. Shortly after, the desired amount of freshly distilled monomer was added into the vessel. The mixture was further agitated for 6 minutes.

THF is a relatively polar solvent with a low boiling point which enables it to be removed easily from the reaction products by simple evaporation. Indeed, when the monomer was the mixture of the two enantiomers, the polymers produced were amorphous and THF was trapped in the polymer and a precipitation in n-hexane was found to be necessary followed by filtration and drying in a dessicator for 5 hours. Even so, in some cases, traces of THF remained and were visible on the NMR spectra of the polymers as well as some water originated from moisture.

5.2. Characterisation

Polymers produced were characterized with respect to structure (^{1}H and ^{13}C NMR spectroscopy) and molecular weight (gel permeation chromatography).

5.2.1. GPC analysis

The polymerization of the range of aliphatic anhydrosulfites prepared, as previously described, was successful provided that the level of purity of the monomers was above 96 %. The results obtained for these polymerizations are presented in table 5.1. The molecular weights determined as polystyrene equivalents were relatively high except for L-PHICAAS due to the low monomer-to-initiator ratio. Additionally, the narrow molecular weight distribution of the polymers was confirmed by GPC.

Determination of the yields and the efficiencies of the initiator could not be effected because of the small quantity of the polymers samples and the loss of materials in the precipitation and filtration process.

Table 5.1. Polymerization of different aliphatic anhydrosulfites with n-BuLi in THF at 25°C.

Poly-α-esters	[M] 10^{-2}.mole	[M] / [I]	$\overline{M_{theor}}$ 10^{-3}.mol.g^{-1}	$\overline{M_n}$ 10^{-3}.mol.g^{-1}	$\overline{M_w}$ 10^{-3}.mol.g^{-1}	$\overline{M_w}/\overline{M_n}$
DL-PHIVAAS	1.7	100	10.00	22.6	26.2	1.16
DL-PHCAAS	1.4	90	10.26	10.8	13.1	1.21
L-PHICAAS	0.4	30	3.42	2.7	3.1	1.15

$[n\text{-BuLi}]_0$ = 1.6 M in hexanes.

5.2.2. NMR studies

The ^{1}H and ^{13}C NMR spectroscopy was performed on samples of the different poly-α-esters synthesised, in solution in deuterated chloroform. For more information on NMR, see section 2. This study was effected in the aim of determining the structure and tacticity of the polyesters synthesised (DL-PHCAAS, DL-PHIVAAS and L-PHICAAS), and consequently defining the mechanism of chain propagation involved in the polymerization of anhydrosulfites.

5.2.2.1. DL-Poly(hydroxy caproic acid) (DL-PHCAAS)

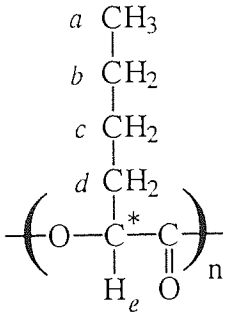

Figure 5.2. Key to NMR spectra of DL-PHCAAS.

The methyl, methine and methylene protons present in the polymer chain of DL-PHCAAS are presented in figure 5.2. In the ^{1}H NMR spectrum of this polymer, the different multiplets could be attributed to the five different protons, in agreement with the peak areas, as shown in table 5.2. and figure 5.3.

From the data obtained in the polymerization of DL-LAAS, the polymerization of DL-HCAAS is expected to yield an atactic polymer. Analysis of the ^{1}H NMR spectrum of DL-PHCAAS revealed a multiplet for the resonance of the ring proton H_e. Thus, this proton appeared to be in different stereospecific environments in the polymer chains, which meant that the polymer formed was atactic. The atacticity of this polymer was also confirmed by the resonance of the methyl protons H_a, which appeared in the shape of a multiplet, instead of a triplet. But ^{13}C NMR was found to be a better technique to determine the tacticity of the polymer, because of the high sensitivity to chain sequences of the methine carbons in the chains, as discussed in section 1.2.1.

Figure 5.3. ^{1}H NMR spectrum of DL-PHCAAS

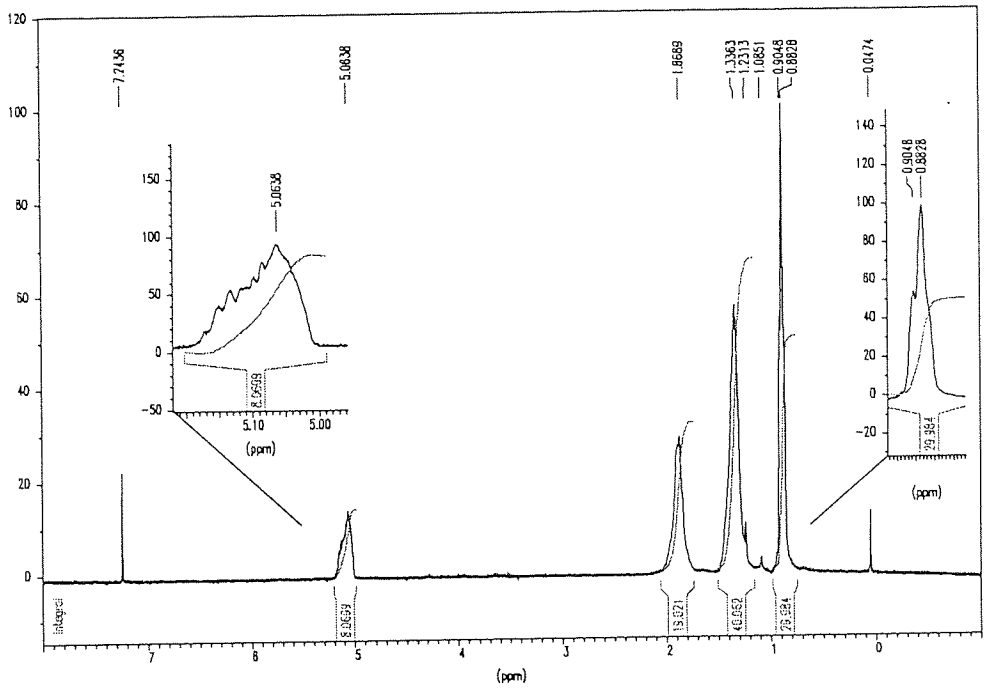

Table 5.2. ^{1}H NMR data of DL-PHCAAS.

Poly-α-ester	δ.ppm	Peak shape	Relative peak area	Assignment
DL-PHCAAS	0.88 - 0.90	pseudo-doublet	30.0	CH_{3a}
	1.23 -1.33	multiplet	40.1	CH_{2b} & CH_{2c}
	1.86	multiplet	19.0	CH_{2d}
	5.06	multiplet	8.1	CH_{e}

Figure 5.4. shows the different resonances obtained for DL-PHCAAS in ^{13}C NMR spectroscopy and their assignments are presented in table 5.3.

Figure 5.4. ^{13}C NMR spectrum of DL-PHCAAS

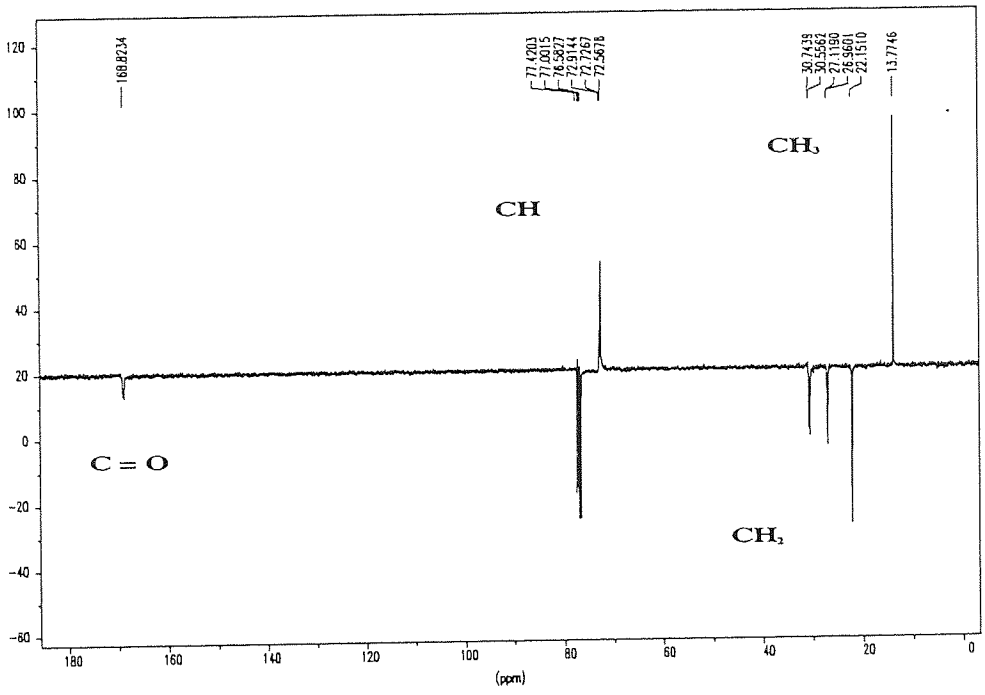

Table 5.3. ^{13}C NMR data of DL-PHCAAS.

Poly-α-ester	δ.ppm	Assignment
DL-PHCAAS	13.77	CH_{3a}
	22.15	CH_{2b}
	26.96 - 27.11	CH_{2c}
	30.55 - 30.74	CH_{2d}
	72.56 - 72.72 - 72.91	CH_e
	168.82	C = O

Like DL-PLAAS, an expansion of the methine and carbonyl regions revealed fine structure, respectively three and eight peaks (and one shoulder). As each methylene proton exhibited also several lines, as shown in figure 5.5., DL-PHCAAS was expected to be atactic.

Figure 5.5. Methylene signals in the ^{13}C NMR spectrum of DL-PHCAAS

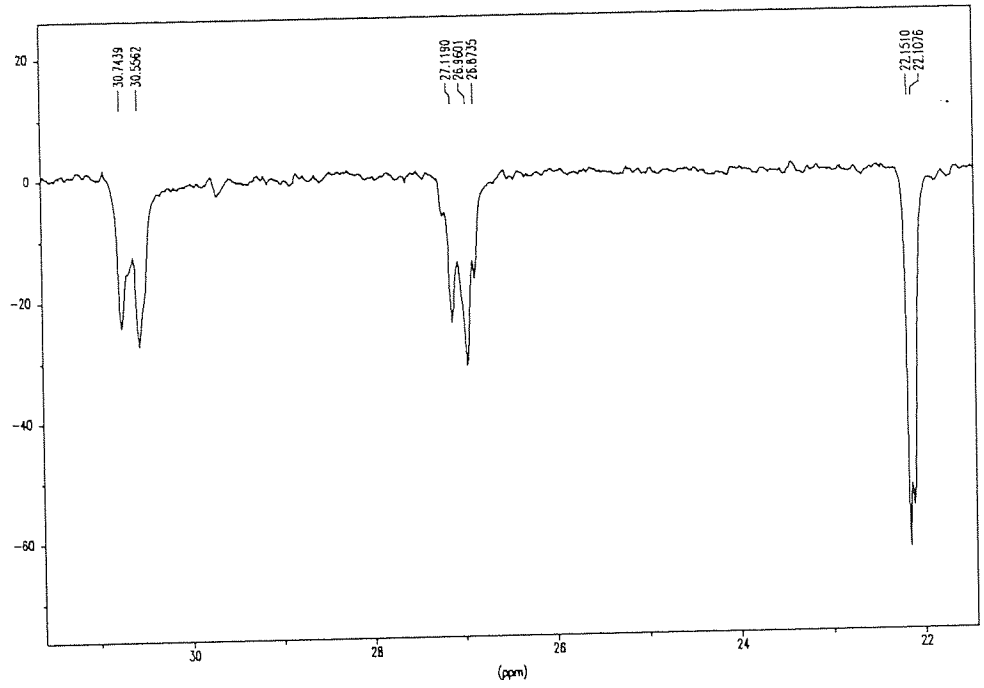

The carbonyl signal of DL-PHCAAS shown in figure 5.6. is relatively similar to the one observed for DL-PLAAS, although there is a better definition of the different peaks in the carbonyl region, probably because of the bulkiness of the substituent on the C(5) carbon. Similarly to DL-PLAAS, the hexad sensitivity of the carbonyl peak was deduced and so the two peaks downfield could be attributed to the hexads mmmmm, mmmmr.

The methine carbon signal presented in figure 5.7. was found to be triad sensitive, as it appeared in the shape of three peaks. The high field peak corresponded to the single peak for isotactic triads mm, the low field peak for syndiotactic triads rr and between them the heterotactic triads rm, mr. For Bernouillian single-addition statistics, DL-PHCAAS would be atactic, since the intensity of the heterotactic peak rm, mr was equal to the intensity of the two other peaks mm and rr.

Figure 5.6. Carbonyl signals in the ^{13}C NMR spectrum of DL-PHCAAS

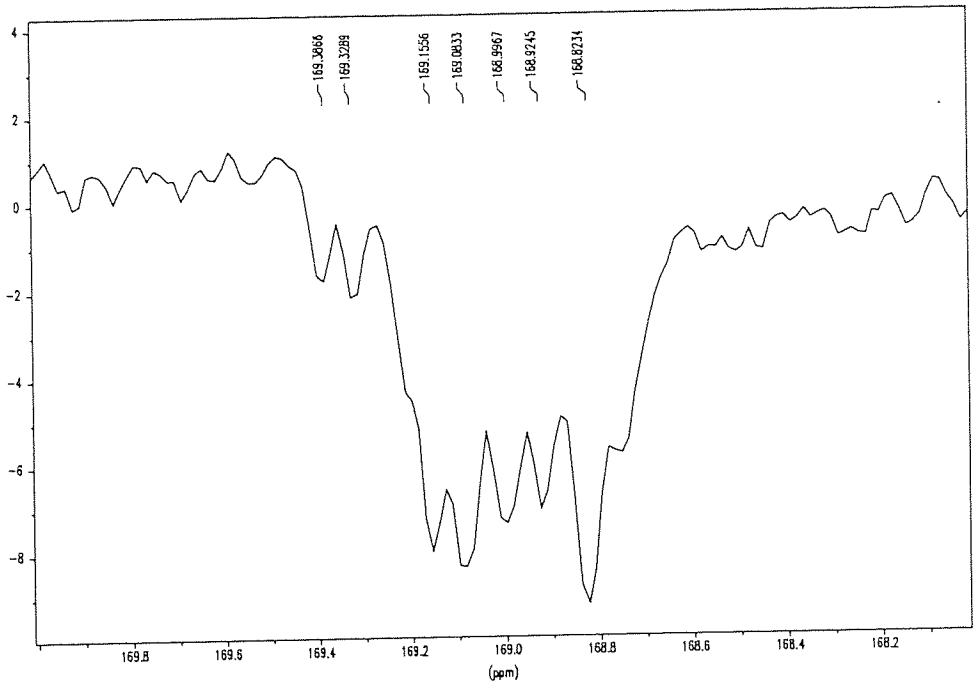

Figure 5.7. Methine carbon signals in the ^{13}C NMR spectrum of DL-PHCAAS

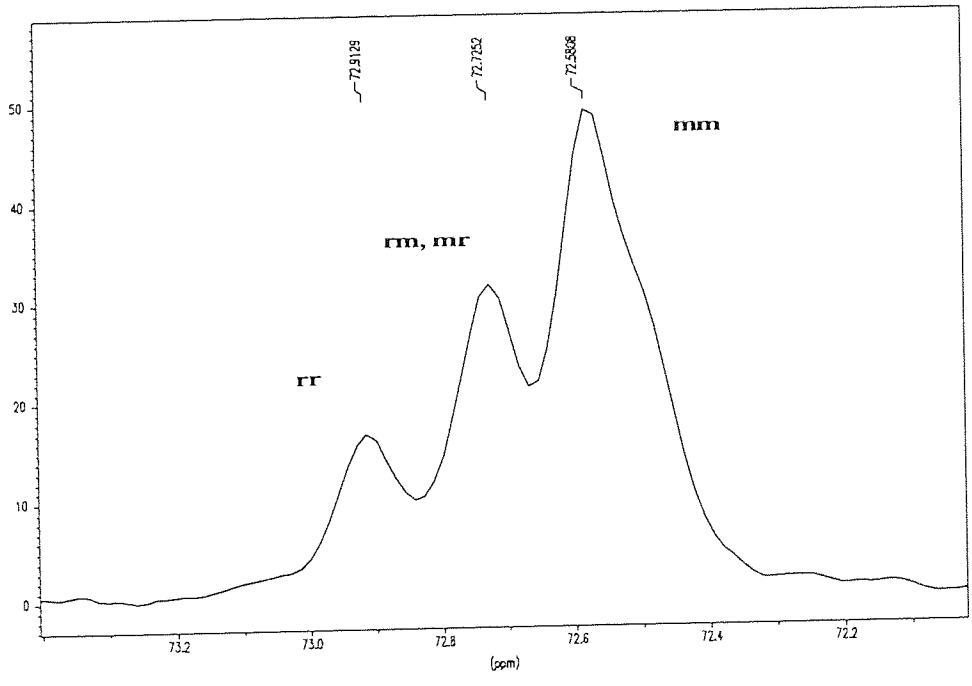

The intensities of the different peaks were determined. It appeared clearly that the presence of isotactic triads was largely predominant, as shown in figure 5.8. and table 5.4. Nearly 60 % of the triads in the atactic polymer DL-PHCAAS were isotactic.

Figure 5.8. Relative peak intensities of the methine carbon signals in the ^{13}C NMR spectrum of DL-PHCAAS

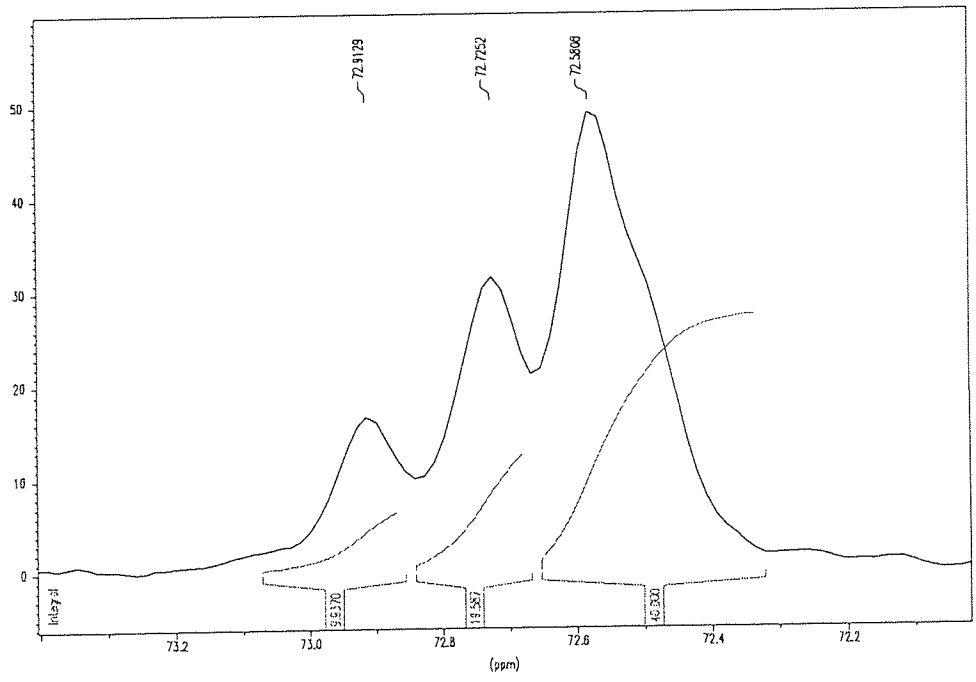

Table 5.4. ^{13}C NMR data of the methine carbon of DL-PHCAAS.

δ.ppm	Relative peak intensity	Assignment
72.58	40	mm
72.72	20	rm, mr
72.91	10	rr

Assuming that a racemic mixture of L and D monomers was of a configurational composition of the type L = D, the anionic polymerization of DL-HCAAS appeared to be stereoselective. Both optical isomers polymerized at the same rate, but D molecules were incorporated preferentially into polymer chains already containing D units, and L molecules into chains containing L units. Therefore the bulkiness of the substituent seemed to be a factor influencing the stereoregulation of the anionic polymerization of anhydrosulfites and so the resulting polymer DL-PHCAAS had a structure predominantly isotactic.

5.2.2.2. DL-Poly(hydroxy isovaleric acid) (DL-PHIVAAS)

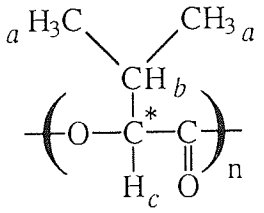

Figure 5.9. Key to NMR spectra of DL-PHIVAAS.

Analysis of the ^{1}H NMR spectrum of DL-PHIVAAS in figure 5.10. revealed three multiplets assigned to the three types of protons present in the polymer unit, shown in figure 5.9. The integral values of the signals confirmed these assignments with the exception of the methyl signal, as presented in table 5.5. As previously explained in section 5.1., DL-PHIVAAS was found difficult to dry. Thus, in this ^{1}H NMR spectrum, it can be seen two signals centred at 1.8 ppm and 3.7 ppm due to the presence of THF along with a signal at 1.7 ppm attributed to water. So hexane with a signal centred at 1.0 ppm might also be present and masked in the methyl protons signal which appeared at the same chemical shift.

The resonance of the methine proton H_c and the methyl protons H_a appeared as multiplets. As in the case of DL-PHCAAS, the ^1H NMR spectrum of DL-PHIVAAS exhibited stereoirregularity. This suggested that DL-PHIVAAS was also atactic with D- and L-hydroxy isovaleric units incorporated in the polymer chain in a relatively random manner. But ^{13}C NMR data gives usually a better representation of the microstructure of the polymer.

It is interesting to mention that the signal of the proton H_d is a pair of multiplets, possibly because of the two configurations D- and L-.

Figure 5.10. ^1H NMR spectrum of DL-PHIVAAS

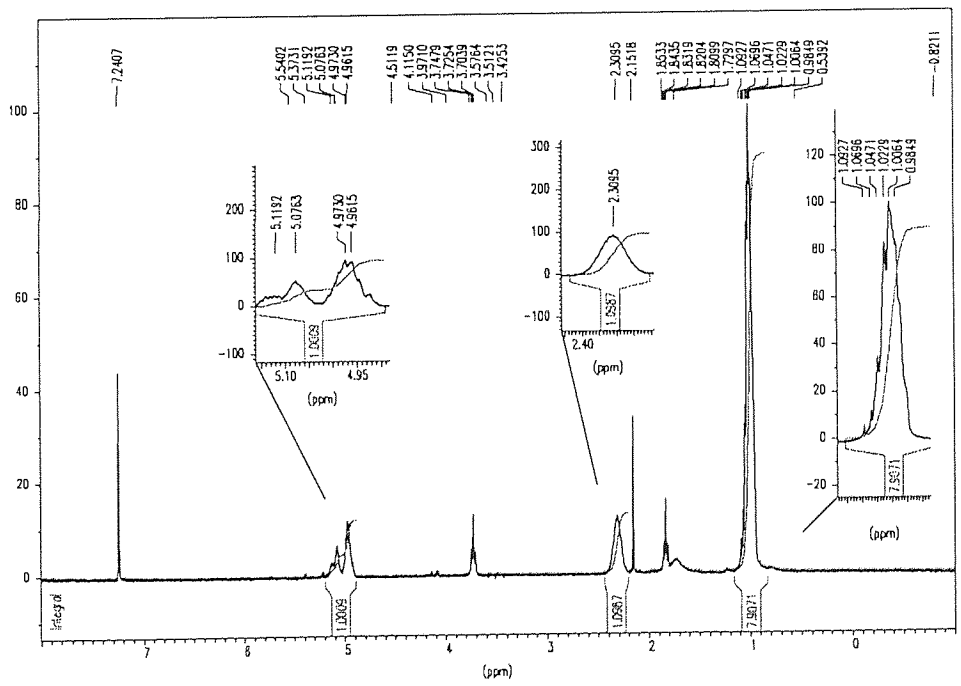

Table 5.5.^1H NMR data of DL-PHIVAAS.

Poly-α-ester	δ.ppm	Peak shape	Relative peak area	Assignment
DL-PHIVAAS	0.98 - 1.09	multiplet	7.9	CH_{3a}
	2.31	multiplet	1.1	CH_b
	4.97	multiplet	1.0	CH_c

The ^{13}C NMR spectrum of DL-PHIVAAS and the corresponding peak table are presented in figure 5.11. and table 5.6., respectively. The two peaks at approximately 25.5 ppm and 67.9 ppm are due to the presence of THF in the polymer.

Figure 5.11. ^{13}C NMR spectrum of DL-PHIVAAS

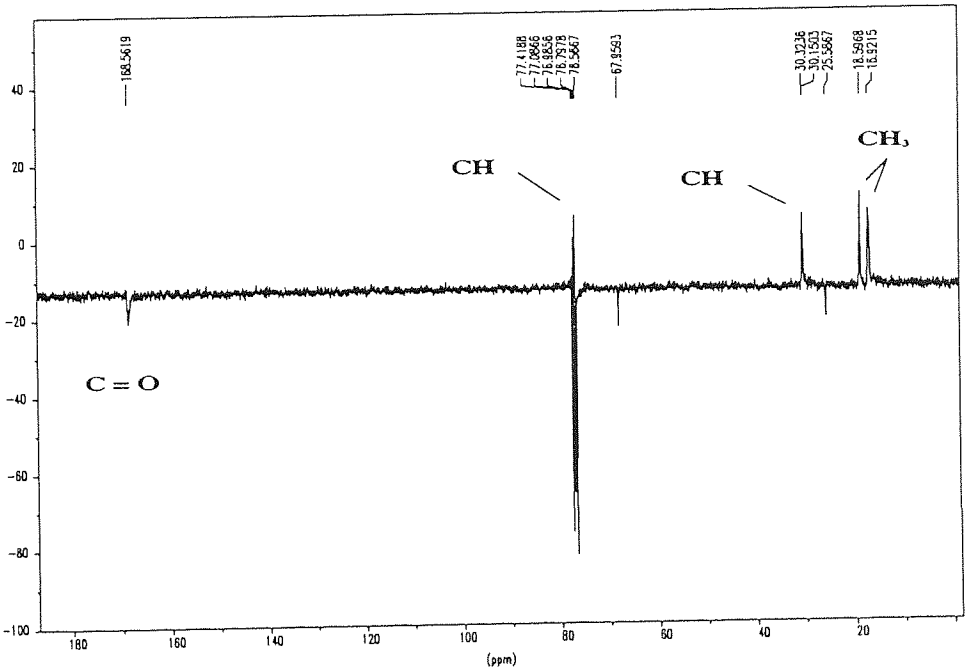

Table 5.6. ^{13}C NMR data of DL-PHIVAAS.

Poly-α-ester	δ.ppm	Assignment
DL-PHIVAAS	16.92	CH_{3a}
	18.59	CH_{3a}
	30.15	CH_b
	30.32	CH_b
	76.79	CH_c
	77.10	CH_c
	168.56	C = O

The ^{13}C NMR spectrum confirmed the atacticity of the polymer, in particular in the carbonyl region where several peaks were observed, as shown in figure 5.12. Because of

the relatively small sample of polymer and the low intensity absorption usually obtained for this functional group, a better definition of the carbonyl signal was not possible. This was probably the reason why this signal differed in shape from the peak obtained for DL-PLAAS or DL-PHCAAS. In particular the downfield small peak which was coinciding with isotactic triads was not observed.

Figure 5.12. Carbonyl signals in the ^{13}C NMR spectrum of DL-PHIVAAS

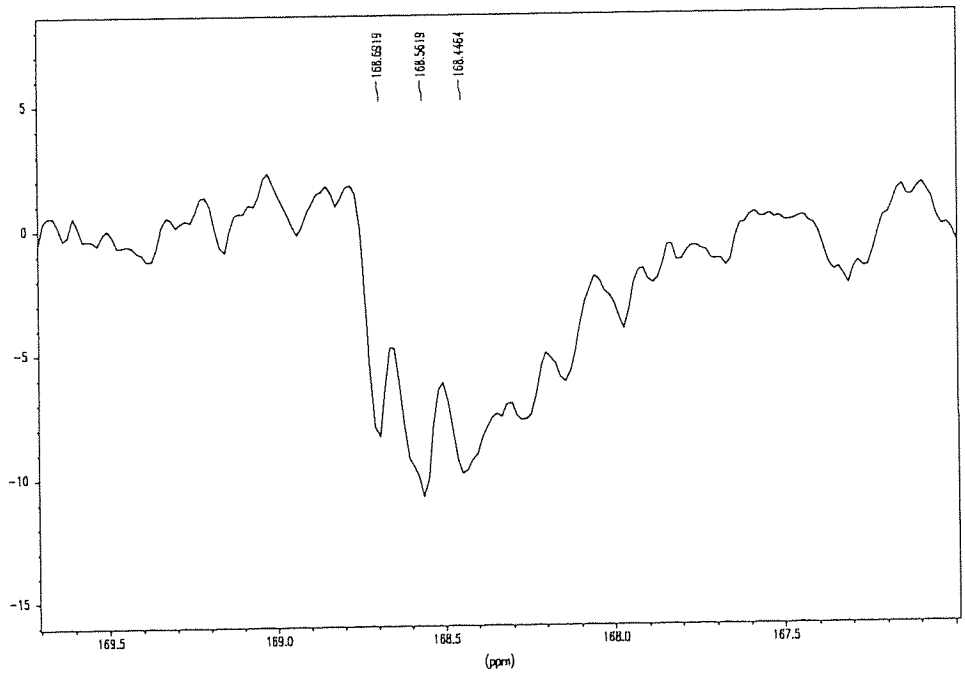

In DL-PHIVAAS, as the signal of the methine carbon CH_c coincided with the three characteristic peaks of *d*-chloroform, this signal was deformed so that no analysis of the stereosequences was possible. The signal of this methine carbon attached to an isopropyl group was shifted downfield compared to the methine carbon attached to a n-butyl group in the DL-PHCAAS chains. Because the electronegativity of the oxygen in the chain was predominant upon the inductive effect of the alkyl group with its electron releasing tendency, the shift was presumably caused by steric effect. When the pendant group was bulkier, there was a shielding effect on the methine carbon and so a higher field was necessary.

Additionally, two signals for the methyl carbons can also be seen in the ^{13}C NMR spectrum of DL-PHIVAAS. This may be explained by restricted rotation around the CH_c-CH_b bond. Indeed, this is in agreement with what is observed for L-PHICAAS in the next section.

5.2.2.3. L-Poly(hydroxy isocaproic acid) (L-PHICAAS)

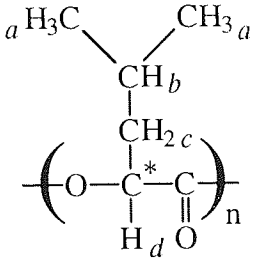

Figure 5.13. Key to NMR spectra of L-PHICAAS.

The structure of L-PHICAAS is described in figure 5.13. where the different protons are represented as H_a, H_b, H_c, H_d and H_e.

The ^1H NMR spectrum of L-PHIVAAS is shown in figure 5.14. The methyl protons resonance appears as a quartet centred at 0.92 ppm, the methylene protons as a multiplet centred at 1.78 ppm whereas the ring proton signal is a quartet centred at 5.06 ppm. The integral values of the signals confirm these assignments, as shown in table 5.7. In this ^1H NMR spectrum, the characteristical signal for THF was also observed at 3.7 ppm and a second signal could be seen at 1.7 ppm if it was not masked by the methylene protons signal. This suggested that a hexane signal might also be hidden by the methyl proton signal.

Analysis of the ^1H NMR spectrum revealed a quartet for the methine proton H_e resonance, instead of a triplet as expected. Just as in the structure of the monomer from which L-PHICAAS was derived, the rotation about the CH_e-CH_d in the polymer seemed to be restricted. This resulted from a similar reason, steric hindrance due to the bulky

isobutyl group. Thus the proton H_e signal was not a triplet but a quartet originating from its coupling with the two non-equivalent protons H_d. Moreover, the methyl protons resonance appeared as two doublets because of the non-equivalence of the two methyl groups.

Figure 5.14. ^{1}H NMR spectrum of L-PHICAAS

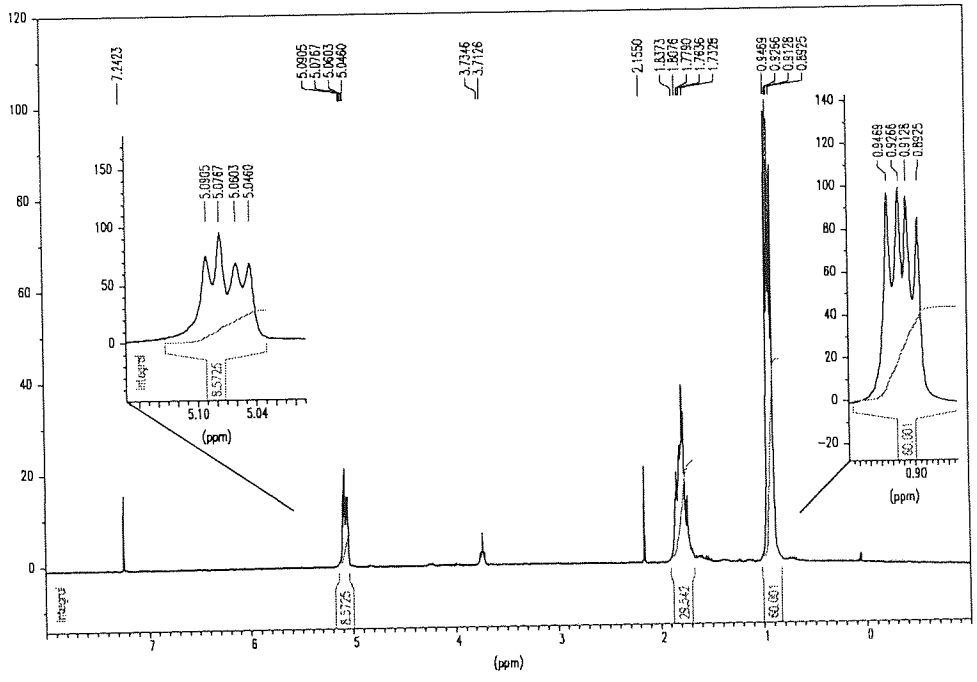

Table 5.7. ^{1}H NMR data of L-PHICAAS.

Poly-α-ester	δ.ppm	Peak shape	Relative peak area	Assignment
DL-PHICAAS	0.89 - 0.94	quartet	60.0	CH_{3a}
	1.73 - 1.83	multiplet	29.5	CH_b & CH_{2c}
	5.04 - 5.09	quartet	8.6	CH_d

The ^{13}C NMR spectrum of L-PHICAAS is shown in figure 5.15. and the peak tables including the assignments of the different carbons are listed in table 5.8.

In this spectrum, the methine and methyl signals appeared as one and two single peaks, respectively. An expansion of the methyl carbon region is shown in figure 5.16. This

confirmed the results obtained from the ^{1}H NMR spectrum, that rotation about the CH_e-CH_d bond was restricted. The two methyl carbons were not equivalent.

Figure 5.15. ^{13}C NMR spectrum of L-PHICAAS

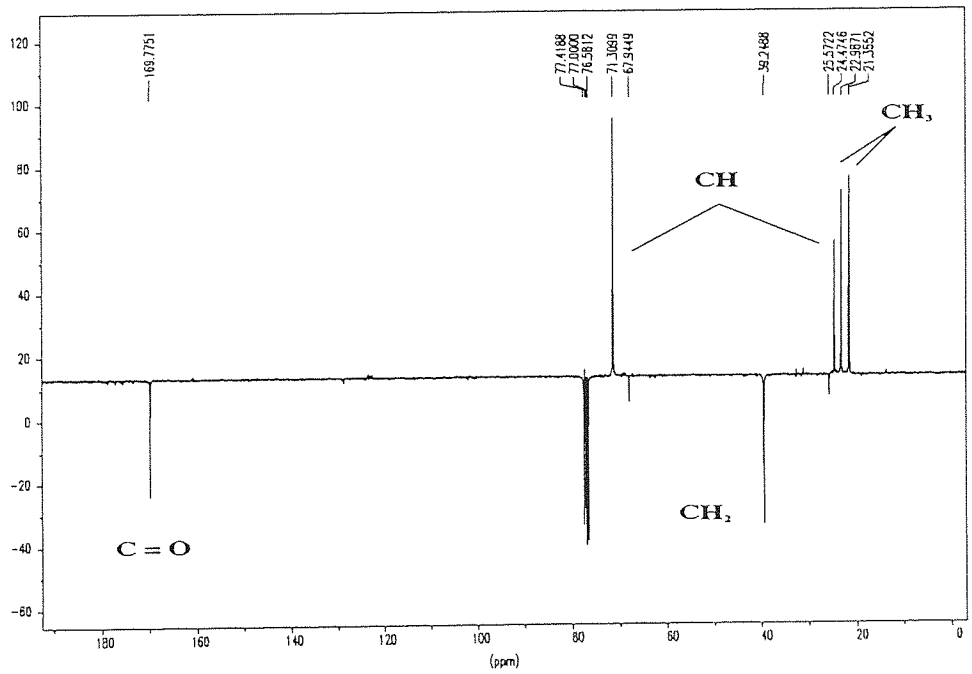

Table 5.8. ^{13}C NMR data of L-PHICAAS.

Poly-α-ester	δ.ppm	Assignment
DL-PHICAAS	21.35	CH_{3a}
	22.98	CH_{3a}
	24.47	CH_b
	39.24	CH_{2c}
	71.30	CH_d
	169.77	C = O

In ^{13}C NMR, the methine and carbonyl carbons are very sensitive to the chains sequences, and as the resonances for these carbons shown in figures 5.16 and 5.17. appeared as single peaks, the isotactic structure of L-PHICAAS could be deduced. Thus, in the structure of L-PHICAAS, the isobutyl group alternates across the plane containing the main chain bonds, as explained and described for L-Polylactic acid in section 1.2.1.

Figure 5.16. Methine and methyl carbons signals in the ^{13}C NMR spectrum of L-PHICAAS

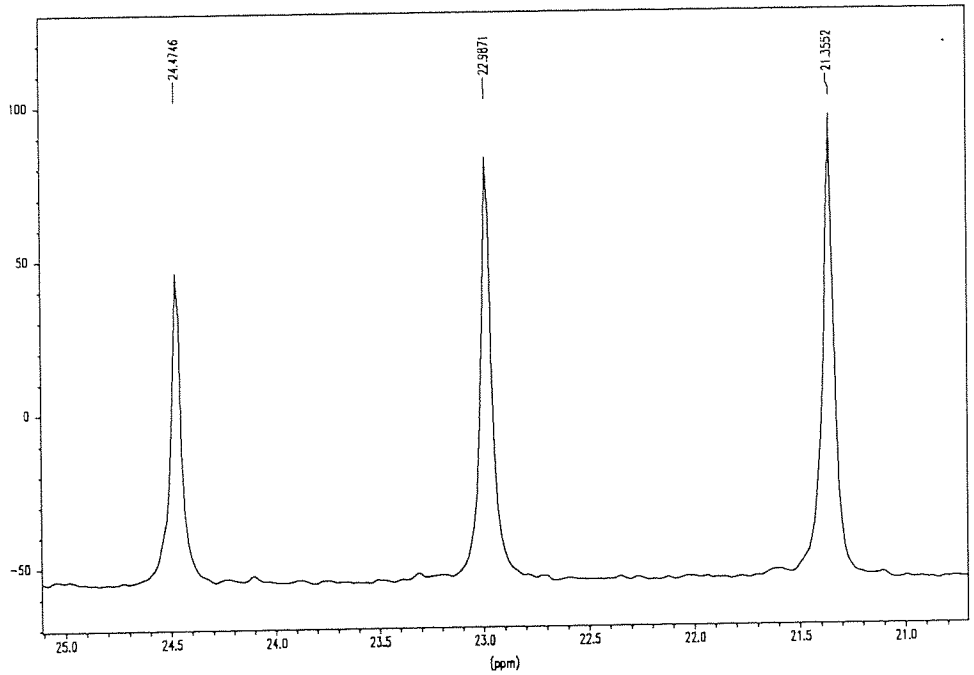

Figure 5.17. Carbonyl signal in the ^{13}C NMR spectrum of L-PHICAAS

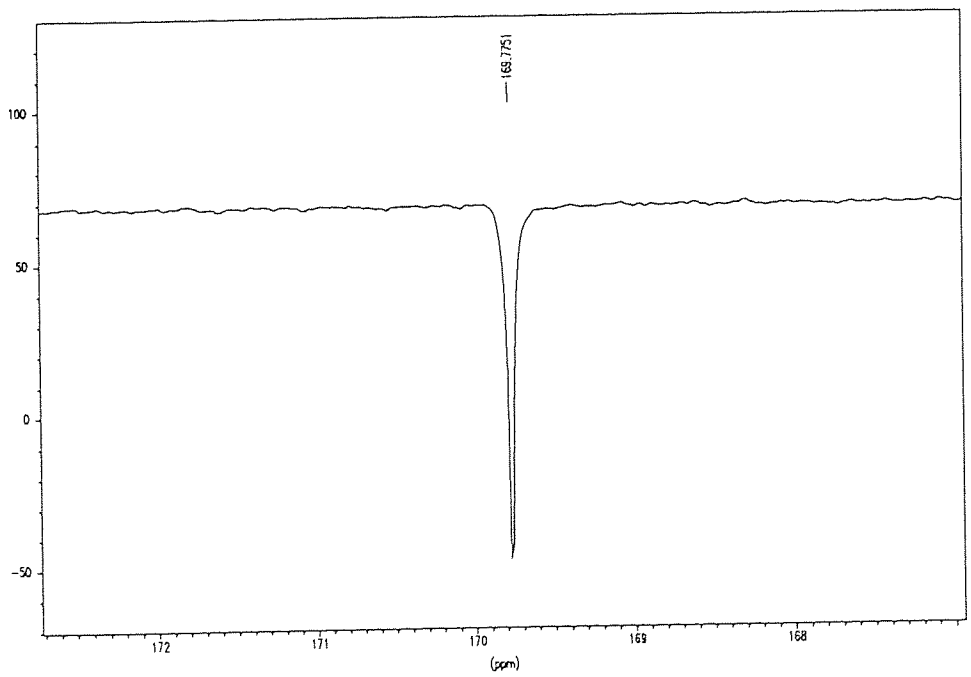

Like DL-PHIVAAS, the two methyl carbons were not equivalent, so two lines were visible in the ^{13}C NMR spectrum of L-PHICAAS, confirming the restriction of the rotation about the CH_e-CH_d bond. Moreover, the shift between the two methyl carbons signals was approximately 1.6 ppm in the spectra of both DL-PHIVAAS and L-PHICAAS, suggesting that the restrictions of rotation in both cases were relatively similar. In figure 5.18., the structure of one unit of L-PHICAAS is described to show the proximity of the bulky isopropyl group with the main chain in the polymer.

Figure 5.18. Structure of one unit of L-PHICAAS

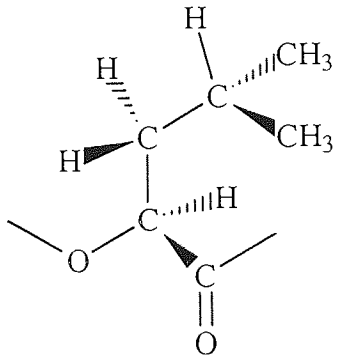

All the NMR data led to the conclusion that the polymer L-PHICAAS produced was purely isotactic with a large pendant group which increased its rigidity. This suggested that similar steric hindrance occurred in DL-PHCAAS and DL-PHIVAAS, this effect being impossible to detect in the ^{1}H NMR spectra of these polymers because of the heterotacticity of their chains. Nevertheless, analysis of the ^{13}C NMR spectrum of DL-PHIVAAS revealed a restriction of rotation in this polymer, as explained in section 5.2.2.2.

5.3. Discussion

The anionic polymerization of aliphatic anhydrosulfites with bulky substituents such as DL-HCAAS, DL-HIVAAS and L-HICAAS was successful. As expected from the study of the polymerization of L- and DL-LAAS in section 4., the anionic polymerization of L-anhydrosulfite yielded a purely isotactic polyester whereas DL-anhydrosulfite led to an atactic polyester. This confirmed that the polymerization of anhydrosulfites did not proceed with racemization of the asymmetric centre. However, the analysis of the ^{13}C NMR spectrum of DL-PHCAAS revealed that this polyester was predominantly isotactic and so the structure of this polymer was not truly atactic like DL-PLAAS. This meant that when the substituent on the anhydrosulfite ring was bulky, the anionic polymerization of anhydrosulfites was stereoselective.

The active propagating species in the anionic polymerization of anhydrosulfite is an alcoholate, as shown in section 4.4. In the example presented in figure 5.19., it can be seen that during propagation, the attack of the alkyl anion on the carbonyl atom will be favoured when the two bulky n-butyl groups, the one in the anhydrosulfite ring and the one at the chain end are the furthest or in other words, when the two asymmetric centres, the one at the active chain end and the one in the anhydrosulfite molecule are both similar. Thus, the polycaproic chain with a L-configuration will attack preferentially a L-monomer and similarly the attack of a D-polycaproic chain on a D-monomer will be favoured. This is the reason why the polymer formed DL-PHCAAS exhibits a structure predominantly isotactic, where most of the bulky n-butyl groups alternate across the plane containing the main chain bonds.

On the other hand, the size of the substituent in the anhydrosulfite ring not only influenced the stereoselectivity of the anionic polymerization of anhydrosulfites, but also affected the flexibility of the resulting polyester. Thus, the polyesters DL-PHCAAS, DL-PHIVAAS and L-PHICAAS with large pendant groups were rather rigid with no free rotation of the pendant groups.

Figure 5.19. Attack of the propagating end of DL-PHCAAS on the anhydrosulfite DL-HCAAS during propagation

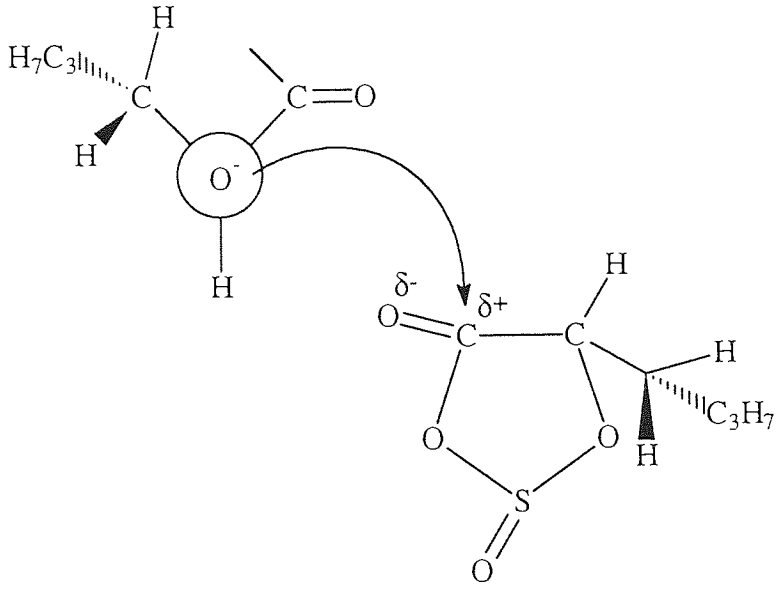

CHAPTER 6

COPOLYMERIZATION OF LACTIC ACID ANHYDROSULFITE WITH ε-CAPROLACTONE

In this chapter, the work has been carried out in collaboration with Dr G. Piquet.

Polymerization of ε-caprolactone can be effected by three different mechanisms categorized as anionic, cationic and coordination. Each method has specific characteristics upon degrees of control of molecular weight, molecular weight distribution and end group composition.

Aluminium alkoxides such as aluminium isopropoxide ($Al(O\text{-}i\text{-}Pr)_3$) [77,78] or tin-containing catalysts such as stannous octoate [24,25] (tin ethyl-2 hexanoate) are effective initiators for the polymerization of ε-caprolactone. These catalysts were found to initiate the cyclic esters by a non-ionic insertion mechanism and to yield living polymers. Teyssie and co-workers [77] reported that the use of aluminium alkoxides, in particular, allowed synthesis of PCL with predictable molecular weight and rather narrow polydispersity. Indeed, these initiators do not cause intermolecular transesterification up to approximately 150°C [78]. Additionally, by an appropriate termination reaction of the living chains prepared by ring-opening polymerization with aluminium alkoxides, three-arm star branched PCL could be synthesised [79].

Various cationic initiators may also be used to polymerize ε-caprolactone. Kricheldorf *et al* [80] conducted copolymerizations of ε-caprolactone with glycolide or lactide with cationic initiators such as ferric chloride, boron trifluoride or triflic acid. In contrast to anionic initiation (discussed in section 1.2.3.), these copolymerizations yielded copolyesters richer in caprolactone.

However, with the objective of generating 'living' systems capable of initiating anhydrosulfites, the anionic polymerization of ε-caprolactone was investigated.

6.1. Preliminary Experiments with ε-Caprolactone

Before performing any copolymerization, the anionic polymerization of ε-caprolactone with butyllithium was examined with the aim of studying its 'living' nature and determining the influence of solvent.

6.1.1. Introduction

The anionic ring-opening polymerization of ε-caprolactone has been extensively studied. It has been reported that ε-caprolactone is a very reactive monomer which is rapidly polymerized by anionic initiators such as butyllithium [81] or potassium *tert*-butoxide [82]. Unlike the ring-opening polymerization of anhydrosulfites, this process is subject to a ring-chain equilibrium given in figure 6.1.

Yamashita and Ito [82] found that the monomer was completely consumed within a few minutes after the introduction of initiator in the system. Also addition of monomer in the reaction mixture resulted in a change of molecular weight distribution in GPC and a simple dilution of the system caused variation of product distribution as well. Thereby, they proposed that the equilibrium involved in the anionic polymerization of ε-caprolactone was 'living'.

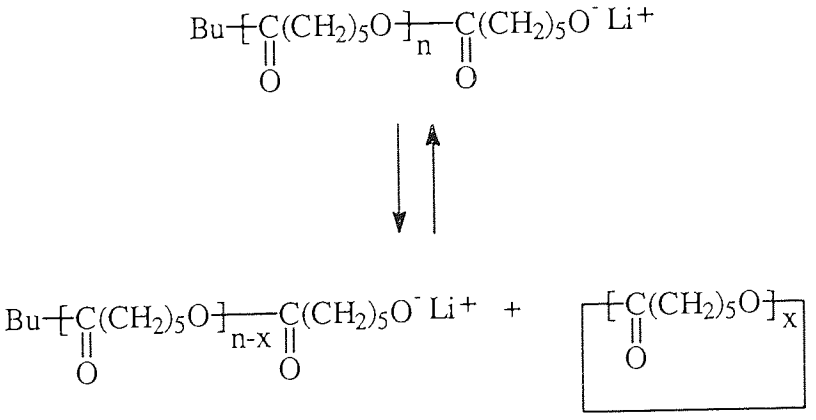

Figure 6.1. Living ring-chain equilibrium in the anionic polymerization of ε-CL in THF with n-BuLi.

Yamashita *et al* [83] observed also that propagation and formation of a linear polymer in the anionic polymerization of ε-caprolactone was then followed by depropagation when the living chains had lost all ability to propagate further. Indeed, if no termination was effected, the living linear chains formed would then either degrade through back-biting reactions to give cyclics oligomers or undergo intermolecular reactions, as shown in figure 6.2. Both intra and intermolecular transesterification broaden the molecular weight distribution. Nevertheless, Penczec *et al* [84] reported that the formation of macrocyclics would occur after much longer time than needed for the polymerization to reach 99 % of monomer conversion.

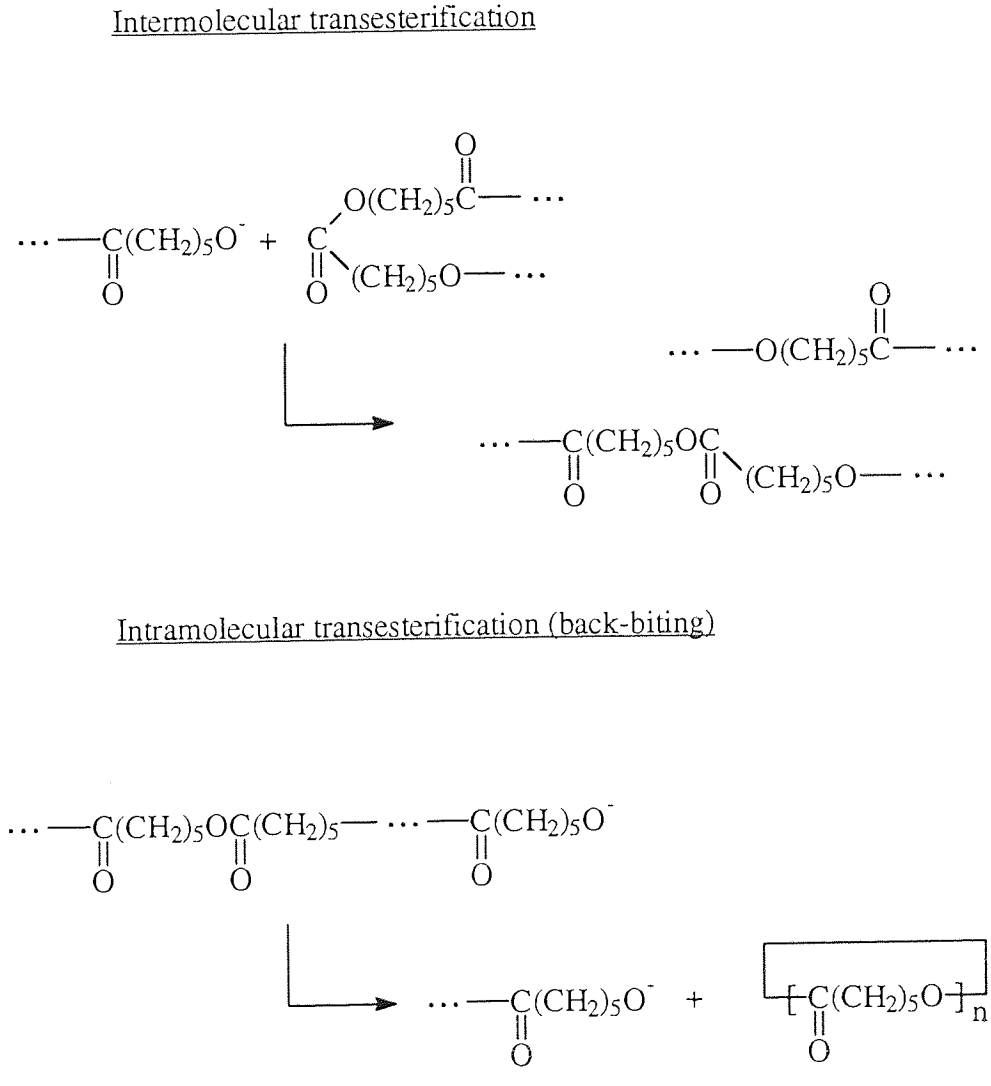

Figure 6.2. Intermolecular and intramolecular reactions of poly(ε-caprolactone) chains.

6.1.2. Experimental

6.1.2.1. ε-caprolactone

In order to remove water, ε-Caprolactone of 99 % purity (supplied by Aldrich Co.) was left over calcium hydride for 3 days, then fractionally distilled under reduced pressure. It was then stored under argon. Figures 6.4. and 6.5. show the ^{1}H and ^{13}C NMR spectra of this compound. They are in agreement with the several relative peak areas as shown in tables 6.1. and 6.2. The structure of ε-caprolactone is described in figure 6.3.

Figure 6.3. Key to NMR spectra of ε-caprolactone.

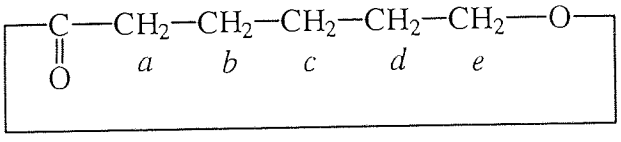

Figure 6.4. ^{1}H NMR spectrum of ε-caprolactone

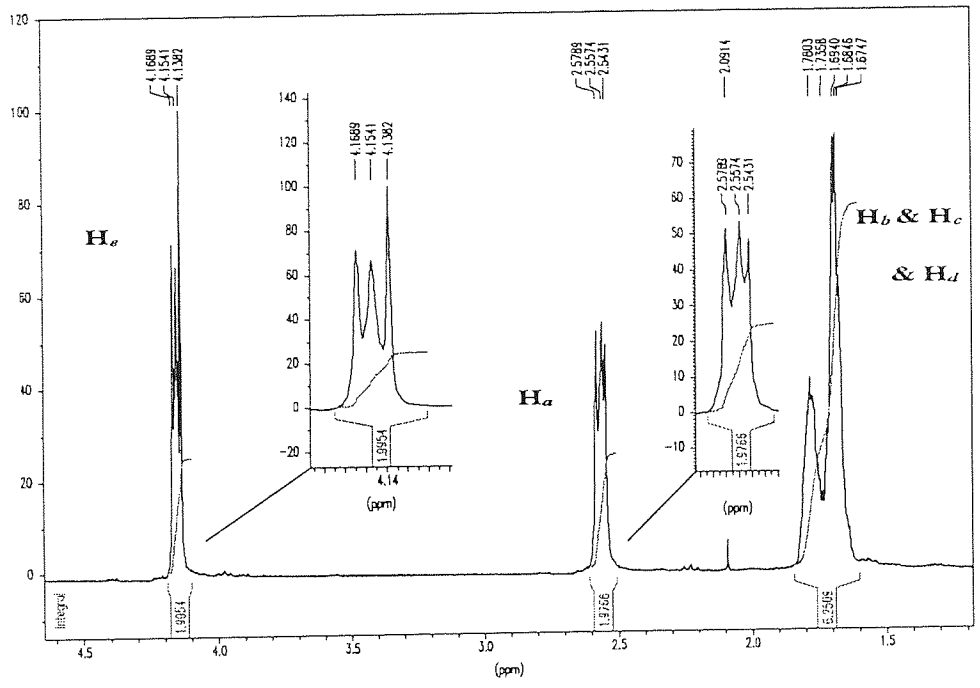

Table 6.1. ^{1}H NMR data of ε-caprolactone.

Monomer	δ.ppm	Peak shape	Relative peak area	Assignment
ε-Caprolactone	1.67 - 1.78	multiplet	6.25	H_b, H_c & H_d
	2.54 - 2.57	triplet	1.97	H_a
	4.13 - 4.16	triplet	1.99	H_e

Figure 6.5. ^{13}C NMR spectrum of ε-caprolactone

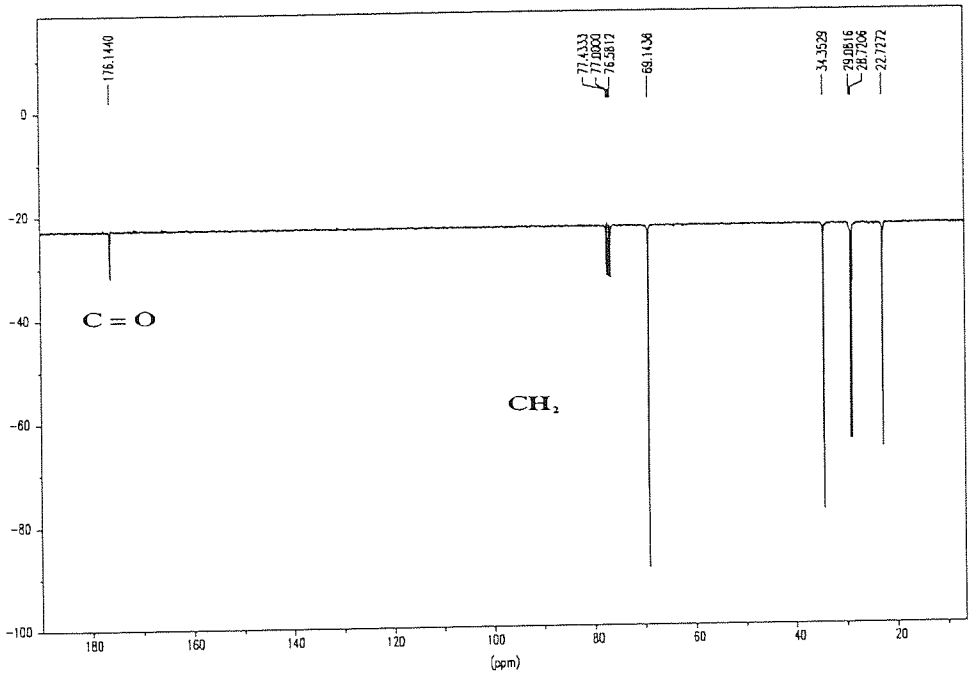

Table 6.2. ^{13}C NMR data of ε-caprolactone.

Monomer	δ.ppm	Assignment
ε-Caprolactone	22.72	CH_{2c}
	28.72 - 29.08	CH_{2b} & CH_{2d}
	34.35	CH_{2a}
	69.14	CH_{2e}
	176.14	C = O

6.1.2.2. Polymerization procedure

The polymerizations were carried out in the same type of vessel as for the polymerization of anhydrosulfites, so that control of temperature was possible, as shown in section 4. The polymerizations were all conducted under argon at 25°C. The solvent was first introduced in the vessel, followed by the initiator in adequate quantity. Shortly after, the

required amount of monomer was injected through a suba seal stopper by syringe. The mixture was then further agitated for 6 minutes.

The polymer formed was precipitated in n-hexane, filtered and dried in a dessicator in order to terminate the polymerization.

6.1.3. Characteristics of the anionic polymerization of ε-caprolactone

6.1.3.1. GPC studies

The polymer samples of PCL were dissolved in THF and then analysed by GPC. For more information about GPC analysis, see section 2. As illustrated in figure 6.6., no trace of oligomers originating from back-biting reactions was observed on the gel permeation chromatographs of PCL.

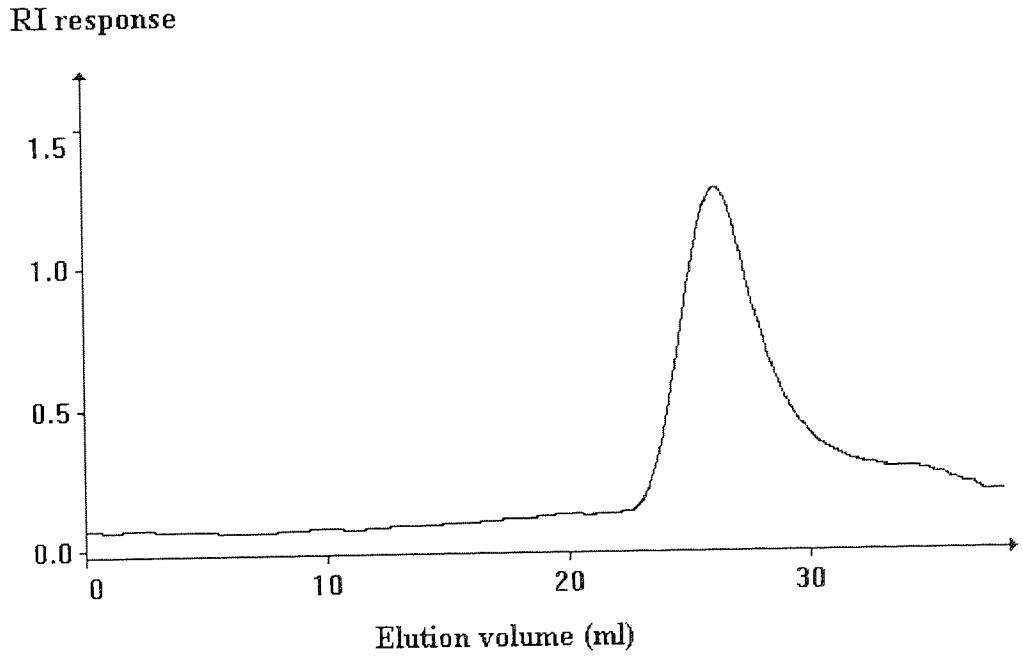

Figure 6.6. Typical GPC trace of PCL initiated by n-BuLi in toluene at 25°C.

6.1.3.2. Effect of the solvent on the molecular weight distribution of polymer

The molecular weights of polymer were higher than the theoretical molecular weights with either solvent, THF or toluene, as shown in table 6.3. This was probably due to side reaction of the initiator with impurities and the solvent in the case of THF, as discussed in section 4.2.1.3. The polydispersities were also rather large because of the occurrence of intra and intermolecular reactions.

In particular, these transesterifications appeared to occur more in THF than in toluene, probably because of the greater reactivity of the active chain ends (free ions) in this solvent than in toluene. A typical GPC trace of PCL is presented in figure 6.6.

Table 6.3. Polymerization of ε-caprolactone with n-BuLi at 25°C with toluene and THF.

Solvent	[M]/[I]	$\overline{Mn}_{theoretical}$ $10^{-4}.mol.g^{-1}$	$\overline{Mn}$ $10^{-4}.mol.g^{-1}$	$\overline{Mw}$ $10^{-4}.mol.g^{-1}$	$\overline{Mw}$ / $\overline{Mn}$
Toluene	50	0.57	2.8	3.8	1.34
	100	1.14	4.2	5.9	1.34
	200	2.28	5.7	7.8	1.34
THF	100	1.14	2.81	4.77	1.69
	150	1.71	4.07	7.02	1.72

As illustrated in figure 6.7. the molecular weights of the polymer produced could be controlled by changing the amount of catalyst used, as decreasing concentration of initiator produced increasing molecular weight. On the other hand, the linear dependence of the molecular weight on the monomer-to-initiator ratio typical of a 'living' system was not exactly obtained, but this did not mean that this polymerization was not living, as observed for PLAAS in section 4.2.1.3.

Figure 6.7. Polymerization of ε-caprolactone with n-BuLi in toluene at 25°C.

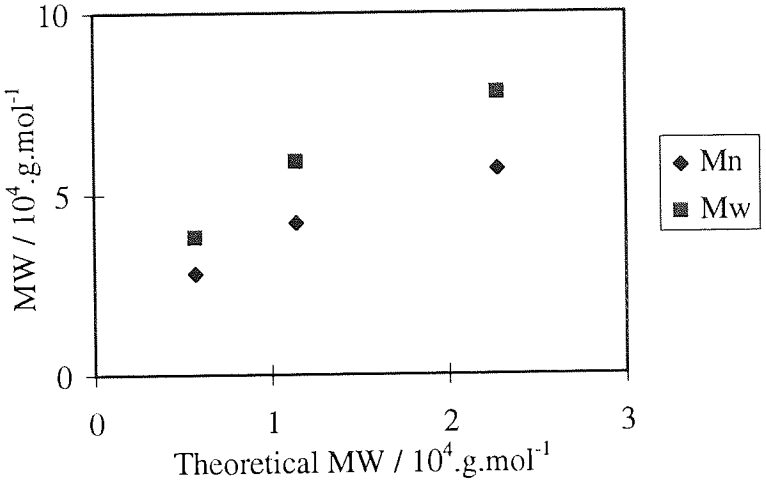

6.1.4. Characterization of poly(ε-caprolactone)

The ^{1}H and ^{13}C NMR spectroscopy was used to characterize the structure of poly(ε-caprolactone) represented in figure 6.8. The NMR spectra are presented in figures 6.9. and 6.10. Additionally, tables 6.4. and 6.5. show the different assignments that could be deduced.

Figure 6.8. Key to NMR spectra of PCL

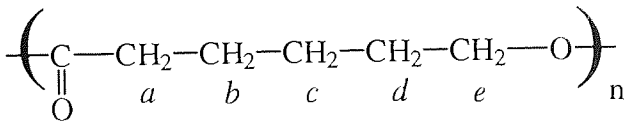

Figure 6.9. ^{1}H NMR spectrum of PCL

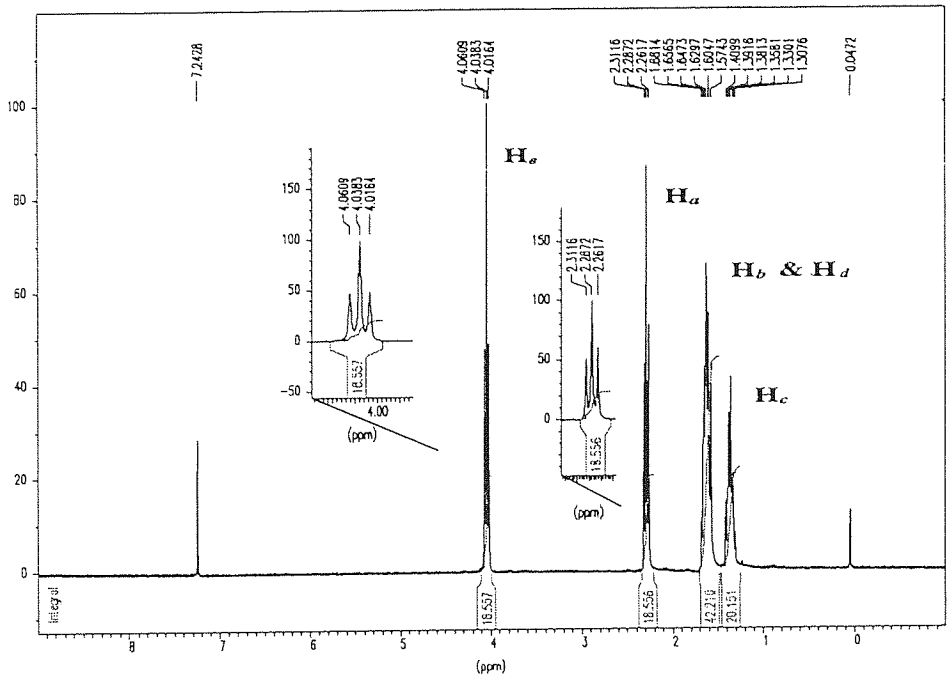

Table 6.4. ^{1}H NMR data of PCL

Polyester	δ.ppm	Peak shape	Relative peak area	Assignment
PCL	1.30 - 1.40	multiplet	20.15	H_b & H_d
	1.57 - 1.68	multiplet	42.21	H_c
	2.26 - 2.31	triplet	18.55	H_a
	4.01 - 4.06	triplet	18.55	H_e

Figure 6.10. ^{13}C NMR spectrum of PCL

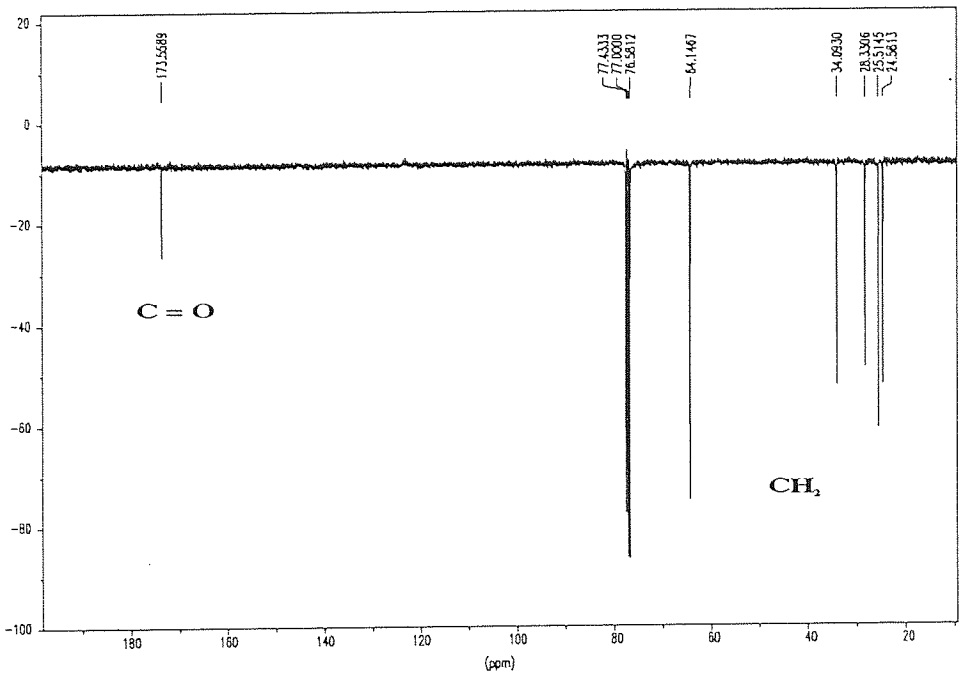

Table 6.5. ^{13}C NMR data of PCL

Polyester	δ.ppm	Assignment
PCL	24.58	CH_{2c}
	25.51	CH_{2b}
	28.33	CH_{2d}
	34.09	CH_{2a}
	64.14	CH_{2e}
	173.55	C = O

6.2. Experimental

The diagram of the copolymerization vessel is presented in section 4.1. All experiments were conducted under argon at 25°C and butyllithium was used as initiator for all polymerizations because of its satisfactory results for the homopolymerizations of ε-caprolactone and the aliphatic anhydrosulfites.

6.2.1. Block-copolymerization

The polymerization of the first monomer (CL or anhydrosulfite) was first carried out, as described in section 4.1. with n-BuLi as initiator and after 6 minutes when the polymerization was complete, the second monomer was added. This mixture was then further agitated for 6 minutes. The polymer solution was poured into a large amount of n-hexane and the resulting precipitate was then filtered and dried in a dessicator.

6.2.2. Random copolymerization

In this experiment, the two monomers involved in the copolymerization were mixed. This mixture was then injected in the polymerization vessel containing the solvent and the initiator n-BuLi and subsequently, was left under stirring for 6 minutes. The product obtained was then precipitated in n-hexane, filtered and dried.

6.3. Block-copolymers poly(ε-CL)-block-poly(LAAS)

6.3.1. GPC analysis

Block-copolymerizations of ε-CL with L- (or DL-) LAAS were first carried out in toluene, a suitable solvent for PCL initiated with n-BuLi at 25°C. But, these conditions turned out to be unsatisfactory. The molecular weight distribution of PCL before addition of LAAS was unimodal and when the addition of LAAS was performed, a bimodal polymer was obtained, as illustrated in figures 6.11. and 6.12. By deconvolution, the estimates of the molecular weight of the two fragments were determined, as shown in table 6.6. The high molecular weight peak increased by the addition of LAAS. This meant that presumably addition of lactic units onto the PCL chains had taken place simultaneously to a homopolymerization of LAAS by the excess of butyllithium, PLAAS corresponding to the low molecular weight peak.

Table 6.6. Block-copolymerization of ε-caprolactone and DL-LAAS with n-BuLi at 25°C in toluene with a ratio n-BuLi:CL:LAAS of 1: 50:50.

Polymer	$\overline{Mn}$ 10^{-4}.mol.g^{-1}	$\overline{Mw}$ 10^{-4}.mol.g^{-1}	$\overline{Mw}$ / $\overline{Mn}$	Observation
PCL before addition of LAAS	3.0	4.1	1.39	unimodal
Poly(ε-CL)-block-poly(DL-LAAS)	3.7 0.69	4.6 0.74	1.26 1.07	bi-modal

Figure 6.11. GPC trace of PCL initiated by n-BuLi in toluene at 25°C before addition of DL-LAAS

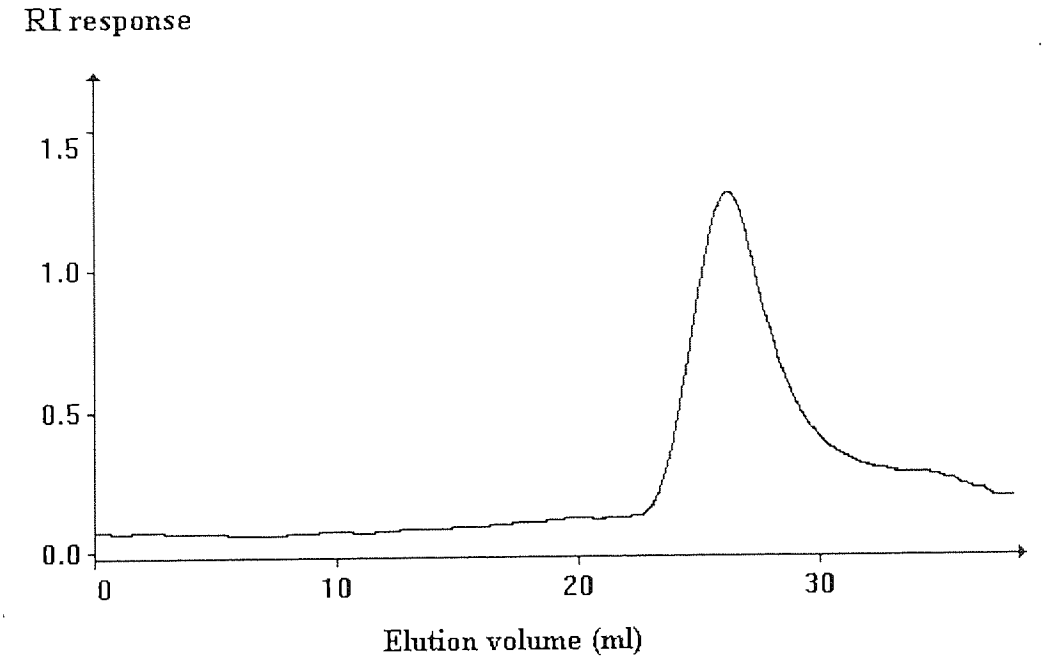

Figure 6.12. GPC trace of copolymer poly(ε-CL)-block-poly(DL-LAAS) initiated by n-BuLi in toluene at 25°C.

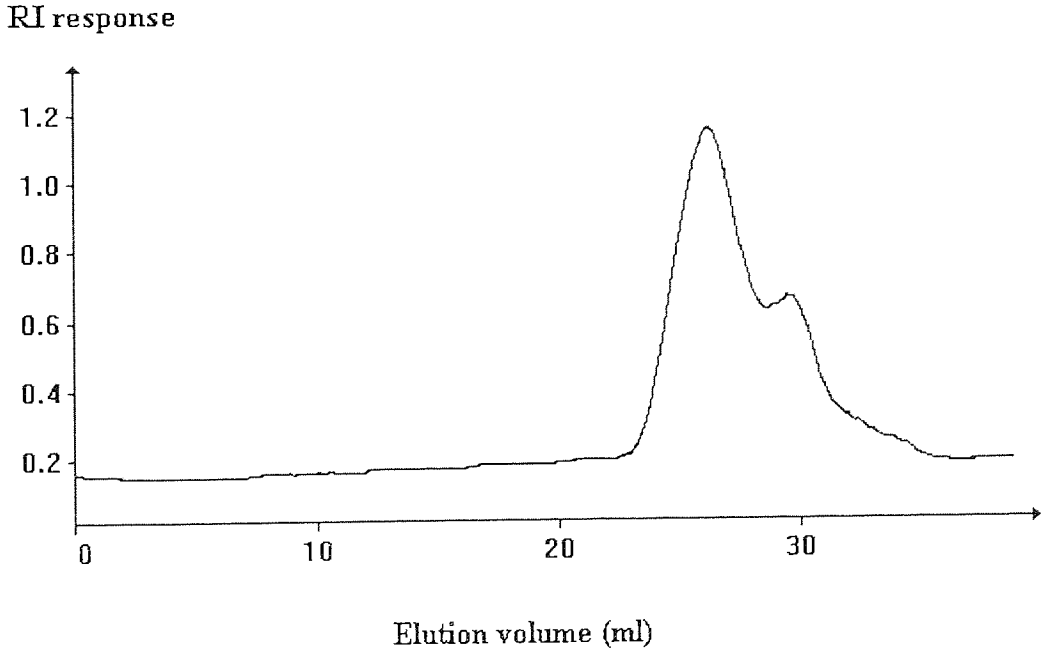

In contrast, when THF was used as solvent, no peak corresponding to the homopolymer PLAAS was observed in GPC, as shown in figure 6.13. In toluene, some initiator n-BuLi was probably still present in the reaction medium after polymerization of PCL and therefore was likely to polymerize LAAS simultaneously with the living PCL chains whereas in THF, residual n-BuLi had completely disappeared after 6 minutes when the addition of LAAS was performed because of its reaction with the solvent presented in section 4.3. Nevertheless, in some cases, the oligomers originating from back-biting were observed, as shown in figure 6.13.

Figure 6.13. GPC trace of copolymer poly(ε-CL)-block-poly(L-LAAS) initiated by n-BuLi in THF at 25°C.

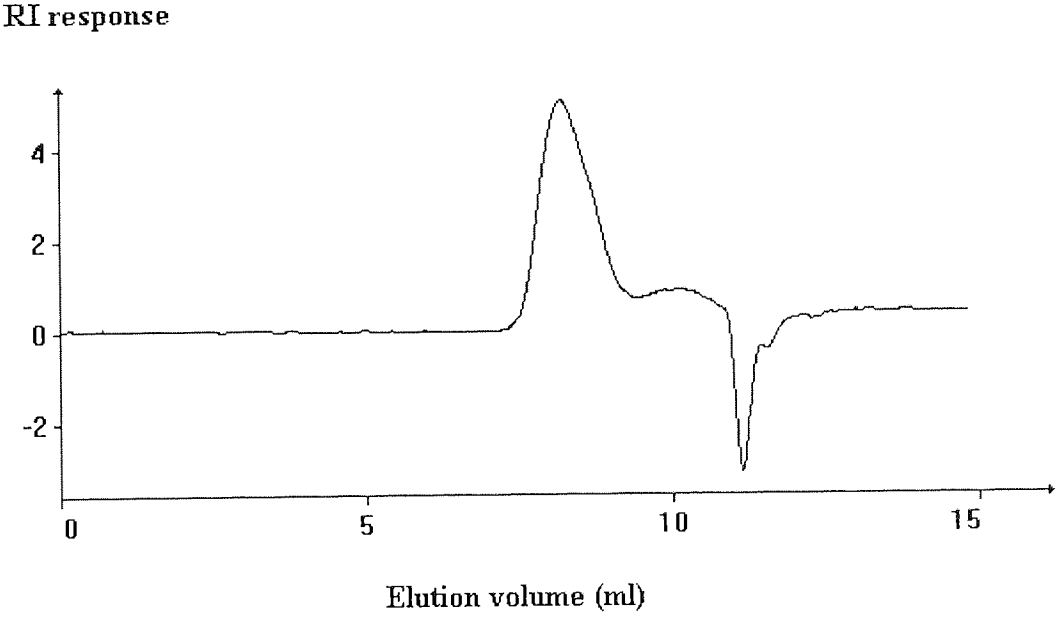

The molecular weights obtained were relatively high, as shown in table 6.7. and the polydispersity between 1.5 and 1.7., as expected for a PCL synthesised in THF, see section 6.1. Additionally, the molecular weights were higher with L-LAAS than DL-LAAS, as observed in their homopolymerization in section 4.

Table 6.7. Block-copolymerization of ε-caprolactone with L- and DL-LAAS with n-BuLi at 25°C in THF with a ratio n-BuLi:CL:LAAS of 1: 50:50.

Sample	Copolymer	$\overline{Mn}$ 10^{-4}.mol.g^{-1}	$\overline{Mw}$ 10^{-4}.mol.g^{-1}	$\overline{Mw}$ / $\overline{Mn}$	Observation
COP 8	Poly(ε-CL)-block-poly(L-LAAS)	2.08	3.15	1.51	unimodal
COP 9	Poly(ε-CL)-block-poly(DL-LAAS)	1.76	2.99	1.70	unimodal

6.3.2. NMR studies

^{1}H and ^{13}C NMR spectroscopy were used to characterize the structure of the polymers prepared. ^{1}H NMR studies were also useful for determining the molar ratio of lactic acid and ε-caprolactone monomer units in the copolymers.

The unimodal polymers COP 8 and COP 9 were analysed by NMR spectroscopy. The spectra exhibited simultaneously the signals for the several protons originating from both blocks PLAAS and PCL, with no additional resonances, so a structure of the A-B type block-copolyesters could be deduced for these copolyesters. The structure of poly(CL)-block-poly(LAAS) is described in figure 6.14. Figures 6.15. and 6.16 show the ^{1}H NMR spectra of poly(CL)-block-poly(L-LAAS) and poly(CL)-block-poly(DL-LAAS), respectively. The corresponding assignments are presented in tables 6.8. and 6.9. In the ^{1}H NMR spectrum of poly(CL)-block-poly(DL-LAAS), in particular, it can be seen a signal at approximately 2 ppm attributed to water and another signal at 0.9 ppm due to n-hexane, this copolyester being difficult to dry.

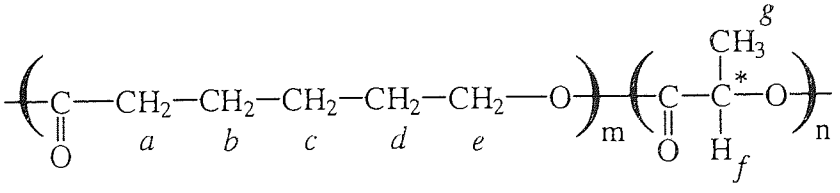

Figure 6.14. Key to NMR spectra of block copolymers poly(ε-CL)-block-poly(LAAS).

Figure 6.15. ^{1}H NMR spectrum of block-copolymer poly(εCL)-block-poly(L-LAAS) / COP 8

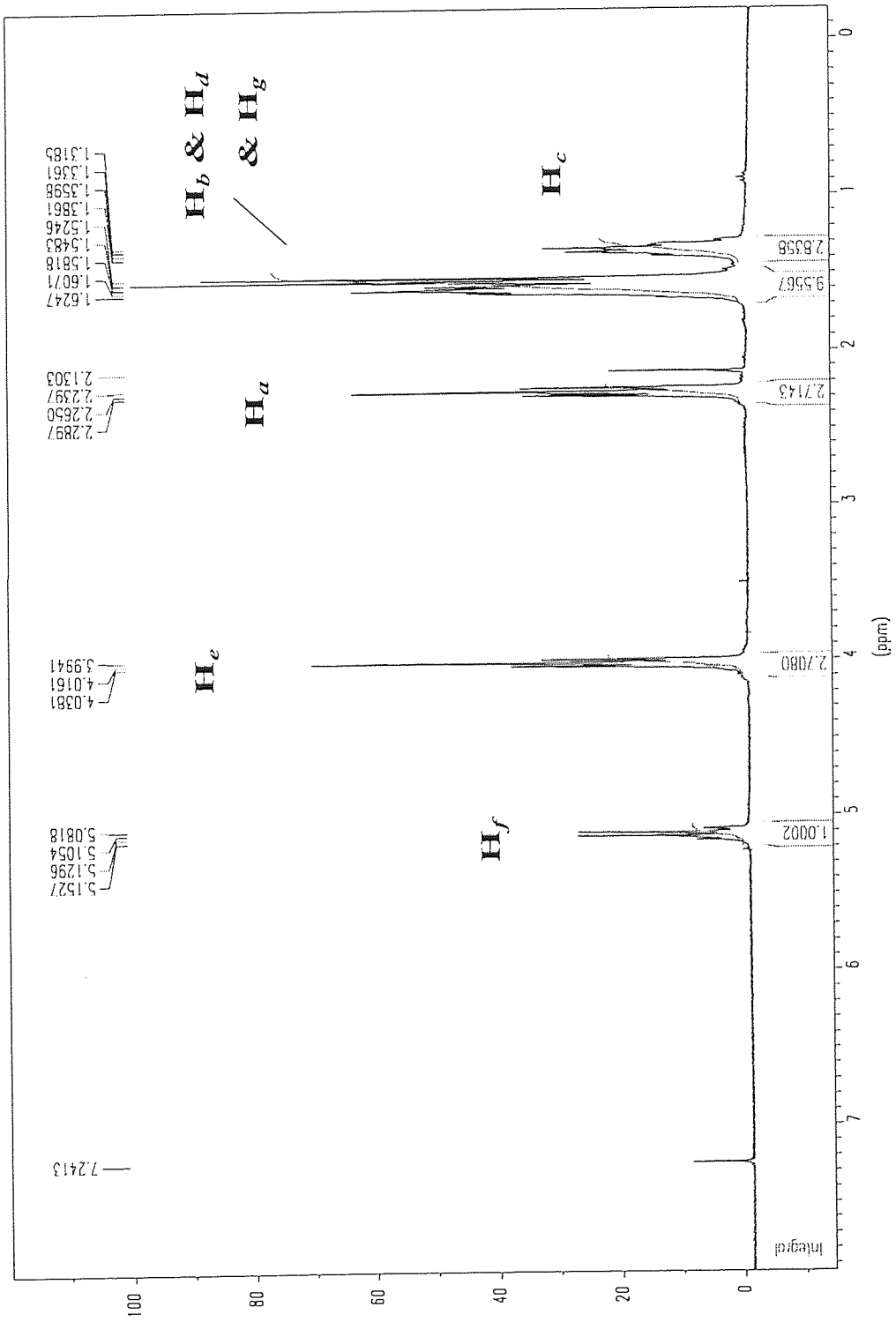

Figure 6.16. ^{1}H NMR spectrum of block copolymer poly(εCL)-block-poly(DL-LAAS) / COP 9

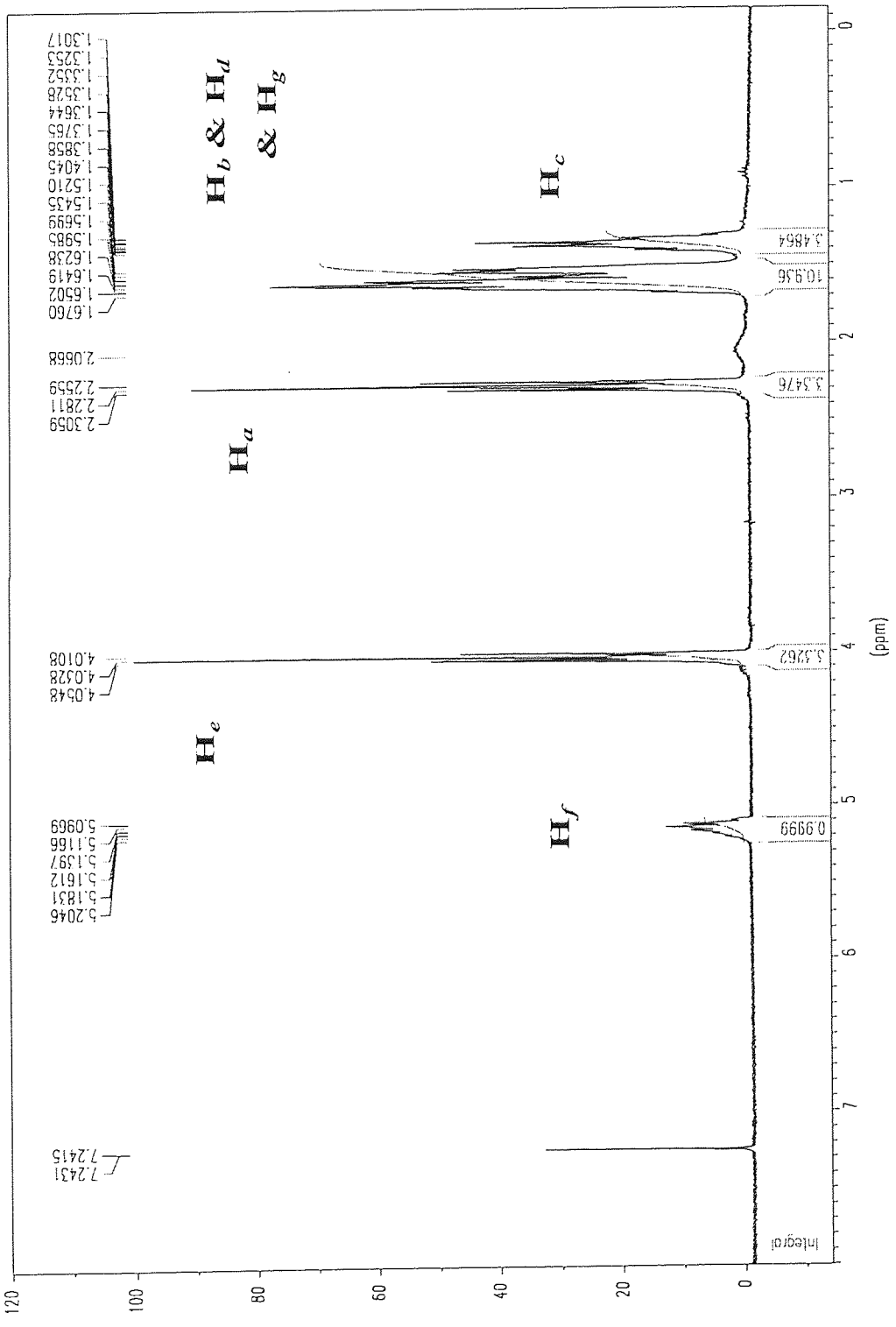

Table 6.8. ^{1}H NMR data of poly(εCL)-block-poly(L-LAAS) / COP 8.

Polyester	δ.ppm	Peak shape	Relative peak area	Assignment
PCL-block-L-PLAAS	1.30 - 1.40	multiplet	3.48	H_c
	1.52 - 1.67	multiplet	10.93	H_b & H_d & H_g
	2.25 - 2.30	triplet	3.34	H_a
	4.01 - 4.05	triplet	3.32	H_e
	5.09 - 5.20	quartet	0.99	H_f

Table 6.9. ^{1}H NMR data of poly(εCL)-block-poly(DL-LAAS) / COP 9.

Polyester	δ.ppm	Peak shape	Relative peak area	Assignment
PCL-block-DL-PLAAS	1.31 - 1.38	multiplet	2.83	H_c
	1.52 - 1.62	multiplet	9.55	H_b & H_d & H_g
	2.23 - 2.28	triplet	2.71	H_a
	3.99 - 4.03	triplet	2.70	H_e
	5.08 - 5.15	multiplet	1.00	H_f

The molar compositions of the copolyesters were calculated from the relative peak areas of the ^{1}H NMR resonance peaks of the methine proton H_f in LAAS at 5.1 ppm and the methylene protons H_e in ε-position in CL at 4.0 ppm. As illustrated in figures 6.17 and 6.18., the two signals did not overlap so that integration was possible.

As expected, the two distinct signals of the methine proton H_f in L- and DL-polylactic chains were observed, a 1:3:3:1 quartet for poly(CL)-block-poly(L-LAAS) and a multiplet for poly(CL)-block-poly(DL-LAAS).

Figure 6.17. Methine proton (H_f) signal of LAAS and methylene proton (H_e) signal of PCL in the ^{1}H NMR spectrum of block copolymer poly(εCL)-block-poly(L-LAAS)

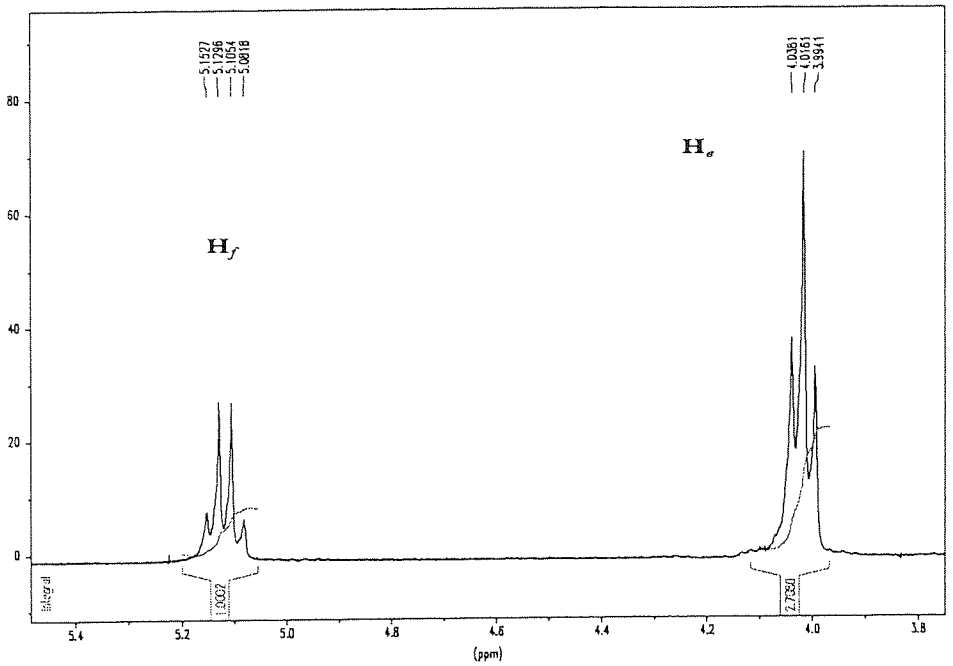

Figure 6.18. Methine proton (H_f) signal of LAAS and methylene proton (H_e)signal of PCL in the ^{1}H NMR spectrum of block copolymer poly(εCL)-block-poly(DL-LAAS)

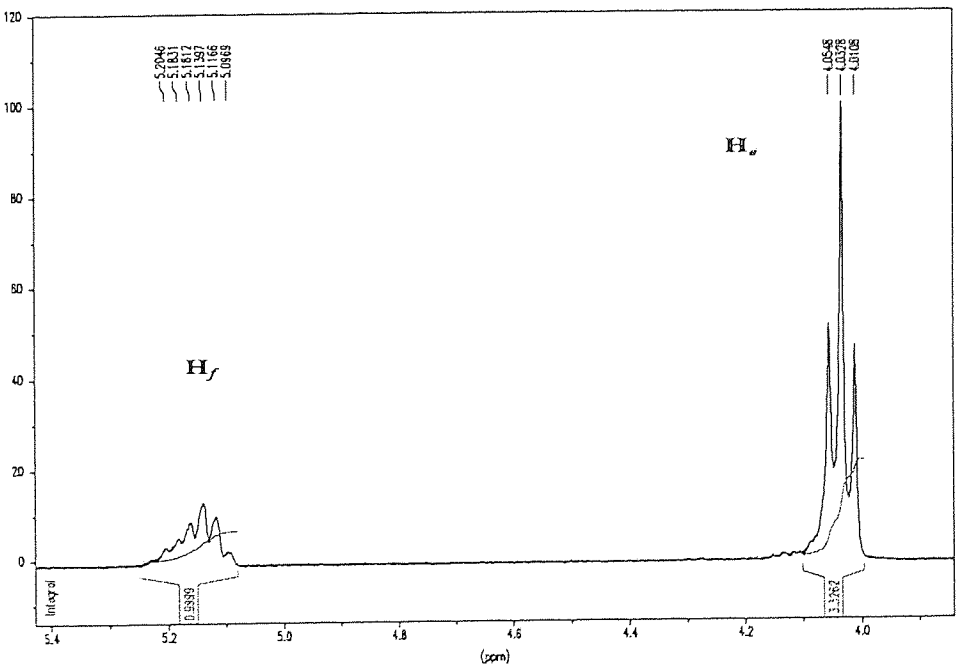

The compositions of the copolymers were found to be in agreement with the feed compositions except for COP 14, as shown in table 6.10., indeed for a monomer-to-initiator ratio of 150 or above the polymer PCL formed was very viscous making the copolymerization more difficult to proceed. This explained the polydispersity close to 2 for this copolymer. Also the incorporation of lactic units onto the polycaprolactone chains was not influenced by the enantiomeric nature of LAAS.

Table 6.10. Block-copolymerization of ε-caprolactone with LAAS initiated with n-BuLi at 25°C in THF with different feed ratios.

Sample	Feed ratio I : CL : LAAS	*	$\overline{Mn}$ 10^{-4}.mol.g^{-1}	$\overline{Mw}$ 10^{-4}.mol.g^{-1}	$\overline{Mw}$ / $\overline{Mn}$	NMR data CL : LAAS
COP 8	1 : 50 : 50	L	2.08	3.15	1.51	55 : 45
COP 9	1 : 50 : 50	DL	1.76	2.99	1.70	58 : 42
COP 14	1 : 150 : 50	DL	3.72	7.50	2.01	62 : 38
COP 15	1 : 100 : 30	DL	2.99	4.80	1.61	77 : 23

* Enantiomeric nature of LAAS.

The ^{13}C NMR spectra of poly(CL)-block-poly(L-LAAS) and poly(CL)-block-poly(DL-LAAS) are presented in figures 6.20. and 6.21., respectively. The several signals were attributed to the different carbons present in the copolyester, as shown in tables 6.11. and 6.12. These spectra exhibited the expected signals for a A-B type copolymer poly(CL)-block-poly(LAAS).

Figure 6.19. ^{13}C NMR spectrum of block copolymer poly(εCL)-block-poly(L-LAAS) / COP 8

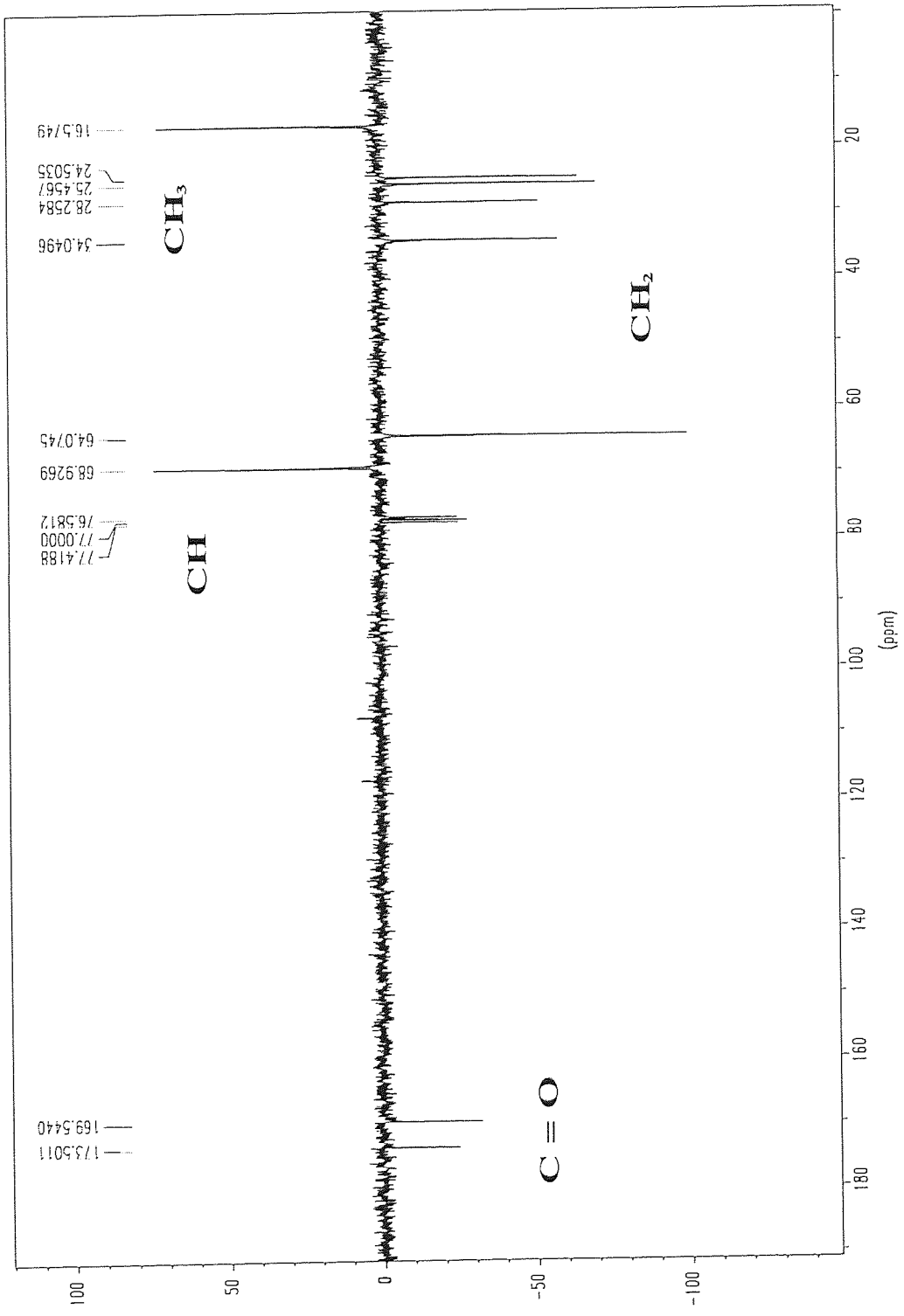

Figure 6.20. ^{13}C NMR spectrum of block copolymer poly(εCL)-block-poly(DL-LAAS) / COP 9

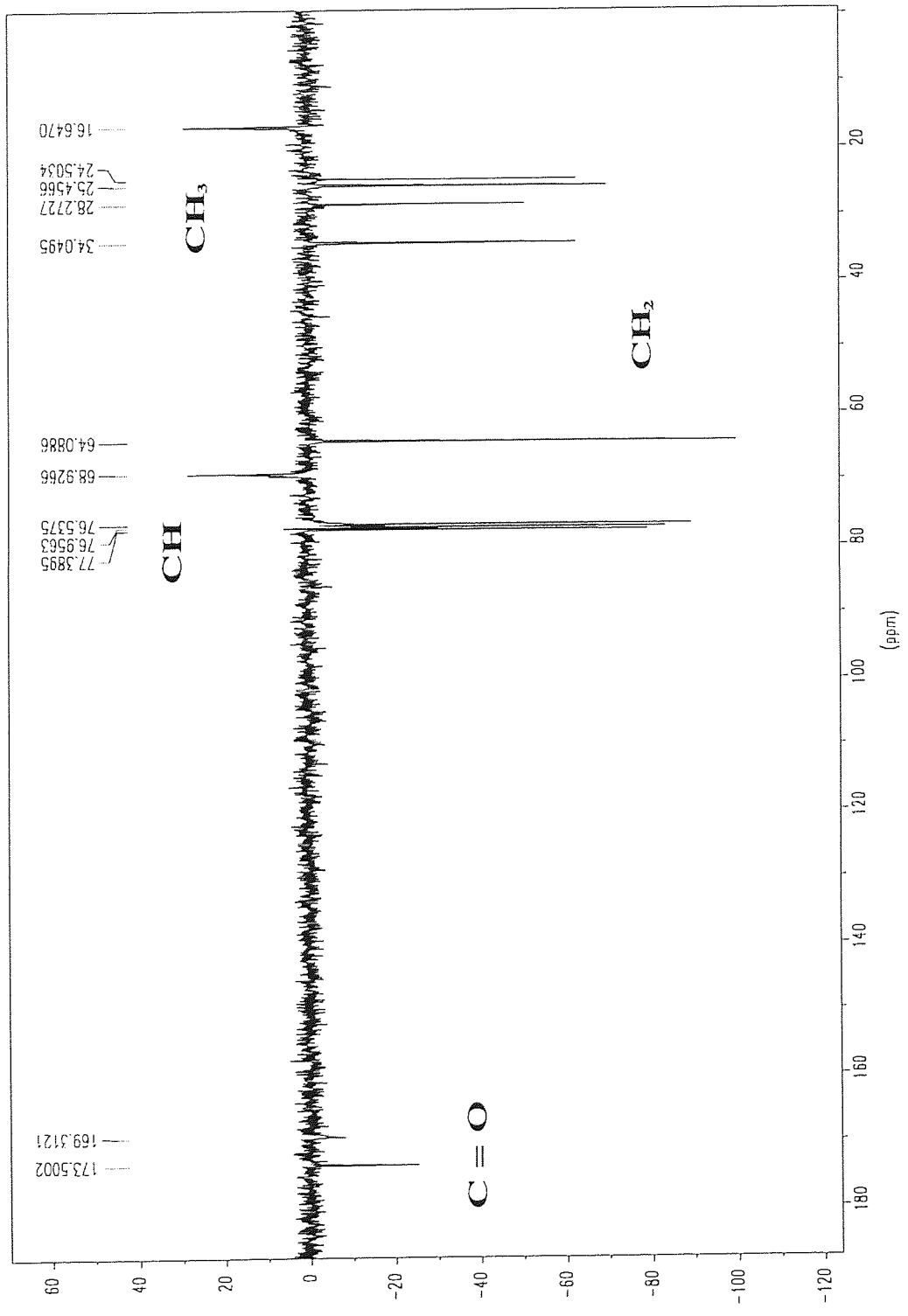

Table 6.11. ^{13}C NMR data of poly(εCL)-block-poly(L-LAAS) / COP 8

Polyester	δ.ppm	Assignment
PCL-block-L-PLAAS	16.57	CH_{3g} (LAAS)
	24.50	CH_{2c}
	25.45	CH_{2b}
	28.25	CH_{2d}
	34.04	CH_{2a}
	64.07	CH_{2e}
	68.92	CH_f (LAAS)
	169.54	C = O (LAAS)
	173.50	C = O

Table 6.12. ^{13}C NMR data of poly(εCL)-block-poly(DL-LAAS) / COP 9

Polyester	δ.ppm	Assignment
PCL-block-DL-PLAAS	16.64	CH_{3g} (LAAS)
	24.50	CH_{2c}
	25.45	CH_{2b}
	28.27	CH_{2d}
	34.04	CH_{2a}
	64.08	CH_{2e}
	68.92	CH_f (LAAS)
	169.31	C = O (LAAS)
	173.50	C = O

As expected, two carbonyl peaks were visible in each ^{13}C NMR spectrum, one from the block polycaprolactone at 173 ppm and the other from the block polylactic at 169 ppm. Additionally, the two types of carbonyl signal at approximately 169 ppm from the polylactic chains were distinguished, a single peak for poly(εCL)-block-poly(L-LAAS)

and several lines for poly(εCL)-block-poly(DL-LAAS), as shown in figures 6.21. and 6.22.

Figure 6.21. Carbonyl signals in the ^{13}C NMR spectrum of block copolymer poly(εCL)-block-poly(L-LAAS) / COP 8

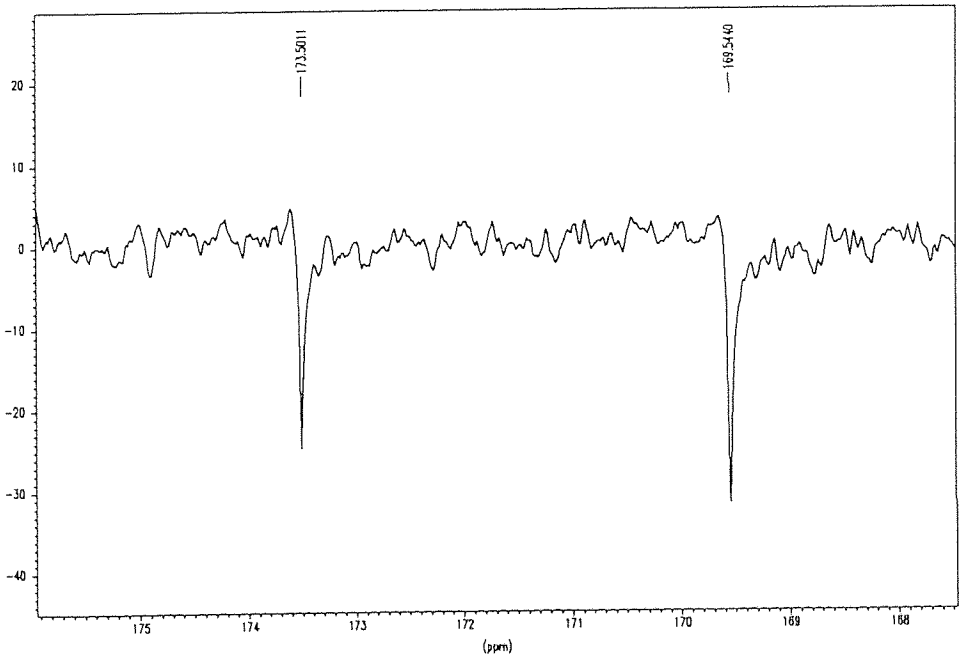

It should be mentioned that the initiation of DL-LAAS by the active PCL chains led to a polymer with stereosequences similar to those obtained for the anionic polymerization of DL-LAAS by butyllithium, as shown in figure 6.23. Indeed, the methine carbon signal is slightly different because of the overlapping of signals originated from lactic units attached to PCL chains. Nevertheless, the block DL-PLAAS in the block copolymers poly(εCL)-block-poly(DL-LAAS) was found atactic with D- and L-lactic units randomly distributed.

Figure 6.22. Carbonyl signals in the ^{13}C NMR spectrum of block copolymer poly(εCL)-block-poly(DL-LAAS) / COP 9

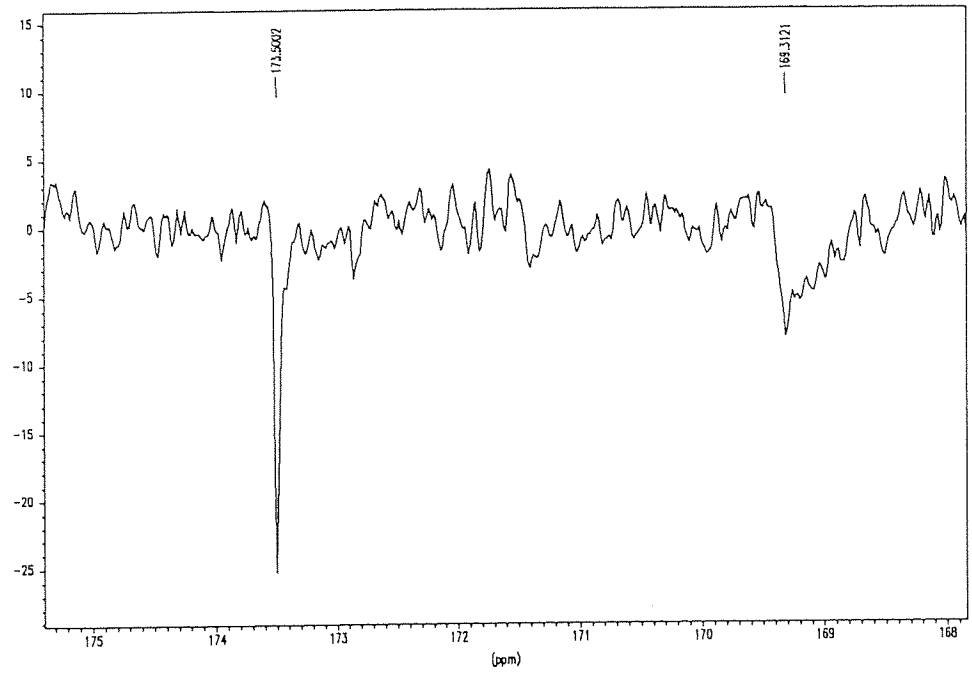

Figure 6.23. Methine carbon signal CH_f in the ^{13}C NMR spectrum of block copolymer poly(εCL)-block-poly(DL-LAAS) / COP 9

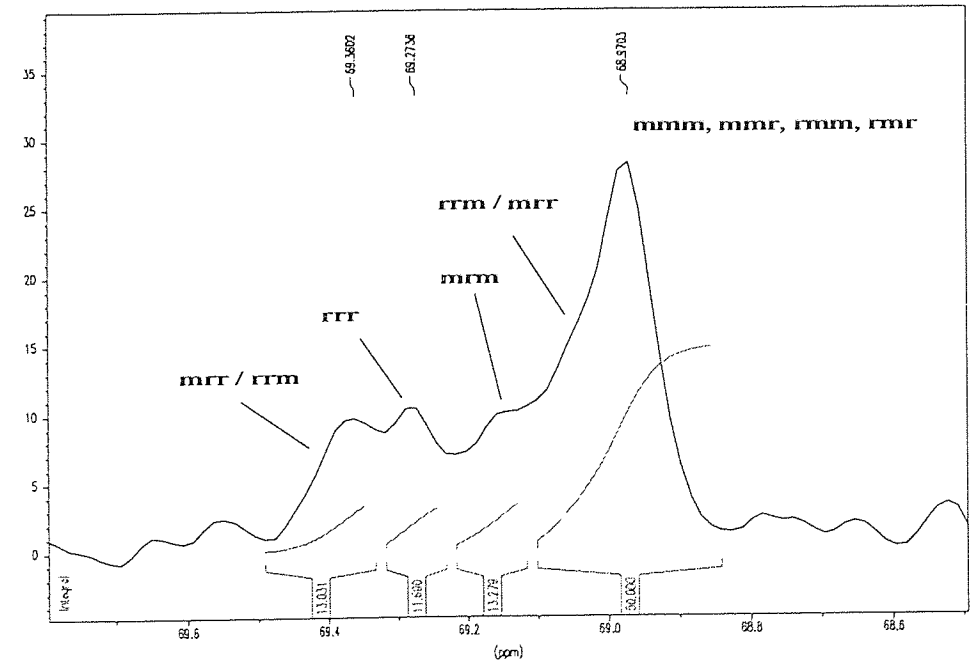

6.3.3. Discussion

The 'living' polycaprolactone chains initiated anionically the polymerization of LAAS. Pure block-copolymers poly(CL)-block-poly(LAAS) possessing unimodal molecular weight distribution were synthesised in THF whereas in toluene, bimodal polymers were obtained. Butyllithium which was not used in the polymerization of ε-caprolactone reacted with THF (for more information, see section 4.2.) whereas in toluene, the excess of butyllithium were still reactive and so could compete with the active chain ends of polycaprolactone as a potential initiator of LAAS. Consequently, in toluene two polymers were formed, the poly(CL)-block-poly(LAAS) and the homopolymer PLAAS. However, in THF, block-copolymers poly(CL)-block-poly(LAAS) with a $\overline{Mn}$ of 2 x10^4 could be synthesised, with either the pure enantiomer L-LAAS or the racemic DL-LAAS. As expected, the ^1H and ^{13}C NMR spectra of these copolyesters poly(CL)-block-poly(LAAS) exhibited signals of a A-B type copolymer. From the ^1H NMR spectra of the copolyesters, the molar ratio of lactic acid and ε-caprolactone monomer units in the copolymers could be determined. The compositions of the block-copolymers were found in good agreement with the feed.

Besides, the block poly(DL-LAAS) in the block-copolymers poly(CL)-block-poly(DL-LAAS) appeared to have an atactic structure similar to the homopolymer DL-PLAAS, meaning that this copolymerization was not stereoselective.

6.4. Block-copolymers poly(LAAS)-block-poly(ε-CL)

The block-copolymerizations of LAAS with ε-CL was also performed under conditions similar to those described in the previous section, for the copolymerization of poly(CL)-block-poly(LAAS). They were carried out in either THF or toluene at 25°C with butyllithium as initiator.

6.4.1. GPC analysis

The results obtained for the copolymerization of LAAS with ε-caprolactone are presented in table 6.13. All the products synthesised presented a rather narrow unimodal distribution, polydispersity between 1.0 to 1.2. in either solvent THF or toluene. Additionally, the molecular weights were smaller than expected by the feed ratio.

Table 6.14. Block-copolymerization of LAAS and ε-CL with n-BuLi at 25°C in THF.

Sample	Feed ratio I:LAAS:CL	*	Solvent	$\overline{Mn}$ 10^{-3}.mol.g^{-1}	$\overline{Mw}$ 10^{-3}.mol.g^{-1}	$\overline{Mw}$ / $\overline{Mn}$	NMR data LAAS:CL
COP 6	1 : 180 : 90	DL	toluene	22.0	26.9	1.22	98 : 2
COP 12	1 : 100 : 50	L	THF	8.9	9.6	1.08	94 : 6
COP 13	1 : 100 : 50	DL	THF	11.3	12.9	1.14	94 : 6

* Enantiomeric nature of LAAS.

6.4.2. NMR studies

The polymers synthesised in this series of copolymerization were then analysed by ^{1}H and ^{13}C NMR in order to define their structure and their molar composition in lactic and caprolactone units. The different protons present in the copolyester poly(LAAS)-block-poly(ε-CL) are shown in figure 6.24.

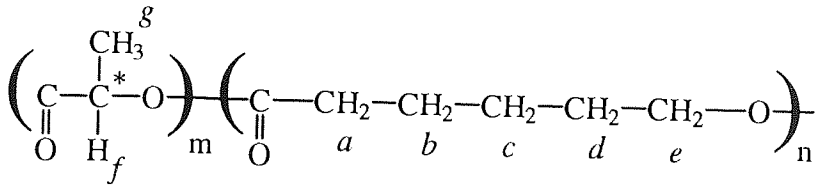

Figure 6.24. Key to NMR spectra of block copolymers poly(LAAS)-block-poly(ε-CL).

The copolymers still contained some unreacted ε-CL. As shown in figure 6.25. for poly(L-LAAS)-block-poly(ε-CL), the characteristics signals of ε-CL were visible in the ^{1}H NMR spectra of the copolyesters, the two triplets centred at 2.57 ppm and 4.17 ppm together with the multiplet at 1.7 ppm. Therefore, the samples of polymer were washed with n-hexane and then dried before analysis by NMR spectroscopy.

The ^{1}H NMR spectra of poly(L-LAAS)-block-poly(ε-CL) and poly(DL-LAAS)-block-poly(ε-CL) are shown in figures 6.26. and 6.27., respectively. The peak tables and the assignments are listed in tables 6.15. and 6.16.

Figure 6.25. ^{1}H NMR spectrum of poly(L-LAAS)-block- poly(εCL) before washing / COP 12.

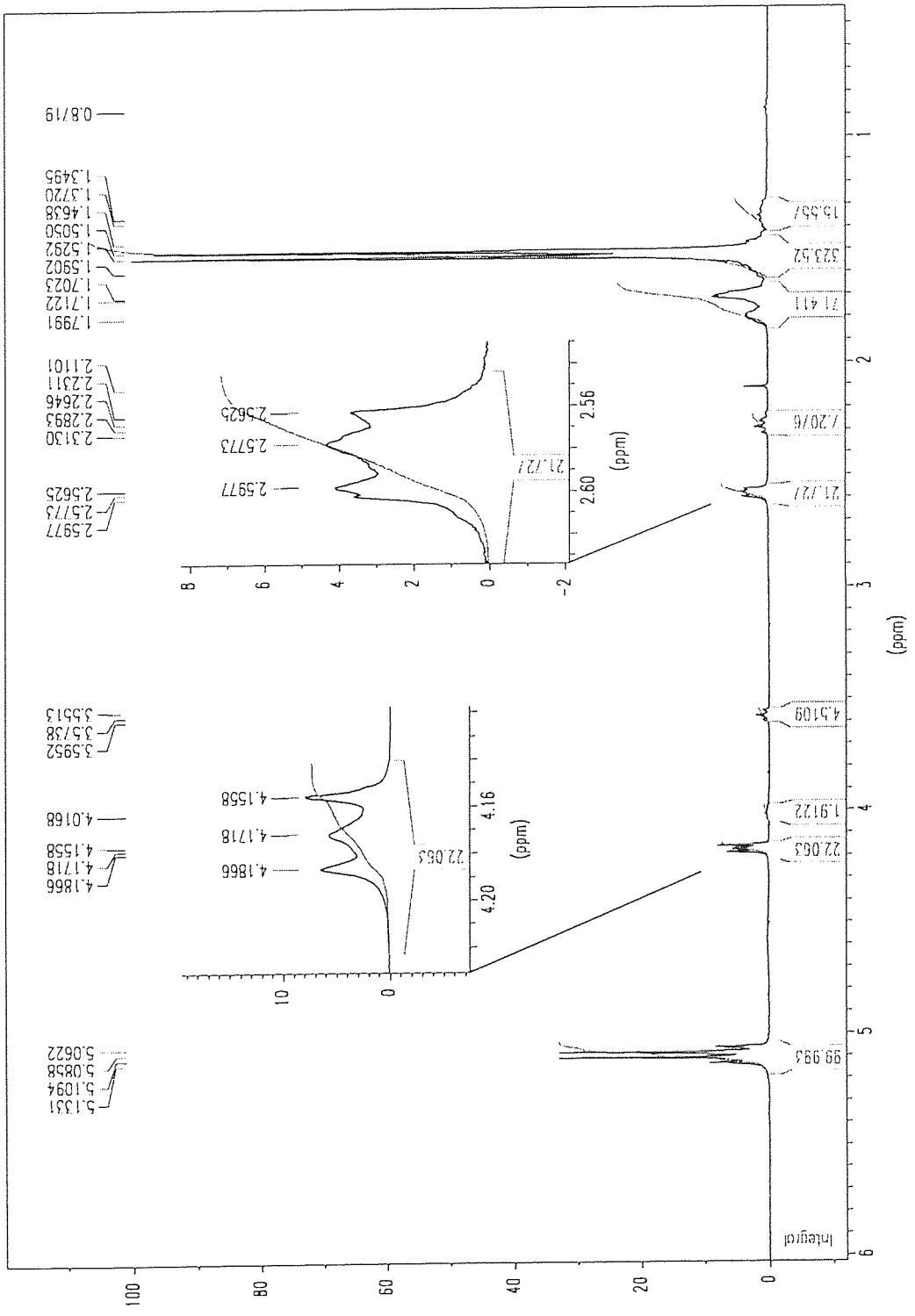

Figure 6.26. ^{1}H NMR spectrum of poly(L-LAAS)-block- poly(εCL) / COP 12.

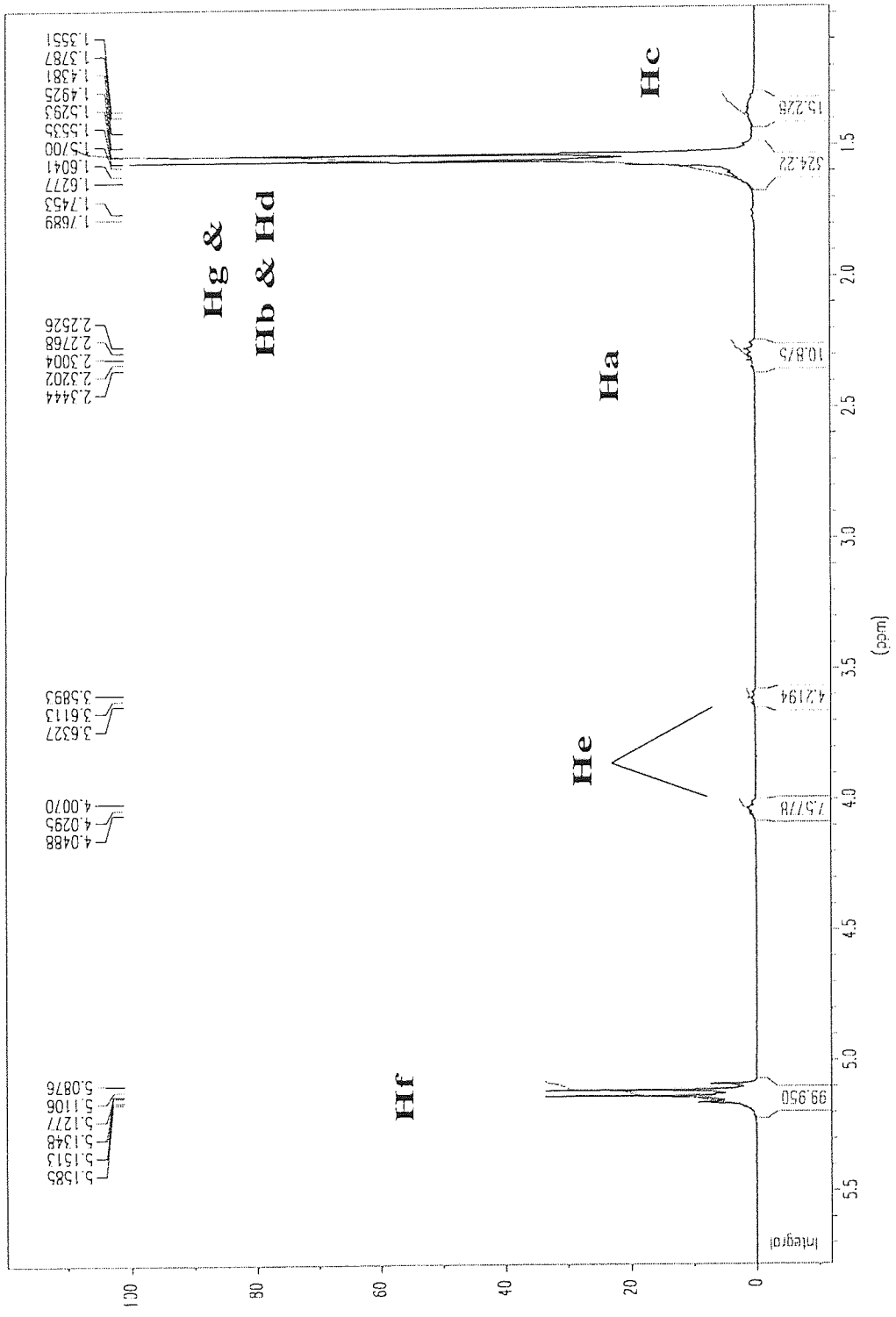

Figure 6.27. ^{1}H NMR spectrum of poly(DL-LAAS)-block- poly(εCL) / COP 13.

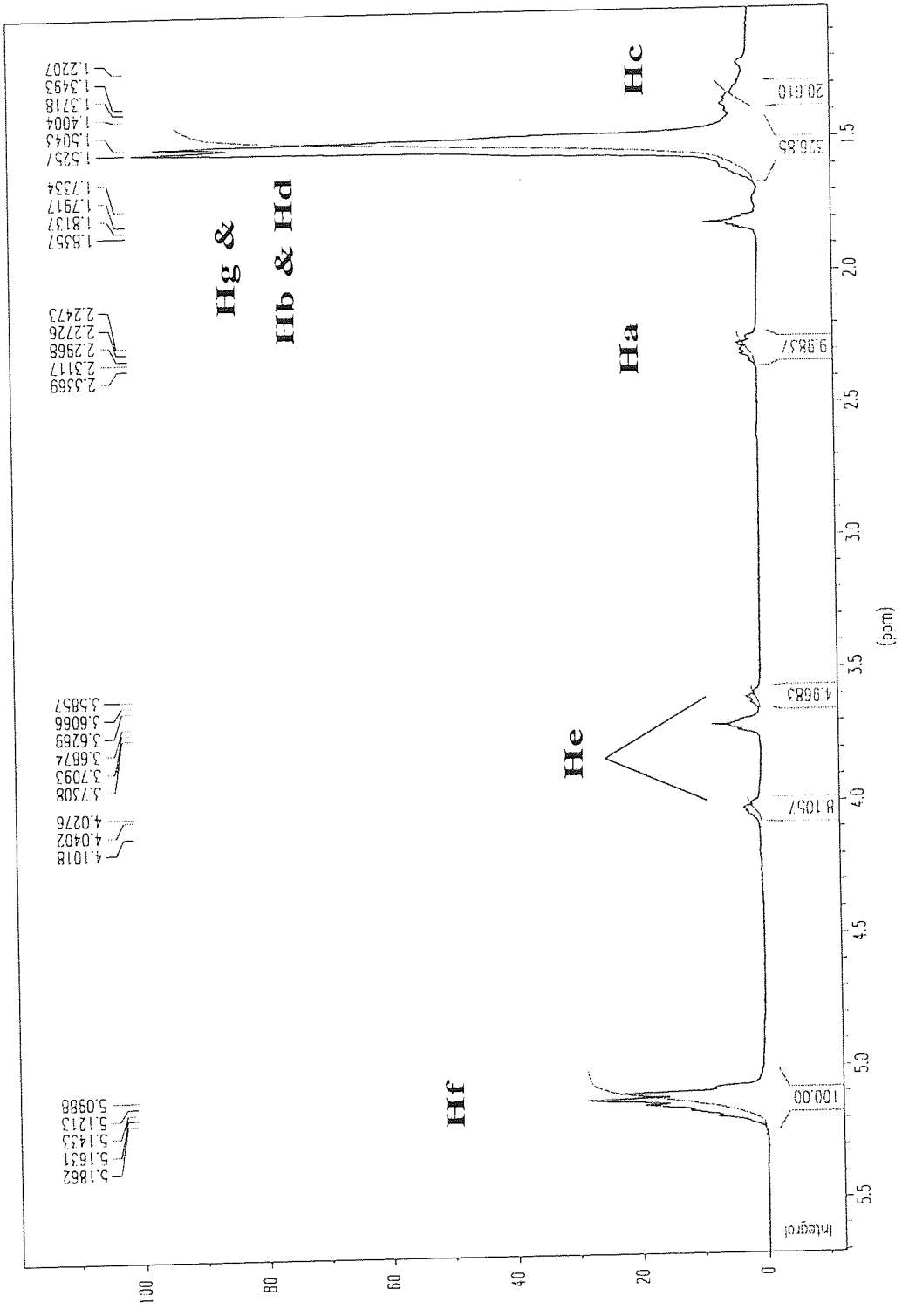

Table 6.15. ^{1}H NMR data of poly(L-LAAS)-block- poly(εCL) / COP 12.

Polyester	δ.ppm	Peak shape	Relative peak area	Assignment
L-PLAAS-block-PCL	1.35 - 1.49	multiplet	15.2	H_c
	1.53 - 1.63	multiplet	324.2	H_b & H_d & H_g
	2.25 - 2.34	multiplet	10.9	H_a
	3.59 - 3.63	triplet	4.2	H_e (end group)
	4.01 - 4.05	multiplet	7.6	H_e
	5.09 - 5.16	quartet	100.0	H_f

Table 6.16. ^{1}H NMR data of poly(DL-LAAS)-block- poly(εCL) / COP 13

Polyester	δ.ppm	Peak shape	Relative peak area	Assignment
DL-PLAAS-block-PCL	1.35 - 1.40	multiplet	20.6	H_c
	1.50 - 1.52	multiplet	326.9	H_b & H_d & H_g
	2.25 - 2.34	multiplet	10.0	H_a
	3.59 - 3.63	triplet	5.0	H_e (end group)
	4.03 - 4.10	multiplet	8.1	H_e
	5.10 - 5.19	quartet	100.0	H_f

Analysis of NMR spectra revealed the appearance of a new signal at 3.6 ppm. Additionally, the signals presumably attributable to the PCL block were smaller than expected and differed in shape from the signals of the homopolymer PCL. The methylene protons H_e resonance appeared as two different signals, one at 3.6 ppm and the other one at 4.1 ppm. This assignment was based on the relative peak areas presented in tables 6.15. and 6.16. and on the consideration that this proton was the closest to the terminated end group, presumably -C$\underline{H}_2$-OH. The resonance of this proton H_e in this position was expected to be shifted upfield compared to its position in a CL unit attached to another CL unit. This is in agreement with results reported by Penczek [84] about the end-group structure in PCL by ^{1}H and ^{13}C NMR spectroscopy.

On the other hand, the signals of the methylene protons H_a and H_e, expected at 2.2 ppm and 4.0 ppm were multiplets, in contrast with the triplets observed in the homopolymer PCL, as shown in figures 6.28. and 6.29. Indeed, if copolymerization took place, a certain number of CL units would be attached to the carboxyl group of a lactic unit and thereby, the resonances of protons in these CL units would be shifted downfield compared to protons in CL units attached to other CL unit. This gave rise to the shape of a multiplet, as a result of two triplets slightly shifted to one another. Additionally, these methylene protons H_a and H_e at the linkage and so close to the block polylactic were sensitive to the stereosequences of lactic unit. This explained the difference between their signals in poly(L-LAAS)-block-poly(ε-CL) and their signals in poly(DL-LAAS)-block-poly(ε-CL), as shown in figures 6.28. and 6.29.

In figure 6.29., the triplet at 3.7 ppm is attributable to THF still present in the copolymer despite the drying of the sample in a dessicator.

Figure 6.28. Signals of methylene protons H_e and H_a of ε-CL units in the ^{1}H NMR spectrum of the block copolymer poly(L-LAAS-block-co-εCL) / COP 12

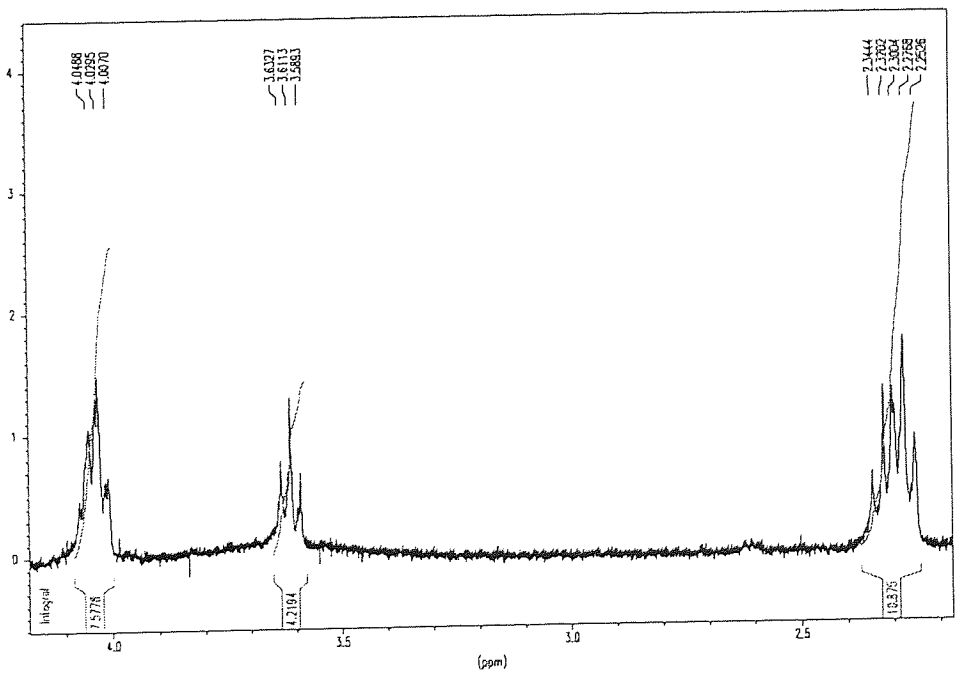

Figure 6.29. Signals of methylene protons H_e and H_a of ε-CL units in the ^{1}H NMR spectrum of the block copolymer poly(DL-LAAS-block-co-εCL) / COP 13

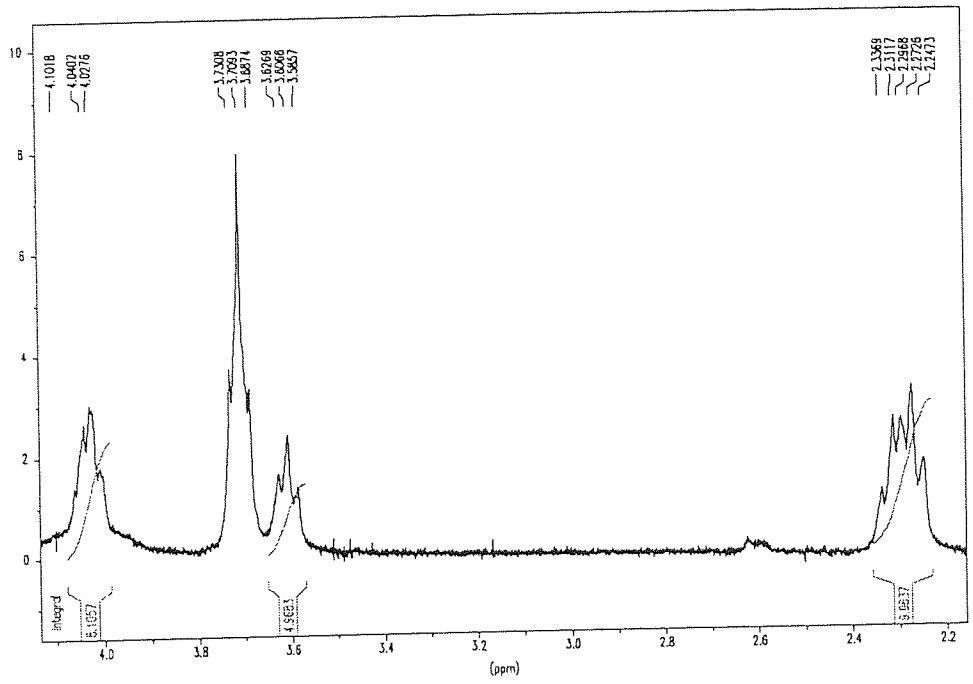

Similarly, the addition of CL unit onto the polylactic chains was clearly visible on the signal of the methine proton H_f, the 1:3:3:1 characteristic quartet at 4.1 ppm was slightly deformed and an expansion of this region revealed the presence of a new small quartet originated from the sequence lactic-CL, as shown in figure 6.30.

From the relative peak areas of signals of the methine proton H_f of block polylactic and the methylene protons H_e of block polycaprolactone, the molar compositions could be deduced. The results are presented in table 6.14.

The incorporation of CL units onto the polylactic chains appeared rather difficult, when an initial feed ratio of 33 % mole of caprolactone was performed, only 6 % of CL was actually incorporated in the copolymer with either L-LAAS or DL-LAAS monomers and in the 6 % moles of CL, 2 % moles were located at the terminated end of the chains.

Figure 6.30. Signals of methine protons H_f in L-PLAAS block in the ^1H NMR spectrum of the block copolymer poly(L-LAAS-block-co-εCL) / COP 12.

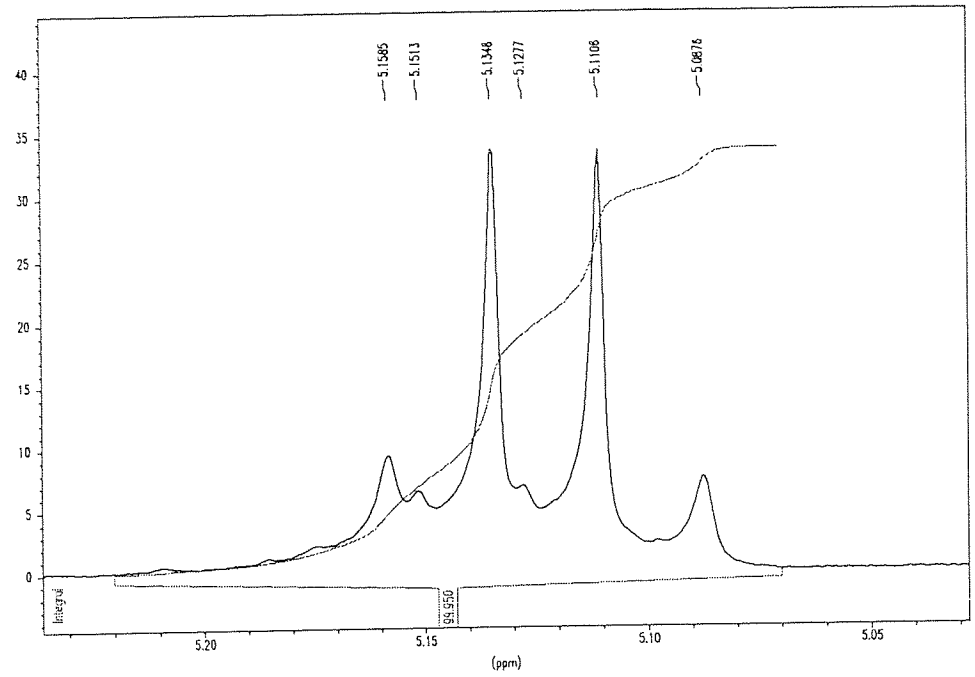

The ^{13}C NMR spectra of block copolymers poly(L-LAAS)-block-poly(εCL) and poly(DL-LAAS)-block-poly(εCL) are shown in figures 6.31. and 6.32., respectively. They confirmed the three different environments of the methylene carbons in a CL unit, CL unit attached to CL unit or attached to lactic unit, and CL bound to a OH group at the end of the chain, as shown in tables 6.17. and 6.18.

The carbonyl peak of CL unit was not detected because of the small incorporation of CL units. On the other hand, the methylene carbon CH_e resonances appeared as two peaks in L-PLAAS-block-PCL, as expected. The resonances of methylene carbons were more complicated in DL-PLAAS-block-PCL because of the several stereosequences of DL-PLAAS.

Figure 6.31. ^{13}C NMR spectrum of block copolymer poly(L-LAAS)-block-poly(ε-CL) / COP 12.

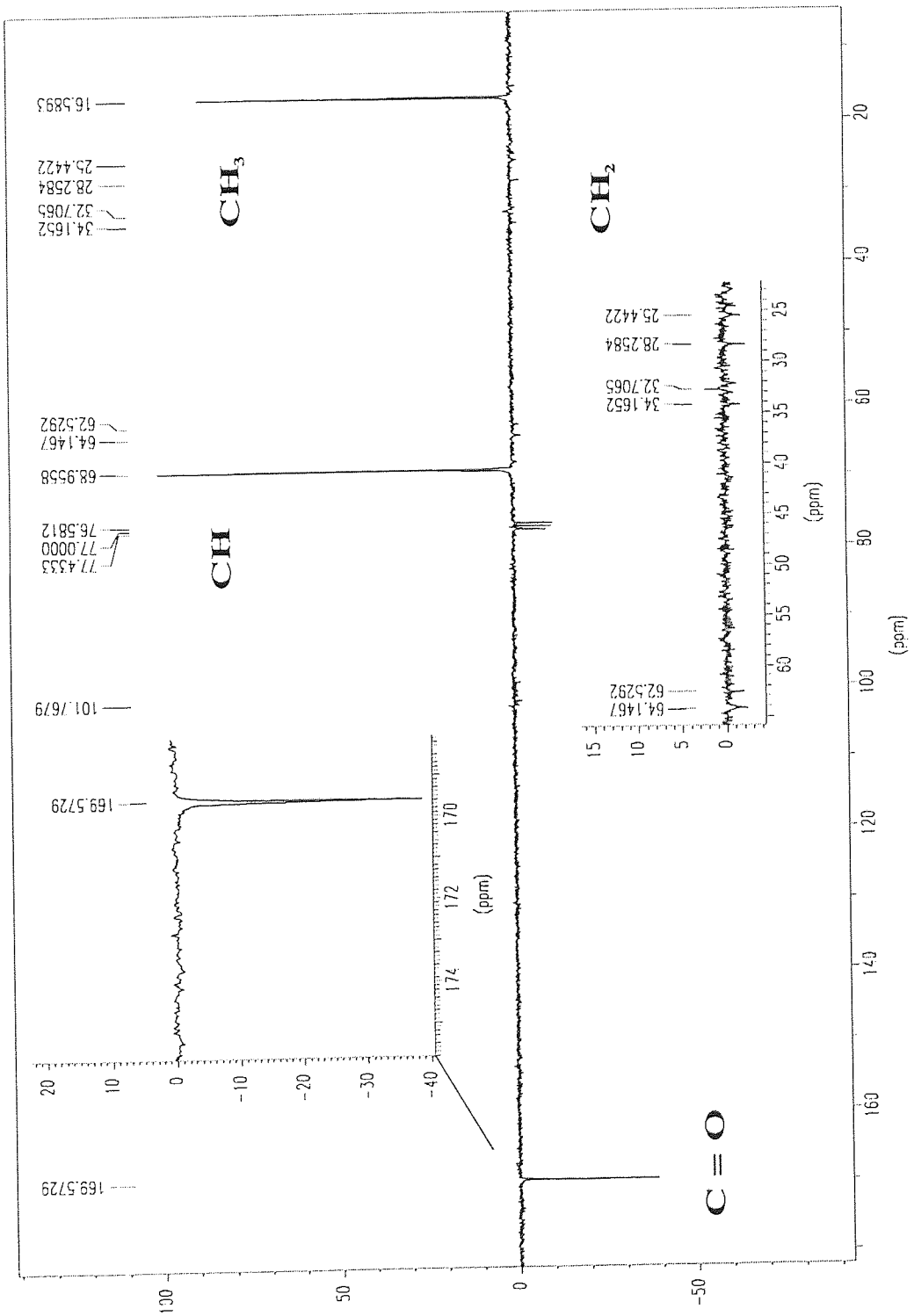

Figure 6.32. ^{13}C NMR spectrum of block copolymer poly(DL-LAAS)-block-poly(ε-CL) / COP 13.

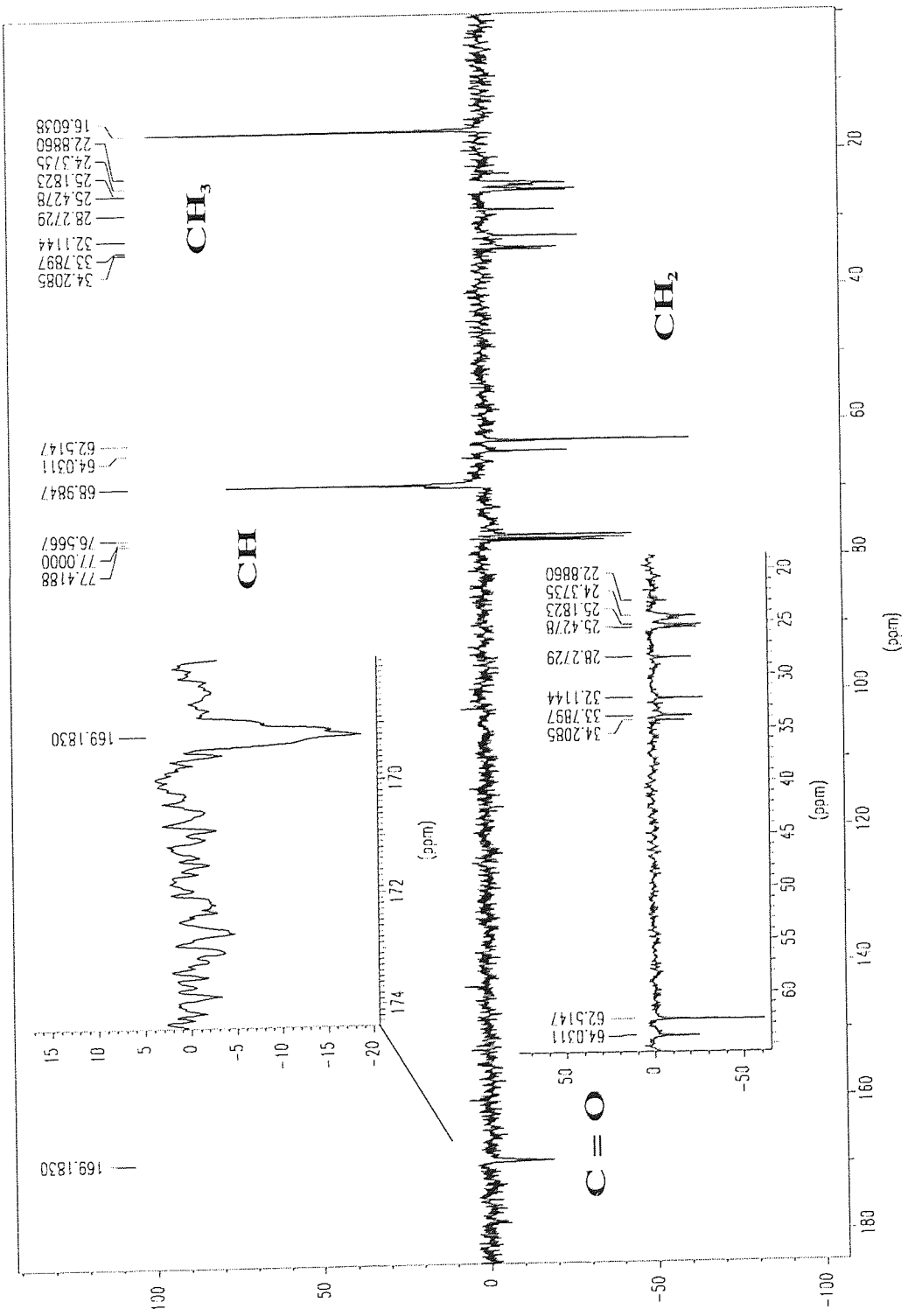

Table 6.17. ^{13}C NMR data of poly(L-LAAS)-block-poly(εCL) / COP 12.

Polyester	δ.ppm	Assignment
L-PLAAS-block-PCL	16.59	CH_{3g} (LAAS)
	25.44	CH_{2c}
	28.25	CH_{2b}
	32.71	CH_{2d}
	34.17	CH_{2a}
	62.53	CH_{2e} (end group)
	64.15	CH_{2e}
	68.96	CH_f (LAAS)
	169.57	C = O (LAAS)

Table 6.18. ^{13}C NMR data of poly(DL-LAAS)-block-poly(εCL) / COP 13.

Polyester	δ.ppm	Assignment
DL-PLAAS-block-PCL	16.60	CH_{3g} (LAAS)
	[22.89 - 34.21]	$CH_{2c\text{ - }2b\text{ - }2d\text{ - }2a}$
	62.51	CH_{2e} (end group)
	64.03	CH_{2e}
	68.98	CH_f (LAAS)
	169.18	C = O (LAAS)

6.4.3. Discussion

The anionic initiation of ε-caprolactone by polylactic chains was rather difficult and only a small incorporation of CL units took place. Indeed, some unreacted CL was found in the copolyesters synthesised. In the ^{1}H and ^{13}C NMR spectra of the copolyesters poly(LAAS)-block-poly(CL), the end group of these copolymers, presumably OH group were clearly visible. Thus, it was possible to determine the percentage of CL at the chain end, approximately 2 % in the total 6 % of CL present in the block-copolymers. That meant that the chains of PCL were rather short.

The polylactic chains were not totally living probably because of the occurrence of aging process and the presence of impurities, as discussed in section 4.3. Therefore, after 6 minutes, a certain number of polylactic chains were terminated and so no CL unit could be added at the end of these chains. Nevertheless, this could not explained the very low percentage of CL present in those copolymers.

Thus, the order in which the two monomers were used appeared to be important. The block-copolymerization of LAAS with ε-caprolactone was not favoured whereas the same block-copolymerization in the reverse order was satisfactory. Although alkoxides were known to initiate ε-caprolactone [82], the active chain ends of PLAAS believed to be alkoxides were not effective initiators for CL. This suggested that either the chain ends of PLAAS were not alkoxides, as proposed in section 4.4. or the only presence of sulphur dioxide released during polymerization of LAAS in the medium interfered with the polymerization of CL. Although sulphur dioxide is a good leaving group, it might not be eliminated in the first stage of ring-opening of anhydrosulfite and so might participate somehow in the initiation of monomers, as shown in figure 6.33.

Therefore, as a future work, it would be interesting to carry out a polymerization of CL initiated by butyllithium with sulphur dioxide bubbling in the reaction medium in order to determine if the only presence of sulphur dioxide can prevent this polymerization to take place.

Figure 6.33. Possible propagating species in the anionic polymerization of anhydrosulfites

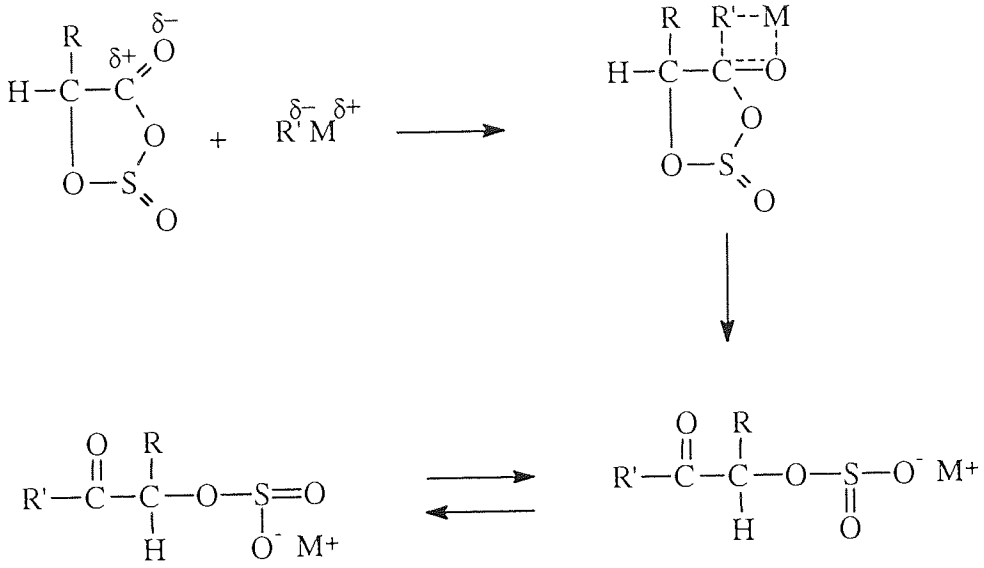

R' = alkyl, amide, or alkoxide

M = Li or K

6.5. Random copolymers poly(LAAS-co-(ε-CL))

The random copolymerization of LAAS and ε-CL was attempted, the experimental conditions are described in section 6.2. The two monomers LAAS and CL were mixed and then polymerization of this mixture was carried out in solution in THF or toluene at 25°C with butyllithium. Products obtained in this copolymerization were characterized by GPC and NMR spectroscopy.

6.5.1. GPC analysis

The results for the random copolymerization of LAAS and ε-caprolactone are summarized in table 6.19. All the polymers produced in this experiment exhibited an unimodal distribution with a polydispersity close to 1.

Table 6.19. Random-copolymerization of LAAS and ε-CL with n-BuLi at 25°C.

Sample	Feed ratio I:LAAS:CL	*	Solvent	$\overline{Mn}$ 10^{-3}.mol.g^{-1}	$\overline{Mw}$ 10^{-3}.mol.g^{-1}	$\overline{Mw}$ / $\overline{Mn}$	NMR data LAAS:CL
COP 5	1:50:50	DL	toluene	12.5	13.6	1.08	98 : 2
COP 7	1:55:55	DL	toluene	13.1	13.8	1.08	98 : 2
COP 10	1:50:50	L	THF	8.4	9.7	1.15	90 : 10
COP 11	1:125:125	DL	THF	10.7	12.6	1.18	96 : 4

* Enantiomeric nature of LAAS.

6.5.2. NMR studies

^{1}H and ^{13}C NMR spectroscopy were performed on the different samples. From these spectra, the structure and the molar composition in both monomers units of the materials obtained could be determined. Figure 6.34. shows the key to NMR spectra of random copolymers poly(LAAS-co-ε-CL).

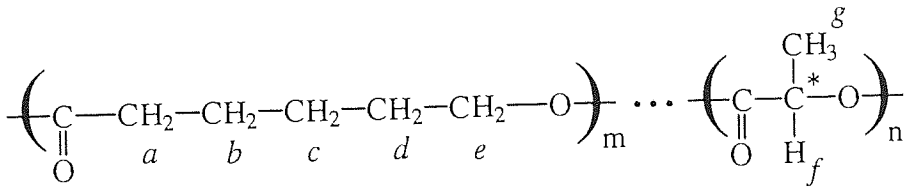

Figure 6.34. Key to NMR spectra of random copolymers poly(LAAS-co-ε-CL).

The ^{1}H NMR spectra of random copolymers poly(L-LAAS-co-ε-CL) and poly(DL-LAAS-co-ε-CL) were relatively similar to the spectra obtained for block-copolymers poly(LAAS)-block-poly(CL), as shown in figures 6.35. and 6.36. Thereby, the assignments of the different signals could be deduced on the basis of similar considerations and these assignments are presented in tables 6.20. and 6.21.

It should be mentioned that as in the case of block-copolymerization of LAAS with CL, the samples to be analysed by NMR still contained unreacted ε-CL, therefore they were washed with n-hexane, filtered and dried.

Figure 6.35. ^{1}H NMR spectrum of random copolymer poly(L-LAAS-co-ε-CL) / COP 10.

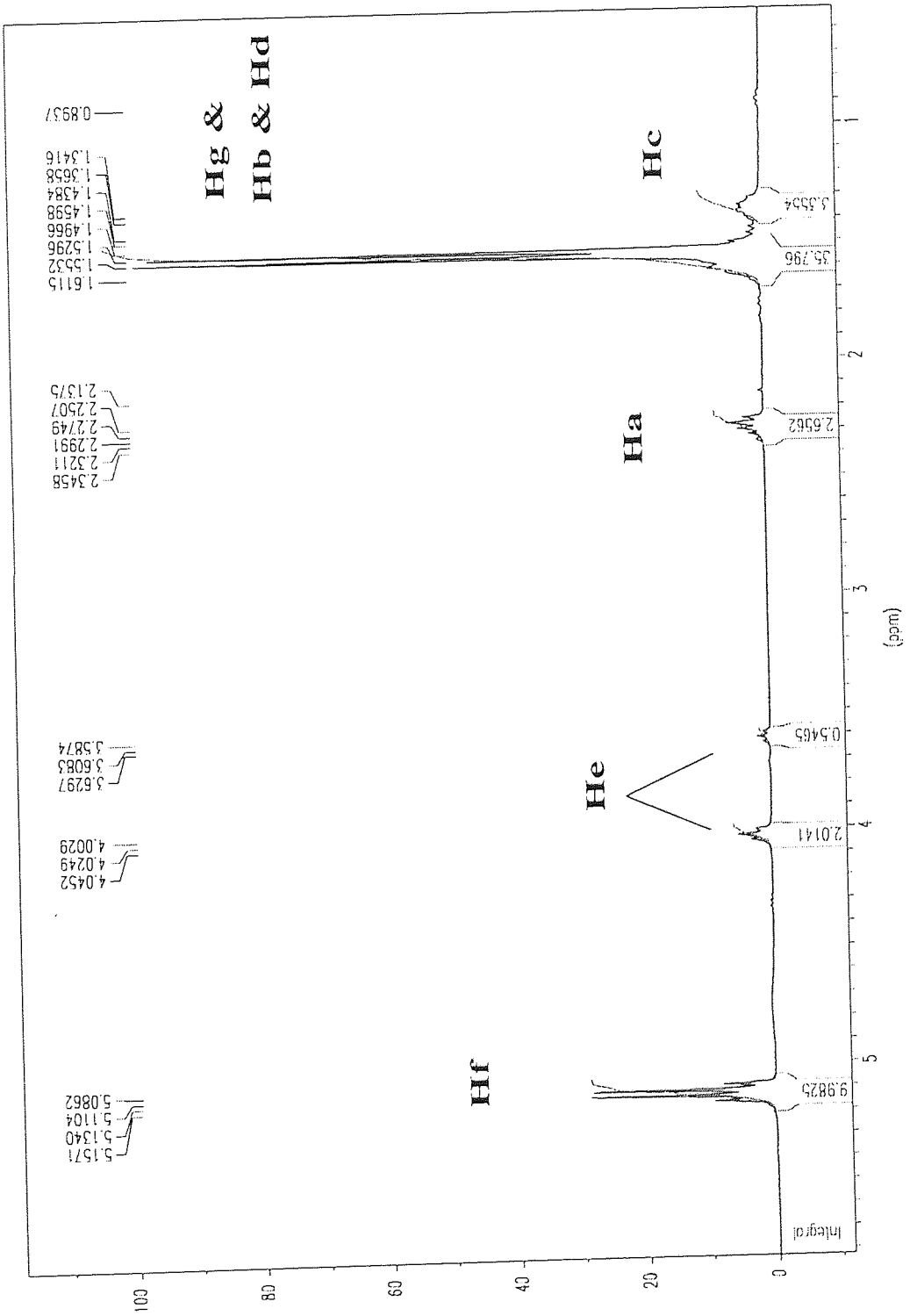

Figure 6.36. ^{1}H NMR spectrum of random copolymer poly(DL-LAAS-co-ε-CL) / COP 11.

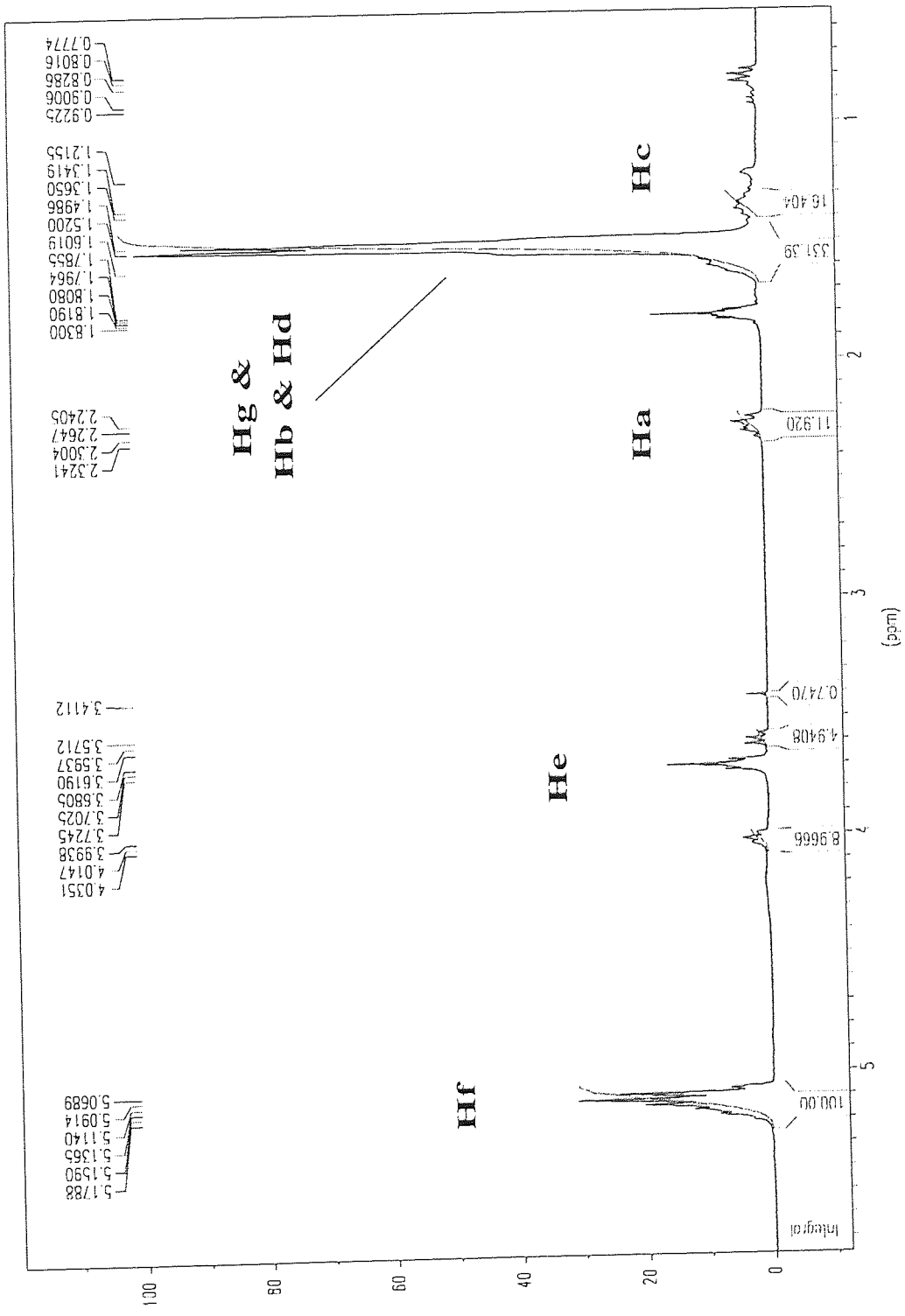

Table 6.20. ^{1}H NMR data of random copolymers poly(L-LAAS-co-ε-CL) / COP 10.

Polyester	δ.ppm	Peak shape	Relative peak area	Assignment
Poly(L-LAAS-co-CL)	1.34 - 1.37	multiplet	3.36	H_c
	1.44 - 1.61	multiplet	35.80	H_b & H_d & H_g
	2.14 - 2.34	multiplet	2.66	H_a
	3.59 -3.63	triplet	0.55	H_e (end group)
	4.00 - 4.05	multiplet	2.01	H_e
	5.09 - 5.16	quartet	9.98	H_f

Table 6.21. ^{1}H NMR data of random copolymer poly(DL-LAAS-co-ε-CL) / COP 11.

Polyester	δ.ppm	Peak shape	Relative peak area	Assignment
Poly(DL-LAAS-co-CL)	1.22 - 1.34	multiplet	16.4	H_c
	1.37 - 1.60	multiplet	331.4	H_b & H_d & H_g
	2.24 - 2.32	multiplet	11.9	H_a
	3.57 - 3.62	triplet	0.8	H_e (end group)
	3.99 - 4.04	multiplet	4.9	H_e
	5.07 - 5.18	quartet	100.00	H_f

These ^{1}H NMR spectra were similar to those obtained for block-copolymers poly(LAAS)-block-poly(CL). The resonance of the methine proton H_f appeared as a 1:3:3:1 quartet in the copolymer poly(L-LAAS-co-CL) and a multiplet in the random copolymer poly(DL-LAAS-co-CL), as observed for a polylactic chain. This suggested that the monomer LAAS was first polymerized and that CL was polymerized in its turn when most of LAAS had been reacted. The difference in reactivity of LAAS and CL was responsible for the formation of these copolymers with blocky structures.

The resonance of the methylene protons H_e appeared as two signals, one multiplet at 3.6 ppm from the -CH_2-OH end group and a multiplet at 4.0 ppm from the sequences CL-

CL and Lactic-CL whereas the resonance of H_a was a multiplet at 2.2 ppm originated from the two same sequences CL-CL and Lactic-CL.

From the relative peak areas of the methylene proton H_e and the methine proton H_f signals, the molar composition could be determined. The incorporation of caprolactone units was found smaller than expected, as shown in table 6.19. and was favoured when the solvent used was THF and the monomer the pure enantiomer L-LAAS.

For COP 10, for example, from a molar feed composition ε-CL : L-LAAS of 50 : 50, only 10 moles of CL was incorporated in the copolymer, in which about 2.5 moles of CL units terminated the chains.

The ^{13}C NMR spectra of random copolymers poly(L-LAAS-co-ε-CL) and poly(DL-LAAS-co-ε-CL) are shown in figures 6.37. and 6.38. whereas the peak tables are presented in tables 6.22. and 6.23. They are in agreement with a structure in block of the copolymer poly(LAAS-co-CL). Additionally, the signal of -$\underline{C}H_2$-OH was visible at 62.5 ppm, as expected.

Figure 6.37. ^{13}C NMR spectrum of random copolymer poly(L-LAAS-co-εCL) / COP 10.

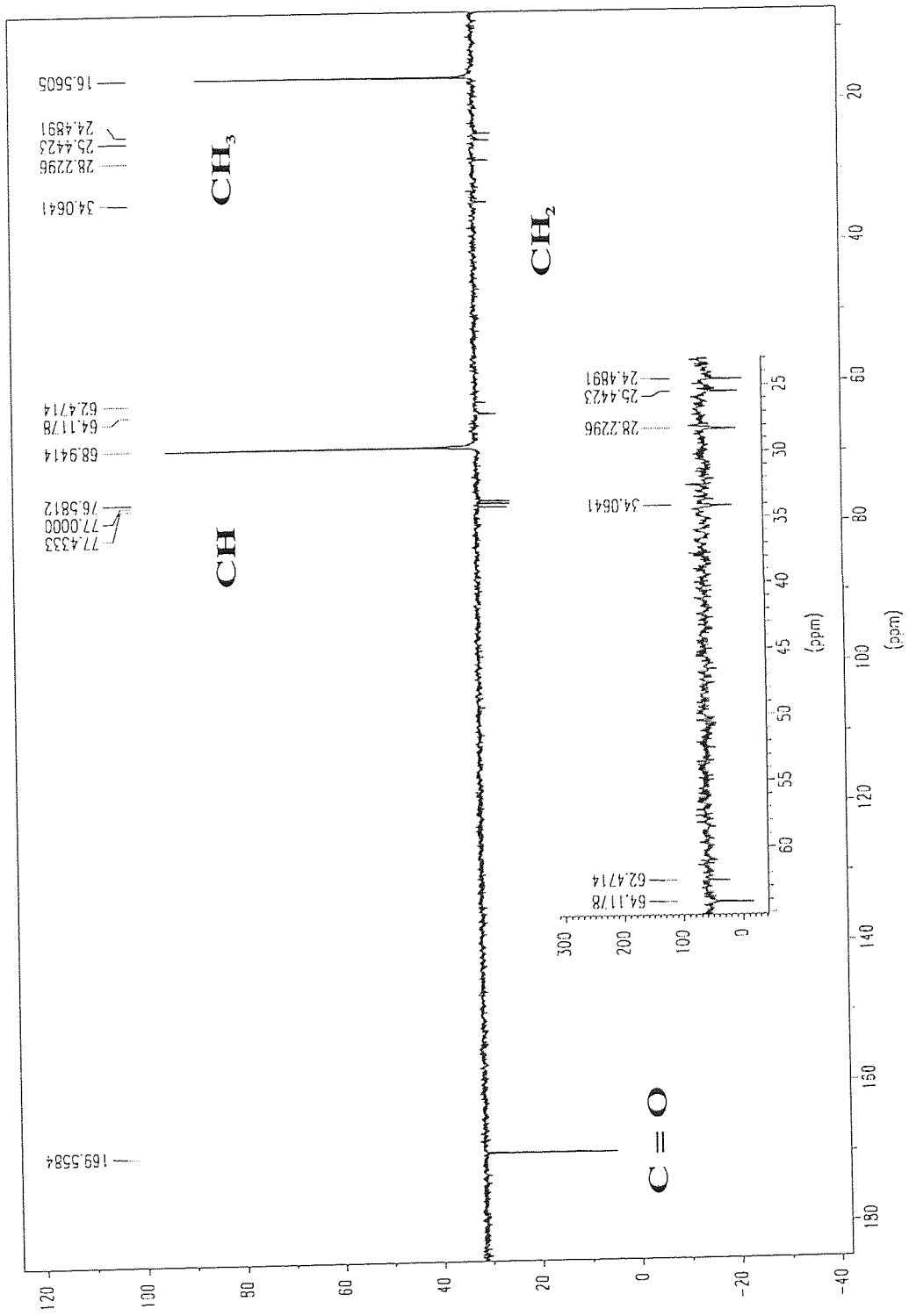

Figure 6.38. ^{13}C NMR spectrum of random copolymer poly(DL-LAAS-co-εCL) / COP 11

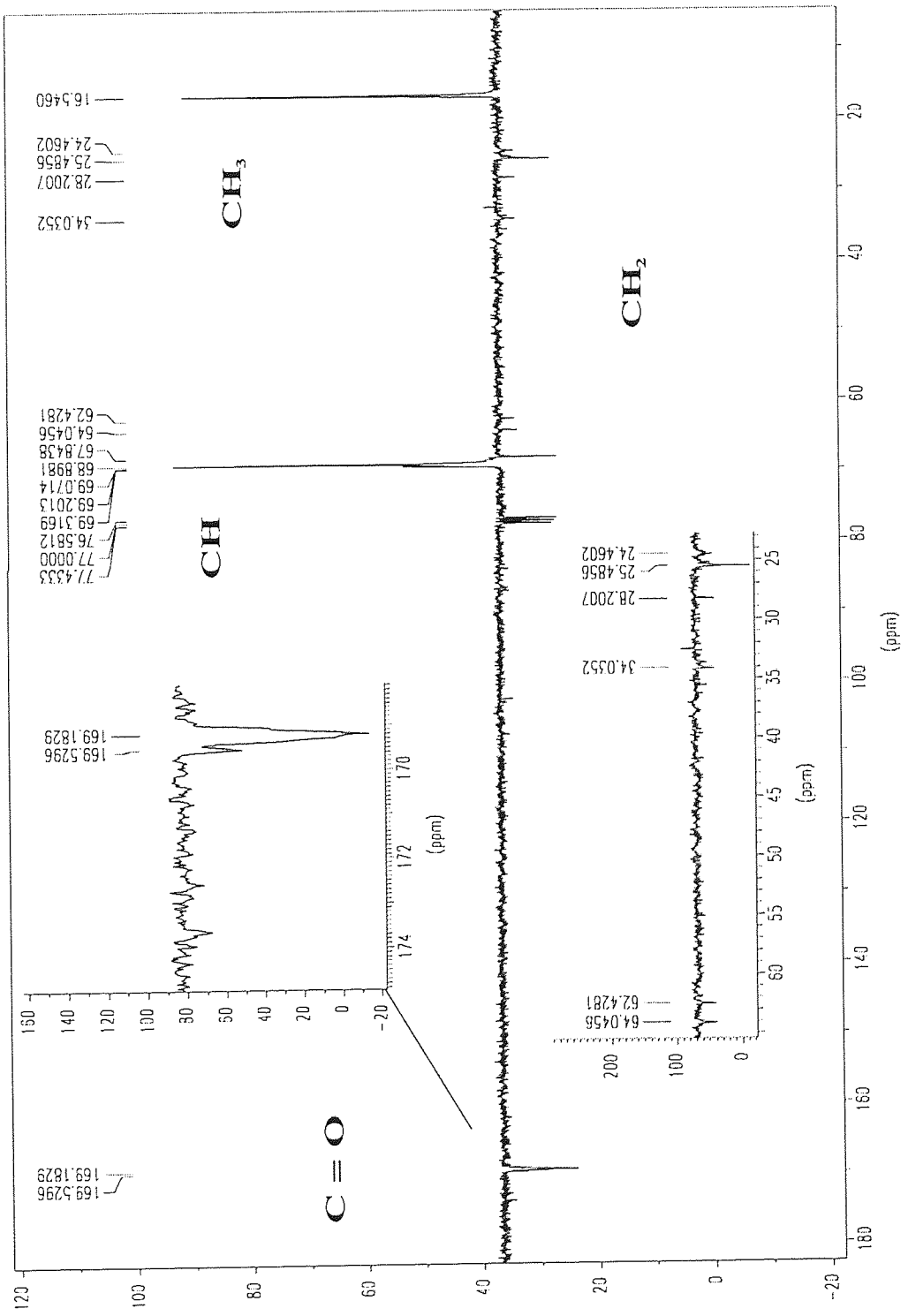

Table 6.22. ^{13}C NMR data of random copolymers poly(L-LAAS-co-ε-CL) / COP 10.

Polyester	δ.ppm	Assignment
Poly(L-LAAS-co-CL)	16.56	CH_{3g} (LAAS)
	24.48	CH_{2c}
	25.44	CH_{2b}
	28.23	CH_{2d}
	34.06	CH_{2a}
	62.47	CH_{2e} (end group)
	64.12	CH_{2e}
	68.94	CH_f (LAAS)
	169.56	C = O (LAAS)

Table 6.23. ^{13}C NMR data of random copolymers poly(DL-LAAS-co- ε-CL) / COP 11

Polyester	δ.ppm	Assignment
Poly(DL-LAAS-co-CL)	16.55	CH_{3g} (LAAS)
	24.46	CH_{2c}
	25.49	CH_{2b}
	28.20	CH_{2d}
	34.04	CH_{2a}
	62.43	CH_{2e} (end group)
	64.05	CH_{2e}
	[68.90 - 69.32]	CH_f (LAAS)
	169.18	C = O (LAAS)

6.5.3. Discussion

The NMR spectra of random copolymers poly(LAAS-co-ε-CL) were relatively similar to the spectra obtained for block-copolymers poly(LAAS)-block-poly(CL). This formation of copolymers with blocky structures could be explained by the difference in reactivity of LAAS and ε-CL in ring-opening polymerization initiated by butyllithium. Indeed, a small percentage of ε-CL copolymerized after all LAAS had been depleted even when the polymerization was continued for 2 hours. Most of ε-CL was found unreacted. It was interesting to note that ε-CL did not yield a homopolymer despite the presence of initiator in the reaction medium.

On one hand, this could be explained if LAAS was more reactive than ε-CL and polymerized first meanwhile the excess of butyllithium reacted with impurities. Thus, once the polymerization of LAAS was complete, the initiator butyllithium was all consumed. So no homopolymerization of ε-CL could take place. As discussed in section 6.4.3., the active chain end of PLAAS might not be an effective initiator for ε-CL so that only a small percentage ε-CL was added onto the PLAAS chains.

On the other hand, the only presence in the medium of sulphur dioxide released during polymerization of LAAS which occurred first might interfer with the polymerization of ε-CL so that neither copolymerization nor homopolymerization of ε-CL could take place.

Additionally, the incorporation of CL at the end of the polylactic chains in the random copolymerization was greater than in the block-copolymerization, 10 % in the random copolymerization of poly(L-LAAS-co-ε-CL) against 6 % in the block-copolymerization of poly(L-LAAS)-block-poly(CL). So the occurrence of aging process might be partly responsible for the low addition of CL units.

Thus, the anionic copolymerization of LAAS and CL with butyllithium did not give access to random copolyesters because of their large difference in reactivity and somehow because of sulphur dioxide.

CHAPTER 7

SYNTHESIS OF NOVEL COPOLYESTERS

In this chapter, the work has been carried out in collaboration with Dr G. Piquet.

The block-copolymerizations of ε-caprolactone with other aliphatic anhydrosulfites than LAAS were conducted. Thereby, novel block-copolyesters such as poly(ε-CL)-block-poly(DL-HIVAAS) and poly(ε-CL)-block-poly(DL-HCAAS) were synthesised and charaterized with respect to molecular weight by GPC and structure by NMR spectroscopy.

7.1. Block-copolymers poly(ε-CL)-block-poly(DL-HIVAAS)

The block-copolymerizations of poly(ε-CL)-block-poly(DL-HIVAAS) were carried out in THF at room temperature under an argon atmosphere initiated by butyllithium. The procedure is described in section 6.2. and the polymerization vessel is shown in section 4.1.

7.1.1. GPC analysis

Block-copolymers of various initiator/monomer1/monomer2 ratios were synthesised in THF. The results are summarized in table 7.1. The molecular weights obtained were relatively high and the polydispersities were about 1.6 - 1.7, in good agreement with the expectations from the ratios and the conditions (THF as solvent).

Table 7.1. Block-copolymerization of poly(ε-CL)-block-poly(DL-HIVAAS) with n-BuLi at 25°C in THF.

Sample	Feed ratio I : CL : HIVAAS	$\overline{Mn}$ 10^{-3}.mol.g^{-1}	$\overline{Mw}$ 10^{-3}.mol.g^{-1}	$\overline{Mw}/\overline{Mn}$	NMR data CL:HIVAAS
COP 16	1 : 100 : 50	30.7	49.8	1.62	72 : 28
COP 17	1 : 70 : 70	26.8	46.8	1.70	65 : 35

7.1.2. NMR studies

^{1}H and ^{13}C NMR spectroscopy were performed on the block-copolymers poly(ε-CL)-block-poly(DL-HIVAAS) in order to determine their structure and their composition.

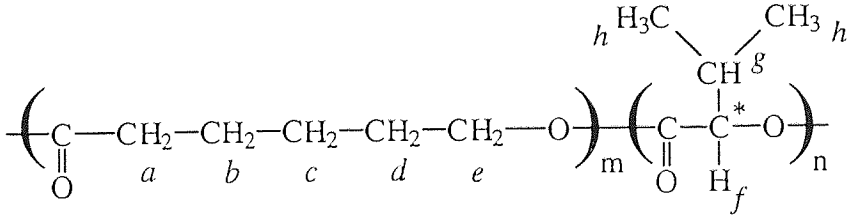

Figure 7.1. Key to NMR spectra of poly(ε-CL)-block-poly(DL-HIVAAS).

The structure of the block-copolymers is described in figure 7.1. and the ^{1}H NMR spectrum of poly(ε-CL)-block-poly(DL-HIVAAS) is presented in figure 7.2. The different assignments were determined in agreement with the integral values, as shown in table 7.2. As the copolymers synthesised had an unimodal distribution and exhibited the signals for protons present in both blocks PCL and PHIVAAS, a structure of A-B type could be deduced for those block-copolyesters.

Figure 7.2. ^{1}H NMR spectrum of poly(ε-CL)-block- poly(DL-HIVAAS) / COP 17.

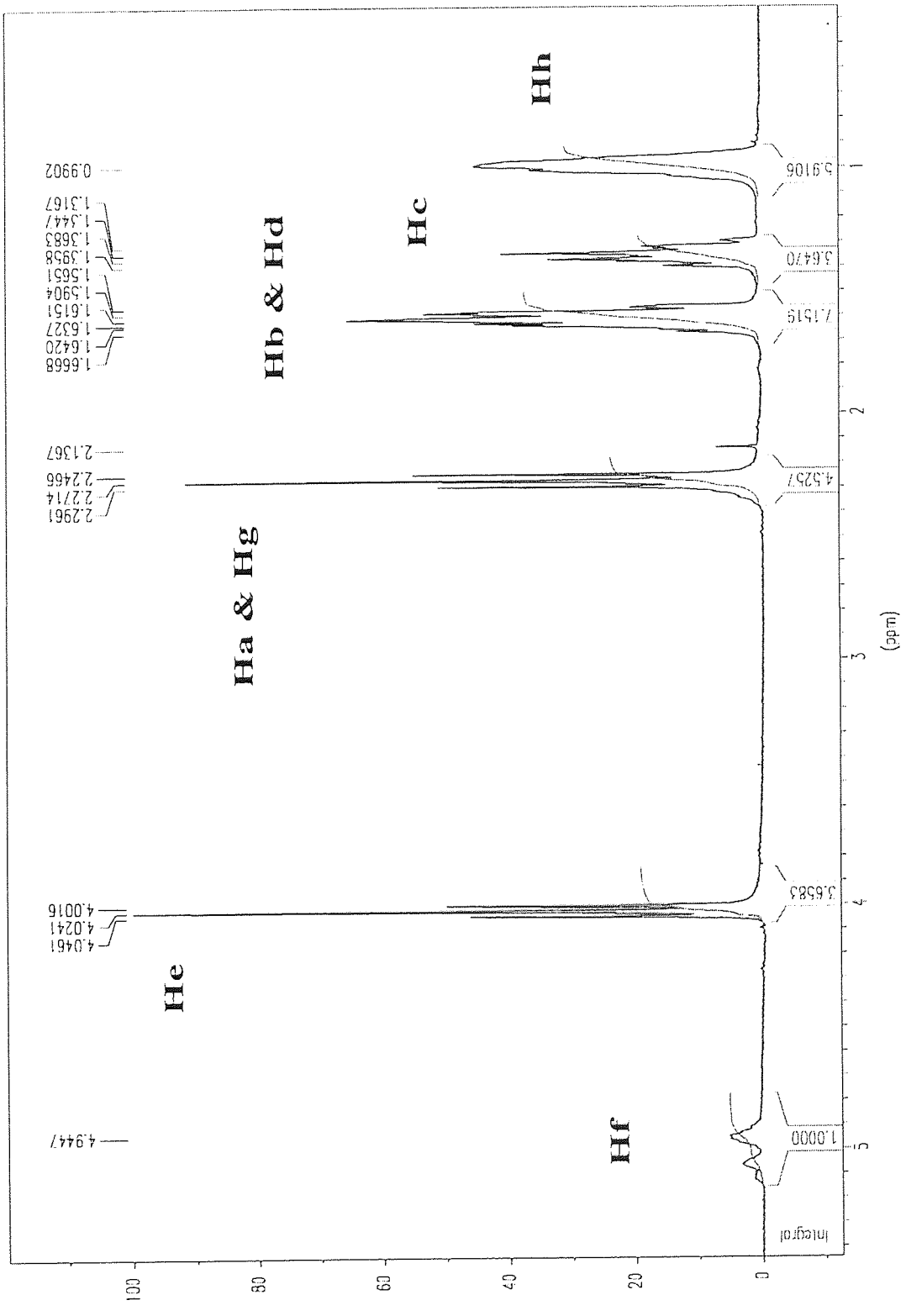

Table 7.2. ^{1}H NMR data of poly(ε-CL)-block- poly(DL-HIVAAS) / COP 17.

Polyester	δ.ppm	Peak shape	Relative peak area	Assignment
L-PLAAS-block-PCL	0.99	multiplet	5.91	H_h
	1.32 - 1.40	multiplet	3.65	H_c
	1.57 - 1.67	multiplet	7.15	H_b & H_d
	2.25 - 2.30	triplet	4.53	H_a & H_g
	4.00 - 4.05	triplet	3.66	H_e
	4.94	multiplet	1.00	H_f

The molar composition was deduced from the relative peak areas of the signals of the methine proton H_f of the block DL-PHIVAAS and methylene protons H_e of the block PCL. The two signals did not overlap so an accurate determination of the composition was possible. The results are presented in table 7.1.

The initiation of DL-HIVAAS by PCL active chains took place and the incorporation of hydroxy isovaleric units appeared less easy than in the case of lactic units, presumably for steric reasons, as explained in section 7.3. For a feed composition in CL : monomer2 of 50 : 50, the copolymer composition was of 65 : 35, compared to 58 : 42 for poly(CL)-block-poly(DL-LAAS).

The ^{13}C NMR spectrum of poly(ε-CL)-block-poly(DL-HIVAAS) is shown in figure 7.3. and the different assignments are listed in table 7.3. They are in agreement with the block-copolyester structure.

As expected for an atactic DL-PHIVAAS block, it can be seen in the ^{13}C NMR spectrum of poly(ε-CL)-block-poly(DL-HIVAAS), several lines for the carbonyl signal at 168 ppm, as shown in figure 7.4.

Figure 7.3. ^{13}C NMR spectrum of block copolymer poly(ε-CL)-block-poly(DL-HIVAAS) / COP 17

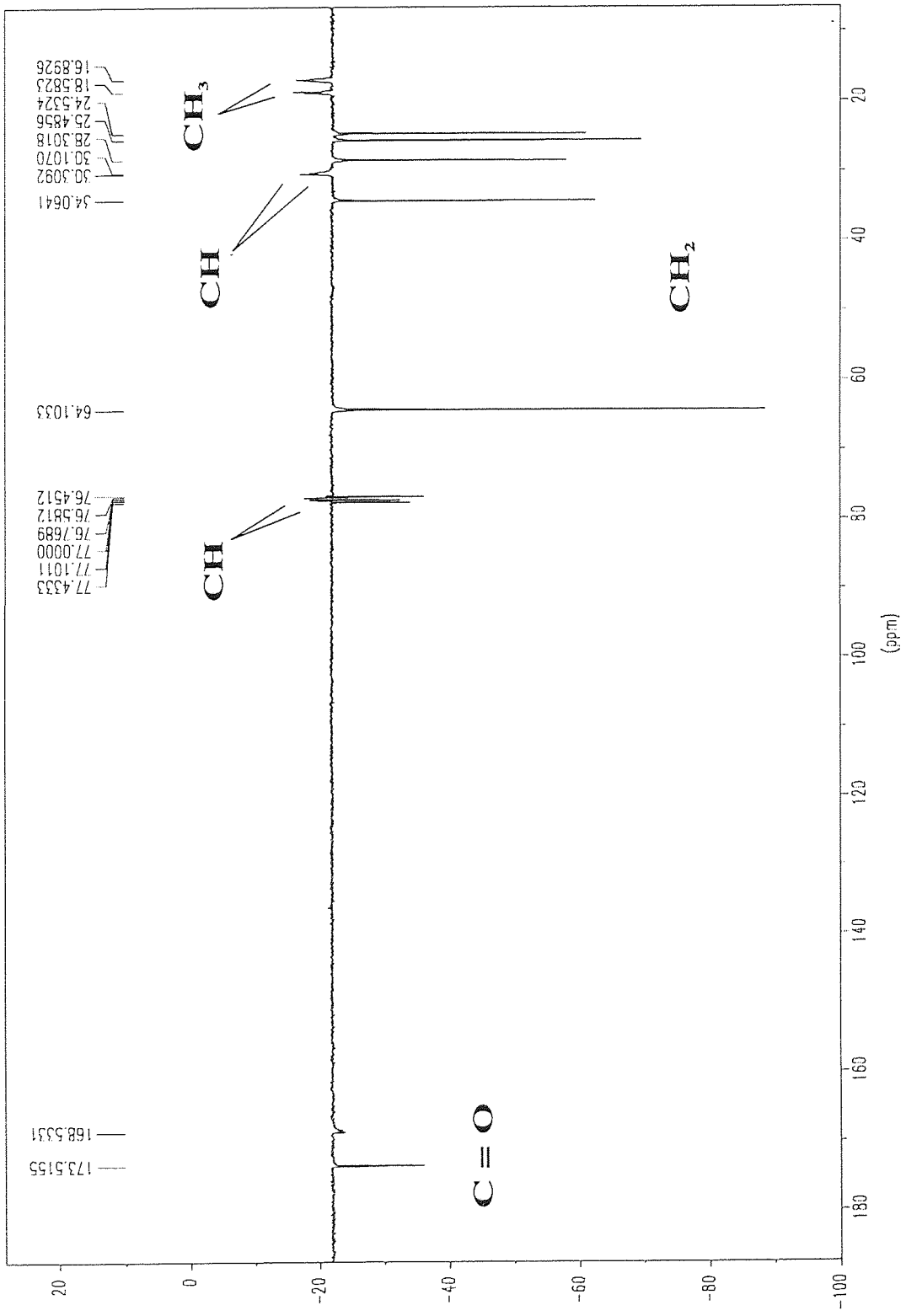

Table 7.3. ^{13}C NMR data of poly(ε-CL)-block-poly(DL-HIVAAS) / COP 17.

Polyester	δ.ppm	Assignment
PCL-block-DL-PHIVAAS	16.89 - 18.58	CH_{3h} (HIVAAS)
	24.53	CH_{2c}
	25.48	CH_{2b}
	28.30	CH_{2d}
	30.10 - 30.31	CH_g (HIVAAS)
	34.06	CH_{2a}
	64.10	CH_{2e}
	168.53	C = O (HIVAAS)
	173.52	C = O

Figure 7.4. Carbonyl signals in the ^{13}C NMR spectrum of poly(ε-CL)-block-poly(DL-HIVAAS) / COP 17

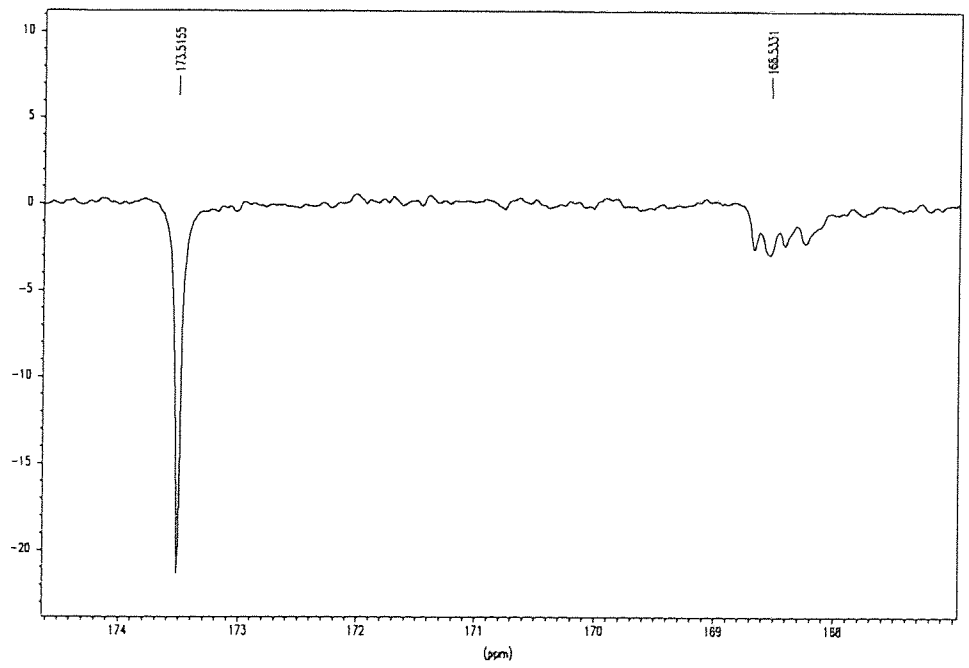

7.2. Block-copolymers poly(ε-CL)-block-poly(DL-HCAAS)

The block-copolymerizations were carried out in similar conditions as for the synthesis of block-copolymers poly(ε-CL)-block-poly(DL-HIVAAS). All the experiments were performed at room temperature in THF.

7.2.1. GPC analysis

The molecular weights and the molecular weight distribution of the copolymers were determined by GPC and are presented in table 7.4.

Table 7.4. Block-copolymerization of poly(ε-CL)-block-poly(DL-HCAAS) with n-BuLi at 25°C in THF.

Sample	Feed ratio I : CL : HCAAS	$\overline{Mn}$ 10^{-3}.mol.g^{-1}	$\overline{Mw}$ 10^{-3}.mol.g^{-1}	$\overline{Mw}$ / $\overline{Mn}$	NMR data CL:HCAAS
COP 18	1 : 50 : 25	25.2	39.7	1.57	77 : 23
COP 19	1 : 35 : 35	45.4	71.0	1.56	69 : 31

7.2.2. NMR studies

^{1}H and ^{13}C NMR spectra were used to characterize the structure of the polymers produced in this copolymerization and to define the molar composition in CL and hydroxy caproic units.

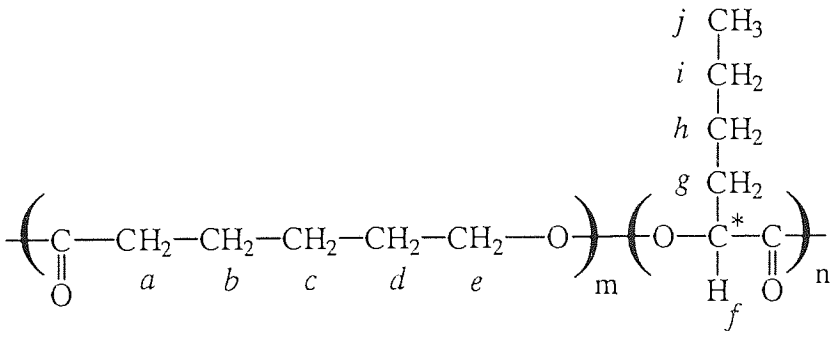

Figure 7.5. Key to NMR spectra of block-copolymer poly(ε-CL)-block-poly(DL-HCAAS)

In figure 7.5., the structure of the block-copolymer poly(ε-CL)-block-poly(DL-HCAAS) can be seen along with the different protons and carbons present in the polymer chains.

The ^{1}H NMR spectrum of poly(ε-CL)-block-poly(DL-HCAAS) and its peak table are shown in figure 7.6. and table 7.5. The different assignments are in agreement with a A-B type copolymer structure.

From the relative peak areas of the signals of H_f and H_e, the molar composition of the block-copolyester was determined, as shown in table 7.4. The incorporation of hydroxy caproic units was found even more difficult than for hydroxy isovaleric units, for a feed composition of 50 : 50, a composition of 69 : 31 was obtained for the copolyesters, probably for steric reasons, as explained in the next section.

Figure 7.6. ^{1}H NMR spectrum of poly(ε-CL)-block- poly(DL-HCAAS) / COP 19.

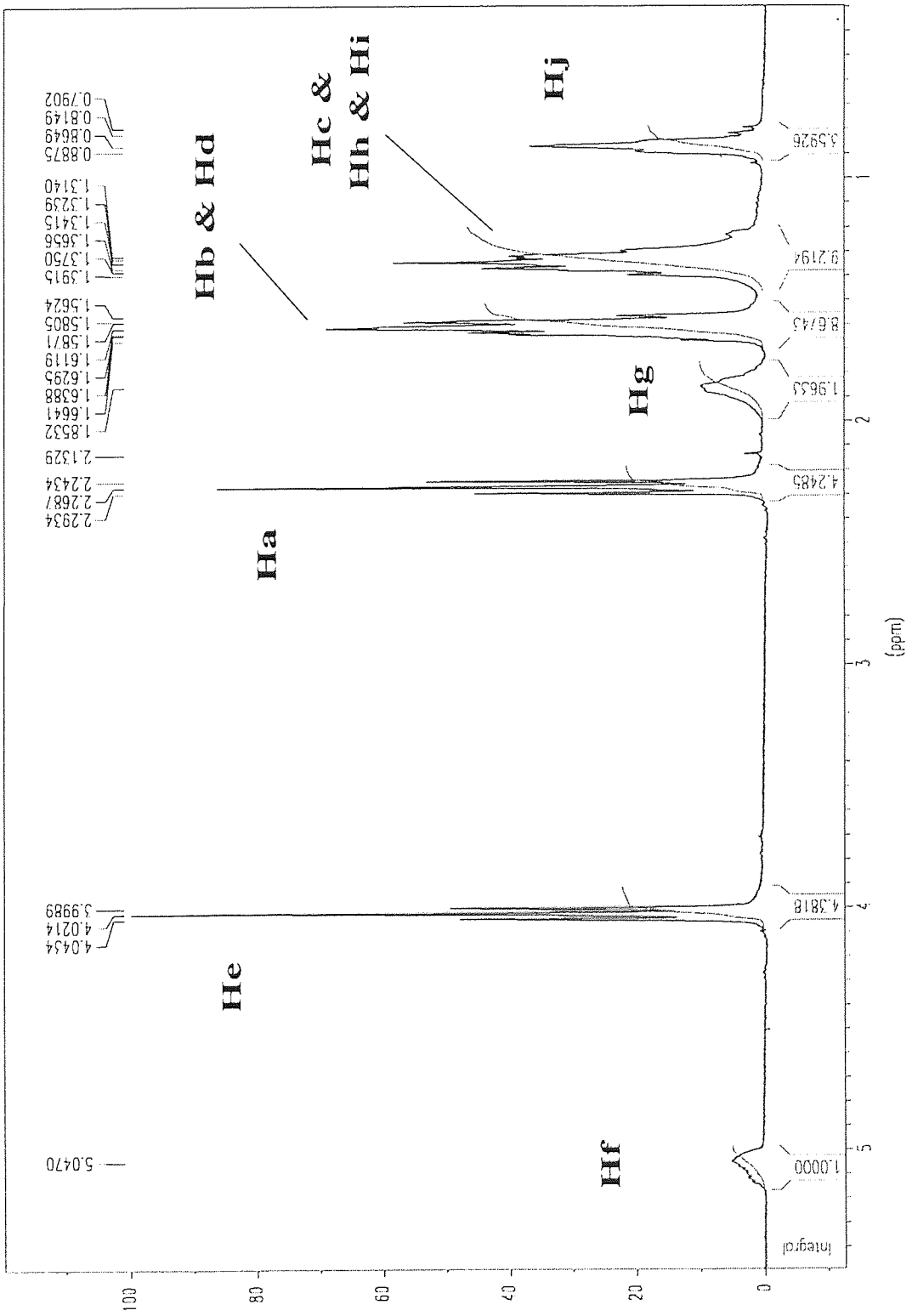

Table 7.5. ^{1}H NMR data of poly(ε-CL)-block- poly(DL-HCAAS) / COP 19.

Polyester	δ.ppm	Peak shape	Relative peak area	Assignment
PCL-block-DL-PHCAAS	0.79 - 0.89	multiplet	3.59	H_c
	1.31 - 1.39	multiplet	9.22	H_c & H_h & H_i
	1.56 - 1.67	multiplet	8.67	H_b & H_d
	1.85	multiplet	1.96	H_g
	2.24 - 2.29	triplet	4.25	H_a
	3.99 - 4.04	triplet	4.38	H_e
	5.05	multiplet	1.00	H_f

The ^{13}C NMR spectrum of block-copolymers poly(ε-CL)-block-poly(DL-HCAAS) and the corresponding peak table are shown in figure 7.7. and table 7.6. They confirmed the block structure of the copolyesters.

The methine carbon signal was similar to the one obtained for DL-PHCAAS, as shown in figure 7.8. This meant that the initiation of DL-HCAAS by active PCL chains yielded block-copolyesters poly(ε-CL)-block-poly(DL-HCAAS) with a block DL-PHCAAS predominantly isotactic, as explained in section 5. The atacticity of the block DL-PHCAAS was confirmed by the several lines observed in the carbonyl and the methylene regions, as shown in figures 7.9. and 7.10.

Figure 7.7. ^{13}C NMR spectrum of block-copolymer poly(ε-CL)-block-poly(DL-HCAAS) / COP 18.

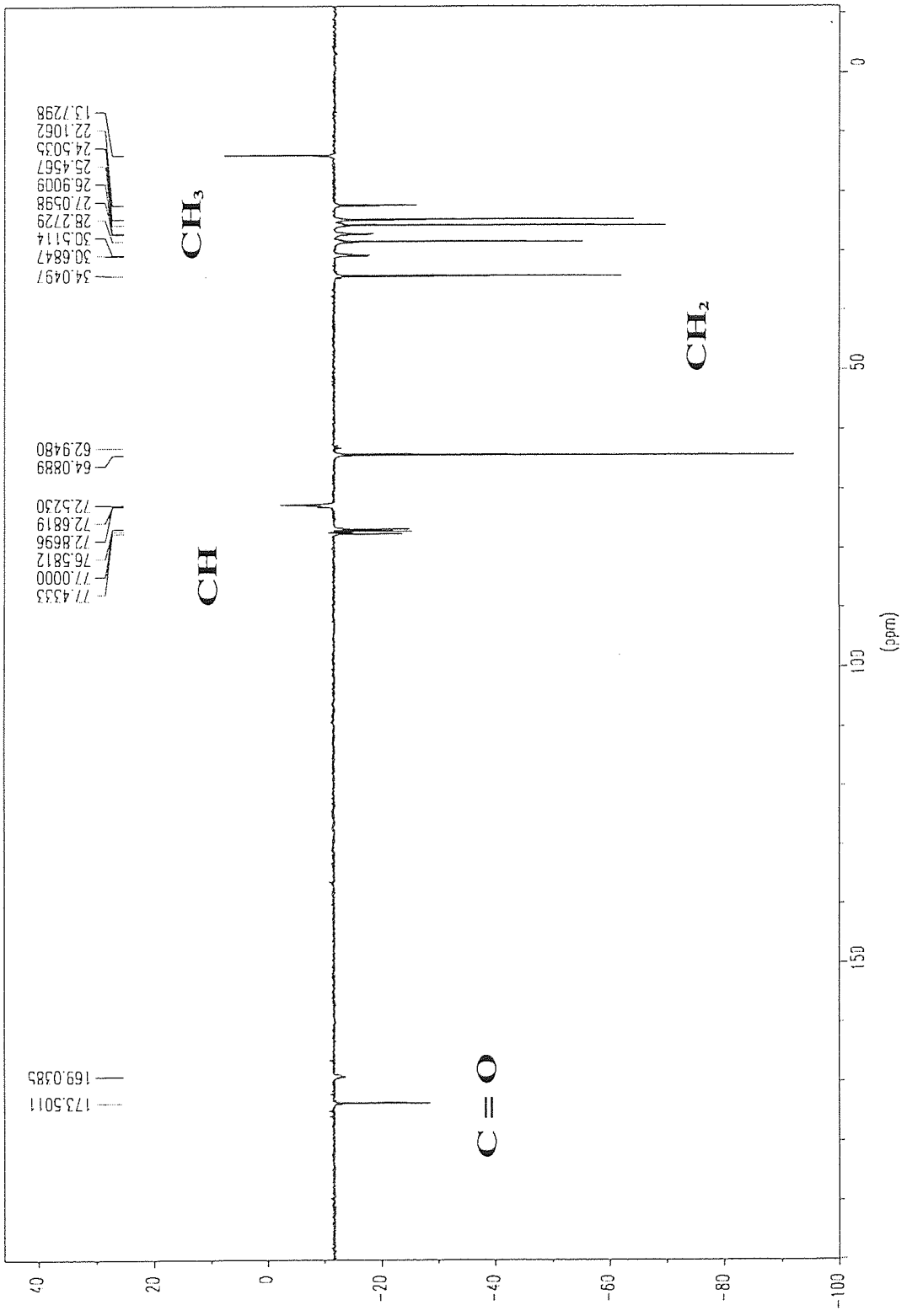

Table 7.6. ^{13}C NMR data of poly(ε-CL)-block-poly(DL-HCAAS) / COP 18.

Polyester	δ.ppm	Assignment
PCL-block-DL-PHCAAS	13.73	CH_{3j} (HCAAS)
	22.11	CH_{2i} (HCAAS)
	24.50	CH_{2c}
	25.46	CH_{2b}
	26.90 - 27.06	CH_{2h} (HCAAS)
	28.27	CH_{2d}
	30.51 - 30.68	CH_{2g} (HCAAS)
	34.05	CH_{2a}
	62.95 - 64.09	CH_{2e}
	72.52 - 72.87	CH_f (HCAAS)
	169.04	C = O (HCAAS)
	173.50	C = O

Figure 7.8. Methine carbon signal CH_f in the ^{13}C NMR spectrum of poly(ε-CL)-block-poly(DL-HCAAS) / COP 18

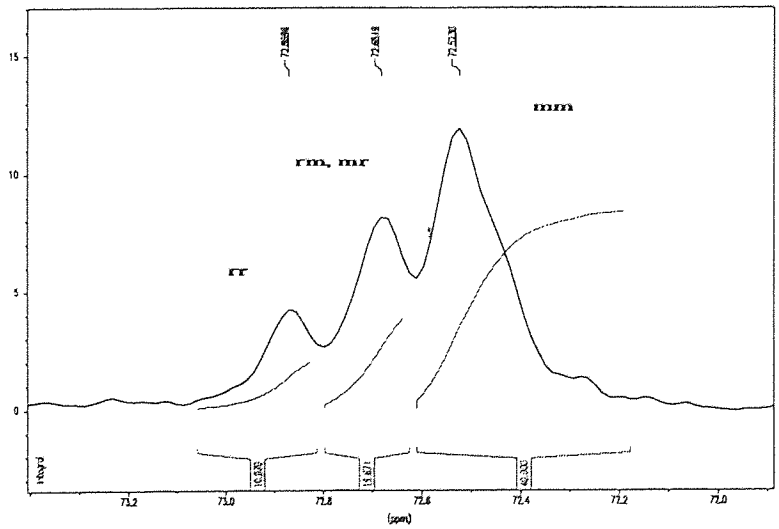

Figure 7.9. Carbonyl signals in the ^{13}C NMR spectrum of poly(ε-CL)-block-poly(DL-HCAAS) / COP 18

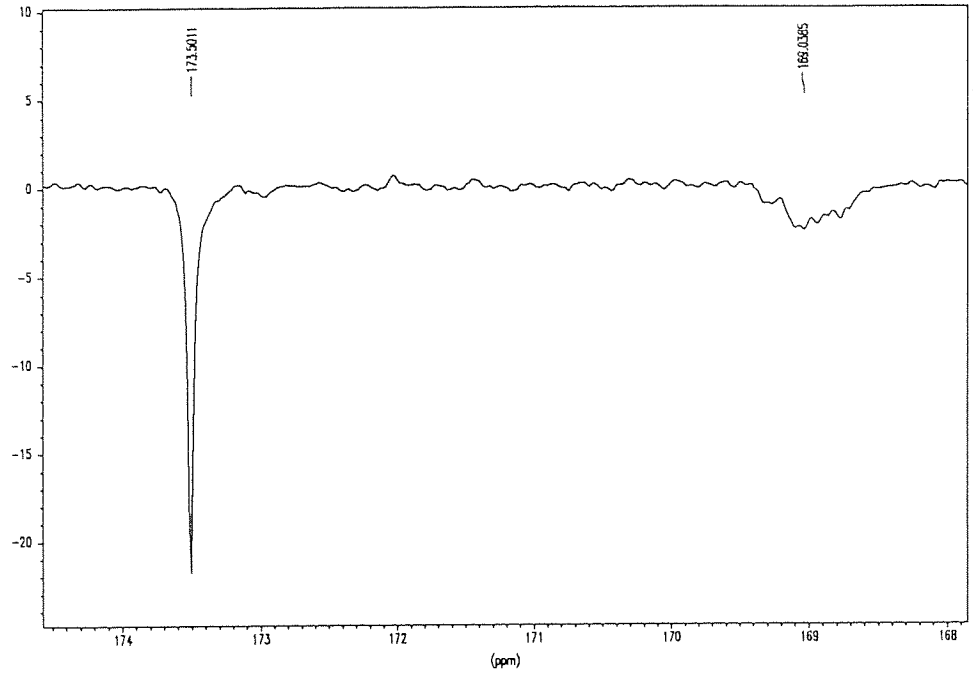

Figure 7.10. Methylene carbons signals in the ^{13}C NMR spectrum of poly(ε-CL)-block-poly(DL-HCAAS) / COP 18

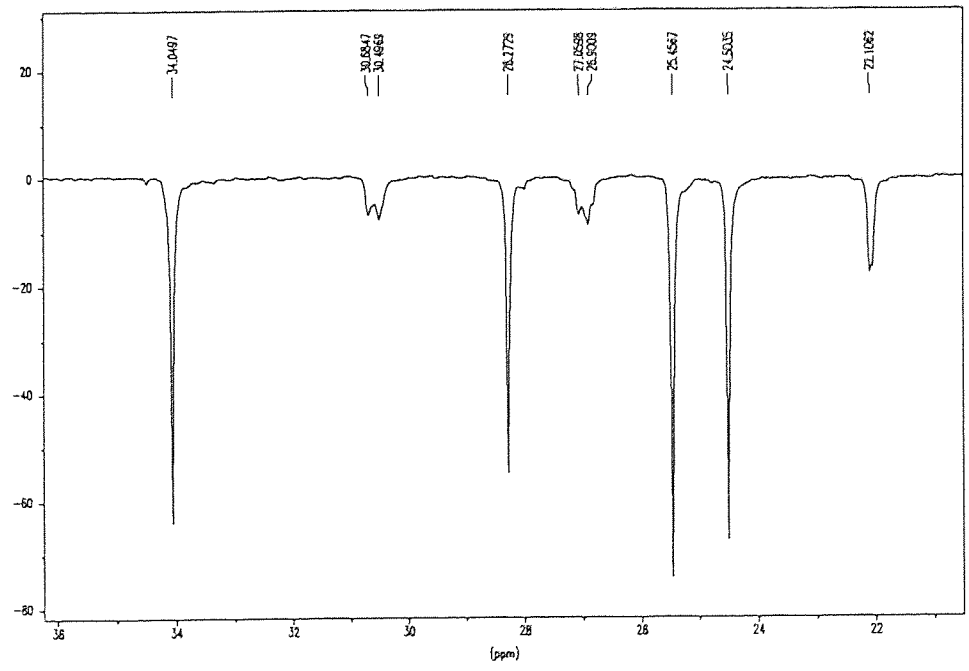

7.3. Discussion

Block-copolymers of ε-caprolactone and aliphatic anhydrosulfites with bulky substituents were synthesised. The copolyesters produced exhibited an unimodal molecular weight distribution in GPC and their ^{1}H and ^{13}C NMR spectra were consistent with a structure of a A-B type copolymer. Nevertheless, the incorporation of anhydrosulfites onto the polycaprolactone chains was reduced compared to LAAS, probably because of steric hindrance induced by the bulky substituent in the anhydrosulfite molecule.

As discussed in section 5.3., when the substituent in the anhydrosulfite molecule was bulky, the anionic homopolymerization of these compounds yielded polymers with structure preferentially isotactic because of steric hindrance. In these homopolymerizations, it was not possible to evaluate the yields because of the small amount of samples and the loss of material in the precipitation and filtration process. Nevertheless, steric hindrance might also affect the percentage of monomer conversion, the propagation proceeding probably with more difficulty in the case of anhydrosulfites with bulky substituents.

In addition, as observed for LAAS (see section 4.5.1.), the enantiomeric nature of the monomer was important. Polymers of higher molecular weight were obtained from L-LAAS than from DL-LAAS, in similar conditions. Although no consistent difference was observed in the copolymerizations of ε-caprolactone with L- and DL-LAAS, the enantiomeric nature of the monomer might also be another reason for the low incorporation of anhydrosulfites units onto polycaprolactone chains. The difference in reactivity between the pure enantiomer and the racemic might be enhanced when the substituent on the C(5) was bulky.

CHAPTER 8

CONCLUSION & SUGGESTIONS FOR FURTHER WORK

CONCLUSION

The anionic ring-opening polymerization of anhydrosulfites was found to provide an interesting and useful route to a variety of poly-α-esters and copolyesters possessing alkyl pendant groups. These materials are of considerable interest for medical application, because of the hydrophobicity of the chains which enhance their biocompatibility. In addition, this process produced polyesters with satisfactory properties in terms of molecular weight, molecular weight distribution and structure. A certain control over these characteristics was also possible.

A certain number of aliphatic anhydrosulfites with different alkyl groups on the C(5), such as methyl, isopropyl, n-butyl and isobutyl were synthesised and the procedure used enabled them to be synthesised with a level of purity satisfactory for polymerization.
Analysis of the NMR spectra of these compounds together with homodecoupling experiments and study of the effect of the temperature on the molecule revealed a very particular structure. As the sulfur atom, too large, is forced out of the plane of the ring, the five-membered anhydrosulfite ring is puckered and thus anhydrosulfites exist in two different conformations. These two forms are in equilibrium and this equilibrium can be

affected by a change in temperature. Additionally, the size of the substituent on the C(5) has a profound effect on the molecule. When the alkyl group is bulky, steric hindrance appears and this results in restricted rotations about the alkyl chains.

Whereas aliphatic anhydrosulfites were successfully purified by distillation and treatment with a metal oxide, aromatic anhydrosulfites, such as benzilic and mandelic acid anhydrosulfites could not be obtained with a level of purity sufficient for polymerization. These compounds decomposed either during distillation or in the packing materials (silica and neutral alumina) during purification by chromatographic techniques.

A wide range of anionic initiators, such as alkali metal alkoxides, alkyls and amides, were found efficient to initiate L-LAAS in THF. The yields of polymers were all relatively high, but the molecular weights and the molecular weight distributions were not similar. Bi-modal distributions were observed for poly(L-lactic acid) initiated either by potassium *tert*-butoxide with a monomer-to-initiator ratio above 200 or by lithium diisopropylamide. In contrast, a relatively narrow molecular weight distribution was obtained with lithium alkyls. High molecular weight poly(L-lactic acid), $\overline{M_n}$ of 37700 was synthesised at room temperature using *tert*-butyllithium, this initiator turned out to be the most successful amongst alkali metal alkoxides, alkyls and amides. The active propagating species for the anionic polymerization of anhydrosulfites was thought to be an alcoholate anion which was regenerating after addition of each subsequent monomer molecule. Additionally, in this mechanism, there was no real termination reactions so that the chain ends were expected to remain active. The 'living' character of the polylactic chains was investigated by adding more monomer when the polymerization was complete and it appeared that a certain number of chains ends remained active whereas others were terminated, probably because of aging processes which involved the reaction of the chain end anions with the solvent THF.

The molecular weights were found to depend on the monomer-to-initiator ratio and were higher than predicted, this was probably due to side-reactions of the initiator with impurities and the solvent THF. Thus, the nature of solvent affected the molecular weight, lower molecular weight polymers were prepared in toluene comparatively to

THF. The polymerization temperature had also a profound effect on the molecular weight, effect which differed from an initiator to another. When potassium *tert*-butoxide was used, increasing temperature yielded increasing molecular weight from 30 to 60°C. In contrast, when the anhydrosulfite was initiated by butyllithium, the molecular weight first increased up to 50°C and then decreased. This could be explained by the occurrence of two simultaneous reactions, polymerization and reaction between butyllithium and THF. Nevertheless, the molecular weight of polymer could be increased substantially, poly(L-lactic acid) with $\overline{M}_n$ of 60600 was produced for a monomer-to-initiator ratio of only 100. Therefore, this process could produce poly(L-LAAS) with a range of molecular weight $\overline{M}_n$ from 5.10^3 to 6.10^4 and a molecular weight distribution rather narrow.

The molecular weight of polymer depended on the basicity of the initiator, the monomer-to-initiator ratio, the nature of the solvent, the temperature, but also on the enantiomeric nature of the monomer. Polymers of higher molecular weight were obtained from L-LAAS than from DL-LAAS, in similar conditions.

L-LAAS led to a highly crystalline, purely isotactic poly(L-lactic acid) while DL-LAAS produced an amorphous polymer with randomly distributed D- and L-lactic units. This gave two indications. On one hand, the formation of L (or DL)-LAAS from L (or DL)-lactic acid did not involve inversion of configuration and this configuration was retained in the ring-opening polymerization, as expected from the mechanisms. On the other hand, this polymerization was not stereoselective.

However, the bulkiness of the substituent was found to be a factor influencing the stereospecificity of this polymerization. Thus, DL-HIVAAS and DL-HCAAS led to preferentially isotactic polymers. The structure of these polymers with bulky pendant groups was also rather rigid. Rotations about the pendant chain were restricted, as clearly observed for L-PHICAAS.

Block-copolymerization of ε-caprolactone with (L- or DL-) LAAS, DL-HIVAAS or DL-HCAAS were successfully carried out in THF and by using butyllithium, as initiator. The molecular weights of copolyesters were all relatively high and the polydispersities about 1.5. In addition, the A-B type block-copolymer structures were revealed by NMR

spectroscopy. The copolymer compositions were close to the feed compositions in the case of poly(CL)-block-poly(LAAS), but when the substituent on the C(5) of the anhydrosulfite ring was bulky, the incorporation of anhydrosulfite units onto the poly(caprolactone) chains was smaller than expected by the feed, probably because of steric hindrance.

Block-copolymerization of (L- or DL-) LAAS with ε-caprolactone catalysed by butyllithium was also conducted in THF and yielded copolymers with relatively high molecular weights and polydispersities close to 1. The NMR spectra of the polymers obtained exhibited a A-B type block-copolymer structure, but the incorporation of ε-caprolactone onto the polylactic chains was rather small. This could be explained if the active chain ends of PLAAS were not alkoxides and so might be ineffective initiators for ε-caprolactone. Alternatively, sulphur dioxide which was released during polymerization of LAAS, might somehow interfer with the polymerization of ε-caprolactone. It is interesting to mention that the terminated-end chains $-CH_2-OH$ were also visible in the ^1H and ^{13}C NMR spectra.

Random-copolymerization of (L- or DL-) LAAS with ε-caprolactone was also performed in THF with butyllithium. This random anionic polymerization yielded polymers with similar structures to block-copolymers poly(LAAS)-block-poly(CL) and did not enable the synthesis of random copolymers because of the large difference in reactivity between LAAS and ε-caprolactone in those polymerization conditions.

SUGGESTIONS FOR FURTHER WORK

Previous research directed towards the synthesis of poly-α-esters of controlled molecular architecture [45-50] resulted in the synthesis of materials with $\overline{M}_n$ less than 10,000. Poly-α-esters synthesised via anhydrosulfites in this project showed useful properties, in particular, the molecular weights were comparable to those produced from cyclic dimers

(lactide or glycolide). A significant increase of monomer purity was certainly an important factor in obtaining high molecular weight polymers but the molecular weights were much higher than predicted. Therefore, it appeared that reduction of initiator efficiency was either due to competitive reactions to polymerization or to a relatively slow initiation by butyllithium. In the latter case, there would be some initiator present at the end of the polymerization. Conversely, in the case where inefficiency of butyllithium resulted from side-reactions, the initiator would all be consumed. These side-reactions might be the reaction of butyllithium with the solvent THF, but more likely to be the reaction of butyllithium with impurities. However, an additional investigation into the extent of the reaction of butyllithium with THF over a short time period, i.e. 15 minutes, should be carried out. It would be also valuable to define the role of chlorine-containing impurities during polymerization reactions even though these compounds were present in small quantities in the reaction medium.

Additionally, because the active chain ends PLAAS were found to be ineffective initiators for ε-caprolactone, these chain ends might not be alkoxides. It may be that the mechanism involved an intermediate stage in which the α-lactone was formed in a similar manner to thermal decomposition of anhydrosulfites or else sulphur dioxide had not been eliminated in the first stage of ring-opening polymerization of anhydrosulfites and participated in the initiation of monomers. Alternatively, sulphur dioxide released in the reaction medium during polymerization of LAAS might prevent the polymerization of CL to take place. It would be therefore interesting to investigate this hypothesis by carrying out a polymerization of CL in the presence of sulphur dioxide.

Since attempts to obtain pure aromatic anhydrosulfites were not successful, an alternative method of synthesising poly-α-esters with aromatic groups could be a route via the anhydrocarboxy derivatives of α-hydroxy acids even though their reactivities were reported to be low compared to anhydrosulfites.

It is felt that the development of copolymers with anhydrosulfites proves to be a very promising area of research. Block copolymerization of ε-caprolactone with anhydrosulfites were successful whereas random copolyesters could not be produced because of the large difference in reactivity between the two monomers. Therefore, it

would be of great interest to investigate other initiator systems which would be susceptible to increase the reactivity of ε-caprolactone relative to the anhydrosulfite and so would favour the incorporation of ε-caprolactone, e.g. aluminium alkoxides. However, it appears that if the two monomers were anhydrosulfites, the reactivities between the two monomers would be rather similar and so the anionic ring-opening polymerization could give access to random copolyesters with interesting structures. Additionally, it is thought that stereocopolymers produced from different proportions of DL- and L-LAAS would be of great interest if it was to study their degradability with respect to structural characteristics.

As anhydrosulfites have proved to be useful in the synthesis of homopolymers and copolymers with interesting properties, a novel approach to the preparation of poly-α-esters and copolymers of α-hydroxy acids with other materials might be a route via anhydrosulfites. In particular, anhydrosulfites may be expected to allow copolymerizations with α-amino acids under mild conditions. These materials, polydepsipeptides, copolymers of α-hydroxy acids and α-amino acids NCAs are very attractive because of their structural similarity to proteins. Furthermore, copolymers of anhydrosulfites and β-hydroxy acids may also be valuable additions to the existing series of synthetic biodegradable materials.

Since the route to the synthesis of polyesters and copolyesters via anhydrosulfites has shown to have certain control over molecular weight, molecular weight distribution and structure, it would be interesting to investigate the biodegradability and behaviour in a biological environment of the homopolymers and copolymers produced with respect to all of these characteristics.

REFERENCES

1 M. Chasin, R. Langer, *'Biodegradable polymers as drug delivery systems'* Drugs and the pharmaceutical sciences, **45**, M. Dekker, New York (1990)

2 J. Leenslag, A. Pennings, R. Bos, F. Rozema, G. Boering, *'Resorbable materials of poly(L-lactide). VI. Plates and screws for internal fracture fixation'*, Biomaterials, **8**, 70-73 (1987)

3 J. Bergsma, W. de Bruijn, F. Rozema, R. Bos, G. Boering, *'Late degradation tissue response to poly(L-lactide) bone plates and screws'*, Biomaterials, **16**, 1, 25-31 (1995)

4 M. Asano, M. Yoshida, I. Kaetsu, *'Biodegradability of a hot pressed poly(lactic acid) formulation with controlled release of LH-RH agonist and its pharmacological influence on rat prostate'*, Makromol. Chem., Rapid Commun., **6**, 509-513 (1985)

5 J. Swarbrick, J. C. Boylan, *'Biodegradable polyester polymers as drug carriers to clinical pharmacokinetics and pharmacodynamics'*, Encyclopedia of pharmaceutical technology, **2**, Dekker, New York (1990)

6 R. Datta, S. Tsai,, P. Bonsignore, S. Moon, J. Frank, *'Technological and economic potential of poly(lactic acid) and lactic acid derivatives'*, FEMS Microbiology Reviews, **16**, 221-231 (1995)

7 F. Bovey, *'High resolution NMR of macromolecules'*, Academic Press, New York and London (1972)

8 M. Bero, J. Kasperczyk, Z. Jedlinski, *'Structure determination of obtained polymers'*, Makromol. Chem. **191**, 2287-2296 (1990)

9 Z. jedlinski, W. Walach,
'Polymerization of L-dilactide and L,D-dilactide in the presence of potassium methoxide', Makromol. Chem. **192**, 2051-2057 (1991)

10 H. Kricheldorf, I. Kreiser-Saunders,
'Polylactones,19 - Anionic polymerization of L-lactide in solution'
Makromol. Chem. **191**, 1057-1066 (1990)

11 H. Kricheldorf, C. Boettcher, *'Polylactones, 21 - Polymerization of L,L-lactide and rac-D,L-lactide with hematin and related porphyrin complexes'*,
Makromol. Chem. **194**, 463-473 (1993)

12 H. Kricheldorf, C. Boettcher, *'Polylactones, 24 - Polymerizations of racemic and meso-D,L-lactide with Al-O initiators. Analyses of stereosequences'*
Makrmol. Chem. **194**, 1653-1664 (1993)

13 H. Kricheldorf, C. Boettcher, *'Polylactones, 25 - Polymerizations of racemic- and meso-D,L-lactide with Zn, Pb, Sb, and Bi salts - Stereochemicals aspects'*
Pure Appl. Chem., A30 (**6** & **7**), 441-448 (1993)

14 G. Schwach, J. Coudane, R. Engel, M. Vert,
'Stannous octoate-versus zinc-initiated polymerization of racemic lactide, effect of configurational structures', Polym. Bull., **32**, 617-623 (1994)

15 H. Fukuzaki, Y. Aiba, *'Synthesis of biodegradable poly(L-lactic acid-co D,L-mandelic acid) with relatively low molecular weight'*
Makromol. Chem. **190**, 2407-2415 (1989)

16 H.Fukuzaki, M. Yoshida, M. Asano, M. Kumakura,
'Synthesis of copoly(D,L-lactic acid) with relatively low molecular weight and in vitro degradation', Eur. Polym. J., **25**, 1019-1026 (1989)

17 K. Imasaka, T. Nagai, M. Yoshida, H. Fukuzaki, M. Asano, M. Kumakura,
'Synthesis and in vitro degradations of low molecular weight copolyesters composed of L-lactic acid and aromatic hydroxy acids'
Makromol. Chem. **191**, 2077-2082 (1990)

18 M. Yoshida, H. Fukuzaki, M. Asano, M. Kumakura,
'Synthesis of biodegradable copoly(L-lactic acid / aromatic hydroxy acids) with relatively low molecular weight', Eur. Polym. J., **26**, 1273-1277 (1990)

19 M. Ajioka, K. Enomoto, K. Suzuki, A. Yamaguchi,
'Basic properties of polylactic acid produced by the direct condensation polymerization of lactic acid', Bull. Chem. Soc. Jpn, **68**, 2125-2131 (1995)

20 D. Gilding, A. Reed, *'Biodegradable polymers for use in surgery - Polyglycolic/poly(lactic acid) homo- and copolymers'*
Polymer, **20**, 1459-1464 (1979)

21 J. rak, J. Ford, C. Rostron, V. Walters, *' The preparation and characterization of poly(D,L-lactic acid) for use as a biodegradable drug carrier'*
Pharma. acta. helv., **60**, 162-169 (1985)

22 F. Chabot, M. Vert, S. Chapelle, P. Granger,
'Configurational structures of lactic acid stereocopolymers as determined by $^{13}C\{^{1}H\}NMR$', Polymer, **24**, 53-59 (1983)

23 M. Bero, G. Adamus, J. Kasperczyk, H. Janeczek,
'Synthesis of block-copolymers of ε-caprolactone and lactide in the presence of lithium t-butoxide', Polym. Bull., **31**, 9-14 (1993)

24 D. Grijpma, A. Pennings, *'Polymerization temperature effects on the properties of L-lactide and ε-caprolactone copolymers'*, Polym. Bull., **25**, 335-341 (1991)

25 G. Perego, T. Vercellio, *'Copolymers of L- and D,L-lactide with ε-caprolactone synthesis and characterization'*, Makromol. Chem. **194**, 2463-2469 (1993)

26 D. Ballard, B. Tighe, *'Studies of the anhydrosulfites of α-hydroxy-carboxylic acids. Part I. Polymerization of anhydrosulfites of α-hydroxyisobutyric acid'* J. Chem. Soc (B), 702-709 (1967)

27 D. Ballard, B. Tighe, *'Studies of the anhydrosulfites of α-hydroxy-carboxylic acids. Part II. Polymerization of glycollic and lactic acid anhydrosulfites'* J. Chem. Soc (B), 976-980(1967)

28 D. Thomas, B. Tighe, *'Studies of the reactions of the anhydrosulfites of α-hydroxy-carboxylic acids. Part III. 'Purification and polymerization of glycollic acid anhydrosulfite'*, J. Chem. Soc (B), 1039-1044 (1970)

29 D. Fenn, M. Thomas, B. Tighe, *'Studies of the reactions of anhydrosulfites of α-hydroxy-carboxylic acids. Part IV. 'Steric and electronic effects in the reaction with alcohols'*, J. Chem. Soc (B), 1044-1048 (1970)

30 B. Evans, D. Fenn, B. Tighe, *'Studies of the reactions of anhydrosulfites of α-hydroxy-carboxylic acids. Part V. Thermal decomposition of benzilic and mandelic acid anhydrosulfites'*, J. Chem. Soc (B), 1049-1052 (1970)

31 G. Blackbourn, B. Tighe, *'Studies of the reactions of anhydrosulfites of α-hydroxy-carboxylic acids. Part VI. Anhydrosulfite synthesis and characterisation'*, J. Chem. Soc (C), 257-259 (1971)

32 G. Blackbourn, B. Tighe, *'Studies of the reactions of anhydrosulfites of α-hydroxy-carboxylic acids. Part VII. Polymerization of anhydrosulfites derived from symmetrically substituted α-hydroxy-acids'*, J. Chem. Soc (B), 1384-1390 (1971)

33 G. Blackbourn, B. Tighe, *'Studies of the reactions of anhydrosulfites of α-hydroxy-carboxylic acids. Part VIII. 'Polymerization of anhydrosulfites of α-hydroxy-cycloalkanecarboxylic acids'*, J. Chem. Soc. Perkin II, 1263- 1268 (1972)

34 A. Crowe, B. Tighe, *'Studies of the reactions of anhydrosulfites of α-hydroxy-carboxylic acids. Part IX. Thermal polymerization of anhydrosulfites of α-hydroxy α-methyl carboxylic acids'*, Br. Polym. J., **6**, 79-89 (1974)

35 A. Crowe, B. Tighe, *'Thermal decomposition of 5,5-(bis-chloromethyl)-1,3,2-dioxathiolan-4-one 2-oxide'*, Chemistry and Industry, 170-171 (1969)

36 G. Blackbourn, B. Tighe, *'Studies in ring-opening polymerization, 5,5-diethyl-1,3,2-dioxathiolan-4-one-2-oxide'*, J. Polym. Sci. Part A1, **8**, 3591-3605 (1970)

37 D. Pedley, B. Tighe, *'Studies in ring-opening polymerization III, 5-methyl-5-propyl and 5-methyl-5-isopropyl-1,3,2-dioxathiolan-4-one-2-oxide'*, J. Polym. Sci., **11**, 779-788 (1973)

38 I. Smith, B. Tighe, *'Phenyl and pentafluorophenyl substituted 1,3-dioxothiolan-2,4-diones : a novel group of heterocyclic monomers'* Chemistry and Industry, 695-696 (1973)

39 I. Smith, B. Tighe, *'Synthesis and characterization of fluorine-containing poly-α-esters II. Thermal and hydroxyl-initiated polymerization of pentafluorophenyl-substituted anhydrosulfites and anhydrocarboxylates of α-hydroxycarboxylic acids'*, Br. Polym. J., **7**, 349-360 (1975)

40 I. Smith, B. Tighe, *'Ring-opening polymerization. V. Hydroxyl-initiated polymerization of phenyl-substituted 1,3-dioxolan-2,4-diones : a model study'* J. Polym. Sci., **14**, 2293-2305 (1976)

41 M. Ali, S. Roy, B. Tighe, *'Anhydrocarboxylate and anhydrosulfite, Derivatives of α-thiocarboxylic acids : Synthesis, purification and characterization'* J. appl. Chem. Biotechnol., **27**, 696-699 (1977)

42 I. Smith, B. Tighe, *'Studies in ring-opening polymerization, 6 Tertiary base initiated polymerization of 5-phenyl-1,3-dioxolan-2,4-dione'* Makromol. Chem., **182**, 313-324 (1981)

43 H. Al-Mesfer, B. Tighe, *'Polymers for biodegradable medical devices, III. Polymerization and copolymerization of cyclics derivatives of tartronic acid'* Biomaterials, **8**, 353-359 (1987)

44 M. Ali, A. Amass, B. Tighe, *'Studies in ring-opening polymerization, 10 Pyridine-initiated polymerization of cyclic anhydrocarboxylates of α-mercapto acids'*, Makromol. Chem., **191**, 199-211 (1990)

45 S. Inoue, K. Tsubaki, T. Tsuruta, *'Synthesis of optically active polymers by asymmetric catalysts. IX. Asymmetric-selective polymerization of β-chloro-α-hydroxy-α-methylpropionic acid anhydrosulfite'* Polym. Lett., **6**, 733-736 (1968)

46 S. Inoue, K. Tsubaki, T. Tsuruta, *'Polymerization of α-hydroxy-carboxylic acid anhydrosulfites by tertiary amines or tertiary amides as catalysts'* Makromol. Chem., **125**, 170-180 (1969)

47 G. P. Blackbourn, *'Some aspects of the synthesis and polymerization of 1,3,2-dioxathiolan-4-one-2-oxides'*,
PhD thesis, University of Aston in Birmingham (1970)

48 A. J. Crowe, *'Ring-opening reactions of some dialkyl substituted 1,3,2-dioxathiolan-4-one-2-oxides'*,
PhD thesis, University of Aston in Birmingham (1975)

49 H. A. Al-Mesfer, *'Polymerization of cyclics derivatives of α-hydroxy acids'*
PhD thesis, University of Aston in Birmingham (1981)

50 L.R. Adams, *'The polymerization of lactic acid anhydrosulphite by anionic initiators'*, PhD thesis, University of Aston in Birmingham (1994)

51 K.C. Frisch, *'Cyclic monomers'*, High polymers, **26**, Wiley interscience (1972)

52 H. Kricheldorf, M. Jonte, *'New polymer syntheses, 8. Synthesis and polymerization of L-lactic acid O-carboanhydride (5-methyl-dioxiolan-2,4-dione)'*, Polym. Bull., **9**,276-283 (1983)

53 S. Inoue, K. Tsubaki, T. Yamada, T. Tsuruta, *'Copolymerization of α-hydroxyisobutyric acid anhydrosulfite with vinyl compounds'*
Makromol. Chem., **125**,181-191 (1969)

54 E. Blaise, A. Montagne, *'Action du chlorure de thionyl sur les acides-alcools'*,
Compt. rend., **174**, 1553-1555 (1922)

55 T. Alderson, *'Polymer from α-hydroxy isobutyric acid'*
U.S.P., 2,811, 511 Assigned to Du Pont de Nemours (1953)

56 J. Rose, C. Warren, *'Polyesters from the anhydrosulfites of α-hydroxy-acids'*, J. Chem. Soc., 791-792 (1965)

57 C. Pitt, *'Non-microbial degradation of polyesters : Mechanisms and modifications'*, Biodegradable polymers and plastics, edited by M. Vert, J. Feijen, A. Albertson, G. Scott, E. Chiellini, Royal Society of Chemistry (1992)

58 S. Ming Li, H. Garreau, M. Vert, *'Structure-property relationships in the case of the degradation of massive aliphatic poly(α-hydroxy acids) in aqueous media, Part 1 : Poly(DL-lactic acid)'*, J. Mater. Sci., Mater. in med., **1**, 123-130 (1990)

59 S. Ming Li, H. Garreau, M. Vert, *'Structure-property relationships in the case of the degradation of massive aliphatic poly(α-hydroxy acids) in aqueous media, Part 2 : Degradation of lactide-glycolide copolymers : PLA37.5GA25 and PLA75GA25'*, J. Mater. Sci., Mater. in med., **1**, 131-139 (1990)

60 H. Pitsner, D. Bendix, J. Muhling, J. Reuther, *'Poly(L-lactide) : a long term degradation study in vivo'*, Biomaterials, **14**, 4, 291-299 (1993)

61 H. Mark, N. Bikales, C. Overberger, G. Menges, J. Kroschwitz, *'Encyclopedia of polymer science and engineering'*, 2nd Edition, Wiley interscience (1985)

62 D. Williams, *'Fundamental aspects of biocompatibility'*, **2**, CRC Press (1981)

63 C. Holten, *'Lactic acid'*, Verlag Chemie (1971)

64 G. Ingram, *'Some further deliberations on the rapid combustion procedure'*, Mikrochim. Acta, **1**, 877-898 (1956)

65 J. homer, M. Perry, *'New method for NMR signal enhancement by polarization transfer, and attached nucleus testing'*,
J. Chem. Soc., Chem. Commun., 373-374 (1994)

66 J. homer, M. Perry, *'Enhancement of the NMR spectra of insensitive nuclei using PENDANT with Long-range coupling constants'*,
J. Chem. Soc. Perkin. Trans., **2**, 533-536 (1995)

67 W.A. Penny, *'Studies in ring-opening - The interactions of some cyclics esters with a bimetallic oxo-alkoxide'*,
PhD thesis, University of Aston in Birmingham (1979)

68 *'The Aldrich Library of FT-IR spectra'*, C. Pouchert,
Aldrich Chemical Co. Inc. (1993)

69 D.S. Breslow, H. Skolnik, *'Multi-sulfur and sulfur and oxygen five and six-membered heterocycles'*, The chemistry of heterocyclic compounds, part one, interscience publishers (1966)

70 M. Bains, *'The covalent character of alkali alkoxides'*,
Canadian J. Chem., **42**, 945-946 (1964)

71 D. Bradley, R. Mehiotra, D. Gaur, *'Metal alkoxides'*, Academic Press (1978)

72 T. Brown, M. Rogers, *'The preparation and properties of crystalline Lithium Alkyls'*, J. Am. Chem. Soc., **79**, 1859-1861 (1957)

73 M. Weiner, G. Vogel, R. West, *'The physical properties and structure of tert-Butyllithium'*, Inorg. Chem., **1**, 654-658 (1962).

74 R. Bates, L. Kroposki, D. Potter, *'Cycloreversions of anions from Tetrahydrofurans. A convenient synthesis of Lithium enolates of aldehydes'*, J. Org. Chem., **37**, 4, 560-562 (1972)

75 M. Szwarc, *'Living polymers : a tool in studies of ions and ions-pairs'*, Science, **170**, 3953, 23-31 (1970)

76 J. Comyn, M. D. Glasse, *'The aging of living α-methylstyryl oligomers'*, Polym. Bull., **18**, 703-709 (1980)

77 Ph. Dubois, R. Jerome, Ph. Teyssie, *'Macromolecular engineering of polylactones and polylactides - 1. End-functionalization of poly(ε-caprolactone)'* Polym. Bull., **22**, 475-482 (1989)

78 H. Kricheldorf, M. Berl, N. Scharnagel, *'Polylactones. 9. Polymerization mechanism of metal alkoxide initiated polymerizations of lactide and various lactones'*, Macromol, **21**, 286-293 (1988)

79 D. Tian, Ph. Dubois, R. Jerome, Ph. Teyssie, *'Macromolecular engineering of polylactones and polylactides. 18. Synthesis of star branched aliphatic polyesters bearing various functional end groups'*, Macromol., **27**, 4134-4144 (1994)

80 H. Kricheldorf, T. Mang, J. Jonte, *'Polylactones. 1. Copolymerization of glycolide and ε-caprolactone'*, Macromol. **17**, 2173-2181 (1984)

81 M. Morton, M. Wu, *'Organolithium polymerization of ε-caprolactone'*, ACS Symposium Series, **286**, 175-182 (1985)

82 K. Ito, Y. hashizuka, Y.Yamashita, *'Equilibrium cyclic oligomer formation in the anionic polymerization of ε-caprolactone'*, Macromol., **10**, 821-824 (1977)

83 K. Ito, Y. Yamashita, *'Propagation and depropagation rates in the anionic polymerization of ε-caprolactone cyclic oligomers'*, Macromol., **11**, 68-72 (1978)

84 A. duda, Z. Florjanczyk, A. Hofman, S. Slomkowski, S. Penczek, *'Living pseudoanionic polymerization of ε-caprolactone. Poly(ε-caprolactone) free of cyclics and with controlled end groups'*, Macromol., **23**, 1640-1646 (1990)

APPENDICES

Appendix 1. Methine signals in the ^{1}H NMR spectrum of DL-LAAS at room temperature

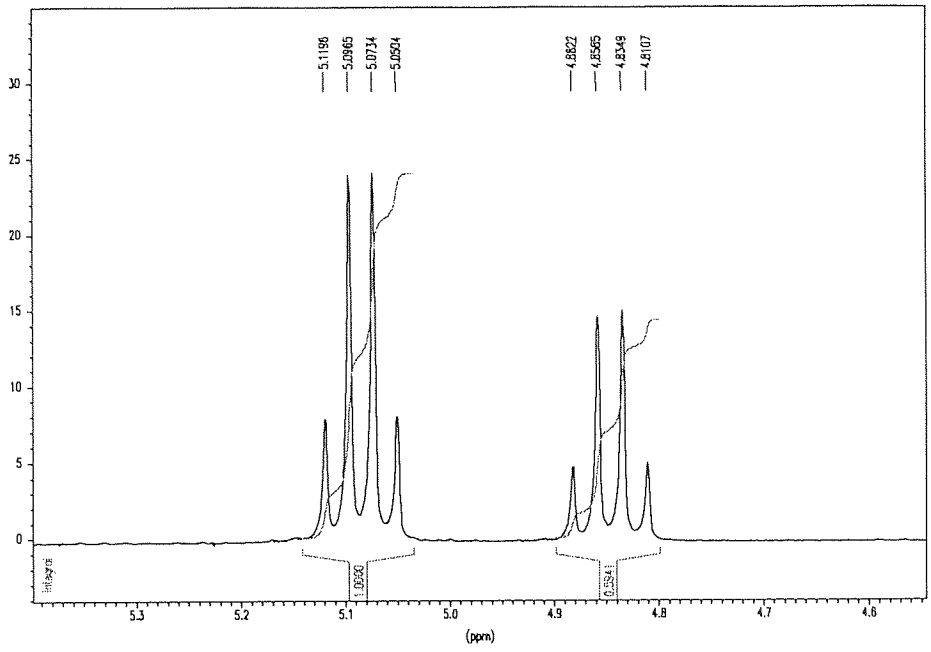

Appendix 2. Methine signals in the ^{1}H NMR spectrum of DL-LAAS at 0°C

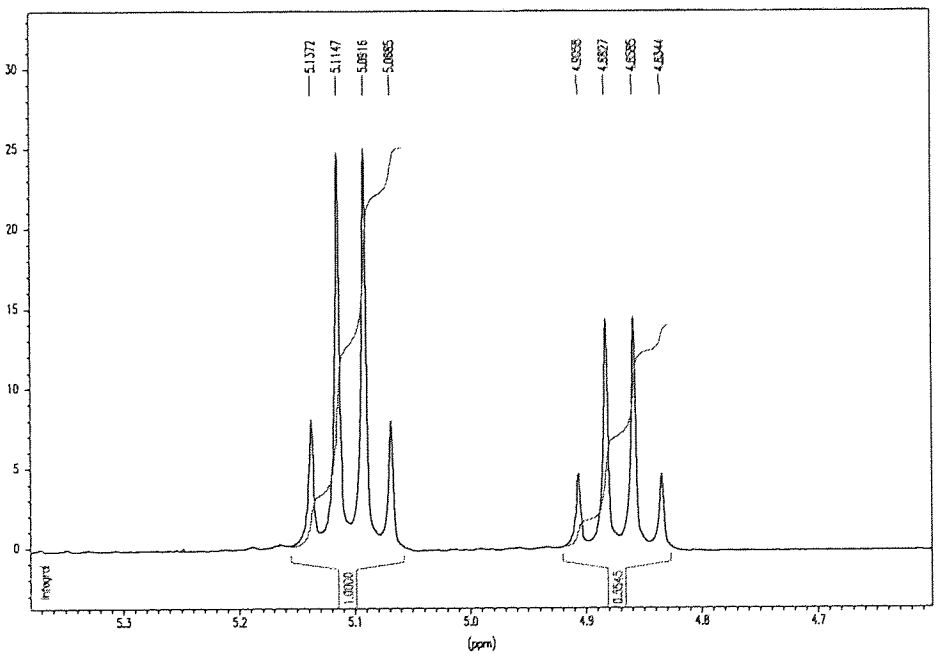

Appendix 3. Methine signals in the ^{1}H NMR spectrum of DL-LAAS at -20°C

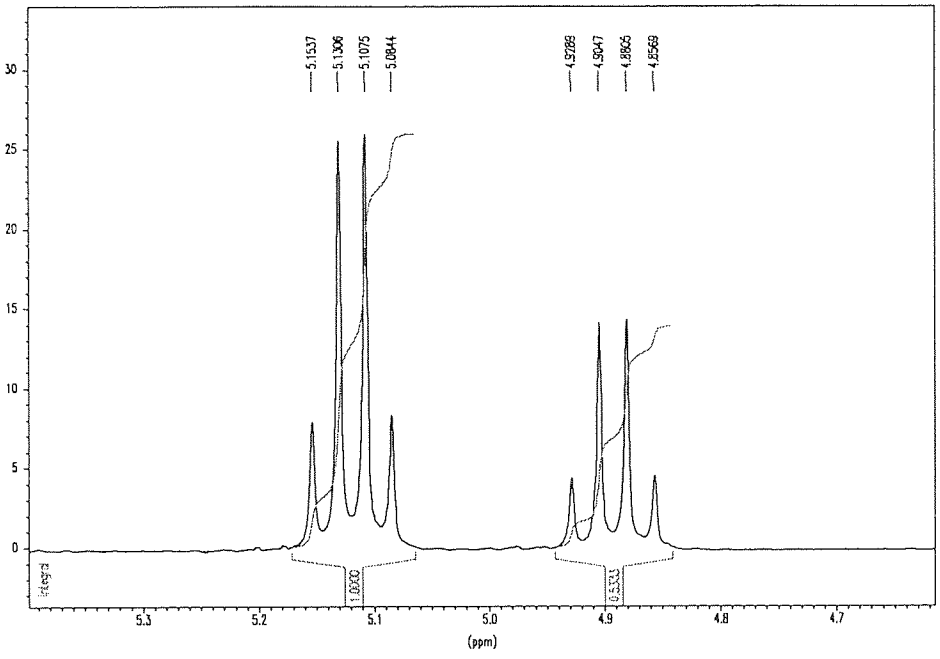

Appendix 4. Methine signals in the ^{1}H NMR spectrum of DL-LAAS at -40°C

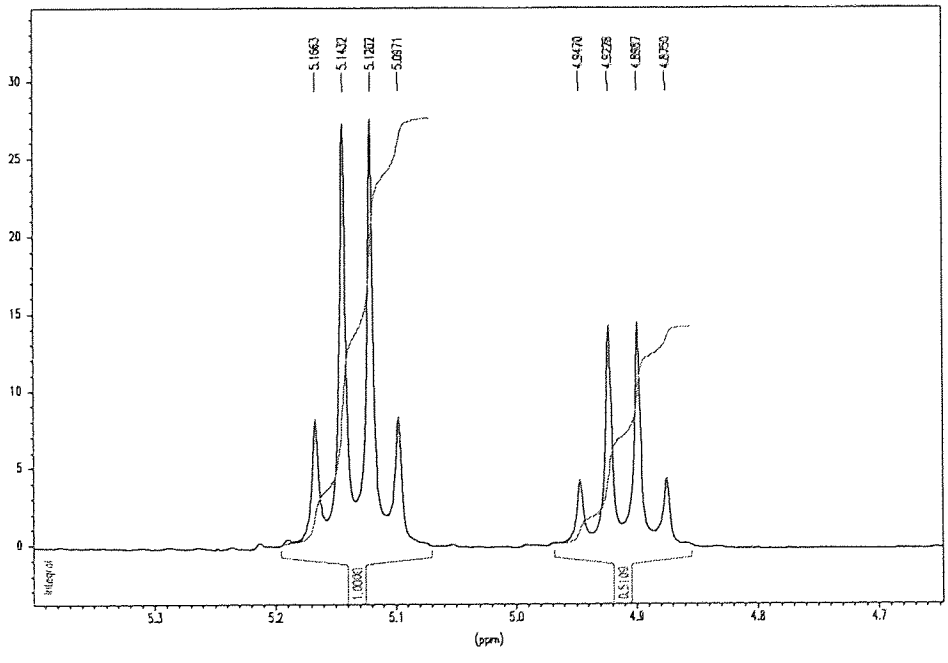

Appendix 5. FT-IR spectrum of DL-HCAAS

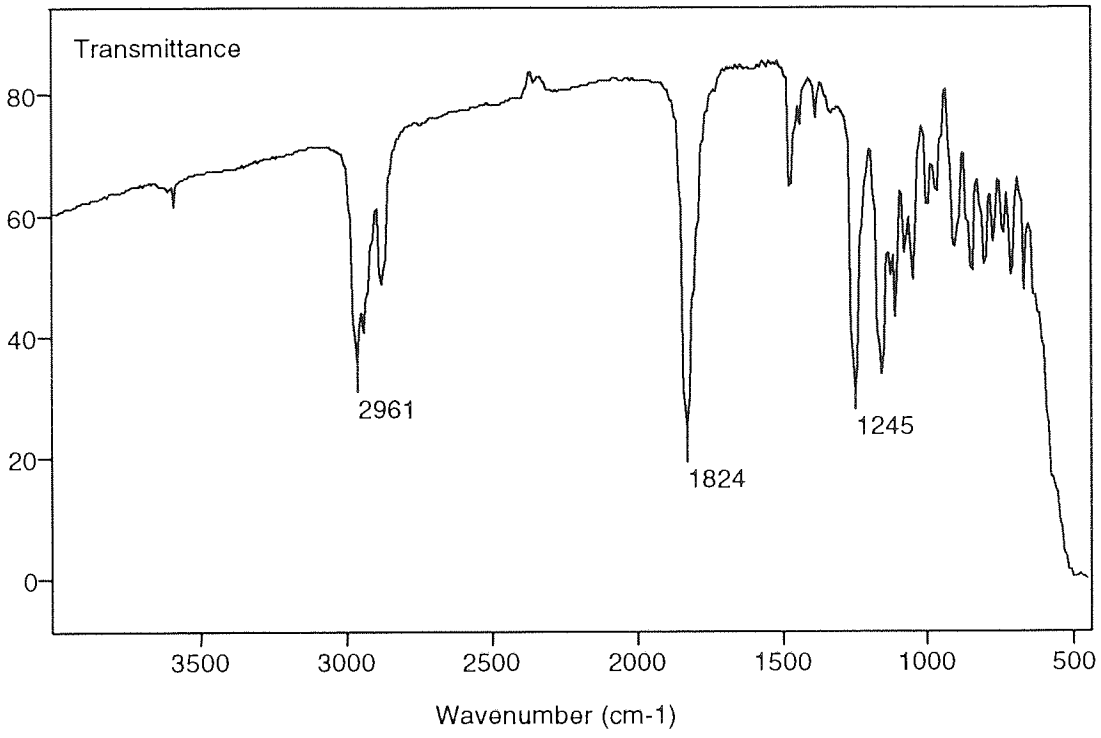

Appendix 6. FT-IR spectrum of L-HICAAS

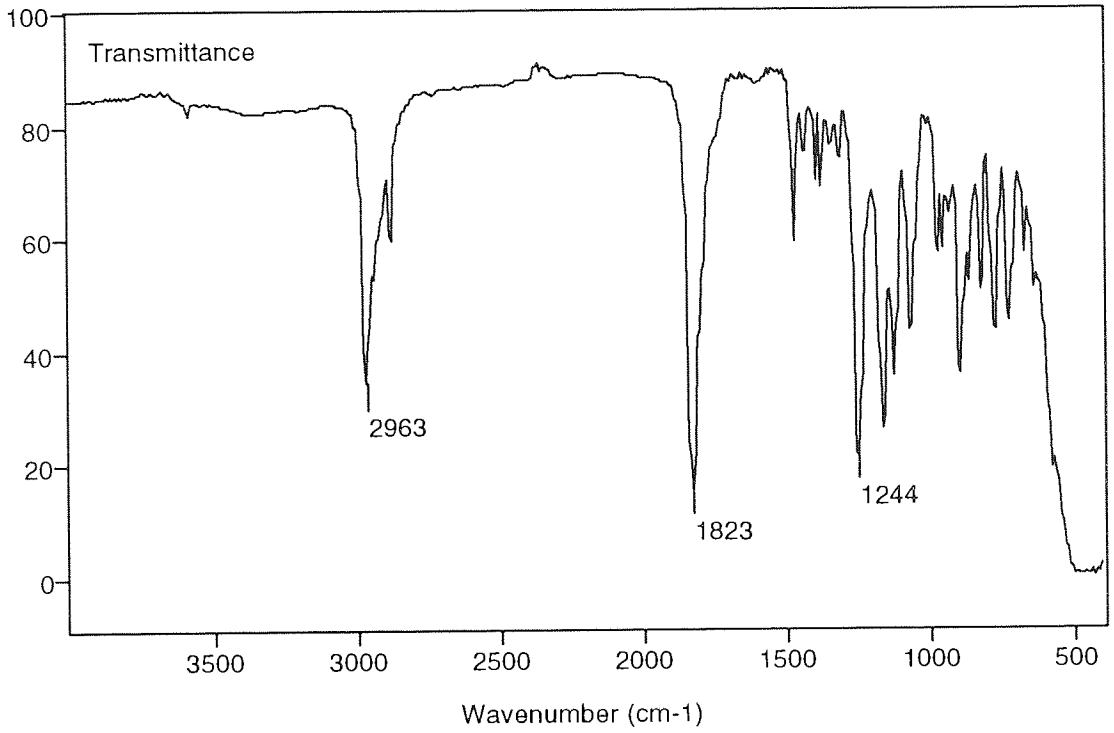

Appendix 7. UV spectrum of LAAS

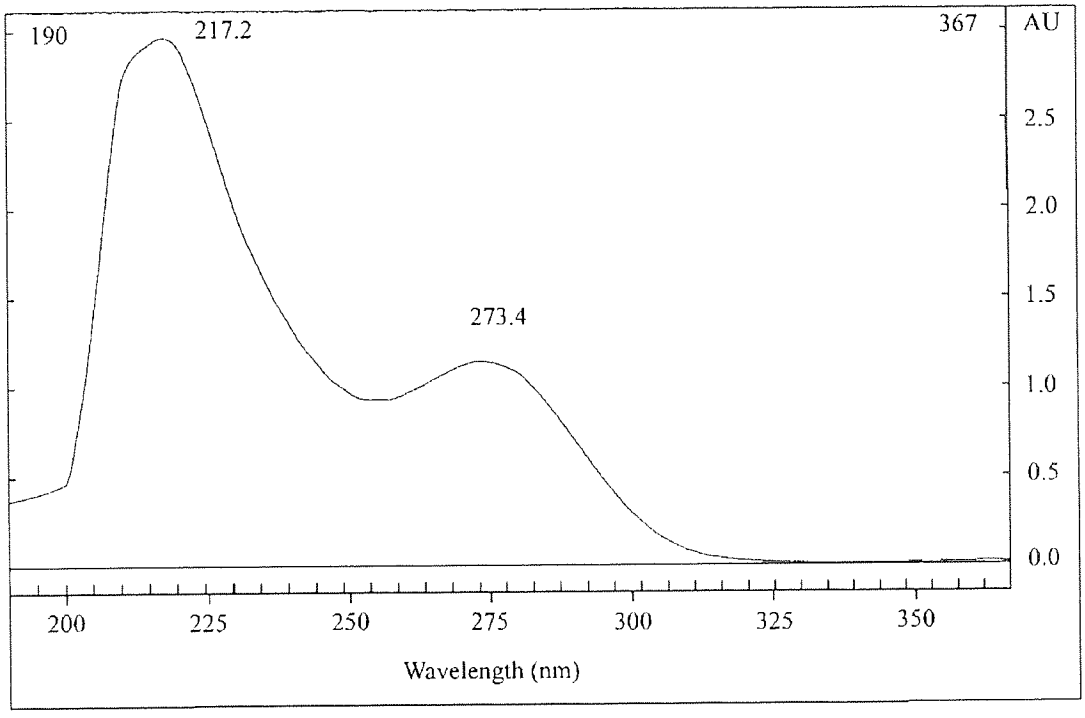

Appendix 8. FT-IR spectrum of the white crystals obtained when MAAS decomposed

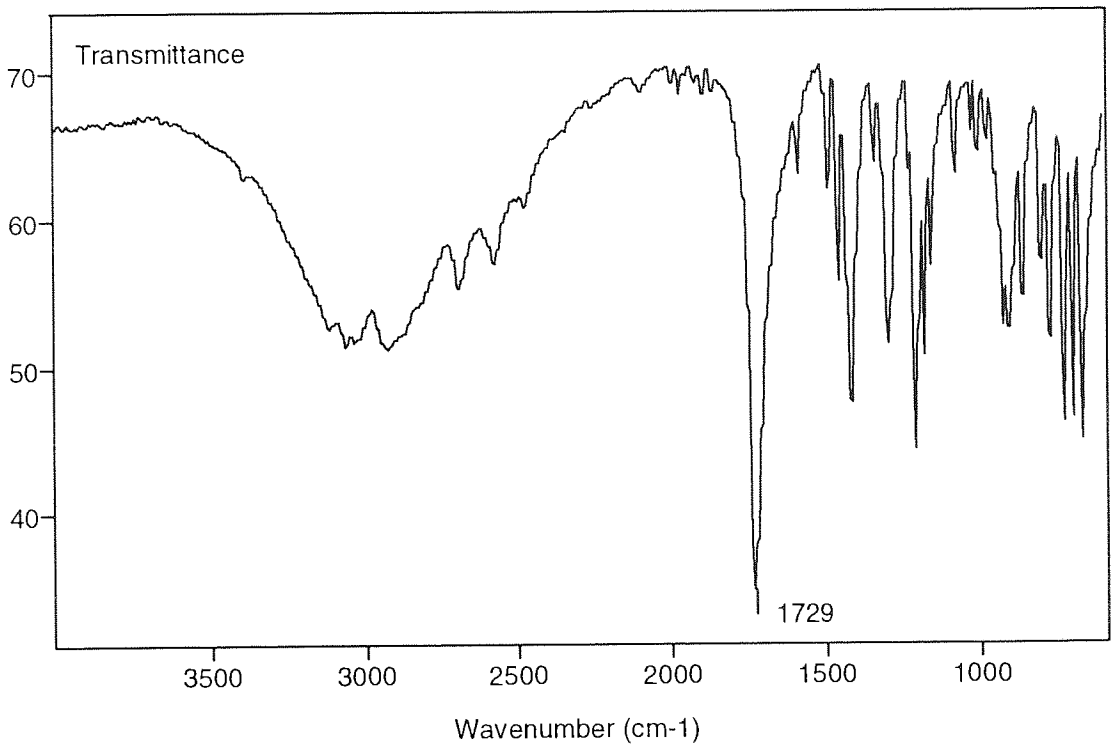

Appendix 9. ^{1}H NMR spectrum of the polymer synthesised in the cationic polymerization of L-LAAS (polyTHF)

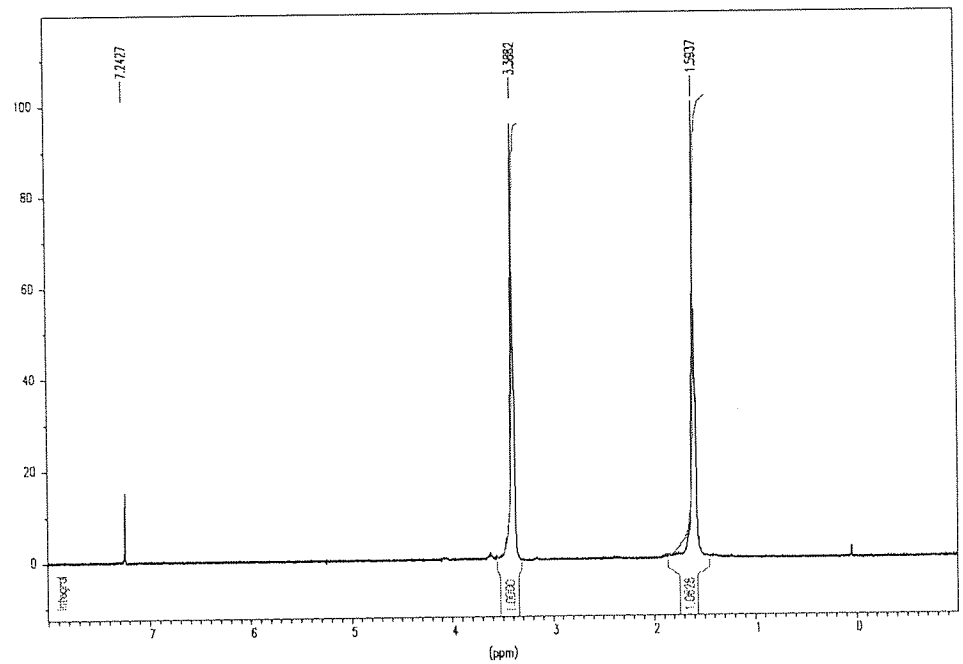

Appendix 10. ^{13}C NMR spectrum of the polymer synthesised in the cationic polymerization of L-LAAS (polyTHF)